

# **Analysis of vegetable oils, seeds and beans by TGA and NMR spectroscopy**

by  
Liesel Retief

*Dissertation presented for the degree of Doctor of Philosophy at the  
University of Stellenbosch*



Promoter: Prof Klaus Koch  
Co-Promoter: Jean McKenzie  
Natural Science Faculty  
Department of Chemistry and Polymer Science

March 2011

## **Declaration**

By submitting this thesis/dissertation electronically, I declare that the entirety of the work contained therein is my own, original work, that I am the sole author thereof (save to the extent explicitly otherwise stated), that reproduction and publication thereof by Stellenbosch University will not infringe any third party rights and that I have not previously in its entirety or in part submitted it for obtaining any qualification.

March 2011

Copyright © 2011 University of Stellenbosch

All rights reserved

## ABSTRACT

Due to the commercial, nutritional and health value of vegetable oils, seeds and beans, the analysis of their components is of much interest. In this dissertation oil-containing food products, specifically vegetable oils, seeds and beans, were investigated.

Selected minor components of three locally produced vegetable oils, namely apricot kernel, avocado pear and macadamia nut oils were investigated using  $^{31}\text{P}$  NMR spectroscopy. These minor components, including 1,2 diacylglycerols, 1,3 diacylglycerols and free fatty acids, were identified in the  $^{31}\text{P}$  NMR spectra of each of the three vegetable oils for the first time. Two approaches were used for the quantification of the minor components present in the spectra. A calibration curve approach used known concentrations of standard minor components to establish calibration curves while a direct correlation approach calculated the unknown concentration of minor components in the vegetable oils using a known amount of standard compound within the analysis solution. These approaches aided in determining the concentration of minor components during storage studies in which vegetable oils were stored in five different ways: exposed to light, in a cupboard, in a cupboard wrapped in tin foil, at  $-8\text{ }^{\circ}\text{C}$  and at  $5\text{ }^{\circ}\text{C}$ . It was found that determining the best storage condition for each oil was difficult since individual minor components were affected differently by the various storage conditions. However, in general the best storage conditions appeared to be  $5\text{ }^{\circ}\text{C}$  and  $-8\text{ }^{\circ}\text{C}$ .

The oil, protein and carbohydrate contents of sesame, sunflower, poppy, and pumpkin seeds, and soy, mung, black and kidney beans were analysed by thermogravimetric analysis and  $^{13}\text{C}$  NMR solid state NMR spectroscopy. It was shown that the first derivative of TGA data for seeds and beans can give valuable information about the carbohydrate, moisture, protein and fat content. This has not been previously demonstrated. For the seeds, the integration of a region between  $270\text{--}480\text{ }^{\circ}\text{C}$  was equal to the sum of the oil and protein content and compared well to quantitative results obtained by other conventional methods. For beans the integration of a region between  $180\text{--}590\text{ }^{\circ}\text{C}$ , gave a value which represented the sum of the oil, protein and carbohydrate content.

$^{13}\text{C}$  solid state NMR spectroscopy, including SPE-MAS, CP-MAS and variable contact time experiments, was carried out on these seeds and beans and gave valuable information on the solid-like and liquid-like components. To our knowledge these seeds and beans have never been previously analysed using this technique.  $^{13}\text{C}$  SPE-MAS NMR spectroscopy indicated that the seeds contained more liquid-like components than the beans. In turn the  $^{13}\text{C}$  CP-MAS NMR spectra indicated that beans had higher levels of solid-like components

than the seeds. These conclusions correlated well with the quantities of liquid-like components and solid-like components that were determined by conventional methods and TGA. Preliminary studies using  $T_{1\rho}H$  experiments on the components present in the seeds and beans led to a few observations. Most interesting is that a model using a two-phase fit in order to determine  $T_{1\rho}H$  values appears to be more accurate than a one-phase model.

## OPSOMMING

Groente olies, sade en bone is 'n onderwerp van groot belang omrede hul kommersiële, voeding en gesondheidswaardes. In hierdie tesis is olie-bevattende voedselprodukte, spesifiek groente-olies, sade en bone geanaliseer. Geselekteerde komponente teenwoordig in klein hoeveelhede in drie lokaal geproduseerde groente-olies, naamlik appelkoos-pit, avokadopeer en makadamia-neut olies is geanaliseer met behulp van  $^{31}\text{P}$  KMR spektroskopie. Hierdie komponente, insluitend 1,2 diasielglyserole, 1,3 diasielglyserole en ongebonde vetsure, is vir die eerste keer geïdentifiseer in die  $^{31}\text{P}$  KMR spektra van die drie groente olies. Twee benaderings is gebruik vir die hoeveelheids-bepaling van die komponente in die spektra. 'n Yking-kurwe metode het gebruik gemaak van bekende hoeveelhede konsentrasies standaard komponente vir die opstel van yking-kurwes, terwyl 'n direkte korrelasie metode gebruik is om die onbekende konsentrasie van komponente in groente olies te bepaal met behulp van 'n bekende hoeveelheid standaard verbinding teenwoordig in die oplossing. Hierdie metodes het gelei tot die bepaling van die konsentrasies van die komponente gedurende vyf verskillende berging toestande wat ingesluit het: Blootgestel aan lig, in 'n donker kas, in 'n donker kas toegevou in tin foelie, bevries by  $-8\text{ }^{\circ}\text{C}$  en in 'n koelkas by  $5\text{ }^{\circ}\text{C}$ . Dit was bevind dat bepaling van die beste bergingstoestand vir elke olie moeilik is aangesien die individuele komponente verskillend geaffekteer word deur die verskeie berging toestande. Die beste bergings toestand oor die algemeen blyk egter om by  $5\text{ }^{\circ}\text{C}$  en  $-8\text{ }^{\circ}\text{C}$  te wees.

Sesamsaad, sonneblomsaad, papawersaad en pampoensaad sowel as sojaboontjie, mungboontjie, swartboontjie en pronkboontjie se olie, proteïen en koolhidraat komponente was geanaliseer met behulp van termogravimetriese analise (TGA) en  $^{13}\text{C}$  soliede toestand KMR spektroskopie. Dit was bevind dat die eerste afgeleide van die TGA data waardevolle inligting lewer oor die komponent inhoud van elk van die sade en bone. Hierdie is nog nie vantevore bevind nie. Vir die sade, was die integrasie van 'n area tussen  $270\text{--}480\text{ }^{\circ}\text{C}$  gelyk aan die som van die olie en proteïen inhoud en het goed vergelyk met die waardes verky deur algemene analitiese metodes. Vir die boontjies, was die integrasie van 'n area tussen  $180\text{--}590\text{ }^{\circ}\text{C}$  gelyk aan die som van die olie, proteïen en koolhidraat inhoud.

$^{13}\text{C}$  vaste staat KMR spektroskopie, insluitende SPE-MAS, CP-MAS en variëerbare kontak-tyd eksperimente, was gedoen en het waardevolle *inligting* gelewer omtrent die

solied-agtige en mobiel-agtige komponente. Hierdie sade en bone is tot ons kennis nog nie van te vore met die tegnieke ondersoek nie.  $^{13}\text{C}$  SPE-MAS NMR spektroskopie het aangedui dat daar 'n groter hoeveelheid mobiel-agtige komponente in sade as in bone teenwoordig is.  $^{13}\text{C}$  CP-MAS NMR spektroskopie het weer aangedui dat daar 'n groter hoeveelheid solied-agtige komponente in bone as in sade teenwoordig is. Hierdie gevolgtrekkings het goed vergelyk met die waarnemings verkry deur konvensionele analitiese metodes en TGA. Voorlopige studies op die komponente van sade en bone deur  $T_{1\rho}\text{H}$  eksperimente het tot 'n paar gevolgtrekkings gelei waarvan die mees interessantste was dat 'n twee-fase model vir die bepaling van  $T_{1\rho}\text{H}$  waardes beter resultate lewer as 'n een-fase model.

## ACKNOWLEDGEMENTS

I wish to thank my supervisor, Prof Klaus Koch, for his assistance during this project, especially for his sympathetic ear during troublesome times and his words of encouragement that always kept me going.

My co-supervisor, Jean McKenzie, I would like to thank for her guidance and availability even though she was not part of the university setup anymore.

A special thanks to my parents, Ean and Ilse Retief, and my husband, Simon Pollock, for their interest and enthusiasm in my project. Their eagerness to try and understand and willingness to listen to newly discovered ideas, aided me greatly in getting my mind around difficult problems. For that I thank them deeply.

## TABLE OF CONTENTS

ABBREVIATIONS.....	12
CONFERENCE PROCEEDINGS AND PUBLICATIONS.....	13
<b>CHAPTER 1: INTRODUCTION TO THE ANALYSIS OF VEGETABLE OILS.....</b>	<b>14</b>
1.1 Introduction to vegetable oils.....	15
1.2 Major and minor components of vegetable oils.....	18
1.2.1 Fatty acids.....	18
1.2.2 Major components: Triacylglycerols.....	21
1.2.3 Minor components of vegetable oils.....	22
1.3 Analysis of vegetable oils.....	23
1.4 Aging and storage of vegetable oils.....	27
1.5 <sup>31</sup> P NMR spectroscopy of olive oil.....	33
1.5.1 Assignment and quantification of <sup>31</sup> P NMR spectra of olive oil.....	33
1.5.2 Identification and authentication of olive oils based on geographical origin and cultivar variety differences by <sup>31</sup> P NMR spectroscopy.....	35
1.6 The investigation of six locally produced oils.....	37
1.6.1 Apricot kernel oil.....	38
1.6.2 Avocado pear oil.....	40
1.6.3 Macadamia nut oil.....	41
1.7 Aims of study.....	42
1.8 References.....	43
<b>CHAPTER 2: ANALYSIS OF VEGETABLE OILS BY <sup>31</sup>P NMR SPECTROSCOPY.....</b>	<b>49</b>
2.1 Introduction.....	50
2.2 Results and discussion.....	51
2.2.1 Assignment of the <sup>31</sup> P NMR spectra of the vegetable oils.....	51
2.2.2 Quantification of <sup>31</sup> P Nuclear Magnetic Resonance spectra.....	55
2.2.2.1 Approach 1.....	56
2.2.2.2 Approach 2.....	58
2.2.3 Limit of Detection and Limit of Quantification.....	61
2.2.3 Storage of vegetable oils.....	63

2.2.4.1	Apricot kernel oil .....	64
2.2.4.2	Macadamia nut oil.....	67
2.2.4.3	Avocado pear oil .....	71
2.2.4.4	Discussion of overall results .....	75
2.3	Conclusions.....	77
2.4	Experimental .....	78
2.4.1	Vegetable oils.....	78
2.4.2	Standard fatty acids.....	78
2.4.3	Storage of oils .....	78
2.4.4	Preparation of stock solution for P-derivitization .....	78
2.4.5	NMR Sample preparation.....	78
2.4.6	Collection of <sup>31</sup> P NMR spectra.....	78
2.5	References.....	79
 <b>CHAPTER 3: THERMOGRAVIMETRIC ANALYSIS OF SEEDS AND BEANS ..</b>		<b>80</b>
3.1	The importance of seeds and beans .....	81
3.1.1	Poppy seed .....	83
3.1.2	Pumpkin seed .....	83
3.1.3	Sesame seed .....	84
3.1.4	Sunflower seed.....	85
3.1.5	Soybean .....	86
3.1.6	Dry beans.....	87
3.1.6.1	Black bean .....	88
3.1.6.2	Kidney bean.....	88
3.1.6.3	Mungbean.....	88
3.2	Thermogravimetric analysis .....	90
3.2.1	Introduction to TGA .....	90
3.2.2	Thermogravimetric analysis as applied to seeds and beans: A literature review.....	94
3.3	Aims of study.....	97
3.4	Results and discussion.....	98
3.4.1	TGA data analysis .....	98
3.4.2	Moisture analysis .....	103
3.4.3	Fat, protein and carbohydrate analyses .....	108
3.4.3.1	Quantification of oil and protein contents of seeds.....	108

3.4.3.2	Quantification by analytical methods applied to beans .....	114
3.5	Conclusions.....	120
3.6	Experimental .....	121
3.6.1	Sample preparation .....	121
3.6.2	Collection of TGA data .....	121
3.6.3	Soxhlet extraction.....	122
3.6.4	Oven gravimetric method .....	122
3.6.5	Dumas-combustion .....	122
3.6.6	Clegg-Anthrone method .....	122
3.7	References.....	123

## **CHAPTER 4: EXPLORATIVE ANALYSIS OF SEEDS AND BEANS BY SOLID STATE**

<b><sup>13</sup>C NMR SPECTROSCOPY</b> .....	126	
4.1	Introduction to solid state NMR spectroscopy .....	127
4.2	Solid state NMR techniques applied to seeds and beans .....	129
4.2.1	Heteronuclear decoupling interactions .....	129
4.2.2	Magic angle spinning (MAS) .....	130
4.2.3	Cross-Polarization (CP).....	132
4.3	Solid state NMR of seeds and beans: literature review .....	133
4.4	Aims of this study .....	138
4.5	Results and discussion.....	139
4.5.1	Seeds.....	139
4.5.1.1	<sup>13</sup> C Single Pulse Excitation-Magic Angle Spinning experiments .....	139
4.5.1.2	<sup>13</sup> C Cross-Polarization-Magic Angle Spinning experiments .....	145
4.5.1.3	Comparison of TGA and Solid-state NMR results.....	149
4.5.2	Beans .....	150
4.5.2.1	<sup>13</sup> C Single Pulse Excitation-Magic Angle Spinning experiments .....	150
4.5.2.2	<sup>13</sup> C Cross-Polarization-Magic Angle Spinning experiments .....	153
4.5.2.3	Comparison of TGA and Solid-state NMR results.....	155
4.5.3	Variable Contact Time application.....	157
4.6	Conclusions.....	169
4.7	Experimental .....	170
4.7.1	Sample preparation for Solid State NMR spectroscopy .....	170
4.7.2	Collection of Solid State <sup>13</sup> C NMR spectra .....	170
4.7.3	Variable Contact Time experiment (VCT).....	171

4.8	References.....	171
-----	-----------------	-----

<b>CHAPTER 5: FINAL CONCLUSIONS</b> .....	174
---	-----

<b>ADDENDUM: PUBLISHED ARTICLES</b> .....	178
---	-----

- Retief, L., Mckenzie J.M., and Koch K.R., A novel approach to the rapid assignment of  $^{13}\text{C}$  NMR spectra of major components of vegetable oils such as avocado, mango kernel and macadamia nut oils, *Magn. Reson. Chem.*, **2009**, 47, 771-781.
- Retief, L., Mckenzie J.M., and Koch K.R., in "Magnetic Resonance in Food Science: Challenges in a Changing World", Identification and quantification of major triacylglycerols in selected South African vegetable oils by  $^{13}\text{C}$  NMR spectroscopy, RSC publishing, London, UK, **2009**, 151-157.

## ABBREVIATIONS

TG	triacylglycerol
DG	diacylglycerol
FFA	free fatty acid
FA	fatty acid
NMR	nuclear magnetic resonance spectroscopy
TGA	thermogravimetric analysis
DTG	first derivative of TGA data
MAS	magic angle spinning
SPE	single pulse excitation
CP	cross polarization
SES	sesame seed
PUM	pumpkin seed
POP	poppy seed
SUN	sunflower seed
SOY	soybean
MUN	mungbean
KID	kidney bean
BB	black bean
P-reagent	2-chloro-4,4,5,5-tetramethyldioxaphospholane

## CONFERENCE PROCEEDINGS

The following posters were presented on results from this project:

1. Retief, L., McKenzie, J.M., and Koch, K.R., *TGA as a Quantitative Tool for the Determination of Seed and Bean Contents*, 39<sup>th</sup> SACI National Convention, Stellenbosch, South Africa, 30 November – 5 December, 2008.
2. Retief, L., McKenzie, J.M., and Koch, K.R., *<sup>31</sup>P NMR Spectroscopy of the Minor Components Present in South African Vegetable Oils*, 39<sup>th</sup> SACI National Convention, Stellenbosch, South Africa, 30 November – 5 December, 2008.

The following poster is being prepared on results from this project:

1. Retief, L., McKenzie, J.M., and Koch, K.R., *<sup>13</sup>C Solid State NMR investigation on whole seeds and beans*, Die Suid-Afrikaanse Akademie vir Wetenskap en Kuns, Studentesimposium, 29 – 30 October, Bloemfontein, South Africa, 2009.

The following oral presentation is being prepared on results from this project:

1. Retief, L., McKenzie, J.M., and Koch, K.R., *Investigation into seed and bean components using TGA and <sup>13</sup>C solid state NMR spectroscopy*, Die Suid-Afrikaanse Akademie vir Wetenskap en Kuns, Studentesimposium, 29 – 30 October, Bloemfontein, South Africa, 2009.

The following publications are being prepared containing results from this project:

1. Publication to be submitted to Magnetic Resonance in Chemistry in 2010: Retief, L., McKenzie, J.M., and Koch, K.R., *Assignment of <sup>31</sup>P NMR spectra of apricot kernel, avocado pear and macadamia nut oils and investigation into storage conditions*.
2. Publication to be submitted to Thermochemica Acta in 2009: Retief, L., McKenzie, J.M., and Koch, K.R., *TGA as a Quantitative Tool for the Determination of Seed and Bean Contents*.
3. Publication to be submitted to Modern Magnetic Resonance in 2010: Retief, L., McKenzie, J.M., and Koch, K.R., *<sup>13</sup>C Solid State NMR investigation on whole seeds and beans*.

# CHAPTER 1: INTRODUCTION TO THE ANALYSIS OF VEGETABLE OILS

*"A scientist in his laboratory is not a mere technician: he is also a child confronting natural phenomena that impress him as though they were fairy tales."*

Marie Skłodowska Curie

November, 1867 – July, 1934



Picture obtained from [http://en.wikipedia.org/wiki/Marie\\_Curie](http://en.wikipedia.org/wiki/Marie_Curie)

## 1.1 INTRODUCTION TO VEGETABLE OILS

Vegetable oils find wide use in pharmaceutical, industrial, nutritional and cosmetic products. These include products such as cooking oils, margarine, salad dressings, food coatings, paints, plasticizers, lubricants, hydraulic fluids, glycerol, synthetic fibres, lecithin, printing inks, medicines, face masks, hand creams, shower gels, soaps, detergents<sup>1,2</sup> and many more too numerous to mention here. “Vegetable” is the term given to any oil from a plant source and so this will include oils such as olive oil, sunflower oil, and many others<sup>1,2</sup>. The focus of this study lies mainly in cold-pressed, i.e. unadulterated, vegetable oils that can be used as food in view of their nutritional value. Figure 1.1 presents data obtained from the Food and Agriculture Organization (FAO) for 2007 indicating the percentage of oil crops produced per continent (from a total amount of 144 805 532 tonnes produced), while Figure 1.2 illustrates the percentage production of each country within Africa.

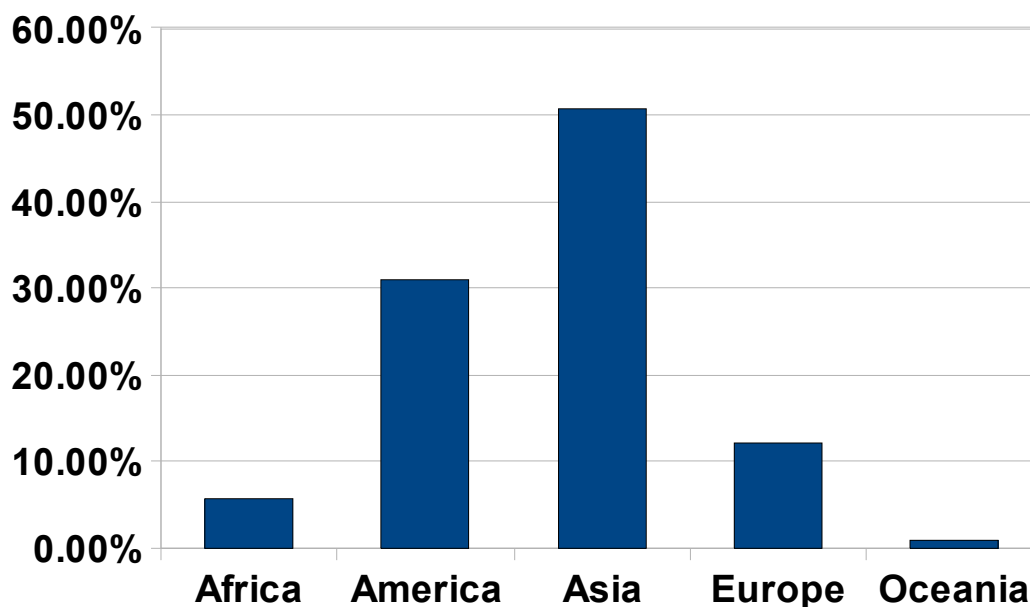


**Figure 1.1:** Percentage oil crop production per continent, adapted from data provided by FAO<sup>3</sup>.

As can be seen from Figure 1.1, Africa's production of oil crops is only 5.64 % of the world's production, with Asia and “the Americas” leading at around 51 % and 31 % respectively. Within Africa (Figure 1.2) Nigeria has the largest production of around 41 %, while all the other countries produce below 6 % each, with South Africa producing only 2.98 % of the oil crops in Africa during 2007. Although South Africa's production of vegetable oils in the world view is low it is still an important commodity within the country and production of oils such as olive oil is certainly on the rise within South Africa.

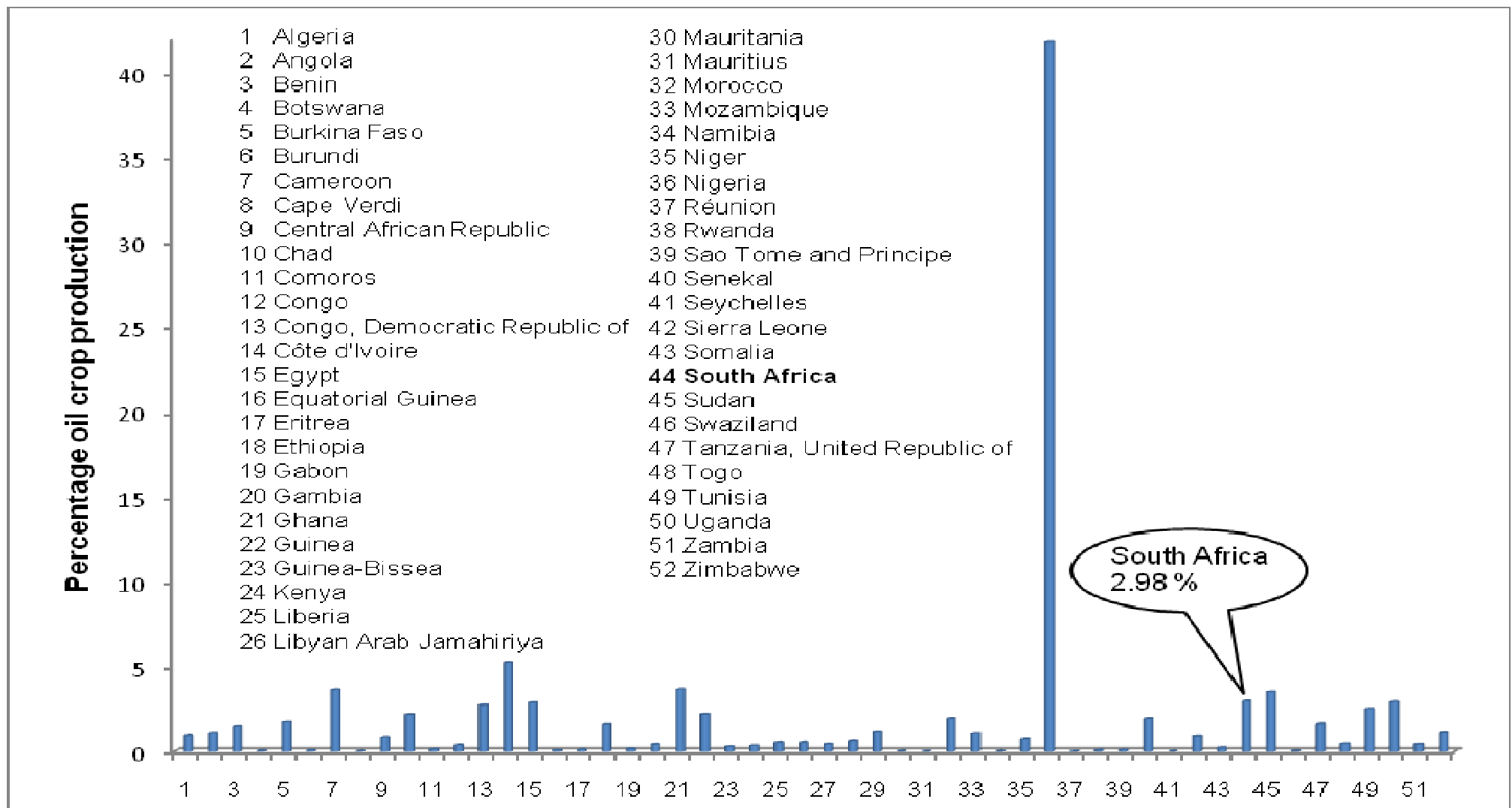


Figure 1.2: Percentage oil crop production within Africa, adapted from data provided by FAO<sup>3</sup>.

Vegetable oils are complex mixtures of which triacylglycerols (TGs) are the major components while the minor components comprise of among others polyphenols, aldehydes, sterols and a variety of volatile compounds<sup>2,4</sup>. The major components are of importance for their nutritional value and also for differentiating between different types of oil. Certain minor components such as polyphenols, vitamins and other antioxidants are understood to be responsible for other health benefits associated with the use of vegetable oils such as their anti-oxidant properties<sup>5,6,7,8</sup>. Several studies have been carried out on the health aspects of vegetable oils, especially olive oil<sup>6-9</sup>. Those carried out on olive oil are discussed briefly in the next few paragraphs as these studies illustrate the important role certain vegetable oils, such as olive oil, play in a healthy diet.

Studies were carried out by Lipworth *et al.* to determine if the incorporation of olive oil instead of animal fats in a diet, reduces the occurrence of certain illnesses associated with the oxidation of fats<sup>9</sup>. This study was concerned with the fact that several cancers, including breast, colon, ovarian, endometrial, prostate, pancreas and oesophageal cancer have been associated with oxidised animal fats. Data confirmed that olive oil does not have cancer promoting properties as some of the other animal fats appear to. These authors suggested that olive oil could even be a promising dietary tool in the prevention of certain types of cancers.

Antioxidants are important compounds that play a protective role in human health, contributing to a decrease in the occurrence of diseases like cancer, atherosclerosis, bowel syndromes etc<sup>6,7,8,9</sup>. Antioxidants such as vitamin E and polyphenols are found as minor components in olive oil<sup>6,7,8,9</sup>. Low-density lipoproteins (LDLs) which are rich in cholesterol and cholesteryl esters can be potentially harmful to the human health and cause diseases such as atherosclerosis. Such diseases have been found to be linked to the oxidatively modified forms of LDL. Antioxidants such as polyphenols have been found to inhibit or decrease the extent of such oxidation of LDLs<sup>6</sup>. Visioli *et al.* reported that the occurrence of coronary heart disease and certain cancers were lower in the Mediterranean areas<sup>6</sup>. This led to their hypothesis that since olive oil, among other foods, is consumed in such large quantities in these regions, this could play an important part in a "healthy diet". Investigation into the biological activity of hydroxytyrosol, oleuropein, luteolin and luteolin aglycon components, which are all found in olive oil, indicated that these compounds had protective properties against the oxidation of LDLs. These authors concluded that substances with high phenol content such as olive oil appear to be

beneficial to any human diet. Manna *et al.* used rats to also investigate this antioxidant property of phenols in olive oil<sup>7</sup>, finding that rats that were fed olive oil as part of their daily diet had a higher content of antioxidants in their serum and therefore increased resistance to oxidation of LDLs. On the other hand, rats that were fed a synthetic diet containing the same fatty acids as olive oil as well as vitamin E did not produce the same results. This led Manna *et al.* to conclude that the minor components present in olive oil such as the polyphenols are important to the human diet. Giovanni *et al.* also carried out a study on the human colon to determine the antioxidative effect of the phenol tyrosol<sup>8</sup>. They found that a diet rich in biophenols, such as tyrosol that is found in olive oil, can lead to the lowering of the risk of inflammatory bowel disease as well as cardiovascular diseases.

Therefore it can be seen that not only are vegetable oils of great value from an economic point of view as shown by the previously mentioned market studies, but these oils also have important health implications. As there is growing interest in the production of these oils in South Africa it is thus relevant to continue characterising these by modern instrumental methods. The better we understand these mixtures, the more effectively they can be applied to products that are of use to the community. In addition we have found that although the major and minor components of olive oil have been extensively studied there are many other vegetable oils produced in South Africa which have only been examined superficially and have not been extensively studied. The focus of this study is therefore specifically to determine quantitatively the major and minor components present in these vegetable oils.

## **1.2 MAJOR AND MINOR COMPONENTS OF VEGETABLE OILS**

The major components present in vegetable oils are triacylglycerols consisting of fatty acids bound to a glycerol backbone. Several of the minor components of vegetable oils such as 1,2 diacylglycerols (1,2 DG) and 1,3 diacylglycerols (1,3 DG) as well as free fatty acids (FFA) are also found in oils.

### **1.2.1 Fatty acids**

Fatty acids differ from one another in the number of carbon atoms in the hydrocarbon chain, the degree of unsaturation (the number of C=C double bonds), and the relative positions of these double bonds in the various chains. There are a number of different opinions about what can be considered the average length of fatty acids, but overall fatty acid chains are considered to have a length of between 12 and 20 carbons. The degree of

saturation of fatty acids plays an important part in their definition. Fatty acids without any C=C double bonds are referred to as *saturated*, while those with at least one double bond are called *unsaturated*. Unsaturated fatty acids can be grouped further into *monounsaturated* (only one double bond is present) and *polyunsaturated* (with two or more double bonds). If unsaturation is present in these compounds, they are found to have a *cis* conformation at the double bond if from a natural source, and the double bonds are usually separated by a methylene group. Fatty acids with *trans* double bonds (called *trans* fatty acids) have usually undergone some form of chemical modification and this is currently a great concern, since *trans* fatty acids can possibly cause diseases such as coronary heart disease, allergies, cancer, and diabetes<sup>10</sup>. Generally for fatty acids in vegetable oils, the first double bond is found between carbons 9 and 10, the second double bond between carbons 12 and 13 and the third double bond between carbons 15 and 16, although exceptions to these double bond positions do occur. Exceptions to these commonly found fatty acids described above, are those with an odd number of carbon atoms, branched or cyclic chains, those with a double bond *trans* conformation and conjugated unsaturation<sup>4,11,12,13,14</sup>.

Table 1.1 shows some common fatty acids found in vegetable oils with their IUPAC nomenclature. However as their trivial names are mostly used when referring to these compounds, these are also shown. According to IUPAC nomenclature the carboxyl carbon is labelled as C1 and thereafter the remaining carbon atoms are sequentially numbered (Figure 1.3). There is a shorthand notation for the description of fatty acids which makes use of two numbers separated by a colon. For instance C18:1  $\Delta^9$  can be used to represent oleic acid. The first number represents the number of carbons in the unbranched hydrocarbon chain; the second number gives the number of double bonds present in the chain; while the symbol  $\Delta^n$  refers to the starting position(s) of the double bonds. In the case of oleic acid the double bond is between C9 and C10, hence  $\Delta^9$ . In polyunsaturated fatty acids in which there are more than one double bond, the double bond positions are separated by a comma, for instance: C18:2  $\Delta^{9,12}$  or C18:2 n9,12. This shorthand notation can be used to represent linoleic acid which has two double bonds, one between C9 and C10 and the other between C12 and C13.

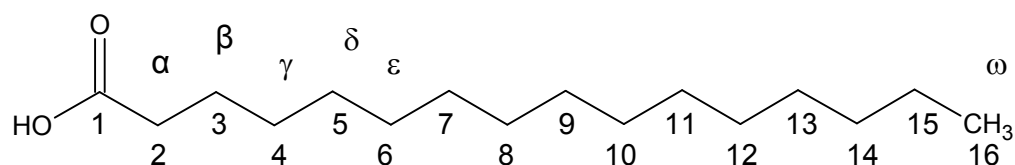


**Figure 1.3:** Structure and numbering of a basic saturated fatty acid.

Another common practice is the use of Greek letters to identify carbon atoms along the fatty acid chain<sup>4,10,13</sup>. The carbon directly adjacent to the carboxyl carbon is designated by the Greek letter  $\alpha$ . Accordingly the following carbons are sequentially numbered  $\beta$ ,  $\gamma$ ,  $\delta$ ,  $\epsilon$ , etc. (Figure 1.3). As illustrated in Figure 1.3, the last carbon in the chain is numbered as  $\omega$  and often the position of the first double bond from the hydrocarbon end (the  $\omega$  carbon end) is referred to as for instance  $\omega 6$ . For this example this means that the first double bond occurs at the sixth carbon atom from the end carbon numbered  $\omega$ , giving the fatty acid the common name of a  $\omega 6$  fatty acid<sup>4,11,14</sup>. Understanding the various methods of naming, whether systematic or not, is required when undertaking research involving fatty acids and their derivatives as often vendors of nutritional products will use whichever jargon serves their marketing needs best.

**Table 1.1:** Some common fatty acids with their IUPAC and trivial names.

Number of carbons	Number of double bonds	IUPAC name	Trivial name
12	0	Dodecanoic	Lauric
14	0	Tetradecoanoic	Myristic
16	0	Hexadecanoic	Palmitic
16	1	<i>cis</i> - $\Delta^9$ -Hexadecenoic	Palmitoleic
18	0	Octadecanoic	Stearic
18	1	<i>cis</i> - $\Delta^9$ -Octadecenoic	Oleic
18	1	<i>cis</i> - $\Delta^{11}$ -Octadecenoic	Vaccenic
18	2	<i>cis</i> - $\Delta^{9,12}$ -Octadecadienoic	Linoleic
18	3	<i>cis</i> - $\Delta^{9,12,15}$ -	Linolenic

20	0	Octadecatrienoic	
22	0	Eicosanoic	Arachidic
24	0	Docosanoic	Behenic
		Tetracosanoic	Lignoceric

### 1.2.2 Major components: Triacylglycerols

Triacylglycerols are the major constituents of vegetable oils. They are non-polar, water insoluble substances composed of three fatty acid residues esterified to a glycerol backbone (Figure 1.4) hence their hydrophobicity<sup>2,4,5</sup>.

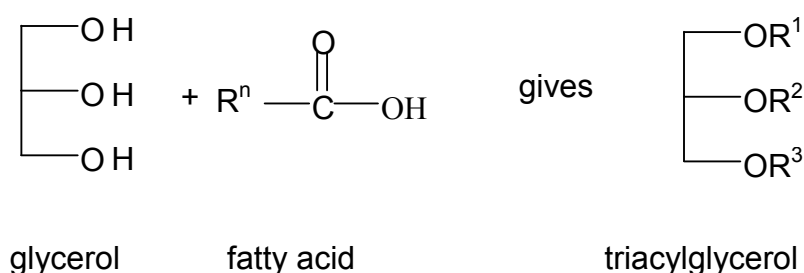


**Figure 1.4:** The structure and constituents of a triacylglycerol, where  $\text{R}^n$  represents a hydrocarbon chain and  $\text{R}^{1,2,3}$  represents three possibly different hydrocarbon chains.

In the case of triolein, all three of the fatty acid residues are olein moieties and hence identical. However in vegetable oils, natural occurring TGs are not only mixtures of different TGs but also TGs where all three fatty acid residue chains within the TG is different as illustrated in Figure 1.5<sup>2,4,5</sup>.

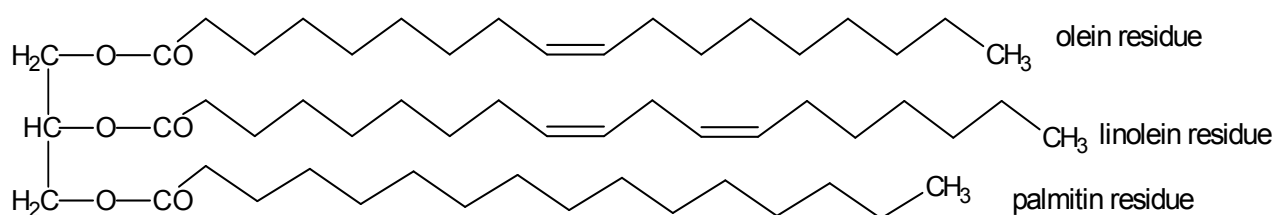


**Figure 1.5:** Structure indicating a hypothetical positional distribution of different fatty acids on the glycerol backbone of a natural occurring TG.

The fatty acids chains on the glycerol backbone can be denoted in two ways. The first is by identifying the two outer chains as  $\alpha$  and the inner chain as  $\beta$ . The other

method is by strictly numbered (sn) identification whereby each chain is identified as sn 1', sn 2' or sn 3'. Refer to Figure 1.6 for the illustration of these numbering schemes<sup>15,16</sup>.

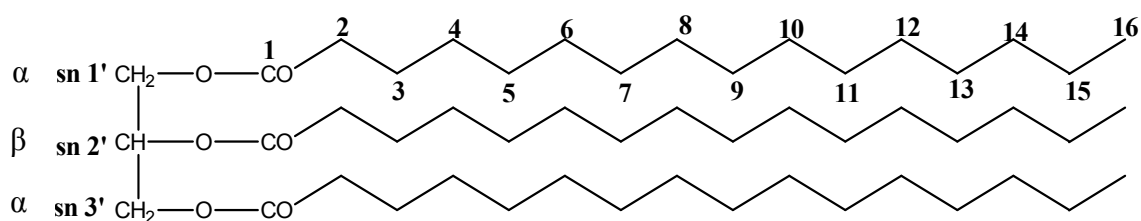


**Figure 1.6:** Numbering scheme for tripalmitin.

Triacylglycerides were previously referred to as triglycerides although both names are still in use. Saturation and chain length plays an important part in the form that TGs are found. For instance those that contain only saturated, long-chain fatty acid groups are solids while unsaturated or short chain fatty acid groups yield liquids<sup>2,4,5</sup>. Note that in this study the strictly numbered notation is used.

### 1.2.3 Minor components of vegetable oils

Several minor components are present in vegetable oils of which many of these components are associated with the colour and distinctive taste of different types of oils as well as their anti-oxidant properties<sup>2,17</sup>. Monoacylglycerols (MGs) and diacylglycerols (DGs) are such components, but if found in significant quantities in a vegetable oil, these often give an indication of adulteration or aging of the oil. This is due to the fact that upon hydrolysis of TGs, the mono- and diacylglycerides form. This hydrolysis occurs naturally in two ways, either enzymatically in the vegetable or fruit, or during storage due to the presence of water and long term exposure to oxygen in air. Formation of MGs and DGs also leads to the presence of free fatty acids (FFA), which are other minor components found in vegetable oils. The hydrolysis can however also occur by the deliberate chemical modification of the vegetable oil content which is referred to as “adulteration” in this context<sup>14,18</sup>. Figure 1.7 illustrates the structures of some of these minor components mentioned. Other minor components of vegetable oils include:<sup>2,17</sup>

- pigments, including chlorophyll and caretonoids
- alcohols
- sterols, including free sterols and sterol esters

- tocols, including tocopherols, tocosterols and tocotrienols
- phospholipids
- squalene
- hydrocarbons, including alkanes, alkenes, polycyclic aromatic hydrocarbons and carotenes

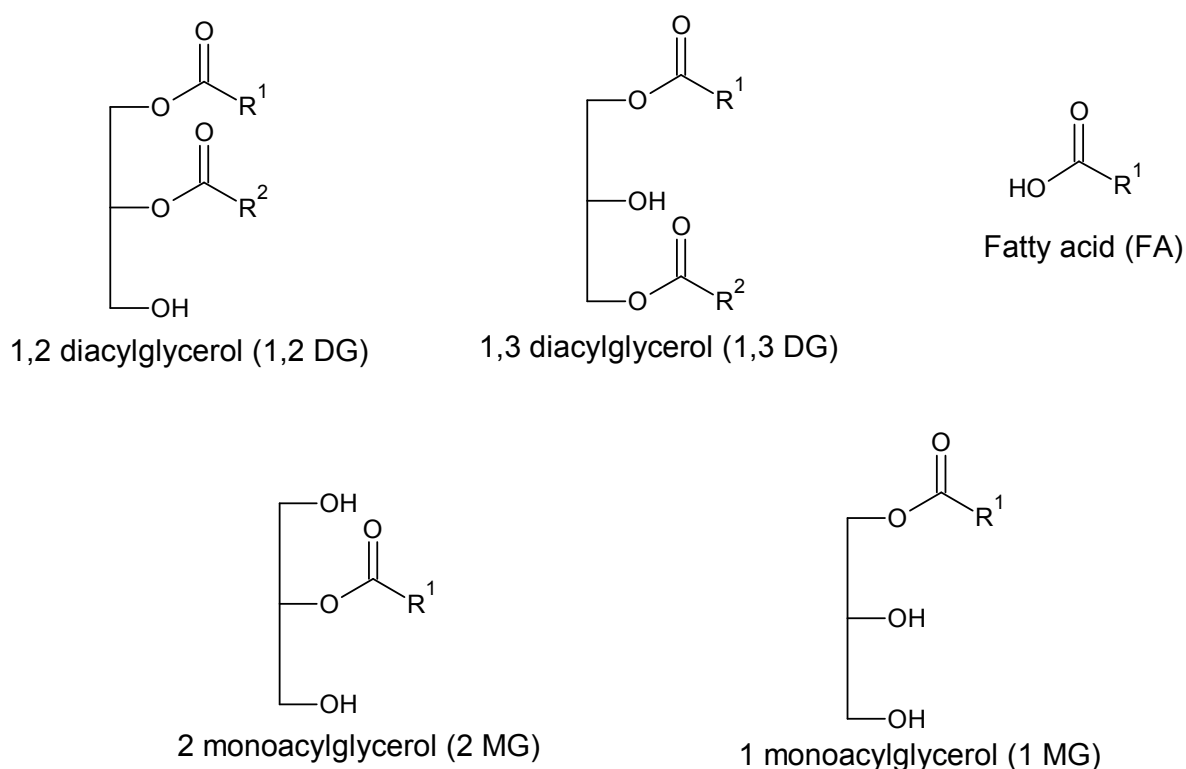


**Figure 1.7:** General structures of diacyl-, monoacylglycerols and fatty acid compounds.

### 1.3 ANALYSIS OF VEGETABLE OILS

A number of analytical techniques have been used for the identification and classification of vegetable oils. Such techniques are used to determine unsaturation, melting point, and acidity, among other things. Titrations have commonly been used for determining average unsaturation and FFA content though more recently the most popular methods for the analysis of vegetable oils are spectroscopic and chromatographic techniques and include Gas-Liquid Chromatography (GC), High Pressure Liquid Chromatography (HPLC), Thin Layer Chromatography (TLC), Mass Spectrometry (MS), Infra-red (IR) spectroscopy (including Near-Infrared and Fourier

Transform IR) and Ultra Violet-Visible (UV-Vis) spectroscopy. Each of these techniques yields information on the qualitative as well as quantitative properties of vegetable oils. Table 1.2 gives a summary of the techniques used for the measurement of vegetable oil properties.

**Table 1.2:** Chromatographic and other analytical techniques for the measurement of chemical properties of vegetable oils<sup>2,19</sup>.

Technique	Detection of property of vegetable oil
GC / GC-MS	Quantitative and qualitative determination of fatty acid composition Determination of tocopherol content Determination of aliphatic alcohol content Determination of sterol composition and content
Head space GC	Determination of volatile halogenated solvent content
HPLC	Determination of tocopherol content
Adsorption spectroscopy	Quantitative determination of Vitamin A
UV adsorption	Identification of fats and fatty acids with conjugated double bonds Detects state of oxidation and changes brought about by technological processes
Emission spectroscopy	Detection of metals in ash of oils
Fluorescence spectroscopy	Detection of adulterants in oil
FTIR spectroscopy	Measurement of <i>cis-trans</i> ratios, iodine values, saponification number, free acid content, peroxide value, anisidine value
Titrations	Determination of FFA content, iodine and peroxide values
TLC	Determination of presence of erythrodiol and uvaol
TLC/GC	Determination of the saturated fatty acids in position 2 of the TG
GC with ECD	Determination of volatile halogenated solvents of olive oil

For the purpose of this dissertation the use of Nuclear Magnetic Resonance (NMR) spectroscopy was of main interest, which is a powerful and increasingly popular method for the analysis of vegetable oils. In general it is ideal to analyze pure compounds by NMR spectroscopy and it is not always the first technique of choice for dealing with mixtures where separation techniques such as GC and HPLC usually

find more use. Although the qualitative and quantitative analysis of vegetable oils by NMR spectroscopy poses some challenges, in recent years the availability of high resolution and new multidimensional NMR techniques has made the analysis of complex mixtures of molecules viable. This is particularly evident in the application of NMR spectroscopy to the analysis of biological fluids in the new field of metabolomics<sup>20</sup>. Thus the application of high resolution NMR for the qualitative and quantitative analysis of vegetable oils is clearly appropriate. Olive oil has been the most thoroughly studied vegetable oil by NMR spectroscopy and the work carried out has indeed demonstrated the versatility of this technique when applied to the analysis of vegetable oils<sup>21-24</sup>.

A significant amount of research has been carried out on the assignment and quantification of minor compounds present in olive oils that can be detected by NMR spectroscopy using 1D and 2D techniques<sup>21-27</sup>. Such compounds include diacylglycerols (DGs), monoacylglycerols (MGs), phenolic compounds, aldehydes, sterols, *etc.* For the identification and analysis of minor components in vegetable oils, <sup>1</sup>H NMR spectroscopy has proven to be very useful. <sup>1</sup>H and <sup>13</sup>C NMR studies on some of the minor components by various groups led to the discovery of new phenolic compounds present in olive oil, including (3,4-dihydroxyphenyl)ethanol derivatives and two (*p*-hydroxyphenyl)ethanol derivatives<sup>25</sup>, pineresinol and 1-acetoxypineresinol<sup>26</sup>, and 4-(acetoxylethyl)-1, 2-dihydroxybenzene<sup>27</sup>. Once these minor components have been detected and identified by <sup>1</sup>H NMR spectroscopy, the technique can be further used for the identification of regional and cultivar differences of vegetable oils<sup>28-40</sup>. Several studies have proven that <sup>1</sup>H and <sup>13</sup>C NMR spectroscopy has great potential to identify and authenticate virgin olive oils by geographical origin and variety<sup>28-40</sup>. A <sup>1</sup>H NMR study by Sachi *et al.* used the minor components of 55 different varieties of extra virgin olive oil samples from four Italian regions as tools to distinguish between regions<sup>28</sup>. <sup>1</sup>H NMR spectroscopy combined with multivariate statistical analysis was used by Sacco *et al.* on the phenolic extracts of 28 Italian extra virgin olive oils of different cultivars and geographic origin<sup>32</sup>. The analytical measurements such as GC give information on the fatty acid composition of the oils and can be used in the discrimination of olive oil variety, while the NMR data classified the oils according to geographical origin. Another use of NMR spectroscopy as applied to the determination of geographical origin is in determining

the year of production of olive oils<sup>36</sup>. In one such study Rezzi *et al.* used <sup>1</sup>H NMR spectroscopy and multivariate analysis on olive oils from various Mediterranean areas<sup>36</sup>. They found that <sup>1</sup>H NMR could successfully be applied for determination of year of production and that chemometric techniques such as multiple linear regressions or generalized pair-wise correlation did not yield better results.

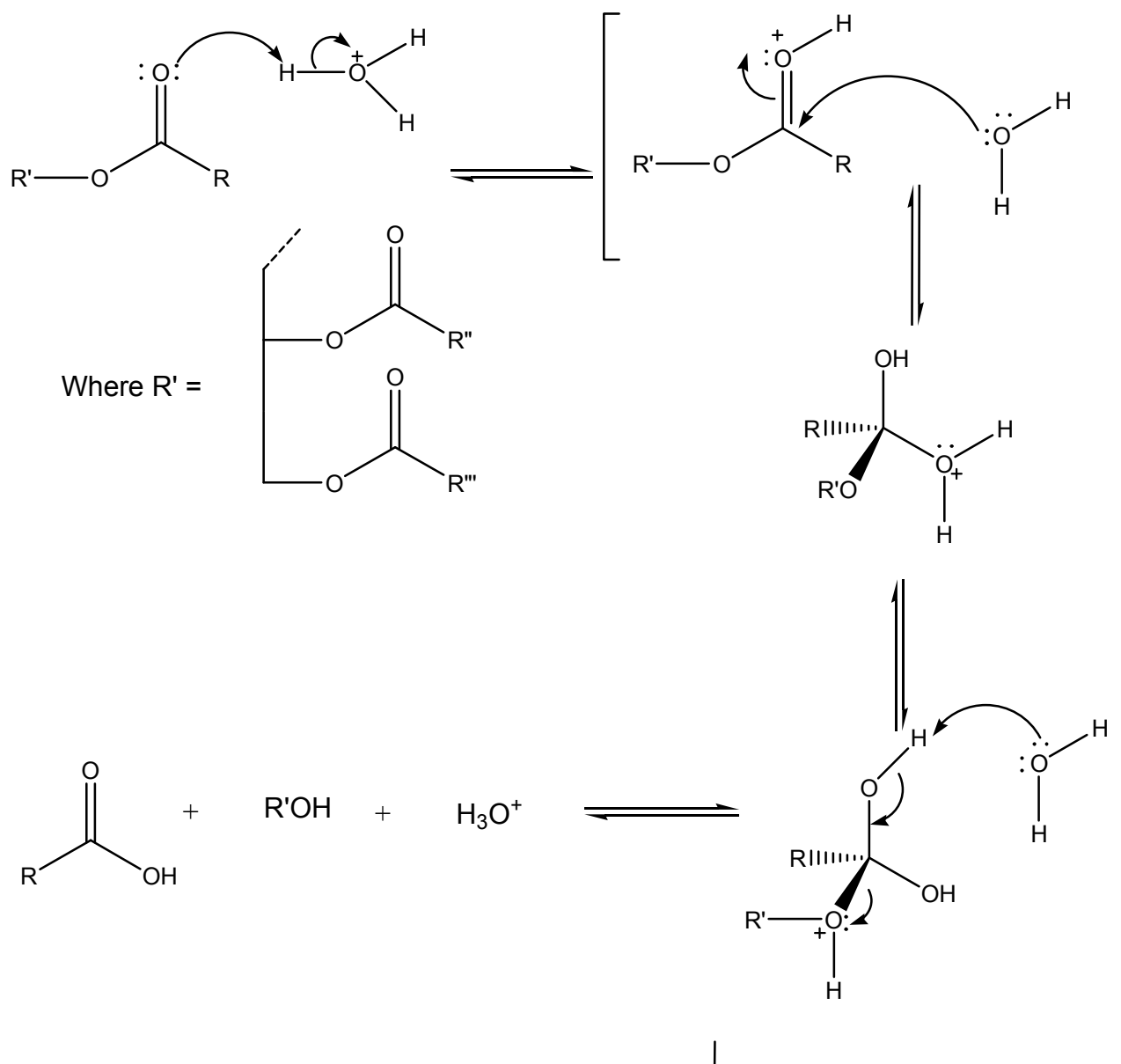
<sup>1</sup>H NMR spectroscopy has also aided in the detection of adulteration. As mentioned already the higher grade olive oil such as virgin and extra virgin olive oil has a high commercial value. As a result adulteration of these oils to try increase the quantity of the oil sold is a concern. This occurs by the addition of other lower quality and value vegetable oils to the vegetable oil of interest, such as sunflower, hazelnut and inferior olive oil. Thus detection of adulteration of olive oils has been studied with a number of analytical techniques including <sup>1</sup>H and <sup>13</sup>C NMR spectroscopy. <sup>1</sup>H NMR spectroscopy has shown that the presence some of these “contaminator” oils can be detected. Moreover properties such as oil’s acidity, iodine value, fatty acid composition and the ratio of 1,2 DG to total DG content can be used to detect adulteration of olive oil with seed oils. In one such study the presence of hazelnut, corn, sunflower and soybean oil could be detected with the use of <sup>1</sup>H NMR and <sup>31</sup>P NMR spectroscopy<sup>41</sup>. Diego *et al.* were successful in developing a method to detect the adulteration of olive oil with low concentrations of hazelnut oil using <sup>1</sup>H and <sup>13</sup>C NMR spectroscopy and the limit of detection for hazelnut oil contamination was found to be about 8 %<sup>42</sup>.

It is therefore evident that <sup>1</sup>H NMR spectroscopy is a valuable tool for the analysis of minor components in vegetable oils. However due to the many substances present in the vegetable oil that are of low concentration, the determination and identification of minor components by <sup>1</sup>H NMR spectroscopy is not simple. In essence using only <sup>1</sup>H NMR spectroscopy one can be at risk of detecting too many substances in a vegetable oil. Hence for studies concerned with the storage of oils, only minor components relevant to the aging of vegetable oils are of interest and therefore a different NMR technique has been used in the literature. A literature survey has shown that <sup>31</sup>P NMR spectroscopy may be a valuable technique for the identification and quantification of certain minor components, relevant to the aging of vegetable oils. These include 1,2 DGs; 1,3 DGs and FFAs (refer to Figure 1.9 in Chapter 1). These minor components were first detected by Spyros *et al.* in olive oil by <sup>31</sup>P NMR

spectroscopy and upon assignment, quantification of these signals aided in the detection of aging and storage of olive oils<sup>14,18,43-54</sup>. Since these studies have only been done on olive oil to our knowledge, and since in general vegetable oil TGs break down into DGs upon aging (refer to Section 1.4 and Scheme 1.1), it may be expected that vegetable oils such as macadamia nut, avocado pear and apricot kernel oils contain the same breakdown components as present in olive oil upon aging. Therefore a review of the literature which deals with the application of <sup>31</sup>P NMR spectroscopy to the analysis of olive oil is discussed in the next section. It should also be noted at this point that olive oil is used throughout this dissertation as a “reference” because of the significant amount of research that has been carried out on this oil by comparison to other vegetable oils, some of which have not been examined by NMR spectroscopy to our knowledge.

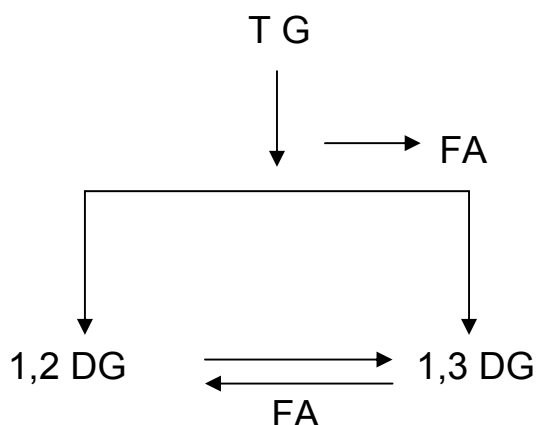
#### **1.4 AGING AND STORAGE OF VEGETABLE OILS**

As mentioned in section 1.2.3, upon storage the main components of vegetable oils, namely TGs, break down into DGs (refer to Scheme 1.1) releasing FFAs. This breakdown (hydrolysis) of TGs during storage occurs due to the presence of water and exposure to light. For the purpose of this study only the reaction mechanism for the hydrolysis of TGs due to the presence of water is discussed, since all oils were sealed upon storage and stored under nitrogen leading to oxidation being ruled out as a mechanism. The hydrolysis mechanism of interest is illustrated in Scheme 1.1<sup>14,18,43</sup>. The hydrolysis is acid-catalysed by the FFAs present in the vegetable oil. The FFAs provides a proton with which a water molecule forms a positively charged hydronium ion. The TG, in the presence of this hydronium ion, undergoes protonation of a carbonyl group of one of the chains on the glycerol backbone and nucleophilic attack occurs to yield a tetrahedral intermediate. The OR' group is converted into a good leaving group by the transfer of a proton to water and elimination of the alcohol group occurs, consequently leading to the formation of a DG and a FFA<sup>44</sup>.



**Scheme 1.1:** Acid-catalysed hydrolysis of the TGs present in vegetable oils.

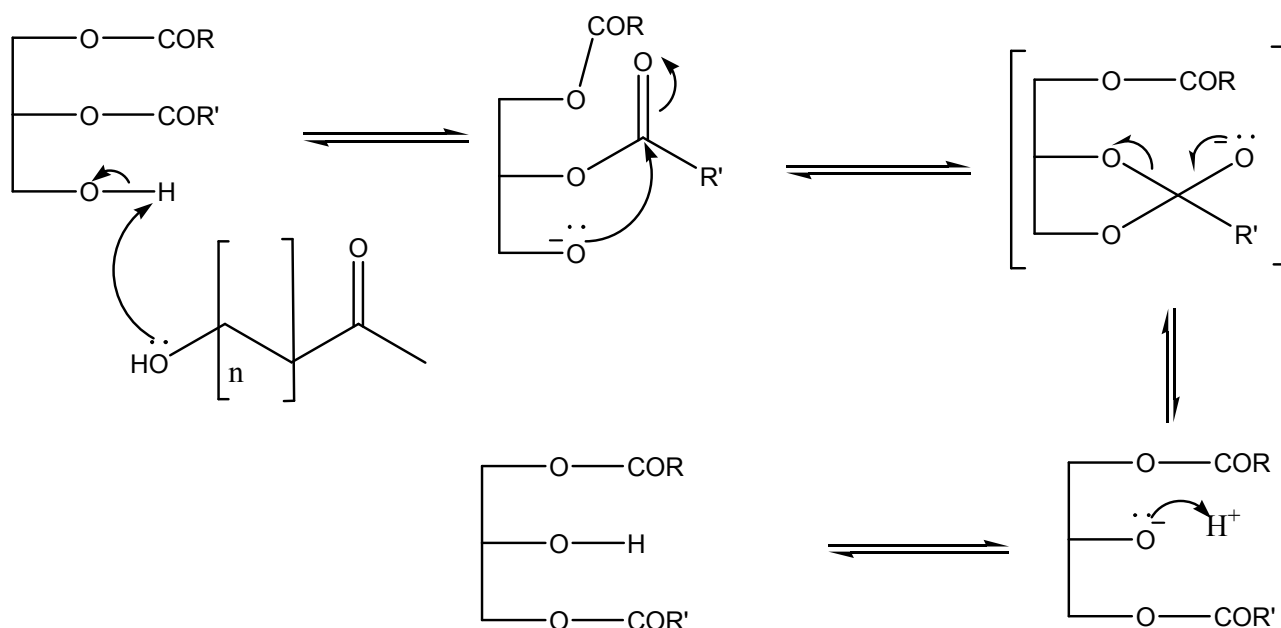
The DGs formed can be in two forms, namely either 1,2 DGs or 1,3 DGs. Upon hydrolysis of the TGs, the released fatty acids behave as catalysts in the isomerisation reaction between the 1,2 and 1,3 DGs (as illustrated in Scheme 1.2).



**Scheme 1.2:** Figure illustrating the breakdown of TGs into DGs and FFAs and the FFA catalysed isomerisation between 1,2 DGs and 1,3 DGs.

The isomerisation between 1,2 DGs and 1,3 DGs occurs via acyl transfer (also referred to as acyl migration) within the molecule, hence an intramolecular reaction, with the formation of an intermediate. This is illustrated in Scheme 1.3 for isomerisation of 1,2 DG to 1,3 DG<sup>27</sup>. The FFA acts as catalyst and abstracts a hydrogen atom from the alcohol group in the DG, yielding an ester enolate ion. Nucleophilic attack occurs within the same molecule between the attacking enolate and carbonyl group giving an unstable intramolecular intermediate. Rearrangement within the molecule occurs and with the uptake of a hydrogen, the isomerised DG is obtained<sup>44,45,46</sup>.

The formation of 1,2 DGs has twice as much chance of taking place as that of 1,3 DGs. This is due to the 1,2 DGs being able to have an OH-group present in the sn 3' position on the glycerol backbone as well as the sn 1' position (obviously a 2,3 DG is equivalent to a 1,2 DG) as opposed to the 1,3 DG of which the OH-group can only be present in the sn 2' position (refer to Figure 1.7).



**Scheme 1.3:** Free fatty acid-catalysed of the isomerisation of 1,2 DG to 1,3 DG present in vegetable oils.

Several studies have been done on the oxidative stability of vegetable oils (aging) with respect to storage conditions. Guillen *et al.* investigated the aging of sunflower oils over ten years which were stored at room temperature and closed off to air<sup>47</sup>. The oils were analysed by FTIR and <sup>1</sup>H-NMR spectroscopy not only to follow the oxidation process but also to investigate primary and secondary oxidation products that formed. During early oxidation stages, <sup>1</sup>H-NMR spectroscopy indicated the presence of hydroperoxides with *cis*, *trans* conjugated double bonds while during advanced stages of aging, hydroperoxides with *trans*, *trans* conjugated double bonds were detected, the latter was however smaller in concentration. The researchers also showed for the first time that hydroxy derivatives with the *cis*, *trans* double bond formation were present and among the primary oxidation components. In the case of alkenals present, it was found that during early oxidation, the concentration of 4-hydroxy-*trans*-2-alkenals were higher than that of 4-hydroperoxy-*trans*-2-alkenals<sup>47</sup>. In another study researchers used corn oil samples stored at room temperature in the dark and closed off to air. The oil samples were stored for different lengths of time, namely 12-103 months, with different air-oil volume ratios and/or air-oil contact surfaces, between the same brand of oil, the same brand of different batches, and oils of different brands. <sup>1</sup>H-NMR spectroscopy was once again used to look at the oxidation and it was found that the degradation of linoleic acyl groups was the most

dominant. During early oxidation stages hydroperoxides and (cis,trans)-conjugated dienic systems were detected with the hydroperoxides higher in concentration than the latter. During intermediate and advanced stages, additional compounds to those found in the early stages, were detected, and included hydroxyl derivatives supporting the (Z,E)-conjugated dienic systems and hydroxyl derivatives with (E,E)-conjugated dienic systems. During advanced stages, aldehydes were found to be present and identified as alkanals, (E)-2-alkenals, (E,E)-2,3-alkadienals, 4-hydroxy-(E)-2-alkenals, 4-hydroperoxy-(E)-2-alkenals and 4,5-epoxy-(E)-2-alkenals<sup>48</sup>. Terskikh *et al.* investigated western redcedar seeds and used various imaging methods and biochemical analyses to investigate compound deterioration<sup>49</sup>. These techniques included those such as GC, <sup>1</sup>H and <sup>13</sup>C NMR spectroscopy, MRI, and western blot analysis. The researchers found that the seeds with poor germination performance indicated the most loss of viability during the prolonged storage and had a greater amount of oxidized proteins present as determined by protein oxidation assays and *in vivo* <sup>13</sup>C NMR analysis. This was probably due to oxidation of the oil in the seeds. Seeds subjected to accelerated aging treatments were found to have higher amounts of oxidised proteins<sup>49</sup>. Brühl *et al.* were interested in identifying the bitter taste that developed upon storage of linseed oil at room temperature<sup>50</sup>. The researchers used a sensory guided fractionated approach, which consisted of five trained sensory panellists. Dilutions of linseed oil in rapeseed oil were prepared and increasing concentrations were given to the panellists to taste and smell until the concentration was detected where the bitter compound was identified. Isolation and identification of the compound by FTIR, NMR, LC-MS and amino acid analyses lead to the determination of its structure as being a methionine sulfoxide-containing cyclic octapeptide, named cyclo (pro-leu-phe-ile-met o-leu-val-phe) (abbreviated as PLFIM OLVF). In the literature this compound is referred to as cyclolinopeptide E but the bitter taste has not previously been associated with it. Sensory evaluation also indicated that the recognition threshold of this compound was 12,3 µmol/L water<sup>50</sup>. The oxidative stability of refined, bleached and deodorized canola and soybean oils, stored for 30 days in the dark at 65 °C, were analysed by Wanasundara *et al.*<sup>51</sup>. The researchers determined the peroxide value (PV), conjugated diene (CD) and triene (CT) contents, 2-thiobarbituric acid reactive substance (TBARS) and *p*-anisidine values. <sup>1</sup>H-NMR spectroscopy was also used to monitor the relative changes in protein absorption pattern of the fatty acids of the oils. During storage and it was

found that the PV, CD, CT and TBARS contents were all higher in canola oil than in soybean oil. The ratio of aliphatic to olefinic protons, as determined by  $^1\text{H-NMR}$ , for both oils increased steadily over storage time and indicated the progressive oxidation of unsaturated fatty acids<sup>51</sup>. Neuberger *et al.* used frequency-selected magnetic resonance imaging to rapidly and non-invasively detect and quantify visually the lipids in living seeds at a variety of stages of time<sup>52</sup>. The method provided quantitative lipid maps with a resolution close to that of the cellular level namely in-plane  $31\mu\text{m} \times 31\mu\text{m}$ . The reliability of the method was tested by using two contrasting grains, namely barley grain and soybean grain. Barley grain is a monocot with 2 % oil and highly compartmentalized, while soybean grain is a dicot with 20 % oil. Electron microscopy and biochemical and gene expression analysis were also done. By identifying steep gradients in the local oil storage at the organ- and tissue-specific scales, these gradients were found to closely coordinate with tissue differentiation and seed maturation<sup>52</sup>.

Other studies have been carried out which link oil stability to oil content using NMR spectroscopy. In one such study the olive oil composition, specifically the fatty acid residues, was determined by NMR spectroscopy in order to understand the effect of thermal stressing of olive oil<sup>53</sup>. Comparison of two methods, namely NMR spectroscopy and Matrix-Assisted Laser Desorption and Ionization Time-Of-Flight (MALDI-TOF) MS, revealed that where MALDI-TOF detected any direct changes, NMR spectroscopy could then provide detailed structural information on the products present with low molecular weight. Separation of oils by chromatographic techniques and subsequent analysis by  $^{13}\text{C}$  NMR spectroscopy has also been used for oil stability predictions and was shown to give better results than those obtained from classical chemical determinations due to the fact that the NMR technique could take more variables into account<sup>53</sup>. Another study showed that the use of chromatographically separated oil fractions increases the discriminative power of NMR spectroscopy and therefore gives better results for the classification of components by  $^{13}\text{C}$  NMR than using the full original oil samples<sup>54</sup>. This is understandable as NMR spectroscopy is typically a technique which is used to best effect when analyzing pure components or simple mixtures.

$^{31}\text{P}$  NMR spectroscopy has also been used to study the DG isomers and free acidity of five extra virgin olive oil samples with different initial acidities as a function of storage time and conditions. It was found that TGs were hydrolyzed and the 1,2 DGs

isomerised to 1,3 DGs over a period of 18 months of storage in different light and temperature conditions. Some samples were kept in ambient temperature in the dark, some in the light and others at 5 °C in the dark. The hydroxyl (from FFAs) and carboxyl (from DGs) groups formed were treated with 2-chloro-4,4,5,5-tetramethyl dioxaphospholane, after which these phosphorylated compounds were subjected to  $^{31}\text{P}$  NMR spectroscopy. Results showed that the structural isomerisation of 1,2 DGs to 1,3 DGs is dependent on the rate of hydrolysis of the TGs, the initial free acidity concentration as well as the storage conditions. The ratio of 1,2 DGs to the total amount of DGs was found to be concentration independent of the time of TG hydrolysis. Based on these studies a quantitative method was developed to estimate the storage time or aging of olive oil. The technique was applied to several oil samples with known and unknown storage history and these were compared with samples of known storage between 10-12 months. It was found that for longer storage periods in the case where the DG isomerisation was close to equilibrium, the calculated values were only an indication and not exact<sup>43</sup>.

This basis of aging, where major components break down into minor components was used for our studies on three different vegetable oils in Chapter 2 with the aid of  $^{31}\text{P}$  NMR spectroscopy. These oils included apricot kernel, avocado pear and macadamia nut oil and the well-studied olive oil was used for comparison.

## **1.5 $^{31}\text{P}$ NMR SPECTROSCOPY OF OLIVE OIL**

### **1.5.1 Assignment and quantification of $^{31}\text{P}$ NMR spectra of olive oil**

A significant amount of research has been carried out on the assignment and quantification of compounds present in olive oils that can be detected by various forms of NMR spectroscopy such as 1D and 2D techniques<sup>16,55-65</sup>. Such compounds include the major components, TGs, as well as some minor components such as DGs, MGs, phenolic compounds, aldehydes, sterols and more. Spyros *et al.* introduced a facile method for the determination of the amount of DGs and MGs in virgin olive oils using  $^{31}\text{P}$  NMR spectroscopy<sup>55</sup>. For detection of the minor components via  $^{31}\text{P}$  NMR spectroscopy, where the molecules themselves did not contain any phosphorus, derivatisation (with 2-chloro-4,4,5,5-tetramethyl dioxaphospholane) was first carried out to incorporate a moiety containing phosphorus to allow for the subsequent  $^{31}\text{P}$  NMR studies. Once the signals in the  $^{31}\text{P}$

NMR spectra were assigned to the minor components present in vegetable oils, quantification of their contents could be determined<sup>55</sup>. Christophoridou *et al.* examined the validity of the technique as a quantitative tool<sup>56,57</sup>. Assignment of the phosphorylated polyphenols in olive oil was done using <sup>31</sup>P NMR spectroscopy and various 2D techniques including <sup>1</sup>H-<sup>1</sup>H COSY, <sup>31</sup>P-<sup>31</sup>P COSY, <sup>1</sup>H-<sup>13</sup>C HMQC, <sup>1</sup>H-<sup>31</sup>P HMQC, <sup>1</sup>H-<sup>31</sup>P NOESY<sup>56,57</sup>. Dias *et al.* compared <sup>1</sup>H and <sup>31</sup>P NMR spectroscopy to conventional analytical methods such as titration, GC and HPLC techniques for the identification and quantification of the major and minor components in olive oil<sup>58</sup>. These components included free acidity, fatty acids, iodine value and phenolic compounds. The standard deviation of the NMR spectroscopic quantitative values compared well to those obtained by the conventional methods except for the total hydroxy tyrosol and total tyrosol values. Linear regression analysis indicated a strong correlation between the two techniques for the quantitative determination of free acids, total hydroxytyrosol and total tyrosol content, total DG, (+)-1-acetoxypinoresinol, (+)-pinoresinol and apegnin values. A good correlation was found between the two techniques for quantification of linoleic acid, free hydroxyl and free tyrosol content and a weak correlation was found for quantification of oleic acid, linolenic acid, saturated fatty acids and luteolin values. Bland and Altman used statistical analysis and results indicated that 96.4 % (for free acidity) and 100 % (for iodine value) of the measurements were within the limits of agreement, while for the rest of the values a range was found of 94 % - 98.5 %<sup>58</sup>. Hatzakis *et al.* developed a non-destructive analytical method to determine the identity and quantity of phospholipids in olive oil<sup>59</sup>. Phospholipids were first extracted from the oils using a 2:1 (v/v) ethanol/water mixture, identified and consequently quantified via <sup>31</sup>P NMR spectroscopy. It was found that the main phospholipids present in olive oil were phosphatidic acid, lyso-phosphatidic acid, and phosphatidylinositol and that for quantitative purposes the sensitivity of the technique was satisfactory with detection limits of 0.25–1.24 μmol /mL<sup>59</sup>.

Other studies have been carried out on the aging of oils using <sup>31</sup>P NMR spectroscopy. As already mentioned, in one study the DG isomers and free acidity were determined of five extra virgin olive oil samples with different initial acidities as a function of storage time and storage conditions. During the study TGs were hydrolyzed and the 1,2-DG isomerised to 1,3-DG over a period of 18 months at

storage conditions of different light and temperature. Some samples were kept in ambient temperature in the dark, some in the light and others at 5 °C in the dark. The hydroxyl (from free fatty acids) and carboxyls (from DG) groups formed were treated with 2-chloro-4,4,5,5-tetramethyl dioxaphospholane, after which these phosphorylated compounds were subjected to  $^{31}\text{P}$  NMR spectroscopy. Results showed that this structural isomerisation was dependant on the rate of hydrolysis of the TG, the initial free acidity as well as the storage conditions. The ratio of 1,2 DGs to the total amount of DGs was found to be concentration independent of the time of TG hydrolysis. Based on these studies a quantitative method was developed to estimate the storage time or age of olive oil. The technique was applied to several oil samples with known and unknown storage history and compared with samples of known storage between 10-12 months. It was found that for longer storage periods where the isomerisation of DG was close to equivalence, the calculated values were only an indication and not exact<sup>43</sup>. Schiller *et al.* used NMR spectroscopy and MALDI-TOF-MS to characterize the effects of thermal stressing on olive oil and linseed oil<sup>60</sup>. They found that both methods gave fast and reliable information on the oil composition and oxidation products formed upon heating. NMR spectroscopy yielded more detailed information on the products with lower molecular weights while MALDI-TOF could more directly detect the changes<sup>60</sup>.

### **1.5.2 Identification and authentication of olive oils based on geographical origin and cultivar variety differences by $^{31}\text{P}$ NMR spectroscopy**

The European Union has implemented laws which protect particular regional foods. The title PDO (Protected Designation of Origin) is given to the names of a variety of foodstuffs such as wine, beer, olives and many others which can be strongly associated with a particular region. Thus for a food to be given a particular label it has to come from that designated region, e.g. for sparkling wine to be classified as Champagne it must indeed have come from the Champagne region in France. Mediterranean olive oils are also PDO classified and so a name that is given to olive oil must correspond to the geographical region in which it is produced. However as olive oils, especially extra virgin olive oil, have high commercial value there is often the threat of olive oils being sold under the incorrect regional name to increase the oil's value or even adulteration of an oil being carried out. Adulteration occurs when lower quality and lower value vegetable oils, such as hazelnut, corn, sunflower and

soybean oils, are added to higher grade oils (such as extra virgin olive oil) to increase the quantity. As a result there is considerable interest in analytical methods to be able to identify the purity of an oil, the geographical origin from which an oil comes, and its cultivar. Thus overall the authentication of these oils is clearly of interest<sup>61</sup>. Fronimake *et al.* looked at the DG content of 96 samples of virgin olive oils, from different regions (Crete, Lesvos, Messinia, Pilion, Zakynthos, Iliia, Halkidik), 15 samples of commercial extra virgin and pure olive oils, 3 samples of refined olive oils and 3 samples of pomace oil<sup>62</sup>. The free hydroxyl groups of the DGs were phosphorylated using 2-chloro-4,4,5-tetramethyldioxaphospholane. 1,2 DG : total DG ratios and total DG content were determined for the virgin olive oil, commercial olive oil, refined olive oil and pomace oil samples. The researchers concluded that <sup>31</sup>P NMR spectroscopy is an efficient tool not only to determine the DG content of oils but also the MG<sup>62</sup>. Fragaki *et al.* obtained the <sup>31</sup>P NMR spectra of 59 samples of three different grades of olive oil samples which were derivatised with the <sup>31</sup>P reagent<sup>63</sup>. 34 were extra virgin olive oils from various regions of Greece, 13 were refined olive oil and 12 lampante oil. With a combination of statistical methods (hierarchical clustering statistical procedure) the researchers were able to classify the three olive oil groups. Applying discriminant analysis to five selected variables the researchers were able to group the 59 samples according to quality with no error. Mixtures were then used of extra virgin olive oil – refined olive oil and extra virgin olive oil – lampante oil, and discriminant analysis allowed extra virgin olive oil adulteration as low as 5 % w/w to be determined. The percentage concentration of the refined olive oil in 6 commercially blended olive oils (virgin olive oils and refined olive oils) from supermarkets could also be determined<sup>63</sup>. Vigli *et al.* used <sup>1</sup>H and <sup>31</sup>P NMR spectroscopy combined with multivariate statistical analysis to classify 192 samples of 13 types of vegetable oils including hazelnut, sunflower, corn, soybean, sesame, walnut, virgin olive oil, rapeseed, almond, palm, groundnut, safflower, and coconut, all from various regions of Greece. The variables that were used, as determined by NMR spectroscopy, were 1,2 DG, 1,3 DG, the ratio of the 1,2DG: total DG, acidity, iodine value and fatty acid composition. A classification/prediction model was set up using discriminant analysis. The model results showed significant discrimination among different classes of oils. Mixtures of olive-hazelnut, corn, sunflower and soybean oils were analyzed by <sup>1</sup>H and <sup>31</sup>P NMR spectroscopy and allowed detection of adulteration of as low as 5 % w/w of fresh virgin olive oil. Clearly DG content

determination is powerful for the classification and detection of adulteration<sup>64</sup>. Petrakis *et al.* did studies using  $^1\text{H}$  and  $^{31}\text{P}$  NMR spectroscopy to characterize monovarietal virgin olive oil (cv. Koroneiki) samples from three regions of southern Greece<sup>65</sup>, namely Peloponnesus, Crete, and Zakynthos, and collected samples in five harvesting years (2001–2006), with the aim to predict their geographical origin. The researchers looked specifically at the contents of fatty acids, phenolics, DGs, total free sterols, free acidity, and iodine number. They were also able to construct successfully a geographical prediction algorithm for unknown samples<sup>65</sup>.

## 1.6 THE INVESTIGATION OF SIX LOCALLY PRODUCED VEGETABLE OILS

From the above discussion it is clear that while olive oil has been extensively studied by  $^1\text{H}$ ,  $^{31}\text{P}$  and  $^{13}\text{C}$  NMR spectroscopy, little in-depth NMR analysis of other vegetable oils has been carried out and reported in the literature. It has been our intention in the past few years to apply some of the NMR spectroscopic methods developed for the analysis of olive oil to other vegetable oils of interest produced in South Africa, such as apricot kernel, avocado pear, grapeseed, macadamia nut, mango kernel and marula oils. Prior to our studies the  $^{13}\text{C}$  NMR spectra of these oils had not been examined or fully assigned. The conventionally used method for the full assignment of  $^{13}\text{C}$  NMR spectra of vegetable oils is by means of standard addition (spiking) of the vegetable oil with a standard triacylglycerol<sup>10</sup>. Comparison of the resulting  $^{13}\text{C}$  NMR spectra of the unspiked and spiked vegetable oil leads to the assignment of the  $^{13}\text{C}$  resonances in the NMR spectrum of the different fatty acid components present in the vegetable oil. Upon application of this method to the  $^{13}\text{C}$  NMR spectra of the above mentioned South African vegetable oils, we encountered some problems<sup>66,67</sup>. Not only did this method have some practical disadvantages including being time-consuming (several spectroscopic runs) and requiring expensive standard triacylglycerols, we found that it was not possible to achieve a full, unambiguous assignment of the  $^{13}\text{C}$  NMR spectra of the desired oils using this technique. Desirous of developing a rapid method for the accurate assignment of the  $^{13}\text{C}$  resonances of the various major components in a vegetable oil, we developed and tested a graphical linear correlation method for the assignment of the  $^{13}\text{C}$  resonances of a vegetable oil<sup>66,67</sup>. The proposed method is based on the reasonable expectation that the  $^{13}\text{C}$  chemical shifts of a fatty acid residue of a particular TG in a given solvent at a specified concentration should all be affected, to a first approximation, in a similar

manner by the factors responsible for the observed concentration dependence. Moreover it may be expected that saturated  $sp^3$  carbon atoms might be differently affected to unsaturated  $sp^2$  carbon atoms for a given fatty acid residue (*vide infra*). On this basis it would be reasonable to expect that  $^{13}C$  shifts of all carbon resonances of a fatty acid of a pure, standard triacylglycerol (e.g. triolein, tripalmitin, etc.) would be linearly correlated to the corresponding fatty acid residues of the triacylglycerols in a vegetable oil mixture in a given solvent at a specified concentration range. Thus the linear correlation method is applied by plotting the chemical shifts of the fatty acid present in the vegetable oil on the y-axis with the corresponding fatty acid chemical shifts of the standard TG on the x-axis and a linear correlation is obtained. The technique was tested and validated with extra-virgin olive oil, for which the  $^{13}C$  NMR spectrum has been well characterized in the literature. This method was found to be especially useful in the crowded areas of the spectrum where peak overlap occurs. The method was also shown to be concentration independent and accurate in the assignment of various vegetable oils, including olive oil. Using this approach one could easily achieve the full assignment of the  $^{13}C$  NMR spectra of the six locally produced South African vegetable oils of interest<sup>66,67</sup>.

In this current dissertation we look specifically at three of the six vegetable oils, namely avocado pear, macadamia nut and apricot kernel oils. Other NMR related research on these three vegetable oils is very limited. Below each of these three oils are briefly discussed, specifically with regards to the NMR research previously carried out by other workers.

### **1.6.1 Apricot kernel oil**

Apricot kernel oil comes from the fruit's nut of the apricot tree, *Prunus armeniaca*, and is light yellow in colour.

Several studies have been done to determine the composition of apricot kernels and their extracted oils from different regions. The oil composition of apricot kernels of eleven varieties found in the Ladakh region of India has been studied by Kapoor *et al.*<sup>68</sup> The researchers found that the pit constitutes 7.3-19.0 weight percentage of the fruit, the kernels 21.9-38 % of the pit from which 27-67 % oil can be obtained. The kernels also contain 20-45 % proteins. The apricot kernel oil was found to contain 51-

80 % oleic, 10-46 % linoleic and 3-11 % palmitic fatty acid residues. UV, IR and NMR techniques were used for this analysis and no unusual fatty acids were found, including those with epoxy, cyclopropene, hydroxyl or other oxygenated functional groups. Although this study involved the use of NMR spectroscopy on the pit of apricot fruit, there was no indication that any NMR analysis was done on the oil itself. Turan *et al.* determined the fatty acid, sn-2 fatty acid, TG, tocopherol and phytosterol compositions of apricot kernel oils from nine different apricot varieties grown in the Malatya region of Turkey<sup>69</sup>. The researchers found that the oil content of the kernels ranged from 40.23-53.19 % with the highest fatty acid content being oleic acid of 70.83 %, with linoleic acid at 21.96 %, palmitic acid at 4.92 % and stearic acid at 1.21 %. The sn-2 position on the glycerol backbone of the TG was mostly occupied by oleic acid at 63.54 %, linoleic acid at 35.0 % and palmitic acid at 0.96 %. The researchers identified eight different fatty acid species, four different tocopherols and six phytosterol isomers. Principal component analysis (PCA) of the lipid components of the oil proved to be a powerful tool to classify the different varieties of the apricot oil with respect to their distribution. Ruiz *et al.* looked at 37 apricot varieties from Spanish cultivars in order to characterize and quantify their phenolic compounds<sup>70</sup>. These varieties were separated into four different groups: white, yellow, light orange and orange. HPLC-MS/MS was used to identify four phenolic compound groups; namely procyanidins, hydrocinnamic acid derivatives, flavonols and anthocyanins and these were quantified by High-Performance Liquid Chromatography-Diode Array Detector (HPLC-DAD). The researchers found that these groups included chlorogenic and neochlorogenic acids, procyanidins B1, B2 and B4, some procyanidin trimers, quercetin 3-rutinoside, kaempferol 3-rhamnosyl-hexoside and quercetin 3-acetyl-hexoside, cyaniding-3-rutinoside and 3-glucoside. The total phenolic content was determined to be between 32.6 -160 mg/100g and no correlation were found between the flesh colour and phenolic content of the different cultivars. In another study by El-Aal *et al.*, apricot kernel oil was extracted and characterized in order to evaluate its use in preparing biscuits and cakes<sup>71</sup>. The researchers used hexane as the extracting solvent and also found the major fatty acid components to be oleic, linoleic and palmitic acid. Chloroform-methanol extracts yielded neutral lipids and TGs as major fractions, while glycol- and phospholipids made up the minor fractions, which includes acylsterylglucosides and phosphatidyl choline as major components. These studies revealed that apricot kernel oil has

excellent properties for preparation of foods, and is comparable to corn oil and did not affect the flavour, colour or texture of the prepared biscuits and cakes. In studies conducted by our group, the major fatty acids present in South African produced apricot kernel oil were analyzed, identified and quantified by  $^{13}\text{C}$  NMR spectroscopy using a novel graphical correlation method as mentioned previously<sup>66,67</sup>. These fatty acids included oleic acid, palmitic acid, linoleic acid and vaccenic and/or eicosenoic acid. Quantification of the fatty acids present in apricot kernel oil by  $^{13}\text{C}$  NMR spectroscopy compared fairly well with those of conventional GC-MS analysis and were found to be  $61 \pm 0.39$  % (w/w) for oleic acid,  $31 \pm 0.56$  % (w/w) for linoleic acid, and  $8 \pm 0.27$  % (w/w) for the saturated fatty acids of which palmitic acid was found to be most predominant. For vaccenic and/or eicosenoic fatty acids, the amounts were too small to be quantified by  $^{13}\text{C}$  NMR spectroscopy.

### 1.6.2 Avocado pear oil

Three avocado tree varieties are found: *Persea Americana* Mill. var. (also known as *P. gratissima* Gaertn), *P. Americana* Mill. var. *drymifolia* Blake (also known as *P. drymifolia* Schlecht. and Cham.) and *P. mubigena* var. *guatemalensis* L. Wms. The oil which is obtained from the fruit of these trees is dark green in colour.

Moreno *et al.* studied the changes that avocado pear oil undergoes with the use of four different extraction methods<sup>72</sup>. These included studying physical and chemical changes, fatty acid profile, *trans* fatty acid content and the identification of volatile components. The researchers found that the major fatty acids present in the oil were palmitic, palmitoleic, oleic, linoleic and linolenic. The results showed that there is an effect on the physical and chemical characteristics of the avocado pear oil, which included the fatty acids present as TGs and volatile compounds, with the use of different extraction methods. It was found that the extraction of oil using solvents resulted in greater deterioration of oils with comparison to using a microwave. In another study Hierro *et al.* were interested in using HPLC with a light scattering detector to identify the TG composition of avocado pear oil<sup>73</sup>. Lipid fractions of two varieties, *Fuerte* and *Hass*, were used. The qualitative compositions were found to be similar, while quantitative differences were found between the two varieties. Four *Persea Americana* varieties including *Zutano*, *Bacon*, *Fuerte* and *Lula* were investigated by Lozano *et al.* for their unsaponifiable matter (UM)<sup>74</sup>. The UM content

of the oils were found to be higher in immature fruits than those for mature fruits, and using UM fractions obtained by HPLC it was found that the sterol and tocopherol content for immature fruit was higher while the tocopherol content was different for each variety. Du Plessis studied avocados of four different cultivars obtained on a monthly basis for the 1978 season from Pretoria, South Africa<sup>75</sup>. The fruit mesocarp was isolated by centrifugation and analyzed for fatty acid, iodine values, phospholipids and FFA contents. Changes in these contents were investigated over time. As mentioned for apricot kernel oil, our group investigated the major fatty acids present in South African produced avocado pear oil. These were analyzed, identified and quantified by <sup>13</sup>C NMR spectroscopy using a novel graphical correlation method as mentioned previously<sup>66,67</sup>. The fatty acids included oleic acid, palmitic acid, linoleic acid, vaccenic and/or eicosenoic acid, and the more uncommonly observed palmitoleic acid. The <sup>13</sup>C NMR shifts for the palmitoleic fatty acids were assigned for the first time in a vegetable oil. Quantification of the fatty acids present in avocado pear oil by <sup>13</sup>C NMR spectroscopy compared fairly well with those of conventional GC-MS analysis and were found to be 62 ± 0.40 % (w/w) for oleic acid plus palmitic acid, 12 ± 0.22 % (w/w) for linoleic acid, around 7 % (w/w) for vaccenic and/or eicosenoic acid, and 21 ± 0.70 % (w/w) for the saturated fatty acids of which palmitic acid was found to be most predominant.

### 1.6.3 Macadamia nut oil

There are two species of the macadamia nut tree with edible fruit, *Macadamia integrifolia* and *Macadamia tetraphylla*, while the fruit of the remaining species, *Macadamia ternifolia*, is inedible. Macadamia nut oil extracted from the fruit is light yellow in colour.

In a study carried out by Holčapek *et al.* the TG and DG content of sixteen different plant oils, of which macadamia nut oil was one, was analyzed<sup>76</sup>. The data was collected using HPLC-MS with atmospheric pressure chemical ionization (APCI) and UV detection. Identification of TGs was achieved using APCI-MS while the characterization of TGs and DGs was carried out with HPLC-APCI-MS. In the same work that was done on avocado pear and apricot oil by our group, the major fatty acids present in South African produced macadamia nut oil were analysed<sup>66,67</sup>. Using the newly developed novel graphical correlation method the fatty acids oleic acid, palmitic acid, linoleic acid and vaccenic and/or eicosenoic acid and the more

uncommonly observed palmitoleic acid were identified and assigned. The  $^{13}\text{C}$  NMR shifts for the palmitoleic fatty acids that were assigned for the first time in a vegetable oil in avocado pear oil were found to be present in macadamia nut oil as well. Quantification of the fatty acids present in macadamia nut oil by  $^{13}\text{C}$  NMR spectroscopy compared fairly well with those of conventional GC-MS analysis and were found to be  $56 \pm 0.36$  % (w/w) for oleic acid, around 16 % (w/w) for palmitoleic acid, around 7 % (w/w) for vaccenic and/or eicosenoic acid, and  $21 \pm 0.70$  % (w/w) for the saturated fatty acids of which palmitic acid was found to be most predominant. For linoleic fatty acid the amount was too small to be quantified by  $^{13}\text{C}$  NMR spectroscopy.

## **1.7 AIMS OF STUDY**

As discussed earlier in this chapter,  $^{31}\text{P}$  NMR spectroscopy has been used by other researchers for the identification and quantification of minor components present in olive oil, specifically DGs, MGs, FFAs, sterols and polyphenols. To our knowledge there are no reports in the literature on the use of  $^{31}\text{P}$  NMR spectroscopy for the determination of minor components in other vegetable oils. We wanted to explore the use of  $^{31}\text{P}$  NMR spectroscopy to identify the minor components of selected locally produced vegetable oils from South Africa, namely apricot kernel, macadamia nut and avocado pear oils. Further quantification studies were to be done in order to aid in detection of aging and storage effects of the minor components present in these oils. Storage conditions included exposure to light, in the dark, in the dark covered in tin foil (to potentially provide better thermal stability), in a fridge at  $5\text{ }^{\circ}\text{C}$  and frozen at  $-8\text{ }^{\circ}\text{C}$ .

Due to our interest in vegetable oils, we also decided to extend our studies to other oil containing food stuffs, namely seeds and beans. These included sesame, poppy, pumpkin and sunflower seeds as well as black, mung, kidney and soybeans. In this study (as presented in Chapter 3) we were interested in investigating the major compounds present in these seeds and beans, specifically oil, carbohydrates and proteins by Thermogravimetric Analysis and solid state NMR spectroscopy. Quantitative values determined from TGA for these compounds were to be compared to those of conventional methods such as Soxhlet extraction (for oil), Dumas-combustion (for protein) and Clegg-Anthrone/UV-Visible spectroscopy (for carbohydrates). Solid state NMR spectroscopic techniques were to be used to aid in

the information obtained on the presence and structure of the compounds present in the seeds and beans as detected and quantified by TGA.

## 1.8 REFERENCES

1. Gunstone, F.D., in "Vegetable Oils in Food Technology; Composition, Properties and Uses", Blackwell Publishing, Ltd., USA and Canada, **2000**, p **33**.
2. Gunstone, F.D., in "The Chemistry of Oils and Fats; Sources, Composition, Properties and Uses", Blackwell Publishing, Ltd., USA and Canada, **2004**, pp 23-24,107-112.
3. Food and Agriculture Organization of the United Nations: <http://www.fao.org>, date of access, 2009.
4. Gunstone, F.D., and Norris, F.A., in "Lipids in Foods; Chemistry, Biochemistry and Technology", Pergamon Press, **1983**, pp 1-8, 29-32.
5. Hoffman, G., in "The Chemistry and Technology of Edible Oils and Fats and Their High Fat Products, Food Science and Technology", Academic Press Limited, San Diego, **1989**, pp 8-10.
6. Visioli, F., and Galli, C. Olive Oil Phenols and Their Potential Effects on Human Health. *J. Agric. Food Chem.* **1998**, *46*, 4292-4296.
7. Manna, C., Galletti, P., Cucciola, V., Montedoro, G., and Zappia, V. Olive oil hydroxytyrosol protects human erythrocytes against oxidative damages. *J. Nutr. Biochem.* **1999**, *10*, 159-165.
8. Giovanni, C., Straface, E., Modesti, D., Coni, E., Cantafora, A., De Vincenzi, M., Malorni, W., and Masella, R. Biochemical and Molecular Action of Nutrients: Tyrosol, the Major Olive Oil Biophenol, Protects Against Oxidized-LDL-Induced Injury in Caco-2 Cells. *J. Nutr.* **1999**, *129*, 1269-1277.
9. Lipworth, L., Martínez, M.E., Angell, J., Hsieh, C., and Trichopoulos, D. Review: Olive oil and Human Cancer: An Assessment of the Evidence. *Prev. Med.*, **1997**, *26*, 181-190.
10. The controversy over trans fatty acids: Effects early in life. *Food and Chemical Toxicology* (2008), *46*, (12), 3571-3579. Publisher: (Elsevier Ltd.), CODEN:FCTOD7 ISSN:0278-6915.
11. McMurray, J., in "Organic Chemistry", Fifth edition, Brooks/Cole, Pacific Grove, **2000**, pp 1118-1120.
12. Bailey, Jr. P.S., and Bailey C.A., in "Organic Chemistry, A Brief Survey of Concepts and Applications", Sixth edition, Prentice Hall Inc., New Jersey **2000**, p 435.
13. Raven, P.H., and Johnson, G.B., in "Biology", Fifth edition, McGraw-Hill Companies, USA, **1999**, pp 45-46.
14. Weiss, T.J., in "Food Oils and Their Uses", The Avi Publishing Company, Inc., Connecticut, **1970**, pp 1-4, 26-38.
15. Vlahov, G., Application of NMR to the study of olive oils, *Prog. Nucl. Magn. Res. Spec.*, **1999**, *35*, 341-357.
16. McKenzie, J.M and Koch, K.R., Rapid analysis of major components and potential authentication of South African olive oils by quantitative <sup>13</sup>C nuclear magnetic resonance spectroscopy, *S. Afr. J. Sci.*, **2004**, *100*, 349 – 354.

17. Hoffman, G., in "The Chemistry and Technology of Edible Oils and Fats and Their High Fat Products, Food Science and Technology", Academic Press Limited, San Diego, **1989**, pp 8-10.
18. Devine, J., and Williams, P.N., in "The Chemistry and Technology of Edible Oils and Fats", Pergamon Press, Glasgow, **1961**, pp 8-11.
19. Commission Regulation (EEC) No 2568/91, *Off. J. Eur. Communities*, **1991**, L248, 1-83.
20. Rochfort, S., *Metabolomics reviewed: A New "Omics" Platform Technology for Systems Biology and Implications for Natural Products Research*, *J. Nat. Prod.*, **2005**, 68, 1813-1820.
21. Mannina, L., and Segre, A., High Resolution Nuclear Magnetic Resonance: From Chemical Structure to Food Authenticity, *Grasas Aceites*, **2002**, 53, 22-33.
22. Mannina, L., Sobolev, A.P., and Segre, A., Olive oil as seen by NMR and chemometrics, *Spectroscopy Europe*, **2003**, 15, 6-14.
23. Shoolery, J.N., Some quantitative applications of  $^{13}\text{C}$  NMR Spectroscopy, *Prog. Nucl. Magn. Res. Sp.*, **1977**, 11, 79-93.
24. Ogrinc, N., Košir, I.J., Spangenberg, J.E., and Kidrič, J., The application of NMR and MS methods for detection of adulteration of wine, fruit juices, and olive oil. A review, *Anal. Bioanal. Chem.*, **2003**, 376, 424-430.
25. Mannina, L., Luchinat, C., Emanuele, M.C., and Segre, A., Acyl positional distribution of glycerol tri-esters in vegetable oils: a  $^{13}\text{C}$  NMR study, *Chem. Phys. Lipids*, **1999**, 103, 47-55.
26. Montedoro, G., Servili, M., Baldioli, M., Selvaggini, R., Miniati, E., and Macchioni, A., Simple and Hydrolyzable Compounds in Virgin Olive Oils. 3. Spectroscopic Characterization of the Secoiridoid Derivatives, *J. Agric. Food Chem.*, **1993**, 41, 2228-2234.
27. Brenes, M., Hidalgo, F.J., García, A., Rios, J.J., García, P., Zamora, R., and Garrido, A., Pinoresinol and 1-Acetoxypinoresinol, Two New Phenolic Compounds Identified in Olive Oil, *J. Am. Oil Chem.Soc.*, **2000**, 77 (7), 715-720.
28. Sacchi, R., Mannina, L., Fiordiponti, P., Barone, P., Paolillo, L., Patumi, M., and Segre, A., Characterization of Italian Extra Virgin Olive Oils Using  $^1\text{H}$ -NMR Spectroscopy, *J. Agric. Food Chem.*, **1998**, 46, 3947-3951.
29. Vlahov, G., Del Re, P., and Simone, N., Determination of Geographical Origin of Olive Oils Using  $^{13}\text{C}$  Nuclear Magnetic Resonance Spectroscopy. I – Classification of Olive Oils of the Puglia Region with Denomination of Protected Origin, *J. Agric. Food Chem.*, **2003**, 51, 5612-5615.
30. Mannina, L., Patumi, M., Proietti, N., Bassi, D and Luchinat, C., Geographical Characterization of Italian Extra Virgin Olive Oils Using High-Field  $^1\text{H}$  NMR Spectroscopy, *J. Agric. Food Chem.*, **2001**, 49, 2687-2696.
31. Shaw, A.D., di Camillo, A., Vlahov, G., Jones, A., Bianchi, G., Rowland, J., and Kell, D.B., Discrimination of the variety and region of origin of extra virgin olive oils using  $^{13}\text{C}$  NMR and multivariate calibration with variable reduction, *Anal. Chim. Acta*, **1997**, 348, 357-374.

32. Sacco, A., Brescia, M.A., Liuzzi, V., Reniero, F., Guillou, C., Ghelli, S., and van der Meer, P., Characterization of Italian Olive Oils Based on Analytical and Nuclear Magnetic Resonance Determinations, *J. Am. Oil Chem. Soc.*, **2000**, *77*, 619-625.
33. Vlahov, G., Improved Quantitative  $^{13}\text{C}$  Nuclear Magnetic Resonance Criteria for Determination of Grades of Virgin Olive Oils. The Normal Ranges for Diglycerides in Olive Oil, *J. Am. Oil Chem. Soc.*, **1996**, *73*, 1201-1203.
34. Vlahov, G., Shaw, A.D., and Kell, D.B., Use of  $^{13}\text{C}$  Nuclear Magnetic Resonance Distortionless Enhancement by Polarization Transfer Pulse Sequence and Multivariate Analysis to Discriminate Olive Oil Cultivars, *J. Am. Oil Chem. Soc.*, **1999**, *76*, 1223-1231.
35. Mannina, L., Dugo, G., Salvo, F., Cicero, L., Ansanelli, G., Calcagni, C., and Segre, A., Study of the Cultivar-Composition Relationship in Sicilian Olive Oils by GLC, NMR, and Statistical Methods, *J. Agr. Food Chem.*, **2003**, *51*, 120-127.
36. Rezzi, S., Axelson, D.E., Héberger, K., Reniero, F., Mariani, C., and Guillou, C., Classification of olive oils using high throughput flow  $^1\text{H}$  NMR fingerprinting with principal component analysis, linear discriminant analysis and probabilistic neural networks, *Anal. Chim. Acta*, **2005**, *552*, 13-24.
37. Mannina, L., Patumi, M., Proietti, N., and Segre, A., P.D.O. (Protected Designation of Origin): Geographical characterization of Tuscan extra virgin olive oils using high-field  $^1\text{H}$  NMR Spectroscopy, *Ital. J. Food Sci.*, **2001**, *13*, 53-63.
38. Guillén, M.D., and Ruiz, A., Edible oils: discrimination by  $^1\text{H}$  nuclear magnetic resonance, *J. Sci. Food Agr.*, **2003**, *83*, 338-346.
39. del Río, C., and Romero, A.M., Whole, Unmilled Olives Can Be Used to Determine their Oil Content by Nuclear Magnetic Resonance, *Horticulture Technology*, **1999**, *9*, 675-680.
40. Mannina, L., Fontanazza, G., Patumi, M., Ansanelli, G., and Segre, A., L., Italian and Argentine olive oils: a NMR and gas chromatographic study, *Grasas Aceites*, **2001**, *52*, 380-388.
41. Vigli, G., Philippidis, A., Spyros, A., and Dais, P., Classification of Edible Oils by Employing  $^{31}\text{P}$  and  $^1\text{H}$  NMR Spectroscopy in Combination with Multivariate Statistical Analysis. A Proposal for the Detection of Seed Oil Adulteration in Virgin Olive Oils, *J. Agr. Food Chem.*, **2003**, *51*, 5715-5722.
42. Diego, L., González, G., Mannina, L., D'Imperio, M., Segre, A., and Aparicio, R., Using  $^1\text{H}$  and  $^{13}\text{C}$  NMR techniques and artificial neural networks to detect the adulteration of olive oil with hazelnut oil, *Eur. Food Res. Technol.*, **2004**, *219*, 545-548.
43. Spyros, A., Philippidis, A., and Dais, P., Kinetics of Diglyceride Formation and Isomerization in Virgin Olive Oils by Employing  $^{31}\text{P}$  NMR Spectroscopy. Formulation of a Quantitative Measure to Assess Olive Oil Storage History, *J. Agr. Food Chem.*, **2004**, *52*, 157-164.
44. McMurray, J., in "Organic Chemistry", Fifth Edition, Brooks/Cole, USA, **2000**, pp 866-868, 948-950.
45. Hamilton, R.J., and Bhati, A., in "Fats and Oils, Chemistry and Technology", Applied Science publishers Ltd., **1980**, Essex, England, pp 86-87.

46. Bruice, P.Y., in "Organic Chemistry", Second edition, Prentice-Hall, Inc., New Jersey, USA, **1998,1995**, pp 841-843.
47. Guillen, M.D., and Goicoechea, E., Detection of primary and secondary oxidation products by Fourier transform infrared spectroscopy (FTIR) and <sup>1</sup>H nuclear magnetic resonance (NMR) in sunflower oil during storage, *J. Agric. Food Chem.*, **2007**, *55*, 10729-10736.
48. Guillen, M.D., and Goicoechea, E., Oxidation of corn oil at room temperature: Primary and secondary oxidation products and determination of their concentration in the oil liquid matrix from <sup>1</sup>H nuclear magnetic resonance data, *Food Chem.*, **2009**, *116*, 183-192.
49. Terskikh, V.V., Zeng, Y., Feurtado, J.A., Giblin, M., Abrams, S.R., and Kermode, A.R., Deterioration of western redcedar (*Thuja plicata* Donn ex D. Don) seeds: protein oxidation and *in vivo* NMR monitoring of storage oils, *J. Exp. Bot.*, **2008**, *59* (4), 765-777.
50. Brühl, L., Matthäus, B., Fehling, E., Wiege, B., Lehmann, B., Luftmann, H., Bergander, K., Quiroga, K., Scheipers, A., Frank, O., and Hofmann, T., Identification of bitter off-taste compounds in the stored cold pressed linseed oil, *J. Agric. Food Chem.*, **2007**, *55*, 7684-7868.
51. Wanasundara, U.N., Shahidi, F., and Jablonski, C.R., Comparison of standard and NMR methodologies for assessment of oxidative stability of canola and soybean oils, *Food Chem*, **1995**, *52*, 249-253.
52. Neuberger, T., Sreenivasula, N., Rokitta, M., Rolletscheck, H., Göbel, C., Rutten, T., Radchuk, V., Feussner, I., Wobus, U., Jakob, P., Webb, A., and Borisjuk, L., Quantitative imaging of oil storage in developing crop seeds, *Plant Biotechnol. J.*, **2008**, *6*, 31-45.
53. Hidalgo, F.J., Gómez, G., Navarro, J.L., and Zamora, R., Oil Stability Prediction by High-Resolution <sup>13</sup>C Nuclear Magnetic Resonance Spectroscopy, *J. Agr. Food Chem.*, **2002**, *50*, 5825-5831.
54. Zamora, R., Gómez, G., and Hidalgo, F.J., Classification of Vegetable Oils by High-Resolution <sup>13</sup>C NMR Spectroscopy Using Chromatographically Obtained Oil Fractions, *J. Am. Oil Chem. Soc.*, **2002**, *79*, 267-272.
55. Spyros, A., and Dais, P., Application of <sup>31</sup>P NMR Spectroscopy in Food Analysis. 1. Quantitative Determination of the Mono- and Diglyceride Composition of Olive Oils, *J. Agr. Food Chem.*, **2000**, *48*, 802-805.
56. Christophoridou, S., Spyros, A., and Dais, P., <sup>31</sup>P Nuclear Magnetic Resonance Spectroscopy of polyphenol-containing olive oil model compounds, *Phosphorus Sulfur*, **2001**, *170*, 139-157.
57. Christophoridou, S., and Dais, P., Novel approach to the detection and quantification of phenolic compounds in olive oil based on <sup>31</sup>P Nuclear Magnetic Resonance Spectroscopy, *J. Agric. Food Chem.*, **2006**, *54*, 656-664.
58. Dias, P., Spyros, A., Christophoridou, S., Hatzakis, E., Fragaki, G., Agiomyrgianaki, A., Salivars, E., Sirgakis, G., Daskalaki, D., Tasioula-Margari, M., and Brenes, M. Comparison of analytical methodologies based on <sup>1</sup>H and <sup>31</sup>P NMR spectroscopy with conventional methods of analysis for the determination of some olive oil constituents, *J. Agric. Food Chem.*, **2007**, *55*, 577-584.

59. Hatzakis, A.K., Boskou, D., and Dais, P., Determination of Phospholipids in Olive Oil by  $^{31}\text{P}$  NMR Spectroscopy, *J. Agric. Food Chem.*, **2008**, *56* (15), 6232–6240.
60. Schiller, J., Süß, R., Petkovič, M., and Arnold, K., Thermal stressing of unsaturated vegetable oils: effects analysed by MALDI-TOF mass spectrometry,  $^1\text{H}$  and  $^{31}\text{P}$  NMR spectroscopy, *Eur. Food Res. Technol.*, **2002**, *215*, 282-286.
61. Dais, P., and Spyros, A.,  $^{31}\text{P}$  NMR spectroscopy in the quality control and authentication of extra-virgin olive oil: A review of recent progress, *Magn. Reson. Chem.*, **2007**, *45*, 367-377.
62. Fronimaki, P., Spyros, A., Christophoridou, S., and Dais, P., Determination of the diglyceride content in Greek virgin olive oils and some commercial olive oils by employing  $^{31}\text{P}$  NMR spectroscopy, *J. Agric. Food Chem.*, **2002**, *50*, 2207-2213.
63. Fragaki, G., Spyros, A., Siragakis, G., Salivaras, E., and Dais, P., Detection of Extra Virgin Olive Oil Adulteration with Lampante Olive Oil and Refined Olive Oil Using Nuclear Magnetic Resonance Spectroscopy and Multivariate Statistical Analysis, *J. Agric. Food Chem.*, **2005**, *53*, 2810-2816.
64. Vigli, G., Philippidis, A., Spyros, A., and Dais, P., Classification of Edible Oils by Employing  $^{31}\text{P}$  and  $^1\text{H}$  NMR Spectroscopy in Combination with Multivariate Statistical Analysis. A Proposal for the Detection of Seed Oil Adulteration in Virgin Olive Oils, *J. Agric. Food Chem.*, **2003**, *51*, 5715-5722.
65. Petrakis, P.V., Agiomyrgianaki, A., Christophoridou, S., Spyros, A., Dais, P., Geographical Characterization of Greek Virgin Olive Oils (Cv. Koroneiki) Using  $^1\text{H}$  and  $^{31}\text{P}$  NMR Fingerprinting with Canonical Discriminant Analysis and Classification Binary Trees, *J. Agric. Food Chem.*, **2008**, *56* (9), 3200–3207.
66. Retief, L., Mckenzie J.M., and Koch K.R., A novel approach to the rapid assignment of  $^{13}\text{C}$  NMR spectra of major components of vegetable oils such as avocado, mango kernel and macadamia nut oils, *Magn. Reson. Chem.*, **2009**, *47*, 771-781.
67. Retief, L., McKenzie J.M., and Koch K.R., in “Magnetic Resonance in Food Science: Challenges in a Changing World”, Identification and quantification of major triacylglycerols in selected South African vegetable oils by  $^{13}\text{C}$  NMR spectroscopy, RSC publishing, London, UK, 2009, 151-157.
68. Kapoor, N., K. L. Bedi, and Bathia A.K., Chemical composition of different varieties of apricots and their kernels grown in the Ladakh region, *J. Food Sci. Tech.*, **1987**, *24*, 141-3.
69. Turan, S., Topcu, A., Karabulut, I., Vural, H., and Hayaloglu, A.A., Fatty acid, triacylglycerol, phytosterol, and tocopherol variations in kernel oil of Malatya apricots from Turkey, *J. Agric., Food Chem.*, **2007**, *55*, 10787-10794.
70. Ruiz, D., Egea, J., Gil, M.I., and Tomás-Barberán, F.A., Characterization and quantitation of phenolic compounds in new apricot (*Prunus armeniaca* L.) varieties, *J. Agric. Food Chem.*, **2005**, *53*, 9544-9552.
71. El-Aal, M.H. Abd., Khalil, M.K.M, and Rahma, E.H., Apricot Kernel Oil: Characterization, Chemical Composition and Utilization in Some Baked Products., *Food Chem.*, **1986**, *19*, 287-298.

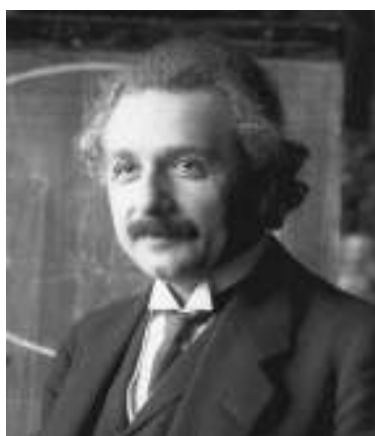
72. Moreno, A.O., Dorantes, L., Galíndez, J., and Guzmán, R.I., Effect of Different Extraction Methods on Fatty Acids, Volatile Compounds, and Physical and Chemical Properties of Avocado (*Persea Americana Mill.*) Oil, *J. Agric. Food Chem.*, **2003**, *51*, 2216-2221.
73. Hierro, M.T.G., Tomás, M.C., Martín, F.F., and María, G.S., Determination of the triacylglyceride composition of avocado oil by high-performance liquid chromatography using a light-scattering detector, *J. Chromatogr.*, **1992**, *607*, 329-338.
74. Lozano, Y.F., Mayer, C.D., and Gaydou, E.M., Unsaponifiable Matter, Total Sterol and Tocopherol Contents of Avocado Oil Varieties, *J. Am. Oil Chem. Soc.*, **1993**, *70*, 561-565.
75. Du Plessis, L.M., 'n Studie van die seisoenale verandering in die samestelling van Suid-Afrikaanse avocado-olie, *Supplement to SA FOOD REVIEW*, **1979**, 114-117.
76. Holčapek, M., Jandera, P., Zderadička, P., and Hrubá, L., Characterization of triacylglycerol and diacylglycerol composition of plant oils using high-performance liquid chromatography-atmospheric pressure chemical ionization mass spectrometry, *J. Chromatogr. A*, **2003**, *1010*, 195-215.

# CHAPTER 2: ANALYSIS OF VEGETABLE OILS BY $^{31}\text{P}$ NMR SPECTROSCOPY

*"A man should look for what is, and not for what he thinks should be."*

Albert Einstein

March, 1879 – April, 1955

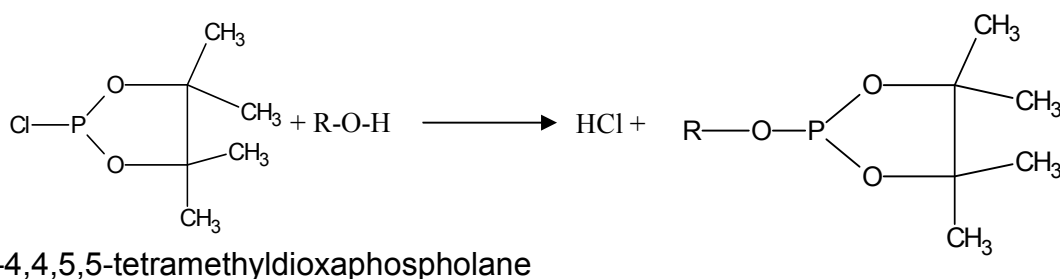


Picture obtained from <http://en.wikipedia.org/wiki/Einstein>

## 2.1 INTRODUCTION

In this chapter the quantitative and qualitative determination of certain minor components in three locally produced vegetable oils, namely apricot kernel, avocado pear and macadamia nut oils are carried out using  $^{31}\text{P}$  NMR spectroscopy. The primary objective of this study was to investigate the applicability of  $^{31}\text{P}$  NMR spectroscopy to examine and determine specific minor components namely, 1,2 DGs; 1,3 DGs and FFAs, in locally produced apricot kernel, avocado pear and macadamia nut vegetable oils.

Before the vegetable oils could be analysed by  $^{31}\text{P}$  NMR spectroscopy, derivatization of the minor components were required. This is necessary since none of the minor components of interest contain a phosphorous atom in their structures and hence in order to be detected by  $^{31}\text{P}$  NMR spectroscopy the labile hydrogens (of the OH and COOH groups) of the minor components are derivatized using 2-chloro-4,4,5,5-tetramethyldioxaphospholane (further referred to as the P-reagent). Since all of the minor components of interest due to age related acid hydrolysis of triglycerides (1,2 DGs; 1,3 DGs and FFAs) contain an OH-group, the P-reagent can react with the components in a substitution reaction in order to incorporate a tetramethyldioxaphospholinate group into their structures, hence making it possible for them to be detected by  $^{31}\text{P}$  NMR spectroscopy. The general reaction is illustrated in Scheme 2.1<sup>1</sup>.



**Scheme 2.1:** Schematic representation of the reaction of 2-chloro-4,4,5,5-tetramethyldioxaphospholane with the OH-groups present in the minor components yielding the minor component (R) containing a tetramethyldioxaphospholinate group.

Experimentally, the method of Spyros *et al.*<sup>1</sup> was used for the derivitization of the minor components. In this method, the vegetable oil is dissolved in a stock solution, containing CDCl<sub>3</sub>, pyridine, cyclohexanol and Cr(acac)<sub>3</sub>. Each of these compounds plays an important role, namely: *Pyridine* reacts with excess HCl gas formed from the phosphorylation reaction (refer to Scheme 2.1) leading to the formation of a pyridinium hydrochloride salt soluble in CDCl<sub>3</sub>. Pyridine is present in excess relative to the P-reagent, since the P-reagent is still a strong derivatizing reagent and the liberated HCl that develops upon further derivatization is capable of leading to the decomposition of the newly formed derivatized minor components, such as DGs and FFAs. CDCl<sub>3</sub> is firstly a NMR solvent ensuring the dissolution of the vegetable oil, and secondly is required to dissolve the formed pyridinium – HCl salt mentioned. The CDCl<sub>3</sub> is also unstable in light, being able to decompose into HCl over time, so that the pyridine will also scavenge any HCl so produced. *Cyclohexanol* is used as internal standard for quantification purposes. Chromium (III) acetylacetonate (Cr(acac)<sub>3</sub>) is used as relaxation reagent since the Cr<sup>3+</sup> atom is paramagnetic and therefore allows faster relaxation of the <sup>31</sup>P nuclei that are to be detected<sup>2,3</sup>.

Once these minor components have been derivatized and detected by <sup>31</sup>P NMR spectroscopy, quantification of the <sup>13</sup>C resonances gives valuable information on the concentration and identity of minor components present within these vegetable oils. These concentrations change upon aging of the oils as discussed in Chapter 1 and consequently storage of vegetable oils is discussed in this study. Three locally produced vegetable oils, namely apricot kernel, avocado pear and macadamia nut oils were stored in five different ways over a period of 8-30 months in order to investigate the effect of different storage conditions on oil degradation and hence minor component concentrations. These storage conditions included exposed to light, in the dark, in the dark covered in tin foil (to provide better thermal stability), frozen in a freezer at -8° C and stored in a fridge at 5° C.

## 2.2 RESULTS AND DISCUSSION

### 2.2.1 Assignment of the <sup>31</sup>P NMR spectra of the vegetable oils

The <sup>31</sup>P{<sup>1</sup>H} NMR spectra of the derivatized minor components of apricot kernel, avocado pear and macadamia nut oils are shown in Figures 2.1-2.3. The spectra were all referenced to a signal that represents the reaction of water (moisture is

present in the oil) with the P-reagent as recommended in the literature; this compound gives a sharp singlet in pyridine/ $\text{CDCl}_3$  at 132.200 ppm<sup>4</sup>, relative to the generally accepted standard reference in  $^{31}\text{P}$  NMR of 85 % aqueous  $\text{H}_3\text{PO}_4$ . Notice that the  $^{31}\text{P}\{^1\text{H}\}$  NMR spectra of the three vegetable oils of interest are similar to the  $^{31}\text{P}\{^1\text{H}\}$  NMR spectrum of olive oil obtained from the literature<sup>5</sup>, although not identical.

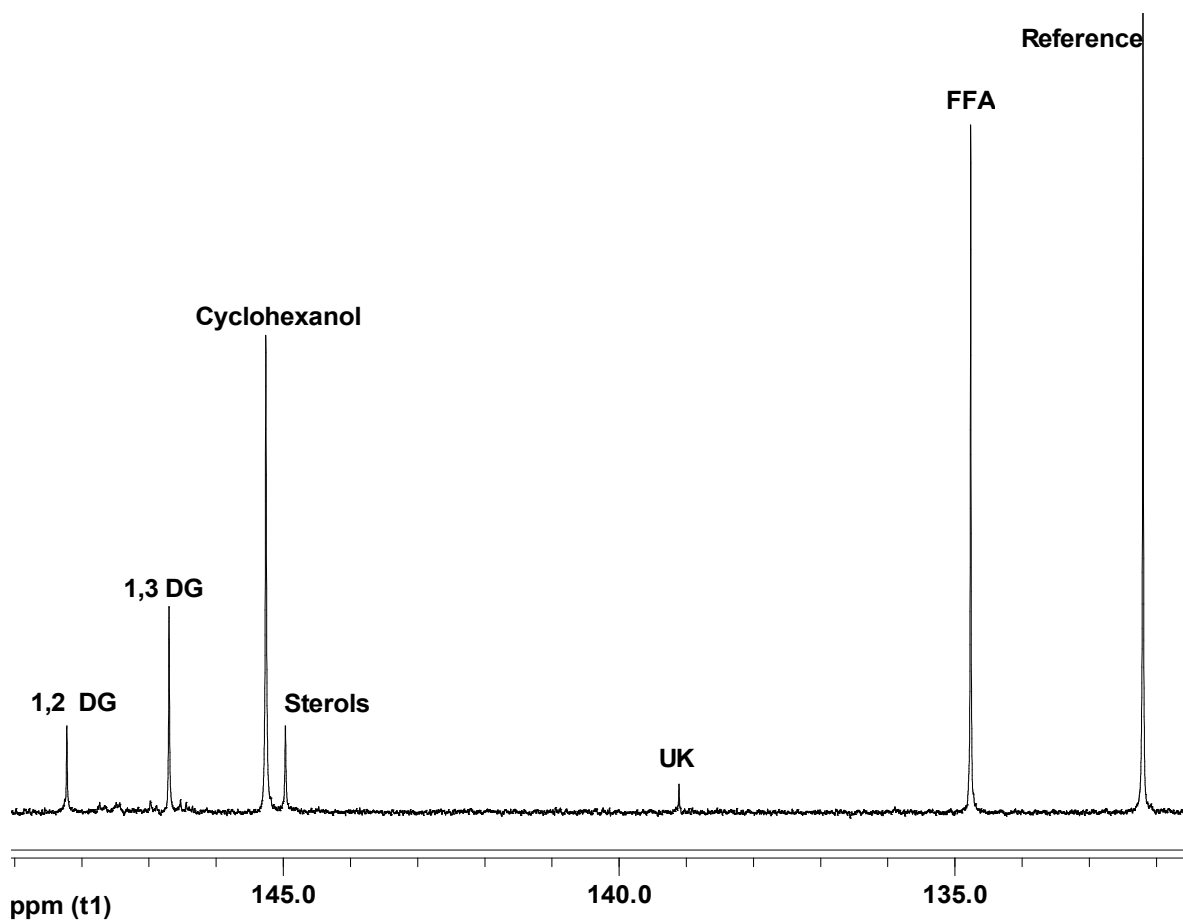


**Figure 2.1:**  $^{31}\text{P}\{^1\text{H}\}$  NMR spectrum of derivatized apricot kernel oil.

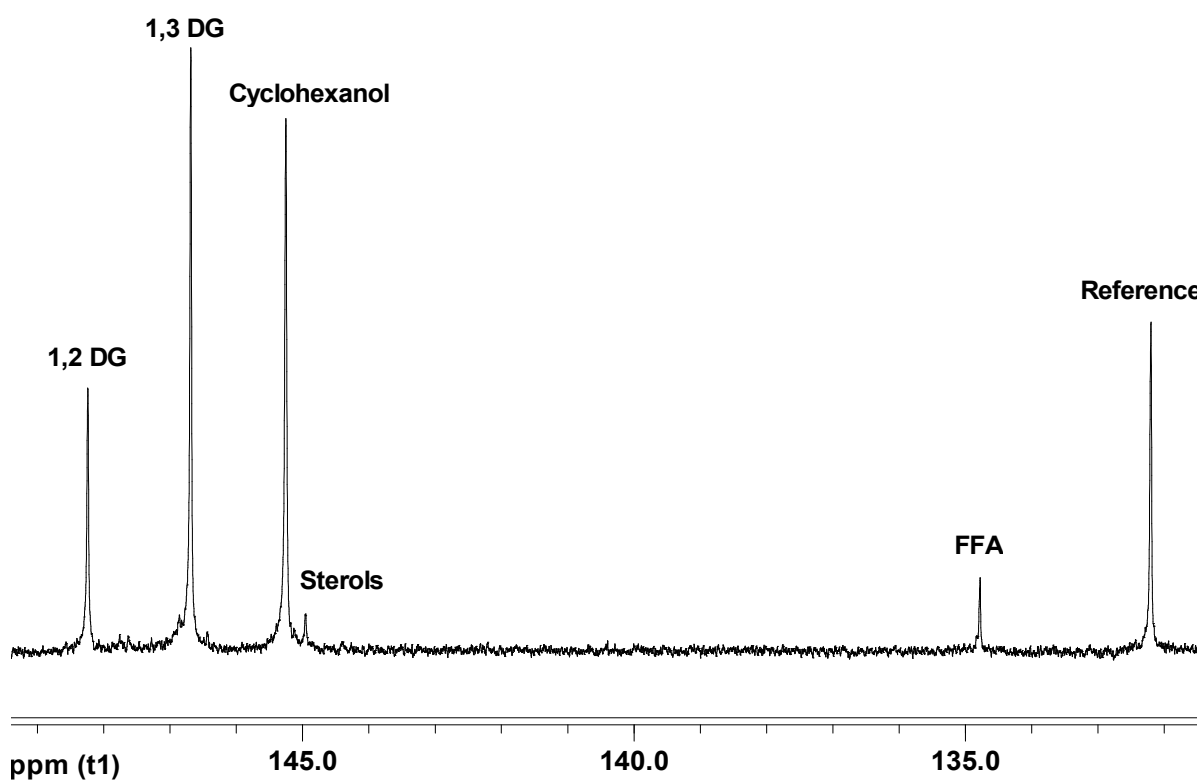


**Figure 2.2:**  $^{31}\text{P}\{^1\text{H}\}$  NMR spectrum of derivatized avocado pear oil.

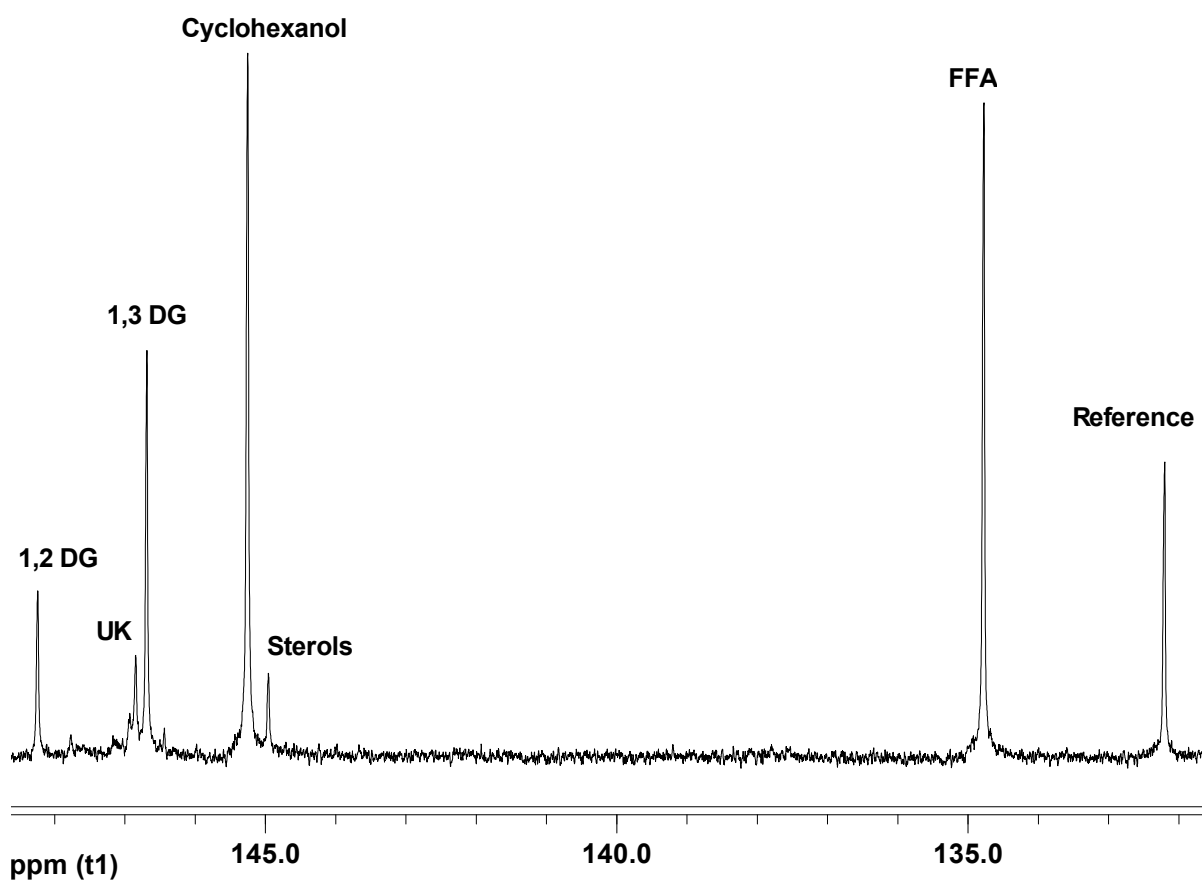


**Figure 2.3:**  $^{31}\text{P}\{^1\text{H}\}$  NMR spectrum of derivatized macadamia nut oil.

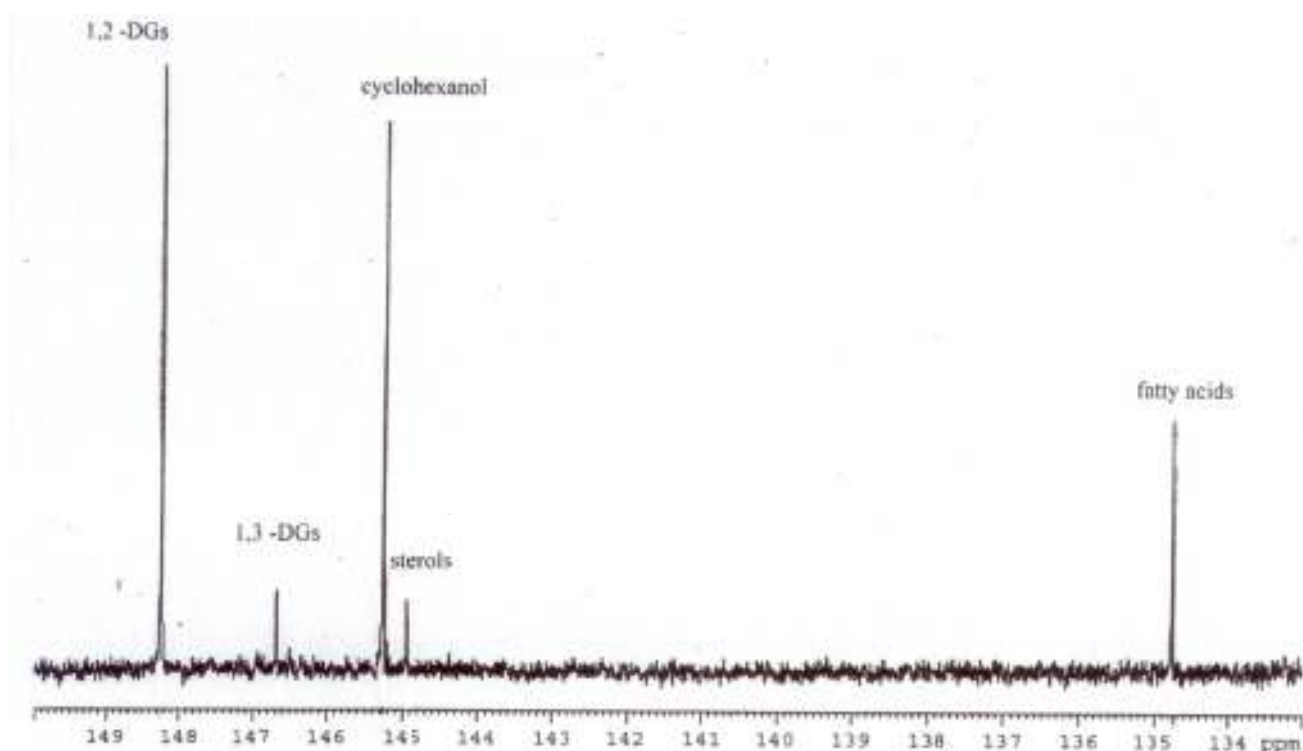


**Figure 2.4:**  $^{31}\text{P}\{^1\text{H}\}$  NMR spectrum of derivatized virgin olive oil taken from Vigli *et al.*<sup>5</sup>.

Due to the similarity of the macadamia nut, apricot kernel and avocado pear vegetable oil spectra with those of the  $^{31}\text{P}\{^1\text{H}\}$  NMR spectrum of olive oil, the majority of the signals in the apricot kernel, avocado pear and macadamia nut oil spectra, representing 1,2 DGs; 1,3 DGs; sterols; FFAs; cyclohexanol and the reference peak, were assigned by comparison to assignments done in the literature for olive oil<sup>1</sup> (refer to Table 2.1). Although similar spectra were obtained for apricot kernel, macadamia nut and avocado pear oils compared to that of olive oil, the spectra were not all identical. Signals are observed in the three vegetable oils that are not present in the olive oil spectrum. These signals are indicated as unknown (UK) on the spectra and in Table 2.1 and are low in concentration as can be observed from the relative intensities. Unknown signals are observed in the  $^{31}\text{P}\{^1\text{H}\}$  spectra for apricot kernel oil at 139.1 ppm and macadamia nut oil at 146.9 ppm. These signals possibly represent polyphenols but due to the low concentrations further work is required to identify them. In the case of each of the compound groups, FFAs, sterols, 1,2 DGs and 1,3 DGs, only one signal is observed representing all the possible compounds present in the vegetable oil, e.g. there is only one signal at 145.0 ppm in the  $^{31}\text{P}\{^1\text{H}\}$  NMR

spectrum of apricot kernel oil, representing all the possible sterols present in the vegetable oil.

**Table 2.1:** Assignment of the  $^{31}\text{P}\{^1\text{H}\}$  NMR spectra of derivatized apricot kernel, avocado pear and macadamia nut oils with comparison to those of derivatized olive oil.

Derivatized compounds of:	Signals present in the $^{31}\text{P}\{^1\text{H}\}$ NMR spectrum of:			
	Apricot kernel oil (ppm)	Avocado pear oil (ppm)	Macadamia nut oil (ppm)	Olive oil (ppm) <sup>1</sup>
Reference/water	132.2	132.2	132.2	132.2
FFA (All)	134.8	134.8	134.8	134.8
UK	139.1			
Sterols (All)	145.0	145.0	145.0	145.0
Cyclohexanol	145.3	145.3	145.3	145.2
UK			146.9	
1,3 DG (All)	146.7	146.7	146.7	146.7
1,2 DG (All)	148.2	148.2	148.2	148.2

### 2.2.2 Quantification of $^{31}\text{P}$ Nuclear Magnetic Resonance spectra

Quantification of the  $^{31}\text{P}\{^1\text{H}\}$  NMR resonances of the FFA and DG components in these spectra, representing the minor compounds present in the vegetable oils, may give information on how storage conditions affect the oil with respect to minor component concentration. Quantification is done by determining the  $^{31}\text{P}\{^1\text{H}\}$  signal integral and hence calculating the concentration of the compound represented by that signal with respect to a reference of known concentration. Care was taken to ensure that the integral was proportional to the concentration by following closely the experimental method recommended by Spyros *et al*<sup>5</sup>. This included the use of an optimum amount of  $\text{Cr}(\text{acac})_3$  to shorten the T1 relaxation of the  $^{31}\text{P}$ -nuclei, addition of a known amount of cyclohexanol as integration standard and use of the same  $^{31}\text{P}$  NMR experimental conditions for all samples. Quantification of the DGs and FFAs were carried out for the samples for different storage conditions and the determination of the concentration of the minor components was performed in two ways.

### 2.2.2.1 Approach 1

Firstly a “direct correlation approach” (DCA) was used, not previously suggested in the literature. This approach is illustrated in Figure 2.5, that upon reaction of 1,2 DGs; 1,3 DGs ; FFAs and cyclohexanol with the P-reagent, one tetramethyldioxaphospholinate group is incorporated into each minor component. Therefore one can assume that the number of moles of P-reagent used to incorporate one tetramethyldioxaphospholinate group into cyclohexanol is proportional to all the derivatized minor components, namely FFAs and DGs. Consequently the integrated area of each signal representing the minor components is proportional to the area integral of the signal representing cyclohexanol. Using the accurately known concentration of cyclohexanol and normalizing the area integral of the derivatized cyclohexanol signal, the molar values of all components could be determined and consequently the concentration of each. For determination of the concentrations, a volume of 0.590 ml (of solution in the NMR tube) was used which included 0.4 ml of the stock solution + 0.175 ml of vegetable oil (150 mg) + 0.015 ml P-reagent). The mole value of cyclohexanol within the sample was determined to be  $8.537 \times 10^{-5} \mu\text{mol}$ . The experimentally determined concentrations of the various minor components in apricot kernel oil are given in Table 2.2 as example.

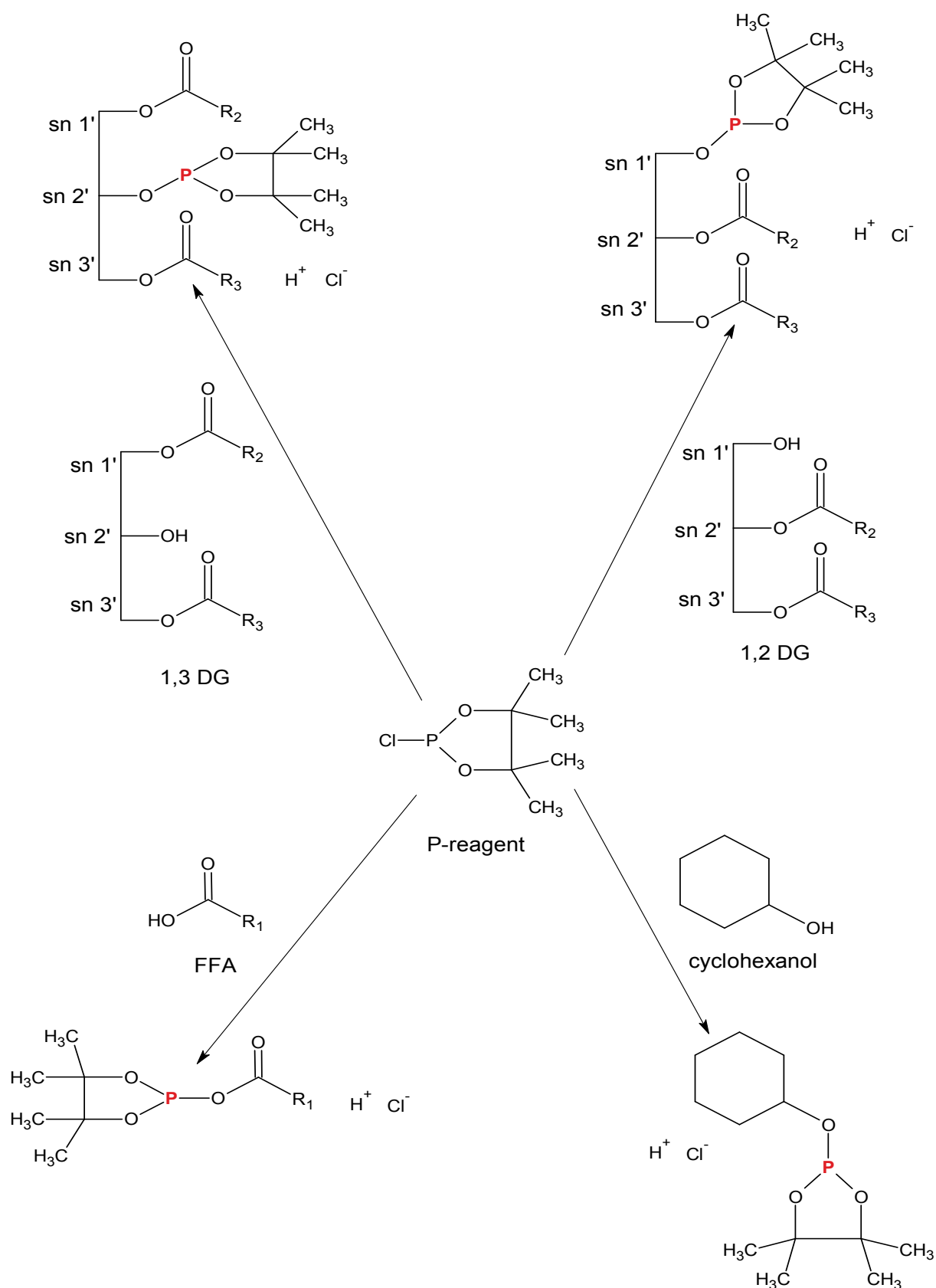


**Figure 2.5:** Illustration of the derivatization of the labile hydrogens present in 1,2 DG; 1,3 DG; FFA and cyclohexanol with 2-chloro-4,4,5,5-tetramethyldioxaphospholane.

**Table 2.2:** Table presenting the integration of the  $^{31}\text{P}\{^1\text{H}\}$  signals and conversion of values to concentration of apricot kernel oil.

Chemical shift (ppm)	Area Integral	Peak assignment	Normalized area integral	Mole value ( $\mu\text{mol}$ )	Concentration $\mu\text{mol/ml}$
148.2	546	1,2 DG	0.153	<0.001	0.221
146.7	1056	1,3 DG	0.295	<0.001	0.426
<b>145.3</b>	<b>3576</b>	<b>cyclohexanol</b>	<b>1.000</b>	<b>0.001</b>	<b>1.447</b>
145.0	573	sterol	0.160	<0.001	0.232
134.8	279	FFA	0.782	0.001	1.131
132.2	6884	water/ref	1.925	0.002	2.785

An average of five integration values of the signal representing the cyclohexanol derivative was determined for five vegetable oil NMR samples in order to determine the relative error percentage of the NMR method. This error was calculated using standard deviation at 95 % CL incorporating the student's t value for five samples. The relative percentage error was found to be 10.4 % and consequently this value was used as a reasonable estimate of the concentration error in the minor components as indicated in Table 2.3.

**Table 2.3:** Concentration in  $\mu\text{mol/ml}$  of 1,2 DGs; 1,3 DGs and FFAs present in fresh apricot kernel, avocado pear and macadamia nut oils.

	1,2 DG concentration ( $\mu\text{mol/ml}$ )	1,3 DG concentration ( $\mu\text{mol/ml}$ )	FFA concentration ( $\mu\text{mol/ml}$ )
<b>Apricot kernel</b>	0.221 $\pm$ 0.023	0.426 $\pm$ 0.023	1.131 $\pm$ 0.023
<b>Avocado pear</b>	0.781 $\pm$ 0.081	1.619 $\pm$ 0.081	0.141 $\pm$ 0.081
<b>Macadamia nut</b>	0.364 $\pm$ 0.038	1.601 $\pm$ 0.038	1.257 $\pm$ 0.038

#### 2.2.2.2: Approach 2

A second approach was suggested in the literature<sup>1</sup> and made use of separately establishing calibration curves<sup>1</sup> and referred to as the “calibration curve approach” (CCA). Standard DGs and FFAs, namely 1,2 dipalmitin; 1,3 dilinolein and oleic acid, were weighed and used to make up solutions with known concentrations. The prepared concentrations for 1,2 DGs were 0.11, 0.16, 0.30 and 0.48  $\mu\text{mol/ml}$ ; for 1,3 DGs were 1.07, 1.39, 2.54 and 3.33  $\mu\text{mol/ml}$ ; for FFAs were 1.27, 2.54, 3.80, 5.10 and 6.34  $\mu\text{mol/ml}$ . Known quantities of these solutions were derivatized and the  $^{31}\text{P}\{^1\text{H}\}$  NMR spectra of the derivatized samples were obtained using the conditions

as defined in Section 2.4.5. As in Sections 2.4.4 and 2.2.1, an exact known concentration of cyclohexanol was added to the stock solution as an internal standard and the peaks in a spectrum could then be integrated and normalized with respect to the cyclohexanol  $^{31}\text{P}\{^1\text{H}\}$  signal integral. A calibration curve was constructed for each standard, where the known concentration of the 1,3 DG; 1,2 DG or FFA sample was plotted on the x-axis against the measured signal integral of the standard with respect to the cyclohexanol internal standard on the y-axis. A linear correlation was obtained for each (refer to Figures 2.6-2.8).

Errors and confidence limits of the calibration curves were estimated as recommended in the literature<sup>6</sup> and are shown in Table 2.4 which lists the confidence limits for the true slope and intercept values of each calibration curve.

**Table 2.4:** True slope and intercept at 95 % CL of the standard calibration curves.

	True slope (at 95 % CL)			% relative error	True intercept (at 95 % CL)		
<b>1,2 DG</b>	0.866	+	0.043	4.95	-0.021	±	0.032
<b>1,3 DG</b>	1.045	+	0.097	9.31	-0.232	±	0.221
<b>FFA</b>	0.547	+	0.506	92.47	0.024	±	0.593

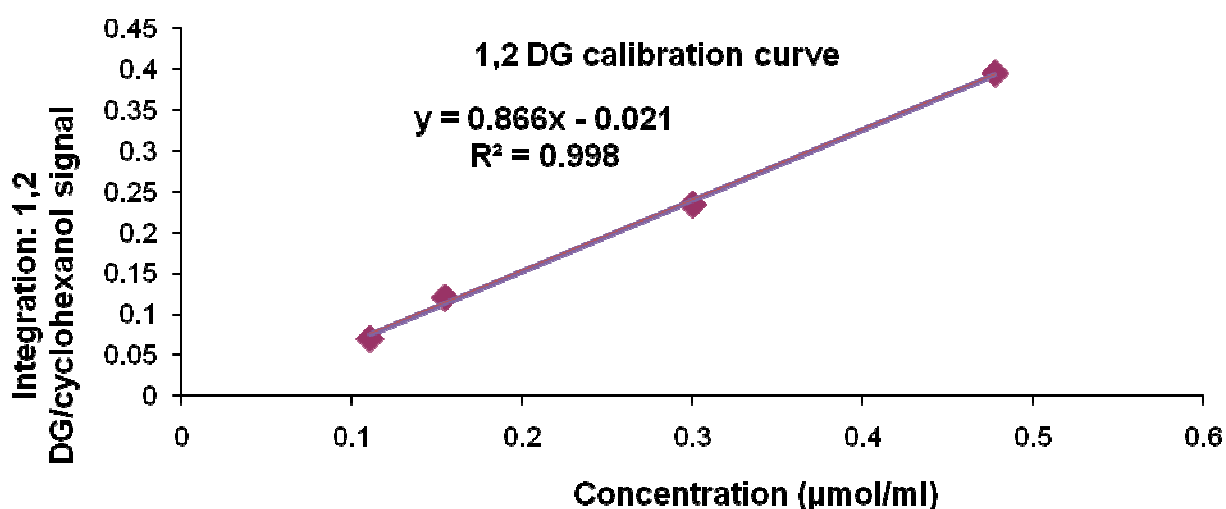


**Figure 2.6:** Calibration curve for 1,2 dipalmitin (1,2 DG standard).

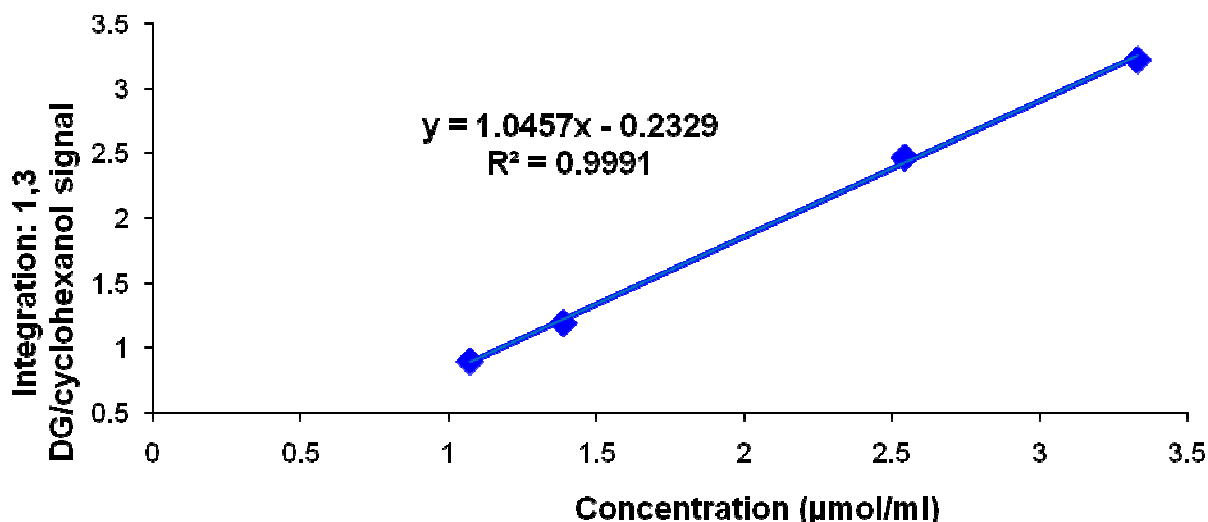


Figure 2.7: Calibration curve for 1,3 dilinolein (1,3 DG standard).

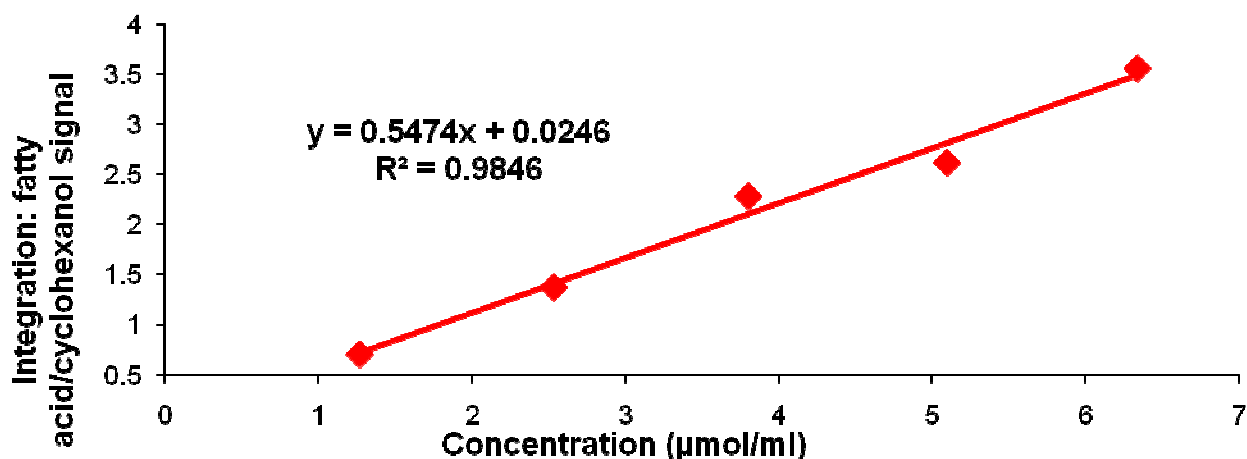


Figure 2.8: Calibration curve for oleic acid (FFA standard).

These calibration curves could be used to determine the concentrations of corresponding compounds present in fresh apricot kernel, avocado pear and macadamia nut vegetable oils. This was done by determining the integration value for each 1,2 DG; 1,3 DG and FFA component of interest with respect to the cyclohexanol area integral from the  $^{31}\text{P}\{^1\text{H}\}$  NMR spectra. The integration value could then be used to calculate the concentration, as read off from the relevant standard curve. Table 2.5 presents these results. Error values for each of the concentration values determined were calculated<sup>6</sup> incorporating the already calculated standard deviations as determined for the calibration curves in Table 2.4.

**Table 2.5:** Concentration in  $\mu\text{mol/ml}$  of 1,2 DGs; 1,3 DGs and FFAs present in fresh apricot kernel, avocado pear and macadamia nut oils.

	<b>1,2 DG concentration (<math>\mu\text{mol/ml}</math>)</b>	<b>1,3 DG concentration (<math>\mu\text{mol/ml}</math>)</b>	<b>FFA concentration (<math>\mu\text{mol/ml}</math>)</b>
<b>Apricot kernel</b>	0.200 $\pm$ 0.008	0.503 $\pm$ 0.067	1.138 $\pm$ 0.203
<b>Avocado pear</b>	0.566 $\pm$ 0.022	1.296 $\pm$ 0.049	0.135 $\pm$ 0.292
<b>Macadamia nut</b>	0.313 $\pm$ 0.009	1.601 $\pm$ 0.046	1.534 $\pm$ 0.184

Comparing the data in Tables 2.3 and 2.5, the two approaches give very similar results. For apricot kernel oil and macadamia nut oil, the two approaches yield similar results for DGs (1,2 and 1,3 DGs) and FFAs concentrations. However for avocado pear oil the results do not compare well for any of the DGs or FFA concentrations.

A possible explanation for the disagreement of results for avocado pear oil between the CCA and DCA methods could be due to matrix effects that interfere with the derivatization. Both the CCA and DCA methods relies on assuming that the reaction yields upon derivitization with the P-reagent are the same for the different OH or COOH species as for the internal standard-cyclohexanol. However from related studies with the P-reagent, this does not seem to be the case as DeSilva *et al.*<sup>7</sup> indicated in their research that reaction yields are varied by class, with long chain alcohols showing the highest reactivity (> 95 % yield), glycerides and cholesterol (> 90 % yield; lyso lipids ( $\pm 65$  %), fatty acids ( $\pm 75$  %) yield, aldehydes (40 %).

In conclusion, both the approaches used (namely CCA and DCA) for the determination of 1,2 DG, 1,3 DG and FFA concentrations in apricot kernel oil and macadamia nut oil lead to similar results, lending confidence in the methods for these two vegetable oils with avocado pear oil being the exception.

### 2.2.3 Limit of Detection and Limit of Quantification

Limit of Detection (LOD) is the least amount of material the instrument can detect because it yields an instrument response significantly greater than a blank<sup>8,9</sup>. For NMR spectroscopy the LOD for a signal is commonly defined as when that signal has a 3:1 signal to noise ratio and the following equation is used to calculate the concentration:

$$LOD = \frac{kS_B}{m}$$

where k is 3 due to the 3:1 signal to noise ratio,  $S_B$  is the standard deviation of five determinations of the blank signal and m is the slope of the calibration curve. Dayrit *et al.*<sup>8</sup> used  $^{31}\text{P}$  NMR spectroscopy on coconut oils and they determined their blank by comparison of the integration between their internal standard and external standard, but since in this study only an internal standard was present; an integration value of the noise (as blank) with respect to the internal standard was used. This was determined working with a 1 ppm area in the NMR spectrum of each of the three oils and choosing 20 random points (signals due to noise) on the baseline.

The Limit of Quantification (LOQ) is the least amount of material that can be quantified using a similar calculation as for determining the LOD<sup>7</sup>. The equation used:

$$LOQ = \frac{kS_B}{m}$$

changes so that k is 10 times the relative  $S_B$  since a 10:1 signal to noise ratio is typically defined as reliably to quantify a signal for NMR spectroscopy (and many other techniques)<sup>10</sup>.

Table 2.6 indicates these values determined for each of the three vegetable oils of interest. In the table a range of values are given for the LOQ and LOD due to incorporation of the error of the slope (given by Table 2.4) since the slope value m is used within the equations to determine the LOD and LOQ values.

**Table 2.6:** LOD and LOQ values determined for apricot kernel, avocado pear and macadamia nut oil analysis by NMR spectroscopy.

		<b>Apricot kernel oil concentration (μmol/ml)</b>	<b>Avocado pear oil concentration (μmol/ml)</b>	<b>Macadamia nut oil concentration (μmol/ml)</b>
	$S_B$	<0.001	0.002	0.003
<b>1,2 DG</b>	LOD	0.001	0.006	0.011
	LOQ	0.003	0.019	0.037
<b>1,3 DG</b>	LOD	0.001	0.005	0.009
	LOQ	0.002	0.016	0.031
<b>FFA</b>	LOD	0.001	0.009	0.018
	LOQ	0.004	0.030	0.059

From data in Table 2.6, in apricot kernel oil a lowest limit of <0.001 μmol/ml concentration of 1,2 DGs was detectable while the lowest limit of concentration

quantifiable was found to be 0.003  $\mu\text{mol/ml}$ . For avocado pear oil these values were slightly higher with a lowest limit of 0.006  $\mu\text{mol/ml}$  detectable and 0.0019  $\mu\text{mol/ml}$  quantifiable. Macadamia nut had the lowest detection limit of 0.011  $\mu\text{mol/ml}$  and the lowest quantifiable limit of 0.037  $\mu\text{mol/ml}$ . Considering the calibration curve data (Table 2.5), the values used to set up the calibration curve for 1,2 DGs are all well above the LOD and LOQ values found for all three vegetable oils, with the lowest value of around 0.1  $\mu\text{mol/ml}$  used, so that in this context it validates the quantitative methods used here. The same situation is observed for the 1,3 DGs and FFAs, where the lowest concentration used for both the calibration curves were around 1  $\mu\text{mol/ml}$ , which is well above the LOD and LOQ values for all three of the vegetable oils in Table 2.6.

Therefore the method used for  $^{31}\text{P}\{^1\text{H}\}$  NMR spectroscopy as well as both the approaches (CCA and DCA) to determine minor component concentrations present in vegetable oils give results reliably above the LOD and LOQ values calculated for the method.

#### **2.2.4 Storage of vegetable oils**

Three vegetable oils (namely apricot kernel, macadamia nut and avocado pear oils) were stored under three conditions. These included storage in the dark, exposed to light, in the dark covered in tinfoil, in a fridge at 5 °C and frozen at -8 °C. Two separate vegetable oil batches were stored at different lengths of time, namely 8 and 27 months for apricot kernel oil; and 8 and 30 months for avocado pear and macadamia nut oils.  $^{31}\text{P}\{^1\text{H}\}$  NMR spectroscopy was used to investigate the effect that storage conditions had on the vegetable oils with respect to formation of minor components and their concentration. Samples of each of these oils stored by different methods were taken for  $^{31}\text{P}$  NMR analysis from the two batches at different times. CCA and DCA approaches were used to analyze the results obtained by  $^{31}\text{P}$  NMR spectroscopy.

Quantitative data obtained from the  $^{31}\text{P}\{^1\text{H}\}$  NMR experiments carried out on each oil were represented in graphs of the concentrations of 1,2 DG; 1,3 DG and FFA components present in the oils. On each graph the concentrations (in  $\mu\text{mol/ml}$ ) were plotted on the primary y-axis and their corresponding percentages (w/w) on the secondary y-axis against the five different storage conditions on the x-axis as

individually determined by the two approaches (namely CCA and DCA). Quantitative results of samples stored at two different time periods were also plotted. Errors were determined as explained earlier in this chapter, with the errors for CCA calculated on each individual sample used, while the error value of 10.4 % was used for DCA as estimated in Section 2.2.2.1.

#### 2.2.4.1 Apricot kernel oil

Results obtained from the  $^{31}\text{P}\{^1\text{H}\}$  NMR experiments of apricot kernel oil are given in Figures 2.9-2.11. Figure 2.9 shows the results obtained for the concentration of 1,2 DGs present in apricot kernel oil. Similar results were observed for the two approaches (namely CCA and DCA) for the determination of concentrations. Both methods gave comparable concentrations of 1,2 DGs found for each storage condition. For both time periods, the concentrations as determined by DCA were slightly higher than that by CCA. Results between the different storage conditions were similar although it would seem as if cooler storage conditions, namely at 5 °C and -8 °C, led to the least amount of 1,2 DGs forming. It is expected that the lower the concentration of the minor component, the better the storage method is due to less degradation of the TGs to DGs and FFAs. Strangely enough storage at longer lengths of time (27 months) lead to lower concentrations of 1,2 DGs with comparison to storage at shorter times (8 months). This is not an indication that longer storage times led to less oil degradation since the process of TG breakdown to DGs and FFAs is irreversible. The lower concentration of components at longer storage times is most likely correlated due to some of the components precipitating out of solution. Sediment was observed in the samples stored for longer periods and resembled waxy substances under a microscope and was confirmed to contain fatty acid chains with  $^{13}\text{C}$  NMR spectroscopy.

Variation in 1,2 DG concentration with different storage methods

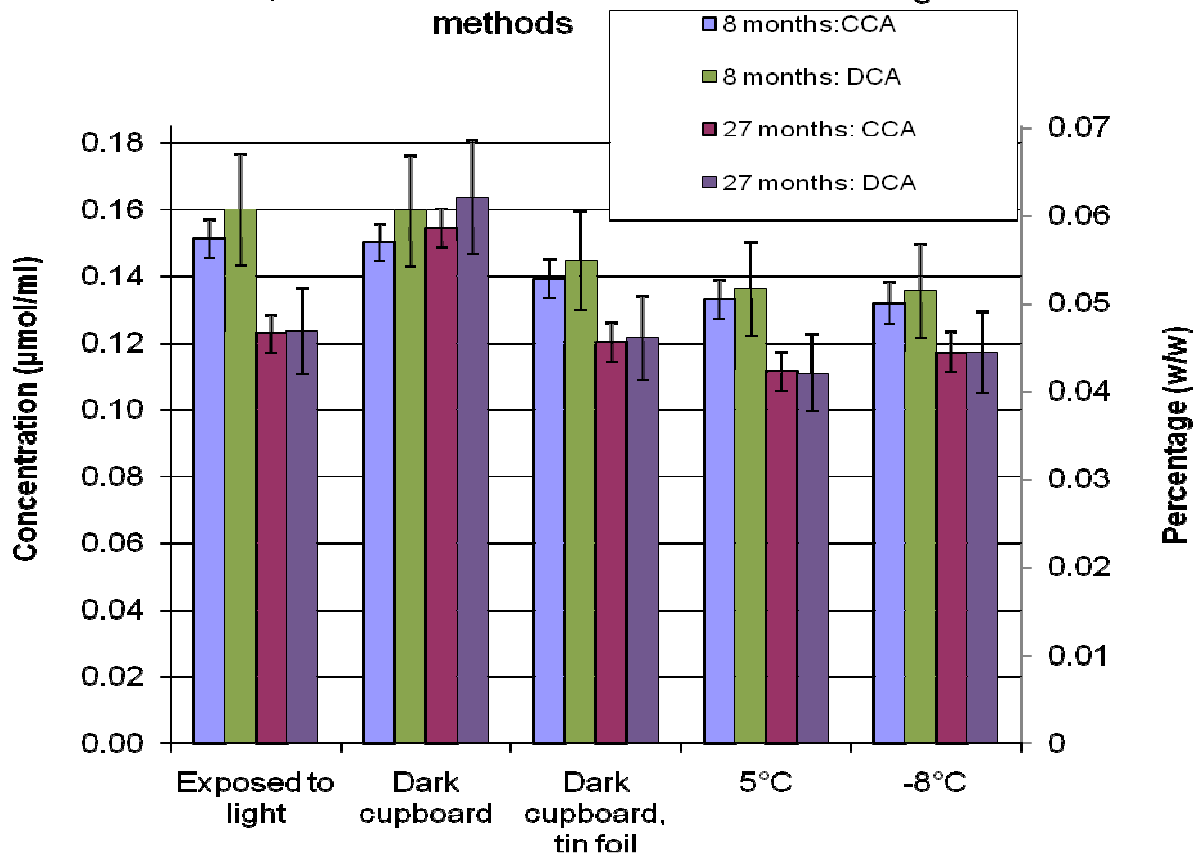


**Figure 2.9:** Variation in 1,2 DG concentration with different storage methods for apricot kernel oil using the direct correlation approach (DCA) and the calibration curve approach (CCA), with error bars ranging from 3.7 % (CCA) to 10.4 % (DCA).

Figure 2.10 illustrates the results obtained for the concentration of 1,3 DGs present in apricot kernel oil. Unlike the situation for 1,2 DGs, similar results were not obtained between CCA and DCA. For both time periods, the concentrations as determined by DCA were much lower than that by CCA for all five storage conditions. There is however still a consistent trend between the storage conditions for both time periods and both methods. Due to the larger error bars of the DCA method, conclusions on the best storage conditions could not be made while the smaller error bars from CCA however indicate that storage at 5 °C led to the least amount of 1,3 DGs forming. Also storage after 27 months and storage after 8 months yield similar results whether it's determined by DCA or CCA.

Variation in 1,3 DG concentration with different storage methods

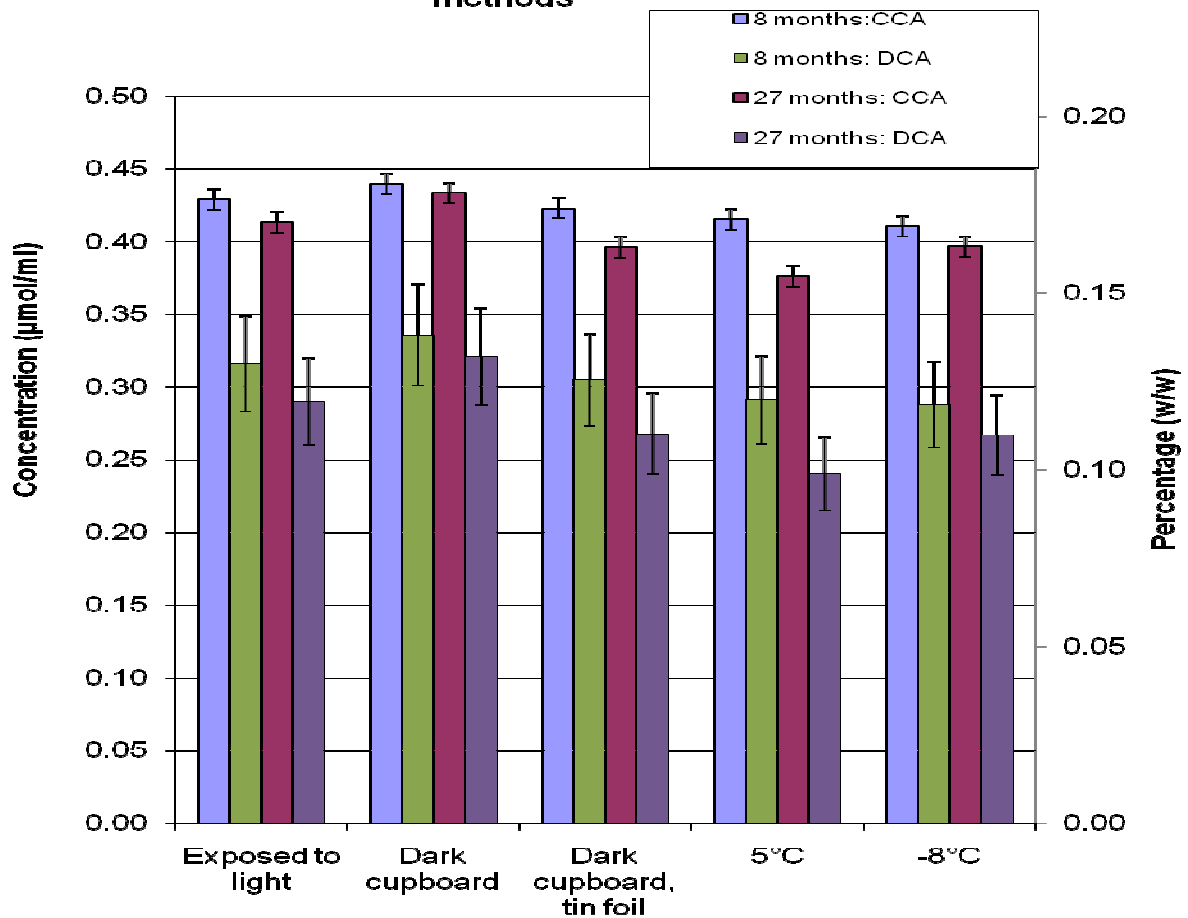


**Figure 2.10:** Variation in 1,3 DG concentration with different storage methods for apricot kernel oil using the direct correlation approach (DCA) and the calibration curve approach (CCA), with error bars ranging from 1.3 % (CCA) to 10.4 % (DCA).

Figure 2.11 illustrates the results obtained for the concentration of FFAs present in apricot kernel oil. The error bars for CCA results are very large making it difficult to compare this method to DCA. This could be an indication that the CCA method is not adequate for application to FFA analysis, for reasons that are yet unknown. Although the DCA results indicated a consistent trend between the storage conditions, it is not possible to differentiate between the storage conditions and consequently no conclusions can be drawn on the best storage method.

**Variation in FFA concentration with different storage methods**

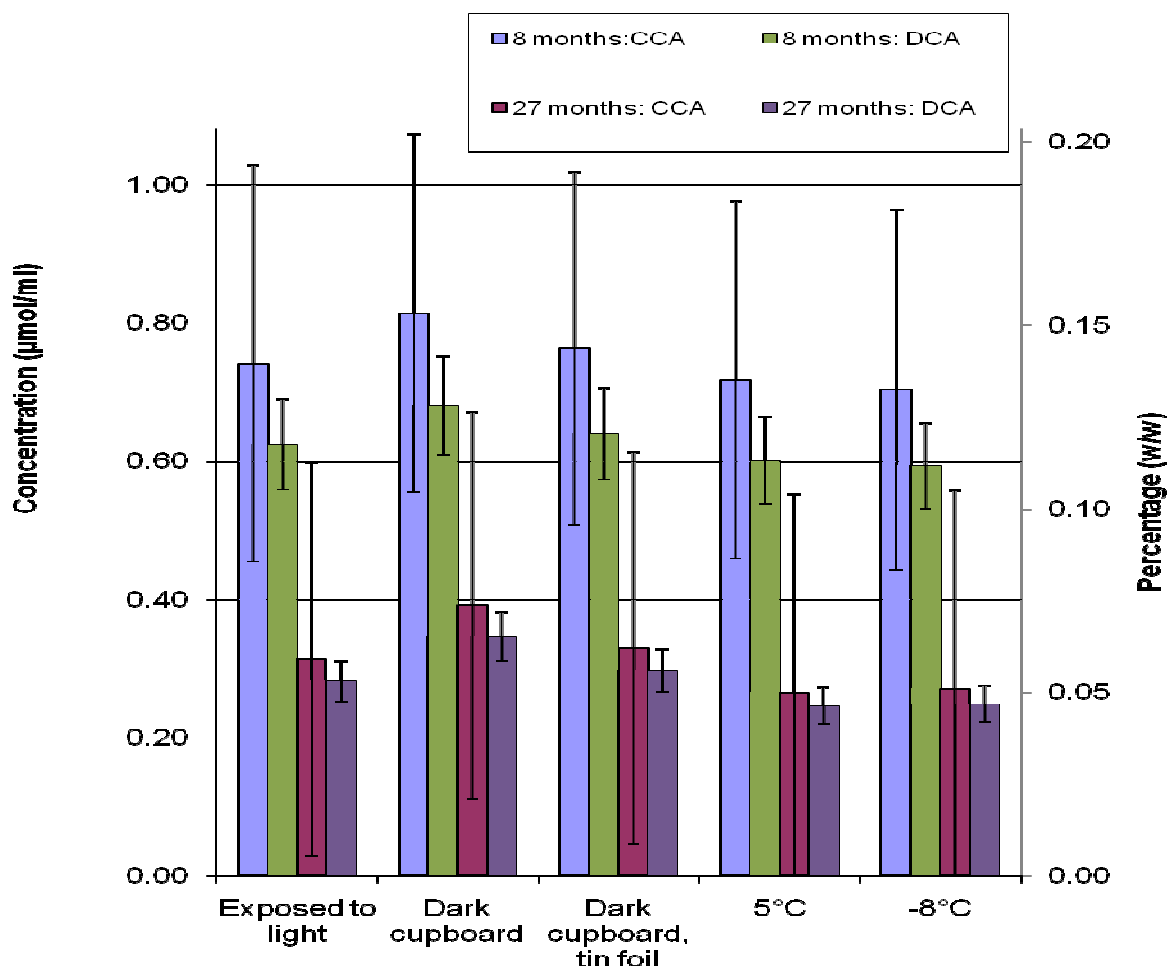


**Figure 2.11:** Variation in FFA concentration with different storage methods for apricot kernel oil using the direct correlation approach (DCA) and the calibration curve approach (CCA), with error bars ranging starting from 10.4 % (DCA).

#### 2.2.4.2 Macadamia nut oil:

Results obtained from the  $^{31}\text{P}\{^1\text{H}\}$  NMR experiments done on macadamia nut oil are indicated in Figures 2.12-2.14. Figure 2.12 illustrates the results obtained for the concentration of 1,2 DGs present in macadamia nut oil. Similar results were observed between CCA and DCA for the comparable concentrations of 1,2 DG determined for each storage condition. For both time periods, the concentrations as determined by DCA were slightly higher than those by CCA. Results between the different storage conditions are quantitatively very close although it would seem as if storage at lower temperatures, namely storage in a fridge at 5 °C and storage in a freezer at -8 °C led to the least amount of 1,2 DGs forming. A trend consistent with apricot kernel oil is

seen for storage at longer lengths of time (30 months) leading to lower concentrations of 1,2 DGs with comparison to storage at shorter times (8 months) with exception of storage in light. In this case oils stored with exposure to light for 30 months had a much higher concentration of 1,2 DGs than those stored for 8 months as is expected since longer storage times lead to more oil degradation. The highest concentration of 1,2 DG is seen for oils stored after 30 months with exposure to light indicating this to be the worst possible storage condition for longer periods of time.

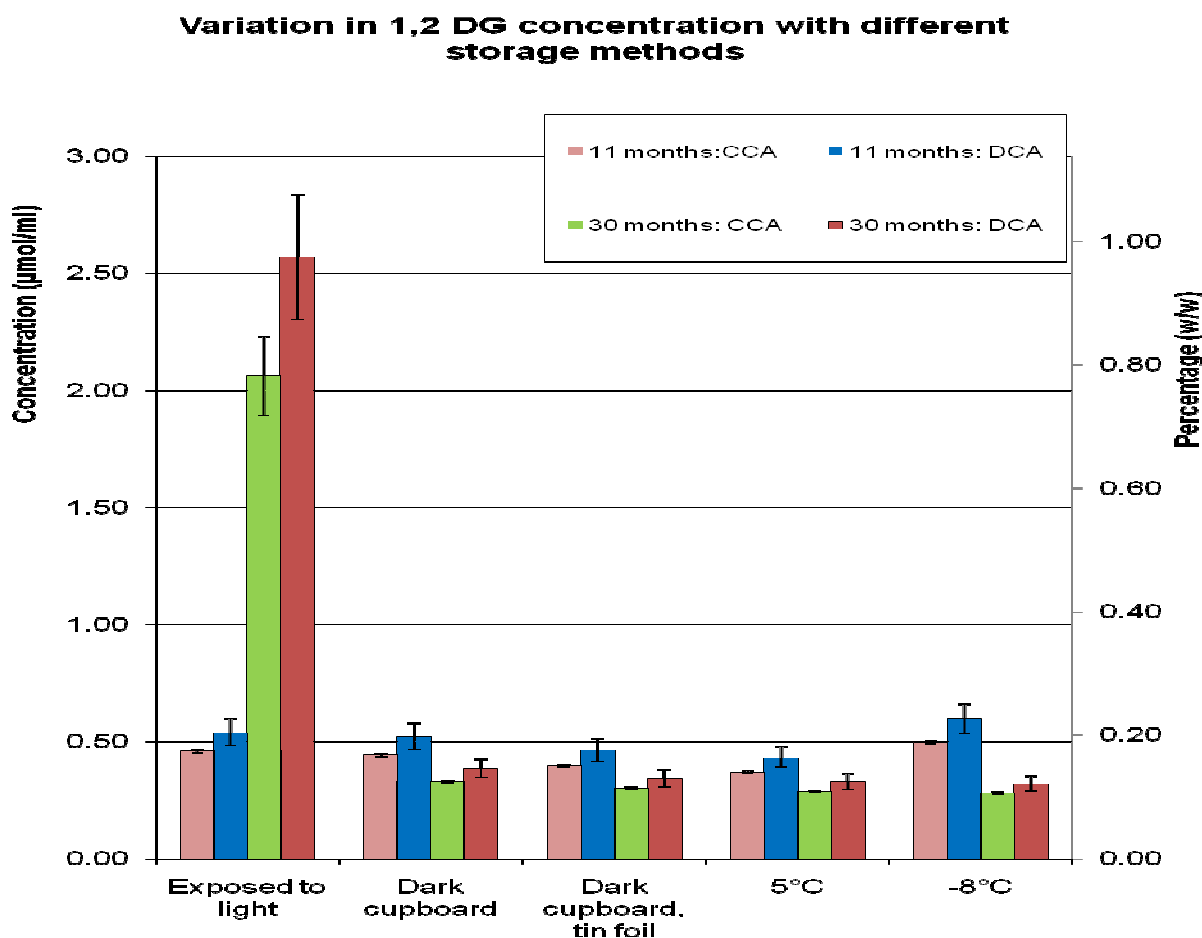
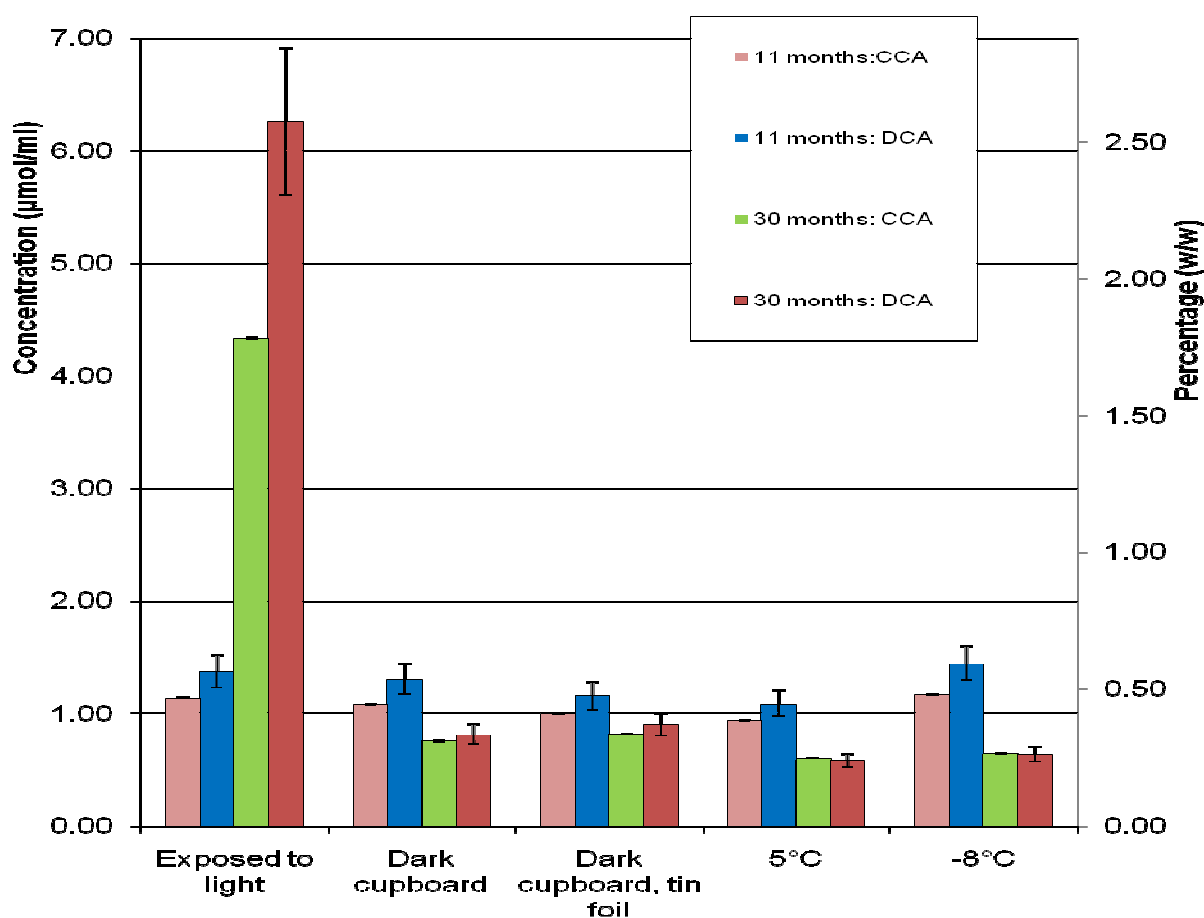


**Figure 2.12:** Variation in 1,2 DG concentration with different storage methods for macadamia nut oil using the direct correlation approach (DCA) and the calibration curve approach (CCA), with error bars ranging from 1.5 % (CCA) to 10.4 % (DCA).

Figure 2.13 illustrates the results obtained for the concentration of 1,3 DGs present in macadamia nut oil. Similar results are observed as for the 1,2 DGs with DCA and CCA yielding comparable concentrations of 1,3 DGs found for each storage condition. For both time periods, the concentrations as determined by DCA were slightly higher than that by CCA. Results between the different storage conditions are

once again similar with the best storage conditions being in a fridge at 5 °C and storage in a freezer at -8 °C. Once again a consistent trend was seen for storage at longer lengths of time (30 months) leading to lower concentrations of 1,3 DGs with comparison to storage at shorter times (8 months) with exception of storage in light. As was the case for the 1,2 DGs; the highest concentration of 1,3 DG is seen for oils stored after 30 months with exposure to light indicating this to be the worst possible storage condition for longer periods of time.

**Variation in 1,3 DG concentration with different storage methods**



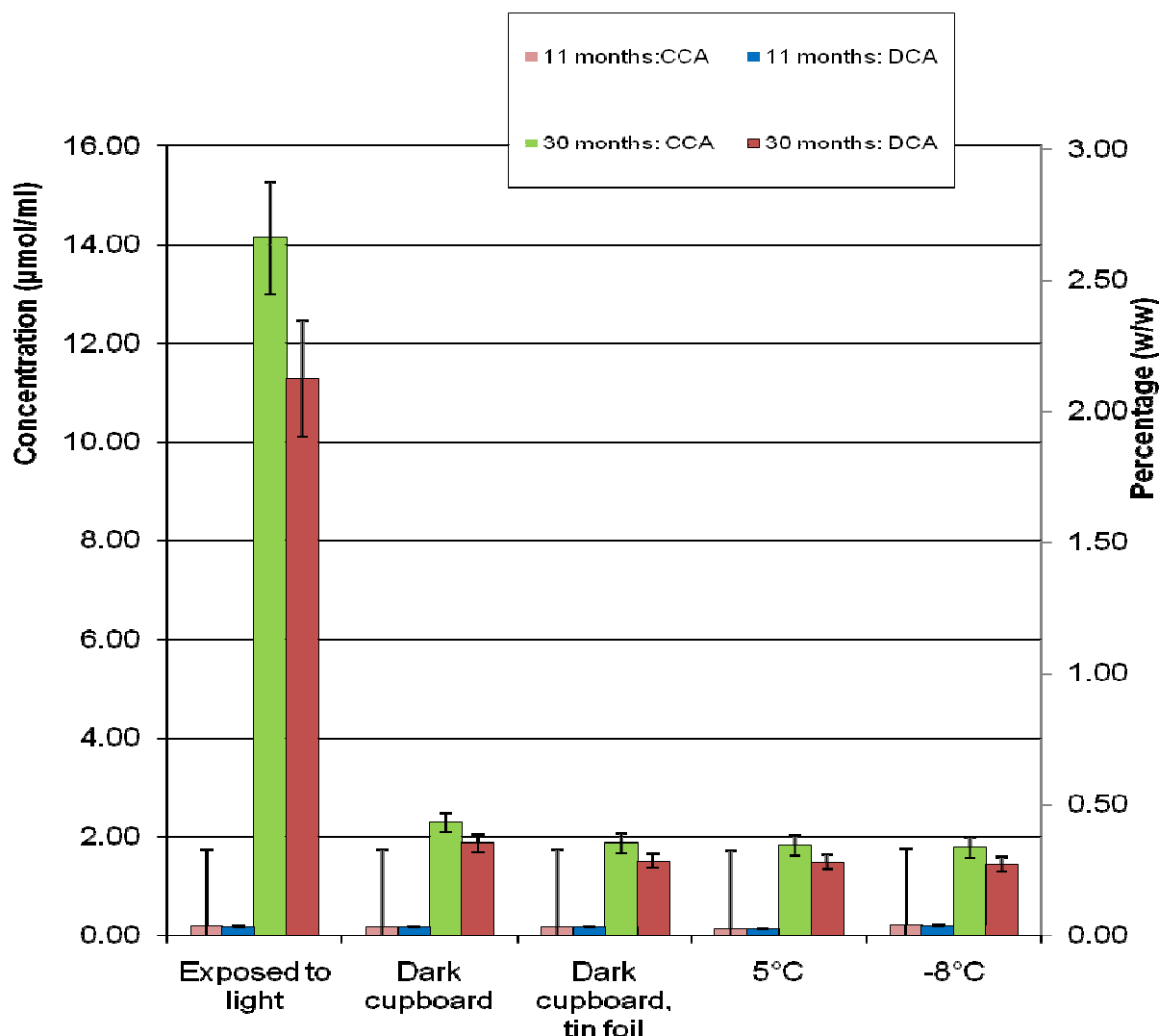
**Figure 2.13:** Variation in 1,3 DG concentration with different storage methods for macadamia nut oil using the direct correlation approach (DCA) and the calibration curve approach (CCA), with error bars ranging from 0.2 % (CCA) to 10.4 % (DCA).

Figure 2.14 illustrates the results obtained for the concentration of FFAs present in macadamia nut oil. Similar results were observed between CCA and DCA for storage of the oils after 30 months having comparable concentrations of FFAs found for each

storage condition. However for storage after 11 months, quantitative values determined by CCA yield results with error bars reaching into the negative, making it difficult to compare this data to that of DCA results obtained. These larger error bars could once again be an indication that the CCA method is not adequate for FFA concentration determination. Based on the results in Figure 2.14 it was not possible to distinguish which of the different storage conditions were the best, although storage after 30 months upon exposure to light yielded the highest concentration of FFAs and consequently it could be concluded that this was the worst storage condition.

Spyros *et al.*<sup>11</sup> found that the formation of DGs and FFAs in olive oil were much faster upon storage of the oil in the light than in the dark and since it is observed that for macadamia nut oil 1,2 DGs; 1,3 DGs and FFAs the worst storage condition is upon exposure to light, it could be that macadamia nut oil in particular has some minor component that decomposes upon exposure to light faster than for other oils (since this rapid increase in components were not observed for apricot kernel oil for instance) which in turn catalyses the TG decomposition.

### Variation in FFA concentration with different storage methods



**Figure 2.14:** Variation in FFA concentration with different storage methods for macadamia nut oil using the direct correlation approach (DCA) and the calibration curve approach (CCA), with error bars starting from 8.1 % (CCA).

#### 2.2.4.3 Avocado pear oil

Results obtained from the  $^{31}\text{P}\{^1\text{H}\}$  NMR experiments done on avocado pear oil are indicated in Figures 2.15-2.17. 1,2 DG; 1,3 DG and FFA concentrations could not be determined for storage of avocado pear oil at the lower temperatures as well as storage in a dark cupboard wrapped in tin foil for storage after 30 months since quantification could not be done on the NMR spectral signals due to the absence of the reference signals and FFA signals in each case. This could most likely be due to the excessive fall out of minor components out of the oil after long periods of time

and hence the concentration of minor components left in the avocado pear solution after 30 months was not sufficient (high enough) to be detected by NMR spectroscopy. Therefore for comparative purposes on storage conditions only results obtained for storage after 11 months are discussed further.

Figure 2.15 illustrates the results obtained for the concentration of 1,2 DGs present in avocado pear oil. Similar results were observed for DCA and CCA with comparable concentrations of 1,2 DGs found for each storage condition. For all storage conditions the concentrations as determined by DCA was slightly higher than that by CCA. Results between the different storage conditions are quantitatively very close although the best storage seems to be at a temperature of 5 °C with the worst being at -8 °C. This is unexpected since usually the lower the temperature the lesser the amount of degradation. However avocado pear with its green coloured oil contains other compounds that could possibly affect the results in a way unknown to us yet.

**Variation in 1,2 DG concentration with different storage methods**

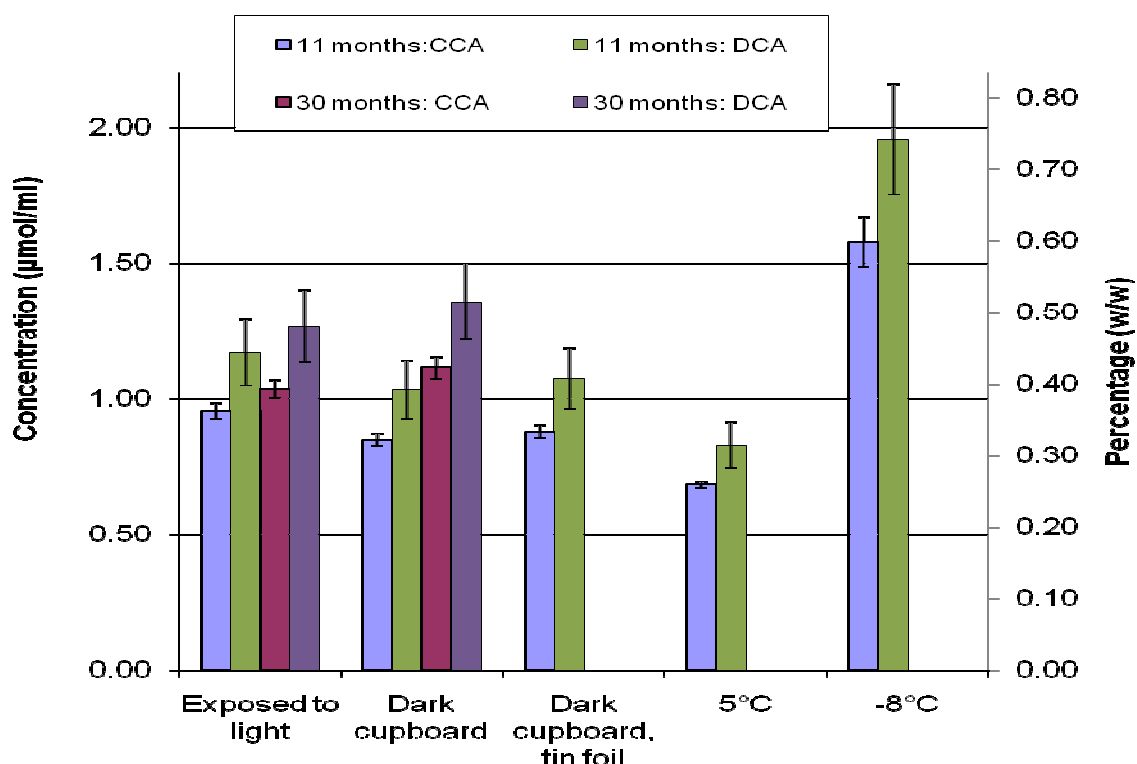


**Figure 2.15:** Variation in 1,2 DG concentration with different storage methods for avocado pear oil using the direct correlation approach (DCA) and the calibration curve approach (CCA), with error bars ranging from 2.1 % (CCA) to 10.4 % (DCA).

Figure 2.16 illustrates the results obtained for the concentration of 1,3 DGs present in avocado pear oil. Unlike the situation for 1,2 DGs similar results were not observed between CCA and DCA for storage at 11 months. Although there was a fairly consistent trend between the storage conditions, the results obtained by DCA were always higher than those obtained by CCA with the exception of the oil stored in a dark cupboard and wrapped in tin foil. In this case the concentrations of 1,3 DGs was much higher as determined by CCA than DCA. Since this was not observed for the 1,2 DGs it could be considered an erroneous calculation and hence an outlier but due to the avocado pear's green colour and the presence of other unknown compounds this data was not so easily discarded. The oil could contain other compounds that could possibly affect the results unknown to us yet. Strangely enough the best storage condition seemed to be storage in a dark cupboard (no tin foil), possibly suggesting that covering the sample in tinfoil results in faster degradation (due to heat from thermal properties of the tin foil) which could lead to the increased the 1,3 DG concentration.

**Variation in 1,3 DG concentration with different storage methods**

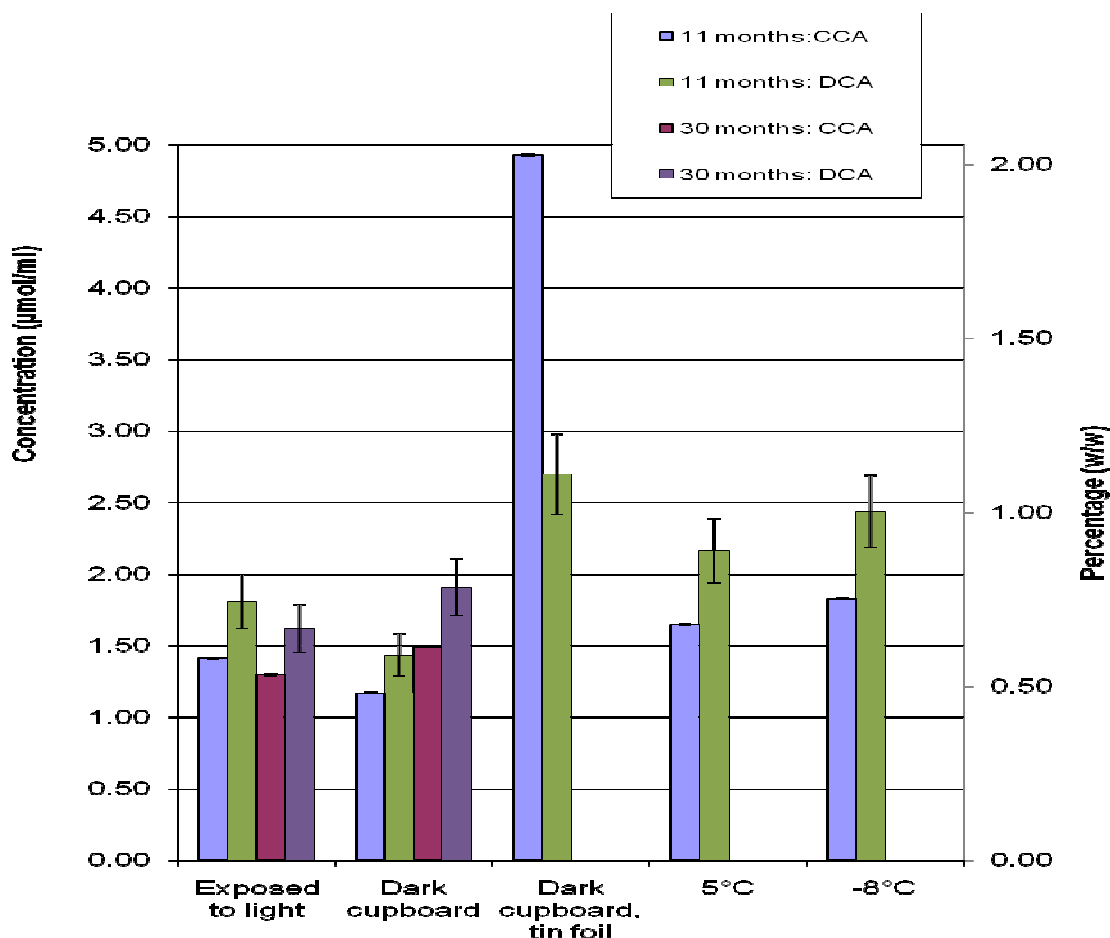


**Figure 2.16:** Variation in 1,3 DG concentration with different storage methods for avocado pear oil using the direct correlation approach (DCA) and the calibration curve approach (CCA), with error bars ranging from 0.09 % (CCA) to 10.4 % (DCA).

Figure 2.17 illustrates the results obtained for the concentration of FFAs present in avocado pear oil. Similar quantitative results were not observed between DCA and CCA methods for storage after 11 months. There was however a consistent trend between the storage conditions, with the results of CCA mostly higher than that of DCA with the exceptions of storage in a dark cupboard and storage with exposure to light. In these cases the FFA concentrations as determined by CCA contain error bars reaching into the negative, making it difficult to compare this data to that of DCA results obtained. These large error bars could once again be an indication that the CCA method is not adequate for FFA concentration determination. Looking at the data obtained from DCA results alone it seems that the best storage methods would be for storage in a dark cupboard or storage upon exposure to light.

**Variation in FFA concentration with different storage methods**

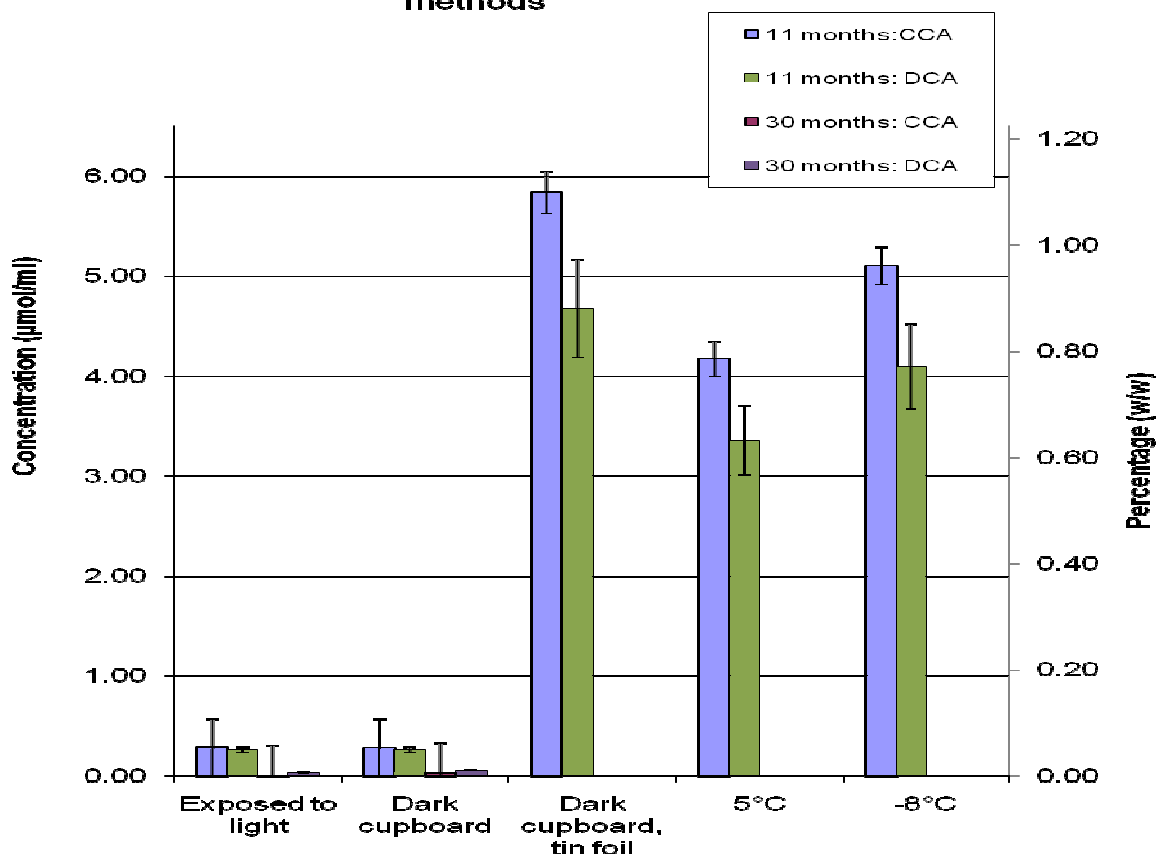


**Figure 2.17:** Variation in FFA concentration with different storage methods for avocado pear oil using the direct correlation approach (DCA) and the calibration curve approach (CCA), with error bars starting from 3.6 % (CCA).

#### 2.2.4.4: Discussion of overall results

A few other general conclusions could be drawn. Firstly, all the oils display roughly a 1:2 ratio of concentration of 1,2 DGs to 1,3 DGs. This is a good indication of oil degradation as explained earlier in Chapter 1. To recap, when TGs break down to form DGs, an isomerization between the 1,2 DGs and 1,3 DGs occur. Since the 1,2 DGs can form double the amount of the 1,3 DGs (due to structural positioning explained in Chapter 1), the equilibrium shifts to the formation of more 1,3 DGs and consequently the relative concentration of the 1,3 DGs are higher than those of the 1,2 DGs. This is nicely observed in all above figures where the relative concentrations of the 1,3 DGs are higher than those for the 1,2 DGs for each of the three vegetable oils. For instance for apricot kernel oil stored exposed to light (Figures 2.8 and 2.9), the 1,2 DG concentration is around 0.15 µmol/ml which is just under half of the concentration of the 1,3 DGs of 0.42 µmol/ml under the same

storage conditions. A similar situation is seen for the macadamia nut oil (Figures 2.11 and 2.12) where the 1,2 DG concentration (around 2  $\mu\text{mol/ml}$ ) is about half the concentration of the 1,3 DGs (around 4.2  $\mu\text{mol/ml}$ ). For avocado pear oil (Figures 2.14 and 2.15), there also seems to be a rough 1:2 ratio where the 1,3 DG concentration of 1.4  $\mu\text{mol/ml}$  is very close to twice the amount of the 1,2 DG concentration of 0.8  $\mu\text{mol/ml}$ . Similar ratios are seen for the 1,2 DG and 1,3 DG concentrations at the other storage conditions for all three vegetable oils.

Secondly, another interesting observation comes to light upon investigation of the 1,2 DG, 1,3 DG and FFA graphs for all three the vegetable oils. Notice that in most cases (with the exception of a few such as the three minor components stored with exposure to light for macadamia nut oil and all cases for avocado pear oil due to lack of comparable data), the relative concentrations of all the samples stored at a longer time period (27 months for apricot kernel oil and 30 months for macadamia nut oil) are lower in concentration to those of the shorter stored samples (8 months for apricot kernel oil and 11 months for macadamia nut oil). This is opposite of what is expected since with time more degradation of the oil would occur and consequently higher concentrations of the minor components. However this is not observed in the current storage studies done. This could be due to some influence by other minor components present in the vegetable oils or possibly connected to the insoluble fat globules detected in the vegetable oils after long storage with indication that some of the minor components of interest (1,2 DGs, 1,3 DGs or FFAs) are falling out of solution and therefore decreasing the actual concentration of these components in solution.

Thirdly, by comparing the two methods, namely the direct correlation approach (DCA) and the calibration curve approach (CCA), similar results seem to be obtained (refer to Tables 2.3 and 2.5). Looking at the three vegetable oils, the concentrations obtained for all three components, namely 1,2 DGs; 1,3 DGs, and FFA compare fairly well between the two different methods. There is however one distinct difference between the two methods and that lies in the error values determined. For the 1,2 DGs the percentage errors calculated for CCA were found to be 3.9 % (apricot), 3.8 % (avocado) and 2.9 % (macadamia nut); while for the 1,3 DGs it was determined to be 13.2 % (apricot), 3.8 % (avocado), 2.9 % (macadamia); and for the FFAs it was determined to be 17.8 % (apricot), 21.6 % (avocado) and 12.0 % (macadamia). Comparison of the errors for the two methods now indicate that the calibration curve

approach might be better for the analysis of concentration of 1,2 DG and 1,3 DGs, while the direct correlation approach would be better suited to use with its relative percentage error (10,4 %) error for FFAs. Also it seems that the direct correlation approach would be the faster, less time consuming option, since no standard calibration curves are required, leading to only one known concentration of compound needed (namely cyclohexanol) and less NMR time required, that being only the one spectrum of the oil itself. However both methods (CCA and DCA) play an important role for interpretation of results as was indicated by the errors just discussed. Therefore, for completeness of storage studies on apricot kernel, avocado pear oil and macadamia nut vegetable oils, both methods were used and compared for their usefulness in the determination of minor component concentrations.

### 2.3 CONCLUSIONS

In conclusion, the  $^{31}\text{P}\{^1\text{H}\}$  NMR spectra of three locally produced vegetable oils, namely apricot kernel, macadamia nut and avocado pear oils were assigned for the first time. The signals in these spectra indicated the presence of the following minor components: 1,2 DGs, 1,3 DGs, FFAs and sterols. These signals were then used for quantitative studies using two methods, namely a calibration curve approach and a direct correlation approach. Both methods proved to be useful. CCA was found to be more useful for the determinations of 1,2 DG and 1,3 DG concentrations while DCA was of use for FFA concentration determination.

Using both these approaches, the quantitative data obtained aided in identification of the best storage conditions for the three vegetable oils. Studies indicated that different storage conditions had an important affect on the minor components and consequently on the freshness of the vegetable oil. No storage situation was found to be exactly similar for each of the three vegetable oils. Determining the best storage conditions for each oil overall is difficult since individual minor components, namely the 1,2 DGs; 1,3 DGs; and FFAs, were upon times affected differently. However keeping this in mind the best storage conditions were storage at 5 °C and -8 °C for apricot kernel, macadamia nut and avocado pear oils.

Finally, for all oils, the 1,2 DG: 1,3 DG ratio was roughly 1:2. Longer storage periods for all of the oils did not indicate higher degradation as would be expected. In fact all minor component concentrations were found to be less compared to shorter storage,

possibly due to the precipitation of components out of solution during longer time periods.

## **2.4 EXPERIMENTAL**

### **2.4.1 Vegetable oils**

Apricot kernel, avocado pear and macadamia nut oils were obtained from Specialized Oils (Paardeneiland, South Africa). The oils received were decanted into clear glass bottles which were then flushed with nitrogen and sealed.

### **2.4.2 Standard fatty acids**

1,2 dipalmitin ( $\geq 99\%$ ), 1,3 dilinolein ( $\geq 99\%$ ), and oleic acid ( $\geq 99\%$ ) were obtained from Sigma-Aldrich for use as standards in the calibration curve approach.

### **2.4.3 Storage of oils**

All oil samples were obtained at two different production dates and stored in five different conditions, namely exposed to light, in the dark, in the dark covered in tinfoil, in a freezer at  $-8\text{ }^{\circ}\text{C}$  and in a fridge at  $5\text{ }^{\circ}\text{C}$ . The oils were stored in clear glass bottles which were flushed with nitrogen and sealed.

### **2.4.4 Preparation of stock solution for P-derivitization**

A 10 ml stock solution was prepared containing 0.6 mg  $\text{Cr}(\text{acac})_3$ , 6.2 ml pyridine and 3.9 ml  $\text{CDCl}_3$ . 14 ml cyclohexanol was added to the solution as an internal standard. The stock solution was stored over activated  $5\text{\AA}$  molecular sieves under  $\text{N}_2$ <sup>1</sup>.

### **2.4.5 NMR Sample preparation**

NMR samples were prepared directly in the NMR tube by adding 150 mg oil, 0.4 ml stock solution and  $\sim 15\text{ }\mu\text{l}$  phosphorous reagent together. These were left to react for 15 min before acquiring spectra<sup>1</sup>.

### **2.4.6 Collection of $^{31}\text{P}$ NMR spectra**

$^{31}\text{P}$  NMR spectra ( $^1\text{H}$  decoupled) were obtained on a Varian <sup>Unity</sup>Inova 400 NMR spectrometer operating at 161.904 MHz for the phosphorous-31 nucleus at  $25\text{ }^{\circ}\text{C}$ . The following acquisition parameters were used: number of scans 64,  $90^{\circ}$  pulse

width; sweep width of 10 kHz; relaxation delay 30 s; memory size 16K (zero-filled to 32K). For quantification, all NMR signals of the standard compounds were deconvoluted five times and the average value used.

## 2.5 REFERENCES

1. Spyros, A., and Dais, P., Application of  $^{31}\text{P}$  NMR Spectroscopy in Food Analysis. 1. Quantitative Determination of the Mono- and Diglyceride Composition of Olive Oils, *J. Agric. Food Chem.*, **2000**, *48*, 802-805.
2. Christophoridou, S., Spyros, A., and Dais, P.,  $^{31}\text{P}$  Nuclear Magnetic Resonance Spectroscopy of polyphenol-containing olive oil model compounds, *Phosphorus Sulfur*, **2001**, *170*, 139-157.
3. Dais, P., and Spyros, A.,  $^{31}\text{P}$  NMR spectroscopy in the quality control and authentication of extra-virgin olive oil: A review of recent progress, *Magn. Reson. Chem.*, **2007**, *45*, 367-377.
4. Jiang, Z. H., Argyropoulos, D. S. and Alessadro, G., *Magn. Reson. Chem.*, **1995**, *33*, 375-382.
5. Vigli, G., Philippidis, A., Spyros, A., and Dais, P., Classification of Edible Oils by Employing  $^{31}\text{P}$  and  $^1\text{H}$  NMR Spectroscopy in Combination with Multivariate Statistical Analysis. A Proposal for the Detection of Seed Oil Adulteration in Virgin Olive Oils, *J. Agric. Food Chem.*, **2003**, *51*, 5715-5722.
6. Miller J.N., Basic statistical methods for analytical chemistry, Part 2. Calibration and regression methods, *Analyst.*, **1991**, *116*, 3 – 14.
7. DeSilva, M. A., Shanaih, N., Gowda, G. A. N., Rosa-Pérez, K., Hanson, B. A., and Raftery, D., Application of  $^{31}\text{P}$  NMR spectroscopy and chemical derivatization for metabolite profiling of lipophilic compounds in human serum, *Magn. Reson Chem.*, **2009**, *47*, S74-80.
8. Dayrit, F.M., Buenafe, O.E.M., Chainani, E.T., and de Vera, I.M.S., Analysis of monoglycerides, diglycerides, sterols and free fatty acids in coconut ( *Cocos nucifera* L.) Oil by P NMR spectroscopy, *J. Agric. Food Chem.*, **2008**, *56* (14) 5765-5769.
9. Long, G.L., and Winefordner, J.D., Limit of Detection, A closer look at the IUPAC definition, *Analytical Chemistry*, **1983**, *55* (7), 46-61.
10. Schievano, E., Guardini, K., and Mammi, S., Fast determination of histamine in cheese by nuclear magnetic resonance (NMR), *J. Agric. Food Chem.*, **2009**, *57* (7), 2647-2652.
11. Spyros, A., Philippidis, A., and Dais, P., Kinetics of Diglyceride Formation and Isomerization in Virgin Olive Oils by Employing  $^{31}\text{P}$  NMR Spectroscopy. Formulation of a Quantitative Measure to Assess Olive Oil Storage History, *J. Agric. Food Chem.*, **2004**, *52*, 157-164.

# CHAPTER 3: THERMOGRAVIMETRIC ANALYSIS OF SEEDS AND BEANS

*“Behold the turtle. He makes progress only when he sticks his neck out.”*

James Bryant Conant

March 26, 1893 – February 11, 1978



Picture obtained from [http://en.wikipedia.org/wiki/James\\_B.\\_Conant](http://en.wikipedia.org/wiki/James_B._Conant).

### 3.1 THE IMPORTANCE OF SEEDS AND BEANS

Many vegetable oils are produced from seeds (such as sunflower oil) and beans (such as soybean oil). Therefore due to seeds and beans being the origin of many oils it was of interest to develop methods for the determination of the major components in seeds and beans by solid state NMR spectroscopy and other methods such as Thermogravimetric Analysis (TGA).

Seeds and beans are an important food source for humans and animals due to their high nutritive value. They consist mainly of proteins, carbohydrates (which are the major source of energy), vitamins and minerals. Usually, the higher the oil content in the seed or bean, the lower the protein content, and vice versa<sup>1</sup>. Seeds are produced world-wide but of specific interest to this study are seeds and beans produced in South Africa.

The seeds of interest included poppy, pumpkin, sesame and sunflower seeds, while the beans included black, kidney, mung and soybeans all produced in South Africa. Figure 3.1 indicates the quantities of specific seeds and beans produced worldwide from information supplied by the Food and Agriculture Organization of the United Nations (FAO) compiled for 2007<sup>2</sup>. Notice that for some of the seeds and beans of interest, data could not be obtained directly. For instance; black, kidney and mung beans are all grouped under “dry beans” while pumpkin seeds are represented in the “pumpkin, squash and gourds” category. From this graph it seems that soybean production is the highest around 216 million tonnes while poppy seed production was the lowest with a value of around 60 000 tonnes. Compared to the other seeds and beans, soybean production greatly outweighs the rest.

Figure 3.2 shows the total worldwide production of seeds and beans with respect to Africa, Asia, America, Europe and Oceania. America is the greatest producer of soybeans while Europe deals more in poppy seeds. Sunflower seeds are produced mostly by Europe while Asia leads in sesame and pumpkin, squash and gourd production. Africa produces a fair amount of seeds and beans while Oceania only produces these products in amounts below 2 % of the total world production.

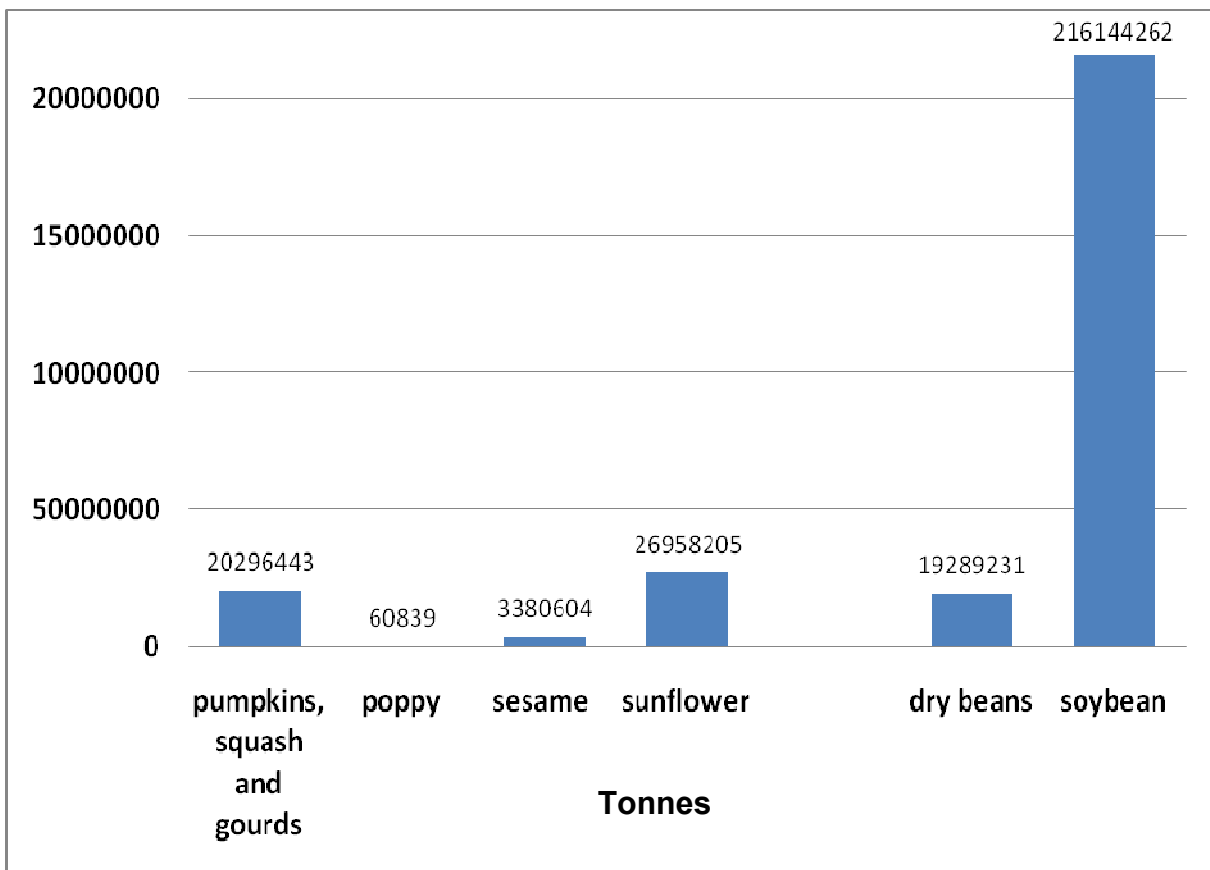


**Figure 3.1:** Total production quantities (in tonnes) of certain beans and seeds worldwide, adapted from data provided by FAO<sup>2</sup>.

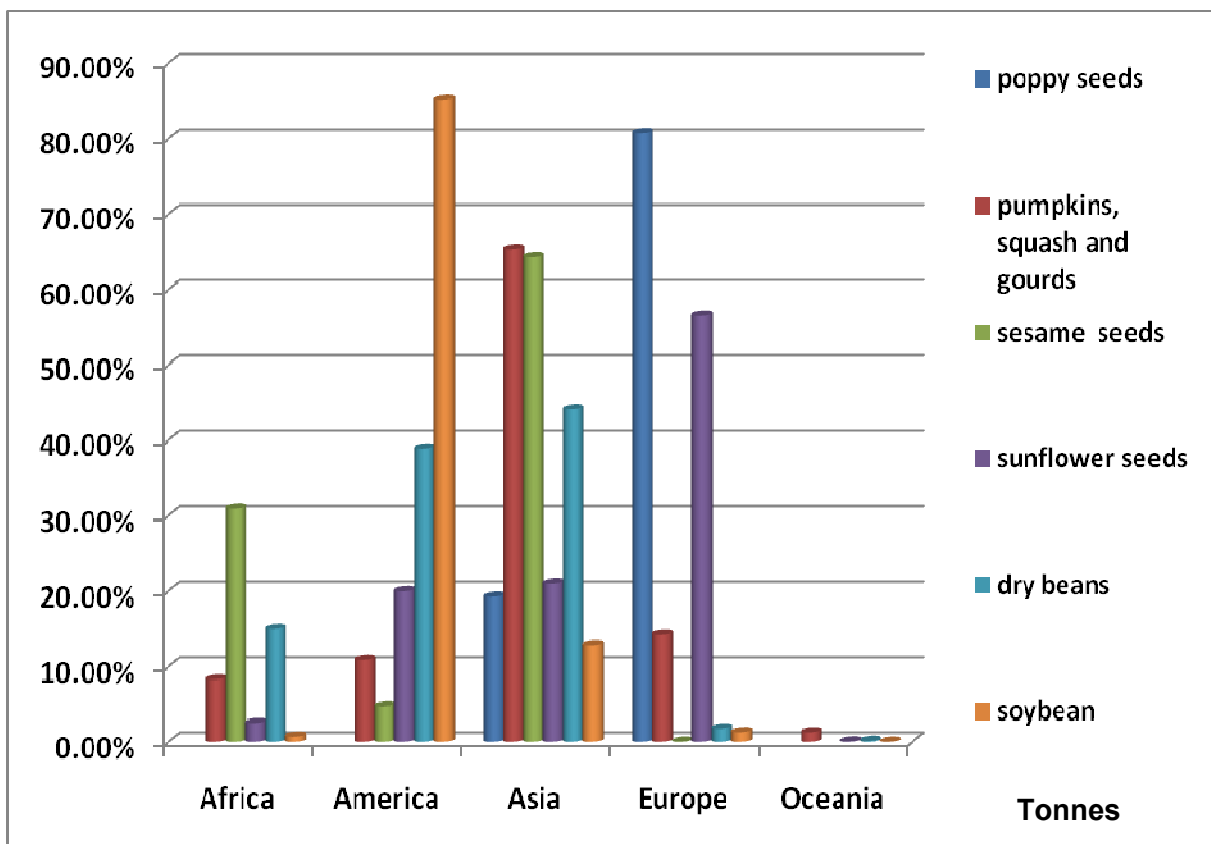


**Figure 3.2:** Production quantities as a percentage of the world total (in tonnes) as produced in separate continents, adapted from data provided by FAO<sup>2</sup>.

In the context of Africa it can be seen from Figure 3.2 that within Africa, the largest production is of sesame seeds (31.93 %) and then dry beans is next (14.98 %), while pumpkin, squash and gourds (8.28 %), sunflower seeds (2.51 %) and soybean production (0.69 %) are all below the 10 % mark.

The following sections discuss the seeds and beans of interest in more detail as well as give more information on the production quantities in individual countries in Africa. The exception is for poppy seed since the FAO database did not indicate the production of such seeds in Africa. Since poppy seeds are found in abundance in the north of Africa<sup>3</sup>, the production quantities could possibly be of too low significance for the FAO database.

### 3.1.1 Poppy seed

Order:	<i>Rhoeadales</i>	
Family:	<i>Papavaraceae</i>	(Poppy family)
Species:	<i>Papaver somniferum</i>	(Opium poppy)

Poppy seed flowers are mainly grown for their oil and in some cases their opium content but are often also grown as garden flowers due to their brilliant yet short-lived bloom. In India the flowers have white petals and white seeds while in France and Germany the petals are coloured (white, pink, yellow, orange, red, and blue<sup>4</sup>) and the seeds are dark. The seed colour can range from slate to blue, while in Turkey the seeds colours can be white, yellow, brown or blue. The average weight of poppy seeds is 0.25-0.5 g per 1000 seeds. The seed is surrounded by a capsule, with some varieties containing pores, which open up when they are mature and the wind scatters the seeds. The seed itself does not contain the opium but the juice obtained by scarring the unripe capsule will yield it. The oil content percentage is about 44-50 % by weight<sup>4</sup>.

### 3.1.2 Pumpkin seed

Order:	<i>Campanulales</i>	
Family:	<i>Cucurbitaceae</i>	(Gourd family)
Species:	<i>Cucurbita Pepo</i>	(Pumpkin and squash)

The pumpkin fruit varies in size, shape and colour. The seeds are between 1.1 and 2.6 cm long, 0.9-1.5 cm broad and 2-4.2 mm thick, with the kernels being about ¾ of the weight of the seeds<sup>5</sup>. Figure 3.3 indicates the production of pumpkins, squash and gourds in tonnes within Africa. Egypt has the highest production of these crops of around 42 % with South Africa producing only around 6 %.

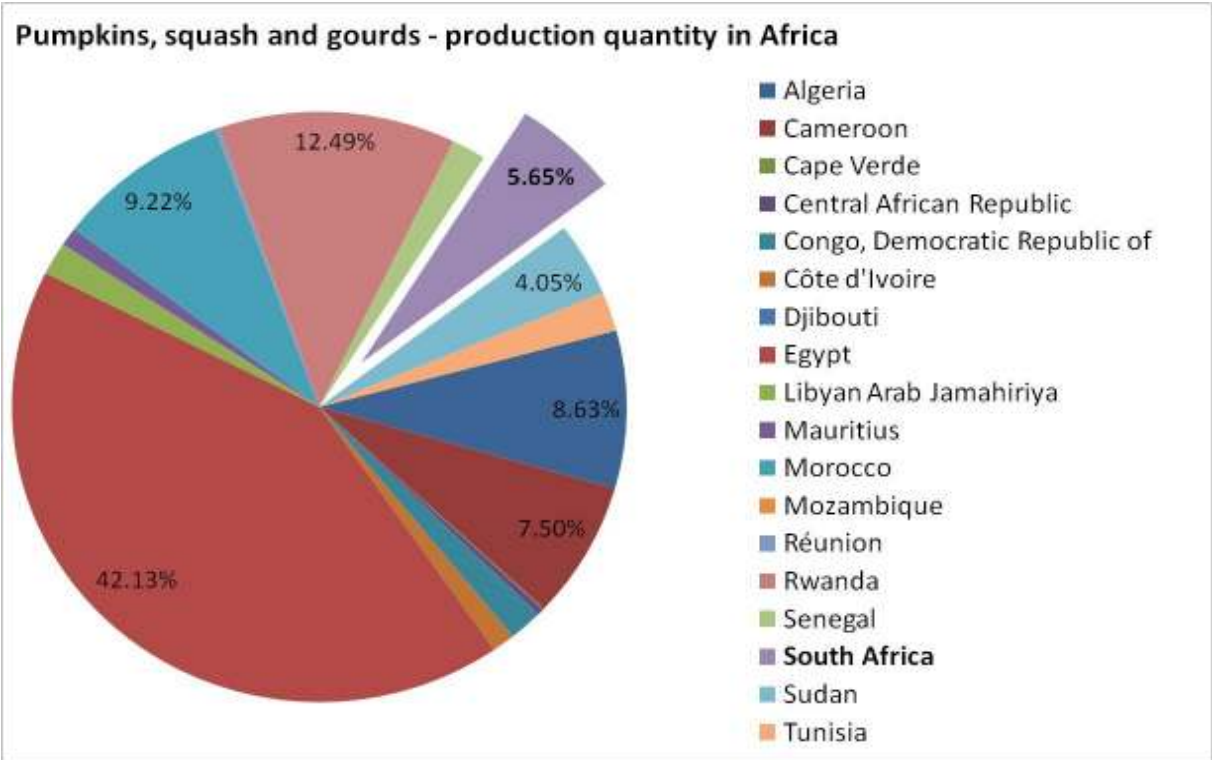


**Figure 3.3:** Production quantities of pumpkins, squash and gourds in various African countries as a percentage of the total tonnes produced in Africa, adapted from data provided by FAO<sup>2</sup>.

**3.1.3 Sesame seed**

Order: *Tubiflorae*  
 Family: *Pedaliaceae* (*Pendalium* family)  
 Species: *Sesamum indicum* (Sesame)

The sesame plant has several names, including “benne”, “til”, “gingelly”, “simsim” and “ajonjol”<sup>5</sup>. The seed is small and varies in size according to its variety and agricultural conditions. Usually they are between 2-3.5 grams per 1000 seeds with an oil content of 44-54 % and protein content of 19-25 % by weight. The lighter coloured seeds are accepted to be of better quality. The seeds have a thin shell covering the kernel,

which is removed by decorticating machines or soaking and rubbing the seed<sup>5</sup>. Figure 3.4 indicates the production of sesame seeds in tonnes within Africa. Sudan has the highest production of this crop at around 25 %, closely followed by Uganda and Ethiopia around 16 %. South Africa does not produce any significant amount of sesame seeds.

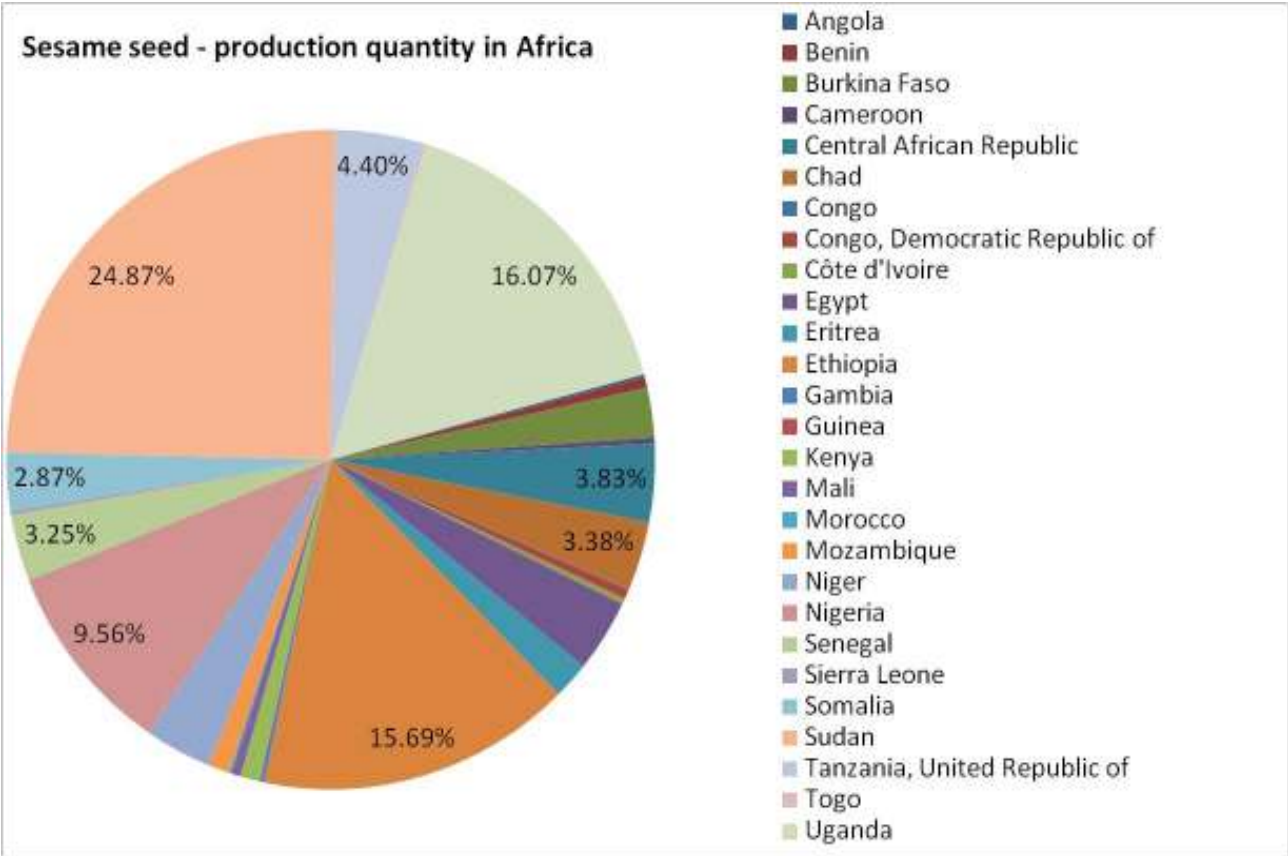


**Figure 3.4:** Production quantities of sesame seeds in various African countries as a percentage of the total tonnes produced in Africa, adapted from data provided by FAO<sup>2</sup>.

**3.1.4 Sunflower seed**

Order: *Campanulales*  
 Family: *Compositae* (Composite family)  
 Species: *Helianthus annuus* (Sunflower)

The sunflower plant occurs in two varieties, namely the tall and dwarf varieties. The dwarf varieties are used for their oil content (oilseeds), due to their shorter and uniform height which makes mechanical harvesting more practical, while the seeds of

the tall varieties are larger in size and are typically used as birdseed. The oil content for sunflower seeds range from 22-36 % by weight and protein content range from 45-55 % by weight. The hulls of the seed are around 40-50 % of the whole seed and contain practically no oil<sup>5</sup>. Figure 3.5 indicates the production of sunflower seeds in tonnes within Africa, indicating that South Africa has the highest production amount around 44 %, with Uganda around 28 % of total production.

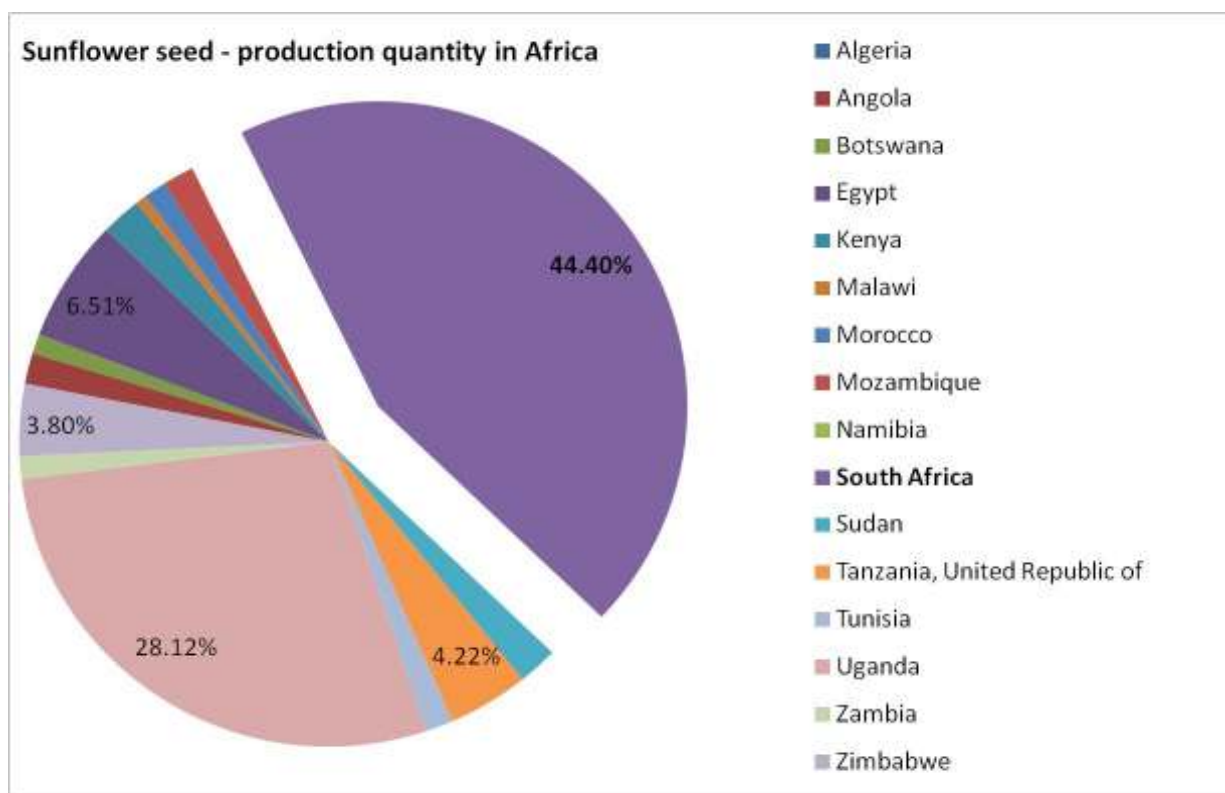


**Figure 3.5:** Production quantities of sunflower seeds in various African countries as a percentage of the total tonnes produced in Africa, adapted from data provided by FAO<sup>2</sup>.

### 3.1.5 Soybean

Order: *Rosalis*  
 Family: *Leguminosae* (Pea, Legume family)  
 Species: *Glycine max* (Soybean)

Soybeans fall under the order of *Rosalis*, which is the largest group of flowering plants<sup>5</sup>. Soybeans are rich in vegetable oil content and produce the biggest quantity of oil as a crop. The seed varies greatly in size, shape and colour of the coat and

colour of the cotyledon. In the wild they are smaller and darker in colour. Commercially produced soybeans have a weight of 10-20 g per 100 seeds while the wild varieties have a weight of about 40 g per 100 seeds. The soybean colours can be yellow, green, brown, black or a combination thereof. The seed cotyledon is around 5-10 % of the weight of the seed, its fat content is less than 1 % and it contains around 7 % protein. The seed as a whole contains around 18-22 % oil, protein content of around 40 % and soluble carbohydrates around 5 or 6 % by weight<sup>5</sup>. Figure 3.6 indicates the production of soybeans in tonnes within Africa. Nigeria produces the most with an amount around 42 % followed by South Africa around 29 %.

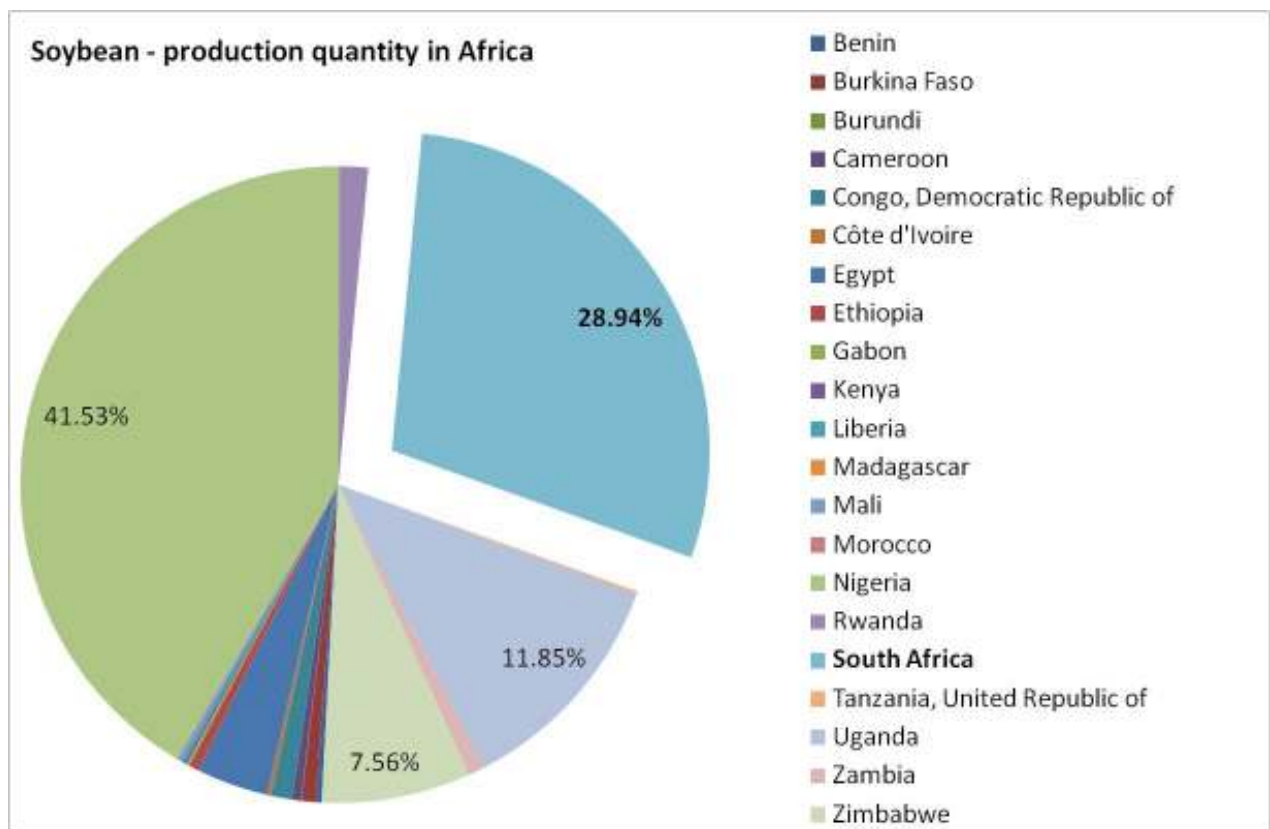


**Figure 3.6:** Production quantities of soybeans in various African countries as a percentage of the total tonnes produced in Africa, adapted from data provided by FAO<sup>2</sup>.

### 3.1.6 Dry beans

“Dry beans” is a general term used for the grouping seeds that originate from the *Phaseolus* plant species. Most of these beans are also referred to as “common

beans” and are regarded as one of the most important field crops in South Africa due to their high protein content and nutritional value. Within each species several types are found differing in size, shape and colour, and within each of these types there are different cultivars that vary only a little from one another, although the differences could be due to adaptability, growth habit, disease resistance and many other factors for the same species. Of the beans that are of interest to us, black bean and kidney bean fall under the *Phaseolus vulgaris* species. Mung bean is considered a “green bean” but often grouped under “dry beans”. This bean has recently been moved from the *Phaseolus* species to *Vigna radiata*<sup>6</sup>.

#### 3.1.6.1 Black bean

Order: *Fabales*  
Family: *Fabaceae*  
Species: *Phaseolus vulgaris*

#### 3.1.6.2 Kidney bean

Order: *Fabales*  
Family: *Fabaceae*  
Species: *Phaseolus vulgaris*

#### 3.1.6.3 Mung bean

Order: *Fabales*  
Family: *Fabaceae*  
Species: *Vigna radiata*; also previously called *Phaseolus mungo*,  
*Phaseolus radiate*, *Phaseolus vulgaris*; *Phaseolus aureus*.

Figure 3.7 indicates the production of dry beans in tonnes within Africa. Production is fairly well spread throughout Africa with Kenya producing around 19 %, closely followed by Uganda (15 %) and Tanzania (10 %). Several countries produce below 10 % of the total including South Africa which produces around 2 %.

### Dry bean - production quantity in Africa

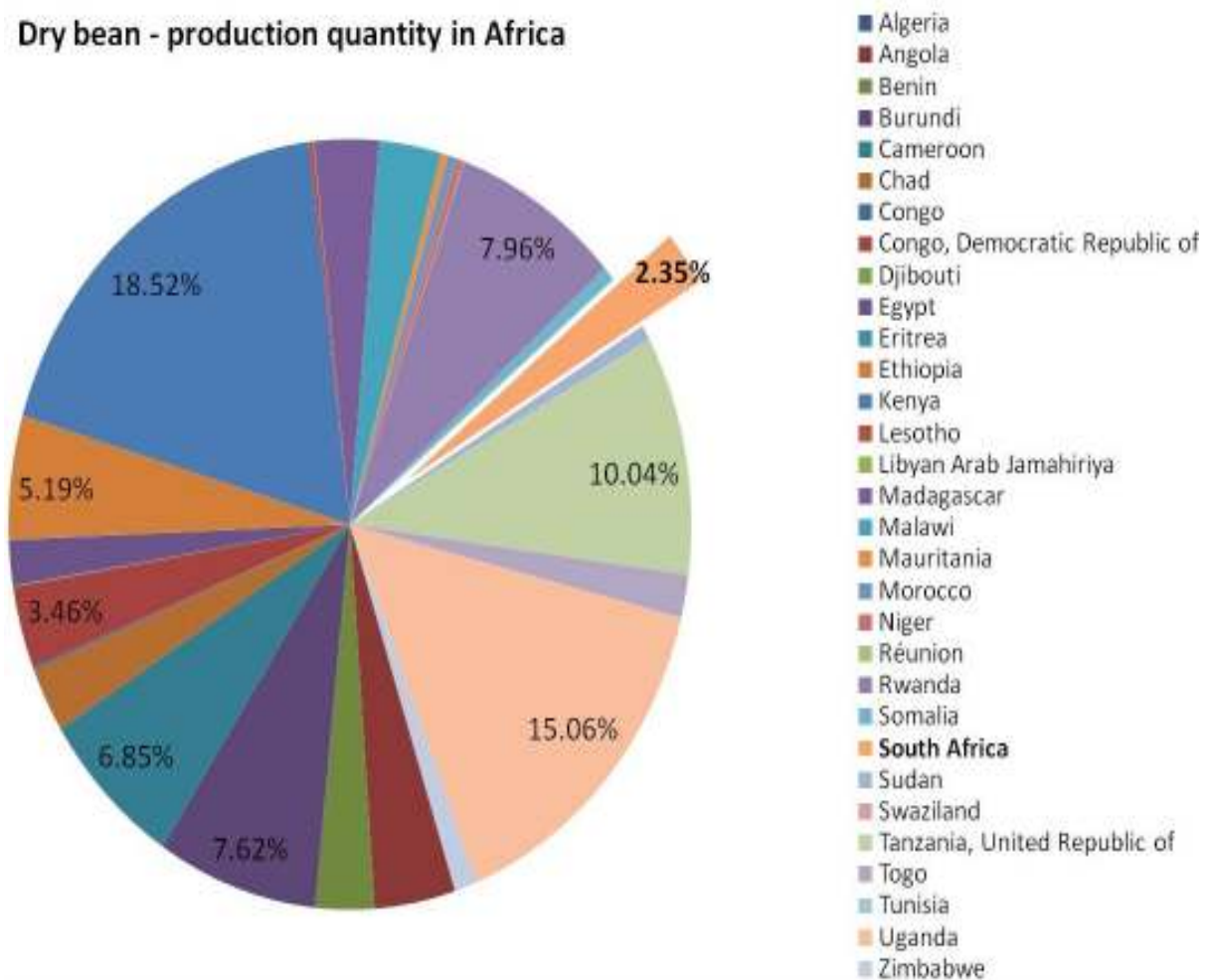


**Figure 3.7:** Production quantities of dry beans in various African countries as a percentage of the total tonnes produced in Africa, adapted from data provided by FAO<sup>2</sup>.

In order to carry out quality control on these food stuffs various analytical methods are used in order to protect mankind against the adulteration of food products. Some of these methods have been extensively researched in the past and some are still under development and scrutiny. Both traditional laboratory techniques and modern analytical methods are used for analysis. One of these traditional methods of interest for this study includes Soxhlet extraction (for extraction of oil), while the modern methods include chromatography and various forms of spectroscopy. Of specific interest to this study are two of the more modern techniques, namely Thermogravimetric Analysis and Solid State Nuclear Magnetic Resonance spectroscopy.

## 3.2 THERMOGRAVIMETRIC ANALYSIS

### 3.2.1 Introduction to TGA

The term thermal analysis (TA) can be applied to any technique where a measurement is taken while the temperature is changed at a chosen rate (usually linearly) or kept constant<sup>7</sup>. Table 3.1 lists some of the main thermal analysis techniques<sup>8,9</sup> which are of specific interest to the analysis of seeds and beans. These different techniques can also be coupled to each other or run simultaneously, (for example TGA-DSC) to yield comparative information, or even coupled to other analytical instruments such as in the case of TGA-FTIR or TGA-MS.

**Table 3.1:** Thermal analysis techniques<sup>7,8</sup>

Technique	Abbreviation	Property
Thermogravimetric analysis	TG or TGA	Change in mass
Differential thermogravimetric analysis	DTG	First derivative of change in mass
Differential thermal analysis	DTA	Temperature difference between sample and reference material
Derivative differential thermal analysis		First derivative of temperature difference
Differential scanning calorimetry analysis	DSC	Heat change supplied to sample
Specific heat measurement		Specific heat
Gas evolution analysis; linear pyrolysis	EGA	Gas thermal conductivity
Pyrolysis		Pyrolysis fragments

Thermogravimetric analysis (TGA) also known as thermogravimetry (TG) is a method where the measurement of mass as a function of heating is recorded. Figure 3.8 shows a TGA instrument. The sample is placed in an aluminium crucible/pan (a). This setup is referred to as an open system since the sample in the crucible is exposed to the atmosphere. The crucible is placed onto a platinum balance (b) and in

turn is mechanically lowered into a furnace (c). When the furnace is heated, heat flows across the system boundaries and the mass lost by evaporation or decomposition is recorded by the balance. The sample is thus continuously weighed as it is heated<sup>7</sup>.

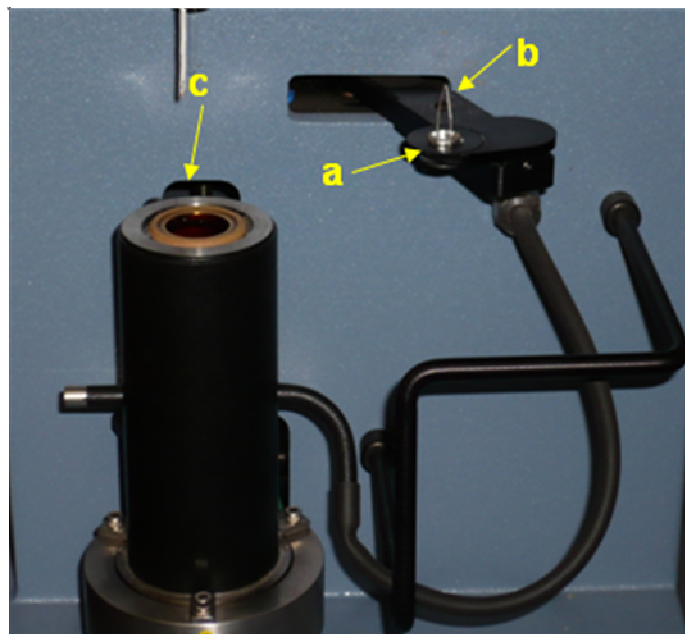


**Figure 3.8:** The TGA Q500 instrument from TG Instruments.

Figure 3.9 shows an example of a TGA curve obtained upon plotting the data for a soybean sample, with increasing temperature on the x-axis and the decreasing sample weight (as a percentage) on the y-axis (a). Figure 3.9 also shows an example of a DTG (first derivative of the TGA data) curve of the same data, with increasing temperature on the x-axis and the first derivative data on the y-axis (b). Both of these curves are termed “thermograms”.

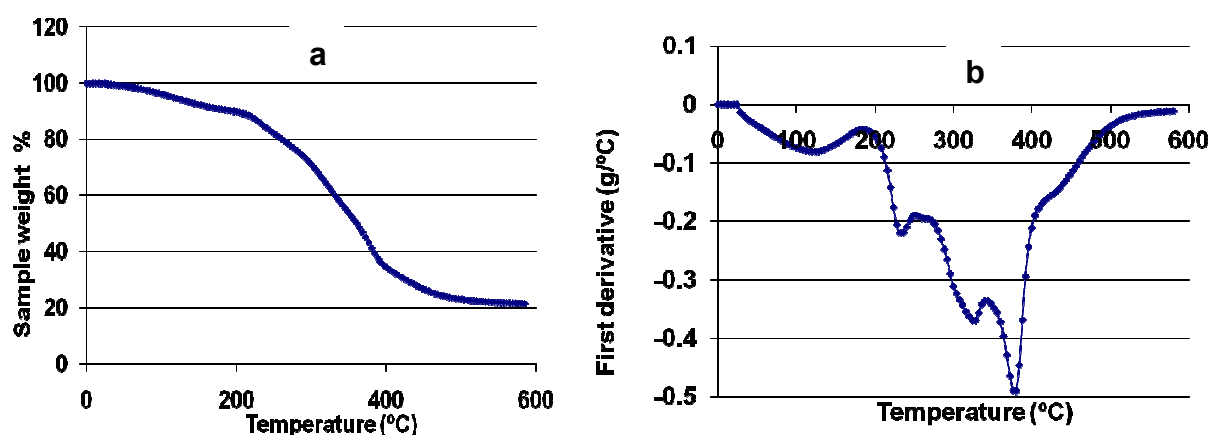


**Figure 3.9:** Examples of a TGA and DTG thermogram for soybean.

TGA can give valuable information on processes or compounds in terms of their thermal stability, degradation, stoichiometric changes, reaction with gases, syndissertation, depositions and/or analytical interactions as well as composition of an original sample and its intermediate compounds or of the composition of the residues obtained after heating<sup>7,8</sup>. Some applications of TGA include studies on:

- 1 corrosion
- 2 volatile organic compounds
- 3 catalysis
- 4 paints and coatings
- 5 etching with gases
- 6 coal conversion and liquefaction
- 7 removal of sulphur oxides from industrial gases
- 8 sorption and permeation of solvent vapours or moisture in plastics
- 9 oxidation and reduction
- 10 pharmaceutical issues such as water sorption and drying
- 11 volatility and vapor pressure
- 12 high-pressure solid-gas reactions
- 13 monitoring nuclear wastes

When using TGA, it is important to keep in mind the factors that can affect the thermogram of a sample. These include instrumental factors and sample characteristics<sup>7</sup>.

Instrumental factors:

- 1.5.1.1.1 furnace heating rate
- 1.5.1.1.2 recording or chart speed
- 1.5.1.1.3 furnace atmosphere
- 1.5.1.1.4 geometry of sample holder and furnace
- 1.5.1.1.5 sensitivity or recording mechanism
- 1.5.1.1.6 composition of sample container

Sample characteristics:

- amount of sample
- solubility of evolved gases in sample

- particle size
- heat of reaction
- sample packing
- nature of the sample
- thermal conductivity

Also of importance for the researcher is the sources of errors listed below that can lead to inaccuracies in the temperature and loss or gain of mass in the data that is obtained<sup>7</sup>.

Some sources of error bias and uncertainty include<sup>7,9</sup>:

sample container air buoyancy  
 furnace convection currents and turbulence  
 random fluctuations in the recording mechanism and  
 balance  
 furnace induction effects  
 electrostatic effects on balance mechanism  
 environment of the thermobalance  
 condensation of volatile products on sample suspension  
 and sample support  
 temperature measurement and calibration  
 weight calibration of recording balance  
 chart paper rulings  
 reaction of the sample with sample container  
 thermal expansion of the balance beam

In the case of the application of TGA to seeds and beans it was important to keep the following factors pertaining to the instrument and sample characteristics in mind as well as some additional possible sources of error:

The *nature of the sample* specifically with reference to the *sample preparation* played an important role as discussed later in more detail. The *furnace atmosphere* used was nitrogen gas. An inert gas was required that would not interact with the sample content such as would be the case for oxygen which could lead to oxidation and

combustion of compounds such as fatty acids or proteins. Other important factors that were kept in mind was to make sure the balance was cleaned before each run, the starting temperature of the room housing the instrument was below that of conventional room temperature, and the instrument furnace was sufficiently cooled down before each run.

### **3.2.2 Thermogravimetric analysis as applied to seeds and beans: A literature review**

Moisture determination by TGA has been of interest when analysing seeds and beans for many years. Tomasetti and co-workers carried out various investigations into the possible use of TGA for this purpose on a number of different samples<sup>10,11,12,13</sup>.

In several articles the researchers compared the values obtained for the moisture loss of different dried seeds, spices, food flours and foodstuffs by TGA to the moisture content obtained from low resolution NMR spectroscopy<sup>10,11,12,13</sup>. These samples included basil seed, cabbage seed, parsley seed, carrot seed, tomato seed, onion seed, lettuce seed, wheat meal, hard corn meal, semolina, rye flour, ground rice, corn flour, potato starch, chick pea flour, soya flour, powdered chestnuts, starch, dry alimentary small paste, toasted ground coffee, toasted ground barley, toasted ground cocoa treated with potassium carbonate and containing traces of natural flavouring, chickpea flour, tea, tobacco, black pepper, powdered milk, soyaseeds, colza seeds, poppy seeds, sunflower seeds, pumpkin seeds, linseeds and sesame seeds<sup>10,11,12,13</sup>. The TGA data of these samples were not only compared to low resolution NMR spectroscopy data but also to the Karl-Fischer method. It was found that TGA was a useful technique to determine not just the moisture content of the samples but also the ash residue content<sup>10</sup> which gives information on the total inorganic/mineral content. Further investigation into the thermal decomposition of the food flours indicated that the ash content was best determined between 650 and 700 °C, whereas the ash content is usually measured at 550 °C by the conventional oven method<sup>11,12</sup>. Tomasetti *et al.*<sup>13</sup> were not only interested in the water loss that plant seeds undergo during TGA, but also in determination of the oil content by low resolution NMR spectroscopy. These authors wanted to optimize a method for two conditions: the type of sample matrix, namely an air or nitrogen stream, and the type of seed sampling, namely whether the seeds should be intact, cut into coarse pieces,

peeled or peeled then cut. The studies indicated that the water loss was independent of the nature of the flowing gas although the degradation processes were found to be different in air or nitrogen stream. This difference in the use of gas is of great importance since air contains oxygen which can affect the degradation process. It was concluded that determination of the ash residue needs to be done under an air stream at approximately 700 °C. In the case of seed sampling the researchers concluded that for small seeds, such as poppy seed, no pre-treatment of the sample (grinding, peeling or cutting) was required. For large seeds, such as pumpkin or sunflower seed, the seeds should be peeled and cut into coarse pieces. For the determination of the oil content of intact seeds, low resolution NMR spectroscopy was found to be a sufficient, precise and accurate technique<sup>13</sup>.

Santos *et al.*<sup>14</sup> carried out chemical and thermal characterization of seeds from *Cnidocolus queritifolius*, commonly known as “faveileira”, found in north-east Brazil. Due to the desertification and agricultural problems in this area, faveileira can be considered as an alternative food source for animal and human consumption<sup>15</sup>. Chemical characterization was done on the flour, kernel and peel of the seed in order to determine the moisture, ash, carbon, nitrogen and protein contents. Association of Official Agricultural Chemists (AOACS) methods were used to determine the moisture, colour, density, iodine content, saponification number and viscosity of the seed oils while the fatty acid content was determined by GC analysis. TGA was used to determine the moisture and ash contents and thermal stabilities. DSC was used to determine the enthalpy of thermal decomposition of components of this seed. The researchers found that the thermodynamic properties of the faveileira seeds are similar to those of other foods and also have an acceptable calorific value. TGA and DSC results indicated good thermal and oxidative stability of the seed. The researchers’ work contributed to incorporation of this seed into the economy for the production of flour for human use, the kernel to be used for the production of edible vegetable oils and the production of other derivatives for animal use<sup>14</sup>.

TGA has also been used for the analysis of green coffee beans. Dyszel<sup>15</sup> analysed green coffee beans, combining TGA with Atmospheric Pressure Chemical Ionization Mass Spectroscopy (APCIMS) to characterize these beans with respect to the origin of country. The author concluded that 1) oxidation products are complex mixtures of which some of these compounds are volatile at low temperatures and some form during the oxidation process; 2) for a single variety of coffee there were fewer intra-

country variations than for inter-country variations and that the inter-country variations were less than the variations found within varieties; 3) the author was successfully able to match an unknown coffee to known coffees and obtain the country of origin<sup>15</sup>. In another study the author studied green coffee beans by Thermogravimetric Analysis/ Atmospheric Pressure Chemical Ionization Mass Spectrometry (TGA/APCIMS) to differentiate between different coffee varieties. The balance effluent or ash obtained from TGA was analysed by negative ionization and photooxidation prior to its entrance into the mass spectrometer. The author compared the ion abundance/temperature curves for selected ions and the MS spectra for specific temperatures of the different beans and showed that it was possible to distinguish between the different coffee beans<sup>16</sup>. Curini and co-workers<sup>17</sup> analyzed eight different coffee varieties by TGA and DSC under a controlled atmosphere using nitrogen, oxygen and air in static and dynamic conditions. The coffee varieties were “America”, “Costarica”, “Kenja”, “Kiwu”, “Paraguay”, “Robusta”, “Santos” and “Zaire”. The researchers concluded that the thermograms could be used to characterize the different coffee varieties and indicate some important conditions under which coffee roasting is performed. The decomposition process of the coffees behaved differently under different atmospheric conditions. The roasting temperature is determined from the initial decomposition temperature. This temperature was found to change to a lower temperature going from nitrogen to static air atmosphere. This initial temperature also differed for each variety of coffee. The researchers were also able to determine the humidity of decaffeinated roasted coffee using the thermograms<sup>17</sup>.

Studies have also been carried out on compounds extracted from seeds and beans. Freitas *et al.* worked on a natural hydrocolloid (galactoxyloglucan) that was extracted from *Jacoba (Hymenaea courbaril)* in order to investigate the effect of oxidation levels on the structure, conformation and thermal properties. TGA was used to determine the kinetics of the degradation reaction and it was found that an increase in the degradation rate was directly dependant on the level of oxidation<sup>18</sup>. Other extracted compounds include seed proteins. Researchers have also studied the thermal properties of the prolamines from rice, wheat and soybeans by TGA, DSC, thermal expansion, X-ray diffraction and infrared spectroscopy (IR) with respect to their structure and physical properties. It was found that the water was lost at about 100 °C, and the transition glass temperature (T<sub>g</sub>) and crystallization temperatures

depends on the amino acid composition of the prolamines. The Tg of the prolamine films were found to be at 175 °C for rice, 172 °C for wheat, and 150 °C for soybean. These amorphous films crystallized to  $\beta$ -crystals with  $\alpha$ -helices at 196 °C for rice, 205 °C for wheat and 199 °C for soybean<sup>19</sup>.

In another study, agricultural by-products, namely wheat straw (WS), sugar beet (SB), corn cobs (CC), rape extracted meal (REM), soya bean hulls (SBH), bagasse (B), almond shells (AS) and olive stone (OS) were analyzed by dynamic and isothermal TGA in two different environments, namely inert (N<sub>2</sub>) and oxidative (O<sub>2</sub>) conditions. This was done in order to evaluate the effect of oxygen on the thermolysis and to compare the environmental impact on the individual samples. It was found that a greater amount of material decomposed (gasified) under oxygen dynamic conditions than an inert atmosphere. Thermooxidation of samples with decreasing effect of oxygen on the samples was found to occur in the following order:

B (32 %, 325 °C) > AS (29 %, 450 °C) > OS (23 %, 450 °C) > SBH (20 %, 475 °C) > WS (21 %, 300 °C) > SB (13 %, 325 °C) > REM (15 %, 500 °C)

From this data the researchers concluded that those materials that form greater residues and of which their degradation course is less affected by oxygen, are less harmful to the environment<sup>20</sup>.

### **3.3 AIMS OF STUDY**

Due to the work done on the oil content of vegetable oils, other oil containing food products were also of interest. Specifically these food products included seeds (poppy, sesame, sunflower and pumpkin) and beans (soy, mung, black and kidney). Initially low resolution solid state-NMR spectroscopy was to be used for this oil determination as it is an easy, reliable and fast technique commonly used in the industry for the determination of oil and moisture content in a variety of food products, such as seeds, beans, chips, nuts, olives, etc. However the use of this instrument was cut short as it became no longer available and consequently an alternative method was sought.

Since previously the moisture content present in seeds and beans had been determined by TGA in the literature, the current study turned to the TGA technique with possibility of determining the fatty acid content as well. This led to the attempted assignment of the first derivative of the TGA data with the aim to explain the full curve

by linking individual peaks with the quantitative loss of components. These components included oil, protein and carbohydrates. This was undertaken in combination with other quantitative studies to determine the major components present in seeds and beans, including fat (by Soxhlet extraction), protein (by Dumas combustion method) and carbohydrates (by Clegg-Anthrone method/ UV-VIS spectroscopy).

### **3.4 RESULTS AND DISCUSSION**

#### **3.4.1 TGA data analysis**

TGA data were obtained of four seeds [sesame (SES), sunflower (SUN), poppy (POP) and pumpkin (PUM) seeds] and four beans [soybean (SOY), mungbean (MUN), black bean (BB) and kidney bean (KID)]. In order to quantitatively determine the compounds present in these seeds and beans, the first derivative thermogram (DTG) was used. This was obtained by plotting the first derivative of the TGA data on the y-axis against the temperature on the x-axis. Refer to Figures 3.10 and 3.11 for the DTGs of all the seeds and beans.

Upon plotting the DTG data, it was found to be difficult to identify the maxima by inspection and thus an analysis program (Findgraph by Uniphiz) was used to manipulate the data to extract maxima by separating peaks clearly. A fourier fit function was used to manipulate the curve until the maxima of the desired peaks could be obtained unambiguously (refer to Figure 3.12).

Figure 3.10: DTG curves of the seeds

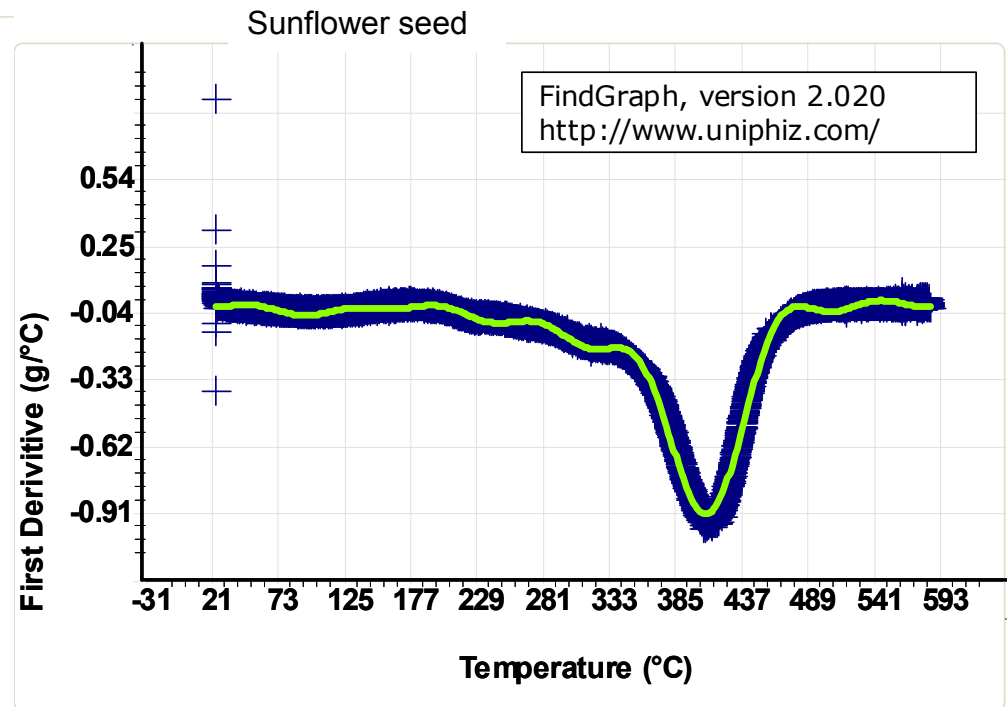
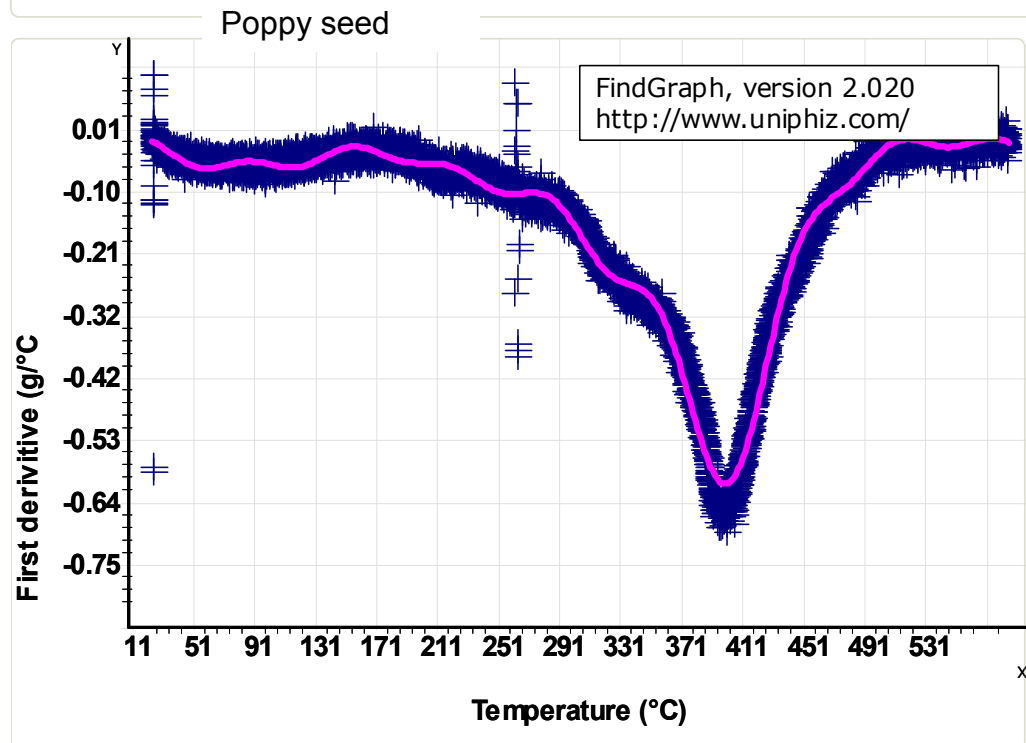
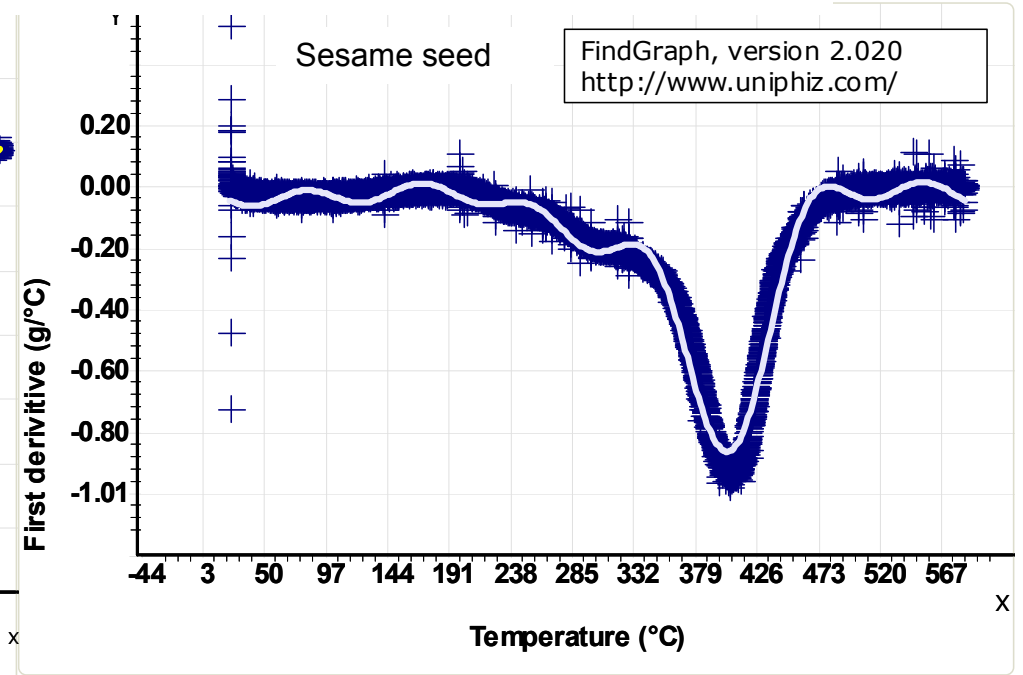
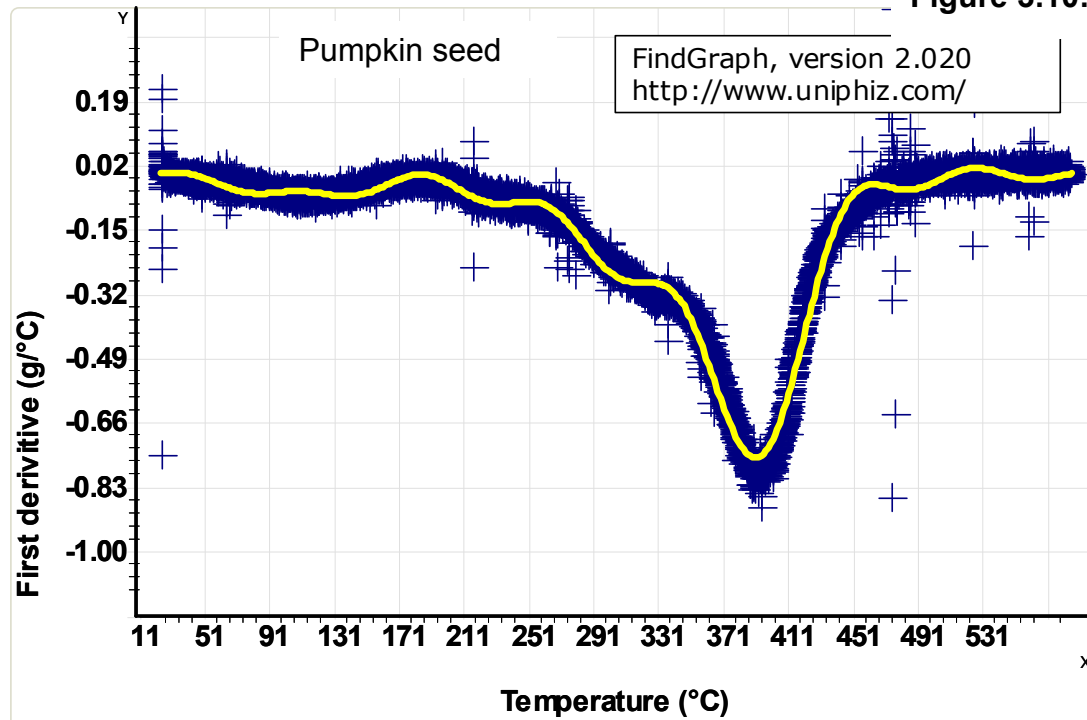
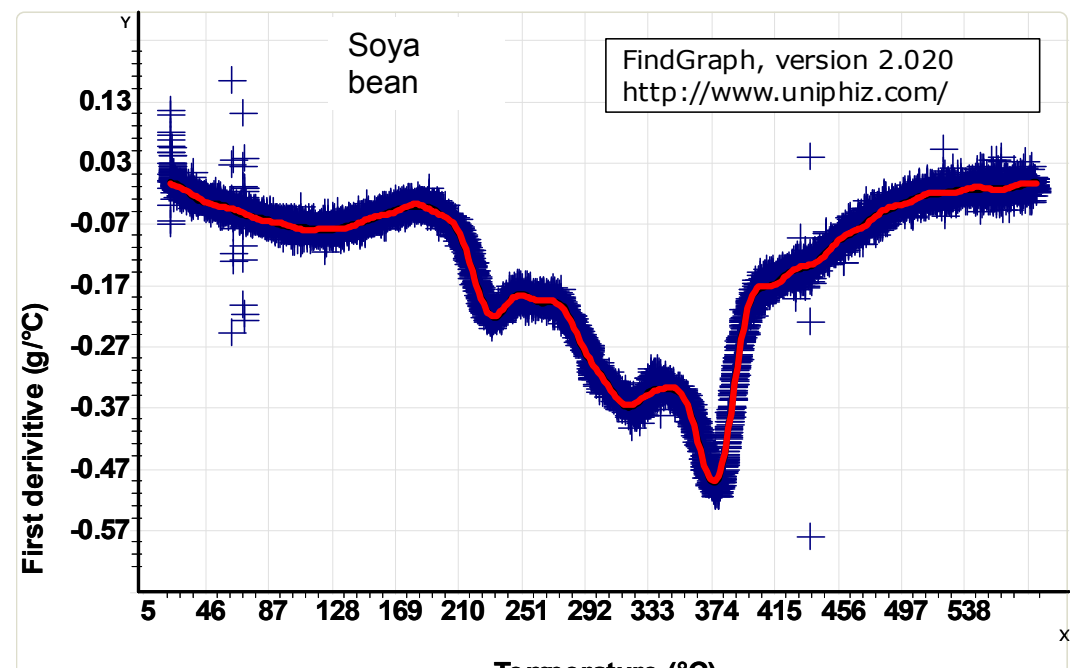
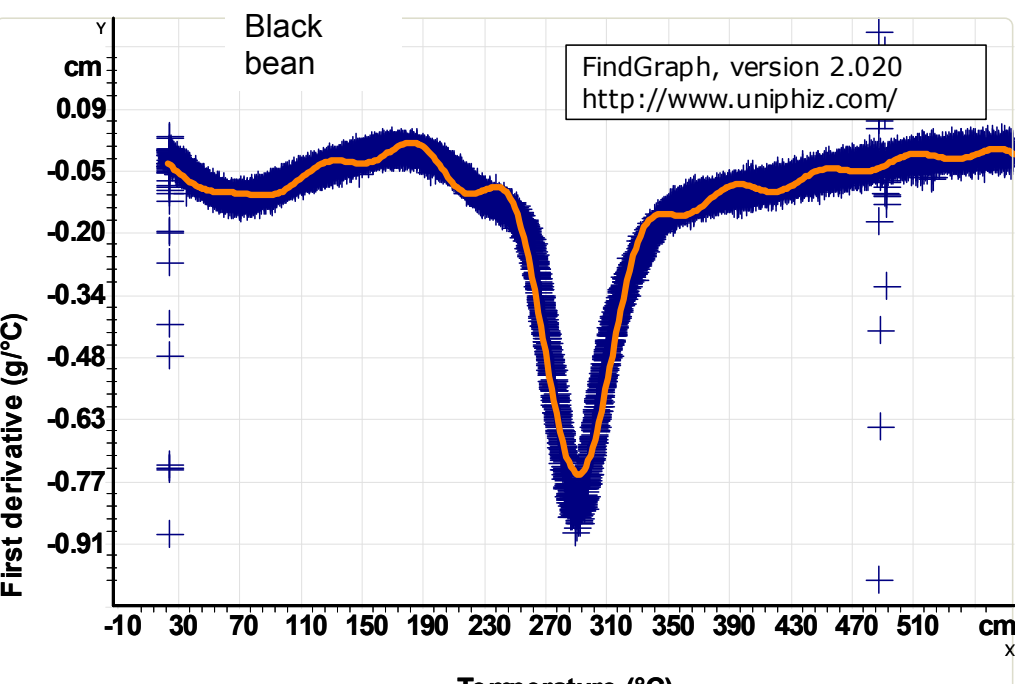
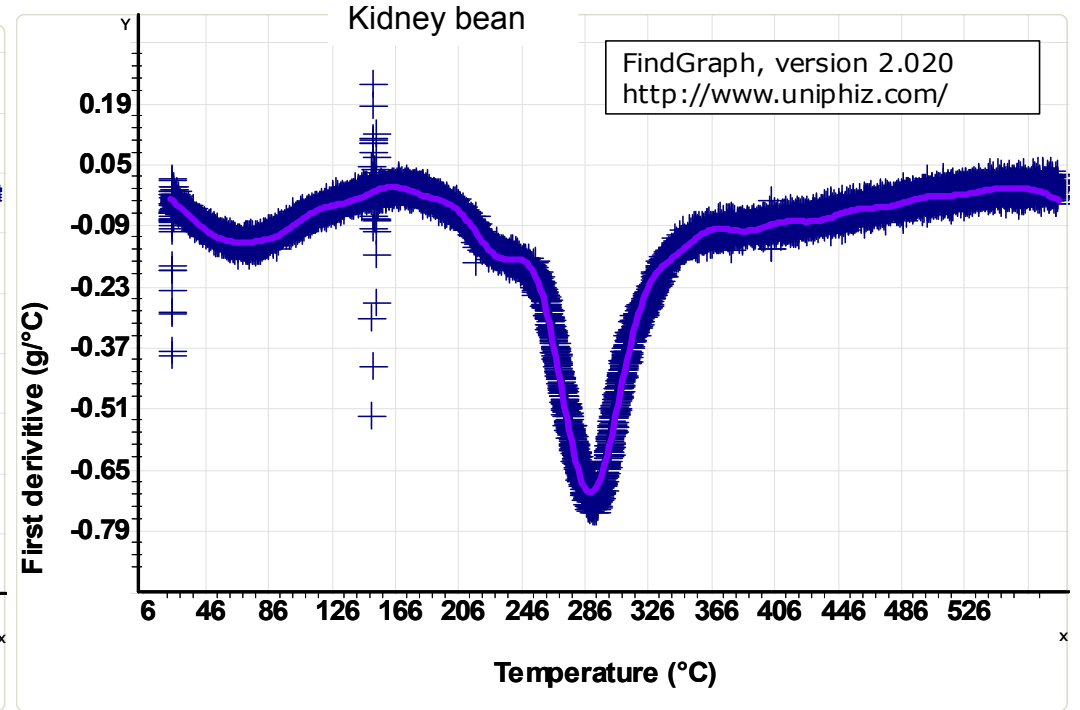
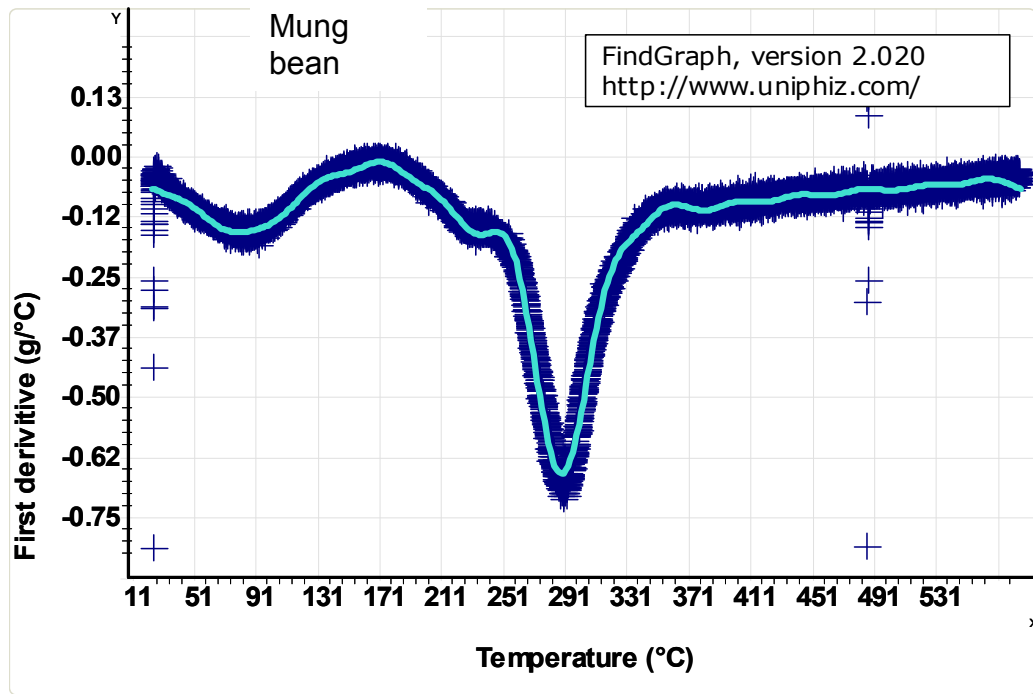
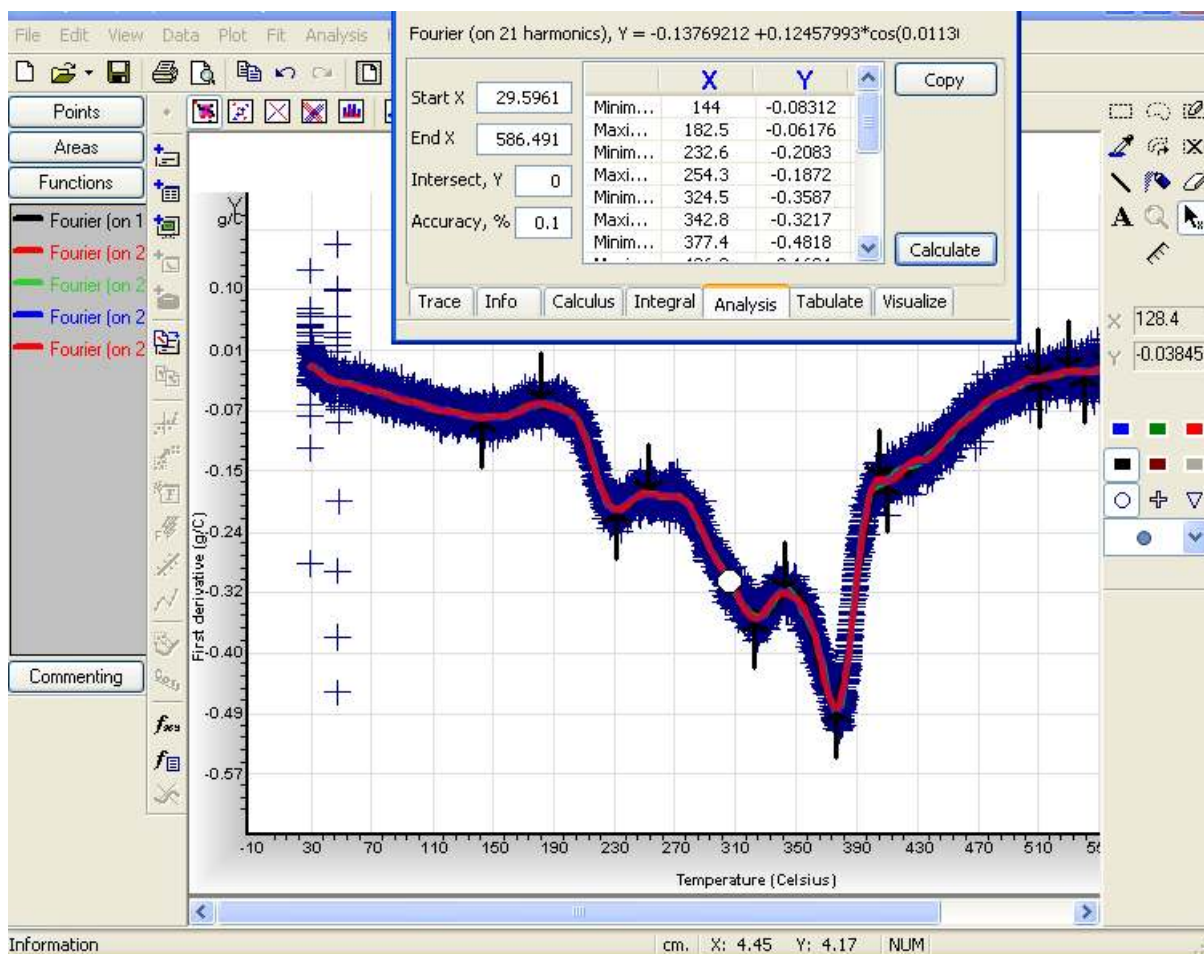


Figure 3.11: DTG curves of the beans





**Figure 3.12:** Screen shot of the main view of the FindGraph software, indicating the maximum and minimum values obtained from the DTG of a soybean sample.

It was observed that the fit with the highest number of harmonics possible gave the best results, since the higher fits would yield the lowest standard errors for the curve, as determined by the program (refer to Figure 3.13).

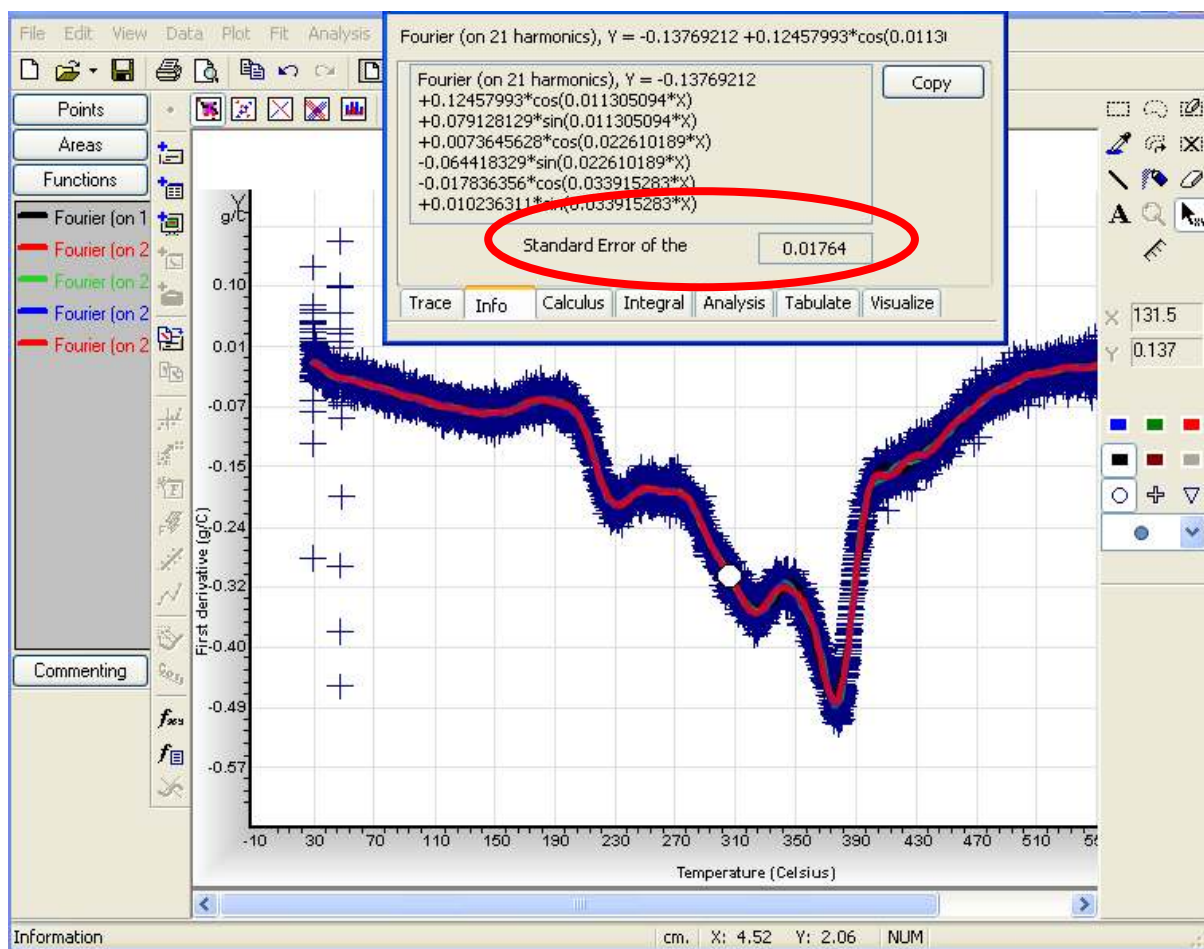


**Figure 3.13:** Screen shot indicating the standard error for the equation describing the DTG of a soybean sample as found by the FindGraph software.

As can be seen from Table 3.2, two sets of data were used to plot the graphs, one which included all the data points collected from the DTG data (full data) and one using data from where the temperature started to increase (increasing temperature). This is due to the fact that as the TGA instrument had to equilibrate first, its temperature slightly fluctuated initially, although usually only in the first decimal place. Notice that the standard errors (in all cases) for the graphs of increasing temperature were found to be lower than those of the full data (refer to Table 3.2).

Several outliers were found in the DTG thermograms, but comparison of the triplicate runs for each individual seed or bean, indicated the outliers were not consistently present. Therefore these outliers were assumed to be due to electronic spikes in the instrument.

**Table 3.2:** Standard errors of the equations fit to the DTGs of seeds and beans based on their full data and from increasing temperature only.

Sample name	Abbreviation	Full data		Increasing temperature	
		Number of harmonics used for fit	Standard error of fit	Number of harmonics used for fit	Standard error of fit
poppy seed 1	POP 1	10	0.95	9	0.03
poppy seed 2	POP 2	7	0.65	8	0.03
poppy seed 3	POP 3	8	1.04	8	0.03
pumpkin seed 1	PUM 1	7	1.25	7	0.03
pumpkin seed 2	PUM 2	7	2.27	7	0.08
pumpkin seed 3	PUM 3	7	1.38	7	0.03
sesame seed 1	SES 1	6	1.15	6	0.04
sesame seed 2	SES 2	7	0.97	6	0.15
sesame seed 3	SES 3	7	1.36	7	0.14
sunflower seed 1	SUN 1	7	1.58	6	0.03
sunflower seed 2	SUN 2	7	0.37	7	0.02
sunflower seed 3	SUN 3	7	0.79	7	0.03
black bean 1	BB 1	13	1.75	10	0.11
black bean 2	BB 2	14	2.20	13	0.03
black bean 3	BB 3	13	2.78	14	0.03
kidney bean 1	KID 1	15	2.66	13	0.02
kidney bean 2	KID 2	15	1.85	12	0.02
kidney bean 3	KID 3	14	1.93	13	0.02
mungbean 1	MUN 1	11	1.02	10	0.04
mungbean 2	MUN 2	13	2.67	9	0.04
mungbean 3	MUN 3	10	3.30	9	0.06
soyabean 1	SOY 1	21	0.02	21	0.02
soyabean 2	SOY 2	7	5.98	19	0.01
soyabean 3	SOY 3	11	0.87	19	0.02

### 3.4.2 Moisture analyses

Determination of the moisture content of the seeds and beans was also carried out using an oven gravimetric method and calculation of the moisture value was done using the following equation (values indicated in Table 3.3):

$$\% \text{ moisture} = \frac{(\text{Original seed weight} - \text{Seed weight without moisture})}{\text{Original seed weight}} \times 100$$

**Table 3.3:** Calculations of moisture content by gravimetry.

<b>SEEDS</b>	<b>Original seed mass (g)</b>	<b>Seed mass after heating (g)</b>	<b>Mass of moisture lost (g)</b>	<b>% moisture content</b>
POP1	2.890	2.661	0.229	7.9
POP2	2.763	2.543	0.220	8.0
POP3	2.874	2.648	0.226	7.9
<b>average</b>				<b>7.9</b>
PUM1	3.004	2.748	0.256	8.5
PUM2	3.370	3.089	0.281	8.4
PUM3	3.374	3.090	0.284	8.4
<b>average</b>				<b>8.4</b>
SES1	1.896	1.800	0.096	5.1
SES2	1.666	1.576	0.090	5.4
SES3	1.707	1.623	0.084	4.9
<b>average</b>				<b>5.1</b>
SUN1	3.466	3.313	0.153	4.4
SUN2	3.117	2.974	0.143	4.6
SUN3	2.803	2.671	0.132	4.7
<b>average</b>				<b>4.6</b>
<b>BEANS</b>				
BB1	2.280	1.918	0.362	15.9
BB2	2.741	2.310	0.431	15.7
BB3	3.275	2.759	0.516	15.8
<b>average</b>				<b>15.8</b>
KID1	3.168	2.748	0.420	13.3
KID2	3.831	3.323	0.508	13.3
KID3	2.884	2.505	0.379	13.2
<b>average</b>				<b>13.2</b>
MUN1	3.761	3.373	0.388	10.3
MUN2	3.503	3.145	0.358	10.2
MUN3	3.907	3.507	0.400	10.3
<b>average</b>				<b>10.3</b>

SOY1	3.102	2.786	0.316	10.2
SOY2	2.971	2.668	0.303	10.2
SOY3	2.917	2.621	0.296	10.2
<b>average</b>				<b>10.2</b>

The gravimetric experiment using an oven for determination of moisture loss was used as comparison to the DTG data obtained, and compared to values obtained from the literature<sup>21,22,23,24</sup>. In the DTGs, the first peak represented the loss due to moisture (refer to Figure 3.14). Using the maximum value of the first peak that was obtained, the moisture content could be determined.

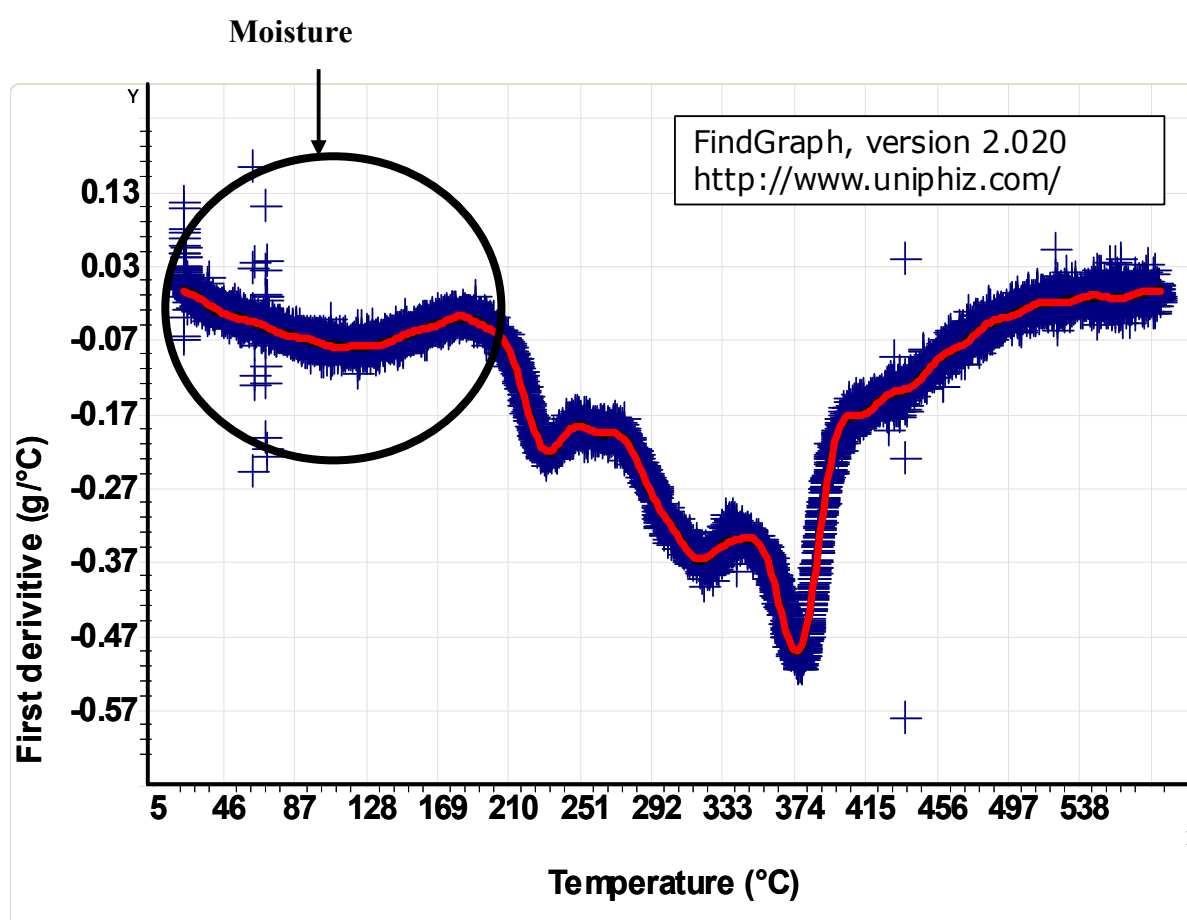


**Figure 3.14:** DTG thermogram of soybean with indication of the peak due to moisture loss.

For the original sample preparation the seeds and beans were all cut into coarse pieces. Table 3.4 gives the results obtained from the oven gravimetric method and from the TGA.

**Table 3.4:** Moisture content determined by TGA and the oven gravimetry method.

SEEDS	TGA Moisture content (% w/w)		Gravimetric analysis Moisture content (% w/w)	BEANS	TGA Moisture content (% w/w)		Gravimetric analysis Moisture content (% w/w)
	increasing temperature	full data			increasing temperature	full data	
POP1	n.a	10.4	7.9	BB1	14.8	14.7	
POP2	n.a	11.0	8.0	BB2	15.0	15.0	
POP3	n.a	11.8	7.9	BB3	14.6	14.5	
<b>average</b>		<b>11.1</b>	<b>7.9</b>	<b>average</b>	<b>14.8</b>	<b>14.7</b>	<b>15.8</b>
PUM1	n.a	10.3	8.5	KID1	13.5	13.5	
PUM2	n.a	10.5	8.4	KID2	13.0	13.2	
PUM3	n.a	13.3	8.4	KID3	12.9	12.9	
<b>average</b>		<b>11.4</b>	<b>8.4</b>	<b>average</b>	<b>13.1</b>	<b>13.2</b>	<b>13.2</b>
SES1	4.8	4.8	5.1	MUN1	11.6	11.4	10.3
SES2	4.9	5.2	5.4	MUN2	12.7	12.6	10.2
SES3	5.0	5.0	4.9	MUN3	11.8	11.5	10.3
<b>average</b>	<b>4.9</b>	<b>5.0</b>	<b>5.1</b>	<b>average</b>	<b>12.0</b>	<b>11.8</b>	<b>10.3</b>
SUN1	4.3	4.6	4.4	SOY1	9.4	9.4	10.2
SUN2	4.9	4.9	4.6	SOY2	9.6	9.9	10.2
SUN3	5.0	5.0	4.7	SOY3	9.4	9.7	10.2
<b>average</b>	<b>4.7</b>	<b>4.8</b>	<b>4.6</b>	<b>average</b>	<b>9.47</b>	<b>9.65</b>	<b>10.2</b>

Looking at Table 3.4, quantitative values obtained for sesame seed, sunflower seed, soybean and kidney beans indicate that the DTG data from increasing temperature as well as full data compare well to those of the conventional gravimetric analysis. In some cases however such as for pumpkin and poppy seeds, the DTG data plotted from increasing temperature could not be quantified. This was due to the fact that no fourier fit of the data could be obtained by the software to yield maxima values. For those specific seeds, the DTG full data and values obtained from the conventional gravimetric method do not compare well. This is also seen for black bean and mung bean where both the increasing temperature and full data values do not compare well to those of the conventional gravimetric analysis. In the literature Tomasetti *et*

*al.*<sup>21</sup> report that for TGA analysis pumpkin seeds need to be prepared by removing the tegument, while poppy seeds due to their small size should be used whole without cutting. Therefore for our studies these two samples were re-prepared in this way and TGA analysis rerun. This was also done for the mung bean sample for which the tegument was detected and therefore also removed. Table 3.5 gives the final results obtained for both techniques yielding more satisfactory comparative values. From the data in Table 3.5 it is evident that with the correct sample preparation TGA can be effectively used to determine the moisture content in seeds and beans. The assignment of the remaining peaks in the DTG thermograms could subsequently be addressed and an analysis of the further quantitative information regarding the content of the seeds and beans could be carried out.

In order to investigate the remaining peaks of the DTGs, it was essential to identify the remaining major components present in the seeds and beans. Conventional methods were used for the determination of the oil content (Soxhlet extraction), protein content (Dumas-combustion) and carbohydrate content (Clegg-Anthrone/UV-is) of seeds and beans. DTG data acquired will only be discussed further where the temperature started to increase consistently since this was found to be more accurate with the lowest standard errors for the fitted curves.

Further analysis of the seeds and beans will be separately discussed.

**Table 3.5:** Moisture content determination by TGA and the gravimetric method using different sample preparation.

SEEDS	TGA Moisture content (% w/w)		Gravimetric analysis Moisture content (% w/w)	BEANS	TGA Moisture content (% w/w)		Gravimetric analysis Moisture content (% w/w)
	increasing temperature	full data			increasing temperature	full data	
<b>Poppy (whole)</b>				<b>Mung bean (without tegument)</b>			
POP1	7.3	8.1	7.9	MUN1	10.9	10.9	10.3
POP2	8.6	7.8	8.0	MUN2	11.7	12.0	10.2
POP3	6.8	8.3	7.9	MUN3	12.2	12.2	10.3
<b>average</b>	<b>7.6</b>	<b>8.1</b>	<b>7.9</b>	<b>average</b>	<b>11.6</b>	<b>11.7</b>	<b>10.3</b>
<b>Pumpkin (without tegument)</b>							
PUM1	7.3	7.3	8.5				
PUM2	8.2	8.2	8.4				
PUM3	7.0	7.1	8.4				
<b>average</b>	<b>7.5</b>	<b>7.5</b>	<b>8.4</b>				

### 3.4.3 Fat, protein and carbohydrate analyses

#### 3.4.3.1 Quantification of oil and protein contents of seeds

Fat content of seeds was determined by the cumbersome Soxhlet method while protein content was determined by the Dumas combustion method. All TGA results are based on the correct sample preparation for each seed as mentioned in the moisture analyses section.

Fat content was determined using the following equation (values indicated in Table 3.6):

$$\% \text{ fat} = \frac{\text{weight of oil}}{\text{original seed weight}} \times 100$$

**Table 3.6:** Values used for the calculation of fat content.

<b>SEEDS</b>	<b>Mass of seed (g)</b>	<b>Mass of fat (g)</b>	<b>Fat content (% w/w)</b>
POP1	9.50	4.03	42.4
POP2	10.90	4.58	42.0
POP3	10.14	4.54	44.8
<b>average</b>			<b>43.1</b>
PUM1	9.95	4.34	43.6
PUM2	10.11	4.43	43.8
PUM3	10.20	4.73	46.4
<b>average</b>			<b>44.6</b>
SES1	9.95	5.83	58.6
SES2	10.16	5.80	57.1
SES3	9.33	5.33	57.1
<b>average</b>			<b>57.6</b>
SUN1	10.08	5.92	58.7
SUN2	9.95	5.72	57.5
SUN3	9.87	5.38	54.5
<b>average</b>			<b>56.9</b>

As can be seen from the triplicate values obtained by Soxhlet extraction determined for each seed, the values fluctuate by up to 2 %. This error combined with the lengthy time it takes to run each experiment makes Soxhlet extraction a cumbersome method.

Protein quantification was achieved by the Dumas Combustion method using a *Leco* instrument. Determination of protein content by Dumas combustion is based on the percentage nitrogen present in the compound compared to a standard, and for proteins the value is multiplied by a factor of 6.25.

Two standards were used, EDTA for protein values higher than 20 % and Alfalfa for protein values below 20 %. Experiments were repeated using Alfalfa as the standard in cases where the protein content of the seed or bean was found to be close to 20 % when using EDTA as a standard. If the true protein content was below 20 % but

the EDTA standard had been used, incorrect results could have been obtained. However referring to Table 3.7, when using Alfalfa as the standard the protein values did not drop below the 20 % mark and therefore all results where EDTA had been the standard were used.

**Table 3.7:** Protein determination using EDTA and Alfalfa as standards.

Standard	EDTA				Alfalfa		
	% N	conversion	Protein content (% w/w)		% N	conversion	Protein content (% w/w)
<b>SEEDS</b>				<b>SEEDS</b>			
POP1	3.4018	6.25	21.3	POP1	3.834	6.25	24.0
POP2	3.2481	6.25	20.9	POP2	3.8794	6.25	24.3
POP3	3.3798	6.25	21.1	POP3	3.8324	6.25	24.0
<b>average</b>			<b>21.1</b>	<b>average</b>			<b>24.1</b>
PUM1	5.4977	6.25	34.4	PUM1	6.0686	6.25	37.9
PUM2	5.452	6.25	34.1	PUM2	5.9654	6.25	37.3
PUM3	5.507	6.25	34.4	PUM3	5.9748	6.25	37.3
<b>average</b>			<b>34.3</b>	<b>average</b>			<b>37.5</b>
SES1	3.6663	6.25	22.9	SES1	4.1526	6.25	26.0
SES2	3.7741	6.25	23.6	SES2	4.1775	6.25	26.1
SES3	3.7418	6.25	23.4	SES3	4.2101	6.25	26.3
<b>average</b>			<b>23.3</b>	<b>average</b>			<b>26.1</b>
SUN1	3.4211	6.25	21.4	SUN1	3.7278	6.25	23.3
SUN2	3.3227	6.25	20.8	SUN2	3.7804	6.25	23.6
SUN3	3.3989	6.25	21.2	SUN3	3.6937	6.25	23.1
<b>Average</b>			<b>21.1</b>	<b>average</b>			<b>23.3</b>

Literature values obtained from the USDA Nutrient Database<sup>25</sup> for oil and protein content in these seeds were found to be: 42 % and 18 % for poppy, 61 % and 20 % for sesame, 50 % and 23 % for sunflower respectively, which compare well with that obtained by the conventional methods. No data was found on the database for pumpkin seeds. By comparing the values obtained in Tables 3.6 and 3.7 to the individual peaks quantified in the DTG thermograms, it was found that none of the

DTG peaks corresponded to the separate values found for protein and oil content. Instead some of the seeds only had one peak in the DTG thermogram while others had two. This is shown in Figure 3.15 where an area from 270–480 °C in the thermogram of each seed represented values close to those of the sum of the protein and oil content (as reported in Table 3.8).

In most cases the sum of the fat and protein content was represented by a certain area in the thermogram. This area was found to be consistent in all the seed thermograms, namely the area under two peaks which are labelled **a** and **b** in Table 3.9 (Figure 3.15). In some cases however only one value could be obtained and this was most likely due to the fact that peak **a** could not be sufficiently separated from peak **b** by the software used and individual maximums could not be obtained. This was exactly the case for poppy seed sample 2 where the separate peaks can be seen by eye but maximums could not be separately determined by the software (refer to Figure 3.5). Notice that peak **b** was observed to always be the largest peak with peak **a** being the smaller peak to the left of peak **b**.

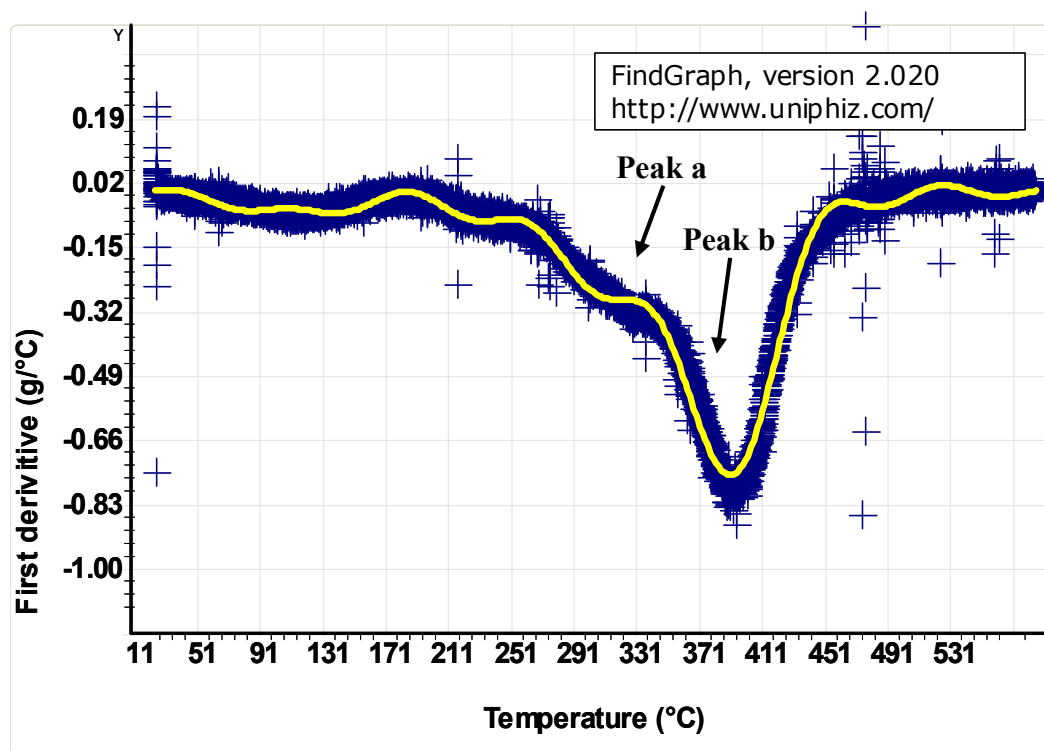


**Figure 3.15:** Graph illustrating the DTG thermogram for pumpkin seed with indication of the peaks of interest for oil and protein content.

**Table 3.8:** Comparison of the fat and protein content values of seeds determined by Soxhlet and Dumas combustion respectively with DTG results.

	Soxhlet and Dumas combustion			DTG		
	Fat content (% w/w)	Protein content (% w/w)	Sum of protein and fat content (% w/w)	Increasing temperature: peak a (% w/w)	Increasing temperature: peak b (% w/w)	Sum of peak a and peak b (% w/w)
POP1	42.4	21.3		63.7		
POP2	42.0	20.9		63.6		
POP3	44.8	21.1		63.9		
<b>average</b>	<b>43.1</b>	<b>21.1</b>	<b>64.2</b>	<b>63.7</b>		<b>63.7</b>
PUM1	43.6	34.4		14.0	59.7	
PUM2	43.8	34.1		16.3	56.6	
PUM3	46.4	34.4		16.0	56.9	
<b>average</b>	<b>44.6</b>	<b>34.3</b>	<b>78.9</b>	<b>15.4</b>	<b>58.2</b>	<b>73.6</b>
SES1	58.6	34.4		14.3	65.2	
SES2	57.1	34.1		13.3	67.5	
SES3	57.1	34.4		14.5	61.3	
<b>average</b>	<b>57.6</b>	<b>23.3</b>	<b>80.9</b>	14.0	64.7	<b>78.7</b>
SUN1	58.7	21.4		10.8	67.4	
SUN2	57.5	20.8		11.0	67.1	
SUN3	54.5	21.2		10.6	67.1	
<b>average</b>	<b>56.9</b>	<b>21.1</b>	<b>78.0</b>	10.8	67.2	<b>78.0</b>

In order to satisfactorily compare content results obtained from TGA and the conventional methods, error determinations were required. Error values were determined for each conventional method as well as for TGA at a 95 % confidence limit (CL) on average for each triplicate experiment. However, since the TGA results are representative of the sum of the oil, protein and carbohydrate values, the error values determined for each individual conventional method could not be used directly for comparison. Therefore the following equation was used:

$$\sqrt{a^2 + b^2 + c^2}$$

where **a** represents the standard errors obtained for Soxhlet extraction, **b** for Dumas-combustion and **c** for Clegg/Anthrone UV-Vis spectroscopy method.

**Table 3.9:** Sum of the oil and protein percentage content obtained for each seed with 95 % CL\* by various methods.

	Sum of the oil and protein percentage content for DTG (% w/w)			Sum of the oil and protein percentage content for conventional methods (% w/w)		
<b>POP</b>	63.7	±	0.4	64.2	±	3.7
<b>PUM</b>	73.6	±	1.2	78.9	±	3.9
<b>SES</b>	78.7	±	6.4	80.9	±	2.3
<b>SUN</b>	78.0	±	0.7	78.0	±	5.5

\* 95 % confidence limit (CL) in each case for triplicate experiments was determined from

$95\% \text{ CL} = \bar{x} \pm t \cdot s_x / \sqrt{n}$ , where  $\bar{x}$  is the mean,  $s_x$  is the standard deviation and  $n$  is the degrees of freedom, namely 3, and  $t$  is the student's  $t$  value determined as 4.303 for three degrees of freedom<sup>26</sup>.

Comparison of the quantitative results (in Table 3.9) obtained via TGA and conventional methods could then be carried out. For most of the seeds, namely poppy, sesame and sunflower seeds the values obtained by TGA compare well with those obtained by conventional methods with at most a two percent difference (such as for sesame seed) while for pumpkin seed incorporation of the standard error values brings one closer to a good comparison between the two methods.

For poppy seed the two values by the different techniques are very close with a very small error in TGA quantification (0.4 %) and a larger error in the conventional methods (3.7 %). However even with incorporation of the slightly larger conventional method's standard error, the quantitative results compare very well between the two techniques. For sunflower seed a very similar situation is seen to that of poppy seed. In this case the conventional method and TGA values are identical up to the first decimal place (78 %) and the standard errors being smaller for TGA (0.7 %) than for the conventional methods (5.5 %). Comparison of the two techniques for sesame seed quantification is also excellent. In this case however, the large conventional

error value (2.3 %) is smaller than the TGA error (6.4 %). These values with incorporation of the standard errors still compare fairly well. Pumpkin seed quantitative values seem to be the only seed to be slightly out. In this case the difference in TGA results (73.6 %) and the conventional method results (78.9 %) is quite large at around 5 %. Standard errors for these two methods, once again show TGA to have a smaller error value (1.2 %) to that of the conventional methods (3.9 %).

In conclusion, for quantification of the components present in seeds, TGA provides data which compares very well to those obtained by conventional methods. For some seeds, this comparison is excellent, such as poppy seed, sesame seed and sunflower seed, while for pumpkin seed the comparison is fair. However it is important to keep standard error determinations of all techniques in mind, and once these errors have been incorporated into the final quantitative values, the TGA quantification of fat and protein contents in all four seeds compare over all very well to that of quantification by conventional methods.

#### 3.4.3.2 Quantification by analytical methods applied to beans

The same protein and oil determinations were carried out on the four bean samples, but unlike the seeds, summation of the values of the protein and oil content did not give results which compared to the two peaks (namely peak **a** and peak **b** in Figure 3.15) in the DTG thermograms. In fact the summation of the values for the protein and oil content (refer to Tables 3.10 and 3.11) were substantially lower than values obtained for the sum of peak **a** and peak **b** in the beans. This led to the investigation of another major component present in beans, namely carbohydrates. Carbohydrate content was determined for seeds using the Clegg-Anthrone /UV-VIS spectroscopy method but the results obtained indicated that the presence of carbohydrates, if any, in seeds is so low that the content could not be accurately determined using this method. However in hindsight, this method was not the best to use since it mainly extracts the soluble carbohydrates from the seeds and beans leaving behind the non-soluble carbohydrates also present and consequently no carbohydrate content was detected for seeds. The incorrect use of carbohydrate extraction and detection method however did not seem to affect results obtained for oil and protein data.

The carbohydrate contents of the beans of interest were determined successfully using the Clegg-Anthrone /UV-VIS spectroscopy method. Table 3.12 gives the results obtained for the carbohydrate determinations. The following equation was used to determine the carbohydrate percentage:

$$\% \text{ carbohydrates} = \frac{25 \times b}{a \times W}$$

where **a** represents the absorbance of the glucose standard and **b** the absorbance of the sample. **W** represents the weight of the original bean flour sample.

**Table 3.10:** Values used for the calculation of fat content.

<b>BEANS</b>	<b>Mass of seed (g)</b>	<b>Mass of fat (g)</b>	<b>Fat content (% w/w)</b>
BB1	9.97	0.26	2.6
BB2	10.06	0.21	2.1
BB3	10.03	0.31	3.1
<b>average</b>			<b>2.6</b>
KID1	10.07	0.13	1.3
KID2	10.09	0.09	0.9
KID3	10.01	0.02	0.2
<b>average</b>			<b>0.8</b>
MUN1	10.50	0.36	3.4
MUN2	9.61	0.20	2.0
MUN3	11.37	0.17	1.5
<b>average</b>			<b>2.3</b>
SOY1	10.01	1.56	15.6
SOY2	10.70	2.00	18.7
SOY3	11.41	2.11	18.5
<b>average</b>			<b>17.6</b>

**Table 3.11:** Protein determination using EDTA and Alfalfa as standards.

Standard	EDTA			Alfalfa			
	% N	conversion	Protein content (% w/w)	BEANS	% N	conversion	Protein content (% w/w)
BEANS							
KID1	2.87	6.25	17.9	KID1	2.88	6.25	18.0
KID2	2.95	6.25	18.4	KID2	2.74	6.25	17.1
KID3	3.02	6.25	18.9	KID3	2.90	6.25	18.2
<b>average</b>			<b>18.4</b>	<b>average</b>			<b>17.8</b>
BB1	3.48	6.25	21.7				
BB2	3.60	6.25	22.5				
BB3	3.68	6.25	23.0				
<b>average</b>			<b>22.4</b>				
MUN1	3.78	6.25	23.6				
MUN2	3.77	6.25	23.6				
MUN3	3.66	6.25	22.9				
<b>average</b>			<b>23.4</b>				
SOY1	5.65	6.25	35.3				
SOY2	5.54	6.25	34.6				
SOY3	5.53	6.25	34.5				
<b>average</b>			<b>34.8</b>				

**Table 3.12:** Determination of the carbohydrate content in beans.

Wavelength (nm)	Standard	a Absorbance	Sample	b Absorbance	w Sample mass (g)	Carbohydrate content (% w/w)
625	Glucose	0.27005	BB	0.32045	1.0007	29.7
625		0.27005	KID	0.47947	1.0016	44.3
625		0.21131	MUN	0.29910	1.0013	35.3
625		0.21131	SOY	0.16220	0.9999	19.2

Literature values obtained from the USDA Nutrient Database<sup>25</sup> for oil, protein and carbohydrate content in these beans were found to be: 1 %, 24 % and 60 % for kidney bean, 1 %, 25 % and 57 % for dry beans (which incorporate black beans), 1 %, 24 % and 63 % for mungbean, 20 %, 37 % and 30 % for soybean respectively.

The oil and protein values obtained by conventional methods compare well with those from the literature while the carbohydrate content determined by the conventional methods were too low in each case. This could possibly be due to the method used for carbohydrate determination which only accounts for soluble carbohydrates.

Upon determination of the carbohydrate content present in the beans, values obtained by analytical methods for the fat, protein and carbohydrate content could then be used in comparison to the TGA results obtained. However as already mentioned unlike the seeds, it was found that the sum of the two peaks, namely peak **a** and **b** as indicated in Figure 3.15, did not give matching results to those of the analytical techniques. Instead the whole of the DTG thermogram, a region from 180-590 °C minus the peak representing the moisture loss, (indicated as Region C in Figure 3.16) gave comparative results (refer to Table 3.12 for these values).

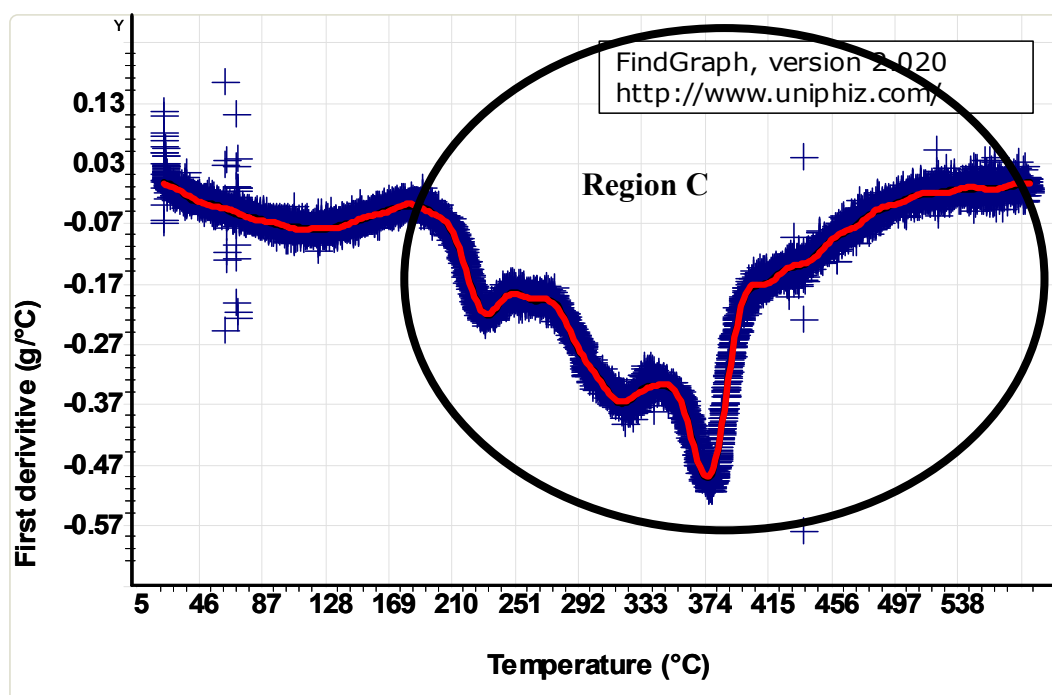


**Figure 3.16:** Graph illustrating the DTG of soybean with indication of the region of interest for oil, protein and carbohydrate content.

Table 3.13 shows the summarized quantitative results (oil plus protein plus carbohydrate content) for each compound with relative errors, determined at a 95 % CL on average for each triplicate experiment run, determined in the same way

as for the seeds. Notice that the oil and protein contents were determined in triplicate while for the carbohydrate content, only a single experiment was done. However the relative percentage error for carbohydrate content was estimated to be at most 3 %.

**Table 3.13:** Comparison of fat, carbohydrate and protein content values for beans determined by conventional methods and DTG.

Sample	Soxhlet, UV-Vis and Dumas combustion				TGA
	Fat content (% w/w)	Protein content (% w/w)	Carbohydrate content (% w/w)	Sum of fat, protein and carbohydrate content (% w/w)	Area C (% w/w)
BB1	2.57	17.91			59.2
BB2	2.07	18.42			59.4
BB3	3.10	18.86			60.1
<b>Average</b>	<b>2.58</b>	<b>22.39</b>	<b>29.65</b>	<b>54.62</b>	<b>59.6</b>
KID1	1.29	21.72			58.8
KID2	0.89	22.48			60.7
KID3	0.24	22.98			61.2
<b>Average</b>	<b>0.81</b>	<b>18.40</b>	<b>44.32</b>	<b>63.53</b>	<b>59.8</b>
MUN1	3.43	23.64			62.0
MUN2	2.03	23.59			62.8
MUN3	1.52	22.89			62.5
<b>Average</b>	<b>2.33</b>	<b>23.37</b>	<b>35.34</b>	<b>61.04</b>	<b>62.4</b>
SOY1	15.63	35.29			66.6
SOY2	18.69	34.64			68.1
SOY3	18.50	34.54			73.4
<b>Average</b>	<b>17.61</b>	<b>34.82</b>	<b>19.19</b>	<b>71.62</b>	<b>70.7</b>

**Table 3.14:** Sum of oil, protein and carbohydrate (% w/w) content obtained for each type of bean at 95 % CL by various methods.\*

	Sum of the oil, protein and carbohydrate percentage content for TGA (% w/w)			Sum of the oil, protein and carbohydrate percentage content for conventional methods (% w/w)		
BB	59.6	±	1.2	54.6	±	3.7
KID	59.8	±	3.2	63.5	±	2.0
MUN	62.4	±	1.0	61	±	1.3
SOY	70.7	±	8.9	71.6	±	1.3

\* 95 % confidence limit (CL) in each case for triplicate experiments was determined from  $95\% \text{ CL} = \bar{x} \pm t \cdot s_x / \sqrt{n}$ , where  $\bar{x}$  is the mean,  $s_x$  is the standard deviation and  $n$  is the degrees of freedom, namely 3, and  $t$  is the student's  $t$  value determined as 4.303 for three degrees of freedom<sup>27</sup>.

Comparison of the quantitative results (in Table 3.14) obtained via TGA and conventional methods can now be carried out. For most of the beans, namely kidney, mung and soybeans the values obtained by TGA compared well with those obtained by conventional methods with at most a three percent difference (kidney bean) while for black bean, taking the errors into account the results appear comparable. For mung bean the two values by the different techniques compared very well with relatively small errors in both techniques at around 1 %. For kidney bean a similar comparison was seen. In this case the standard error of the conventional methods (2.0 %) was smaller than for TGA (3.2 %). However once again as was the case with mung bean, the error values for both techniques were very close together and taking these values into account the final quantification values for kidney bean compare well. Comparison for soybean quantification via the two techniques also compared very well. Like kidney bean, the conventional method error value (1.3 %) was smaller than the TGA error (8.9 %). Although a large error was observed for TGA, the values still compared well. As was the case with pumpkin seed, black bean seemed to be the only bean for which values obtained via the two different methods varied. In this case the TGA data (59.6 %) and the conventional method data (54.6 %) difference were quite large at around 5 %, as for pumpkin

seed. Standard errors for these two methods indicated that TGA had a smaller error value (1.2 %) to that of the conventional methods (3.7 %). Taking these error values into account however makes the comparison between the data become more acceptable.

### **3.5 CONCLUSIONS**

During an investigation into the use of TGA as a quantitative tool to determine the moisture, oil, protein and carbohydrate content of seeds and beans, it was shown that TGA gave valuable information on the content in seeds (where all seeds were ground into coarse pieces with the exception of poppy seed being used whole) and beans (where all beans were ground into coarse pieces and the tegument removed from mung bean and kidney bean). The thermograms obtained from the plot of the first derivative of the TGA data with respect to the temperature indicated certain regions of peaks corresponding to the mass loss of the compounds of interest as determined by conventional methods. These methods included Soxhlet extraction for oil, Dumas-Combustion for protein and Clegg-Anthrone/UV-VIS method for carbohydrates. It could possibly be that these peaks are indeed the bulk of the oil/protein/carbohydrates but that because these components are made up of mixtures the DTG peaks overlap and so the information for each component can't be isolated from the DTG. For seeds, a region consisting of two peaks between 270–480 °C gave quantitative results for the oil and protein content, while for beans, a region between 180-590 °C gave quantitative results for the oil, protein and carbohydrate contents. For all the seeds and beans tested, the TGA results compared very well to those of the conventional methods and hence the conclusion can be drawn that TGA is another useful technique for the determination of the sum of the oil, protein and carbohydrate content in seeds and beans. It is interesting that although the conventional method used to determine carbohydrate content in the seeds and beans only accounted for the soluble carbohydrates, comparable values were found in the TGA thermograms. Possibly the carbohydrate content for seeds could be detected separately from the oil and protein content while for the beans the non-soluble carbohydrates ends up as part of the ash residue. This requires further investigation.

Although it was not possible to use the DTG thermogram to distinguish between the individual oil, protein and carbohydrate content, the beauty of the discussed TGA

technique however lies in the use of this information in a subtraction method to determine desired values. For instance, using conventional methods, two or three separate experiments are required to obtain oil, protein and carbohydrate contents. For analytical purposes each of these experiments needs to be done in triplicate. One of these conventional methods, namely Soxhlet extraction (for determination of oil content) is a long, messy and cumbersome procedure taking about 16 hours, while TGA takes at maximum one hour to obtain data for a seed or bean. The other two conventional methods are fairly rapid in obtaining results as well, namely a three minute run per sample via Dumas combustion and about an hour for the Clegg-Anthrone/UV-Visible spectroscopy method. By obtaining results for protein and carbohydrate content by the two above mentioned conventional methods and results from TGA, one can cut out the need to use the cumbersome Soxhlet extraction method. The oil content of a seed or bean can now be determined by subtracting the protein content (for seeds) or protein and carbohydrate content (for beans), determined by the conventional methods, from the relevant quantitative data obtained from the TGA results, thus yielding a faster option to determine the oil content.

In the next chapter, high resolution solid-state NMR spectroscopy is discussed as a method to investigate the seeds and beans and to possibly gain some further insight to the differences between the DTG thermograms obtained for the seeds and beans, namely the regions where the mass loss of the components of interest were found.

## **3.6 EXPERIMENTAL**

### **3.6.1 Sample preparation**

The beans and seeds were commercially obtained and were prepared in different ways for each experiment. In some cases they were used whole with or without their tegument (for TGA). For cases where the beans and seeds needed to be cut into coarse pieces (for TGA and gravimetric analysis by oven) or ground up into flour (for Soxhlet, Dumas combustion method and UV-Visible spectroscopy), a coffee and spice grinder was used taking care not to create too much heat in order to limit moisture loss. To achieve this only short cycles of the grinder were used. The grinder was cleaned using water and wiped dry with paper.

### **3.6.2 Collection of TGA data**

Experiments were conducted on a TGA Q500 instrument from TG Instruments, with the sample weight ranging between 3 and 10 mg. Seeds and beans were analysed in triplicate to minimize random errors caused by the factors mentioned in the introduction to the TGA section in Chapter 3, of which sample particle size and preparation were found to be of most importance. All experiments were conducted under a flux of nitrogen, maintained at a flow rate of 75 ml/min. The sample was initially isothermally stabilized at 30 °C for one min and then a ramp rate of 10 °C/min was used up to a maximum temperature of 590 °C<sup>1</sup>. FindGraph software from Uniphiz was used to process the data.

### **3.6.3 Soxhlet extraction**

The oil content of the seeds and beans was determined in triplicate using Soxhlet extraction. 10 g of sample was ground into a flour and placed into a thimble. A 250 ml round bottom flask used for the extraction was filled with approximately 150 ml hexane. The oil bath temperature was kept at approximately 100 °C for the 16-18 hours during which the Soxhlet extraction was allowed to run. The solvent was removed via rotary evaporation leaving the desired oil product. The oil percentage was determined by the mass (oil % = (mass of oil (g)/mass of sample used for extraction (g)) x 100)<sup>27</sup>.

### **3.6.4 Oven gravimetric method**

The water content was determined in triplicate using an oven gravimetric method. Samples were cut into coarse pieces and placed inside glass polytops. Samples were left in an oven at approximately 105 °C for 15-17 hours and then cooled down under vacuum for 30-45 minutes. Moisture loss was determined by the mass difference of sample before and after the experiment<sup>28</sup>.

### **3.6.5 Dumas-combustion**

Quantification of the protein content of the seeds and beans was carried out in triplicate using a Leco Nitrogen Analyzer FP528 (Dumas-combustion method). Seeds and beans were ground into flour before analysis. 1 mg of the flour was then used with Alfalfa and EDTA as standards. Protein content was determined using the conversion factor of 6.25 as is standard for seeds and beans.

### 3.6.6 Clegg-Anthrone method

Before the carbohydrate content in the seeds and beans could be determined, the carbohydrate fraction was extracted. This was done using the Clegg-Anthrone method<sup>29,30</sup>. Anthrone reagent was prepared as follows: 165 ml distilled water and 380 ml concentrated sulphuric acid were added to a 2 L flask and cooled down to room temperature before 750 mg anthrone was added and the mixture stored at 5 °C. A 100 ml standard glucose solution was prepared by dissolving 100 mg glucose in distilled water and diluted 10 times. Perchloric acid solution was made by addition of 279 ml perchloric acid to 100 ml distilled water and cooled to room temperature before use.

Extraction of carbohydrates: Approximately 1.0 g of the ground sample (flour) was accurately weighed, dissolved in 10 ml distilled water and 13 ml of the perchloric acid solution and manually stirred for 20 minutes. Distilled water was used to make the solution up to 100 ml and the solution was filtered using N°541 Whatman, Schleicher & Schuell filter paper. The extract was diluted to 250 ml with distilled water and shaken well.

Determination of the carbohydrate content: 10 ml of the extract was diluted to 100 ml using distilled water. 1 ml of sample, distilled water and the standard glucose solution were separately transferred to glass vials. 5 ml of the anthrone reagent was added to each vial and mixed. The vials were placed in a water bath and heated for approximately 12 min at 90 °C, after which they were rapidly cooled down to room temperature under cold running water and transferred to 0.5 cm cuvettes. Absorbances of the solutions were collected using an Agilent 8453E UV-visible Spectrophotometer at 625 nm.

### 3.7 REFERENCES

- 1 Information bulletin number 269: seeds and their role in fruit production compiled and issued by Fruit and Fruit Technology Research Institute, Stellenbosch, 1975.
- 2 Food and Agriculture Organization of the United Nations:  
<http://www.fao.org>, date of access, 2009.
- 3 [www.frenchgardening.com/aujardin.html?pid=31322166539680](http://www.frenchgardening.com/aujardin.html?pid=31322166539680), date of access, 2009.
- 4 [Bernáth](#), J., Poppy: the genus Papaver, Harwood Academic Publishers, **1998**.
- 5 Eckey, E. W., Vegetable fats and oils, Reinhold publishing corporation, New York, **1954**.
- 6 Liebenburg, A.J., Dry bean production, Department of Agriculture, South Africa.
- 7 Wendlandt, W.W.M.; Thermal methods of analysis, Interscience publishers, **1964**, Chapter 2.

- 8 Brown, M.E., Introduction to thermal analysis, techniques and applications, Chapman and Hall, London, New York, **1988**, p 3.
- 9 Czarnecki, J., and Šesták, J., Practical thermogravimetry, *J. Therm. Anal. Calorim.*, **2000**, 60, 759-778.
- 10 Tomasetti, M., Campanella, L., and Aureli, T., Thermogravimetric analysis of some spices and food products. Comparison with other analytical methods for moisture content determination (part 3). *Thermochim. Acta*, **1989**, 143, 15-26.
- 11 Tomasetti, M., and Campanella, L. Determination of water in plant samples: a comparative thermogravimetric and NMR study on different species of seeds, *Thermochim. Acta*, **1986**, 105, 179-190.
- 12 Tomasetti, M., Campanella, L., Delfini, M., and Aureli, T., Determination of moisture in food flours. A comparative thermogravimetric and NMR study, part 2, *Thermochim. Acta*. **1987**, 120, 81-95.
- 13 Tomasetti, M., Campanella, L., Aureli, T., and Sammartino, M.P., TG and NMR analysis of commercial plant oil seed, *Thermochim. Acta*, **1991**, 190, 131-141.
- 14 Santos, J.C.O., Dantas, J.P., Medeiros, C.A., Athaide-Fiho, P.F., Conceicao, M.M., Santos Jr., J.R., and Souza, A.G., Thermal analysis in sustainable development, Thermoanalytical study of faveleira seeds (*Cnidocolus Quercifolius*), *J. Therm. Anal. Calorim.*, **2005**, 79, 271-275.
- 15 Dyszel, S. M. Characterization of green coffee beans by combined thermogravimetric analysis/atmospheric pressure chemical ionization mass spectrometry, *Thermochim. Acta*, **1985**, 87, 89-98.
- 16 Dyszel, S. M. Comparison of various green coffees by thermogravimetric analysis/atmospheric pressure chemical ionization mass spectrometry (TGA/APCIMS). Part 2, *Thermochim. Acta* **1986**, 104, 85-92.
- 17 Curini, R., D'Ascenzo, G., Materazzi, S., Chiacchierini, E., De Angelis Curtis, S., and Lucchetii, M.C., Characterization of coffees by thermoanalytical methods, *Ann. Chim-Rome*, **1991**, 81, 625-638.
- 18 Freitas, R.A., Martin, S., Paula, R.C., Feitosa, J.P.A., and Sierakowski, M.R., Effect of the oxidation level on the thermogravimetric kinetics of an oxidized galactoxyloglucan from *Hymenaea courbaril* (Jatoba) seeds. *Thermochim. Acta.*, **2004**, 409, 41-47.
- 19 Magoshi, J., Becker, M.A., and Nakmura, S., Thermal properties of seed proteins. *J. Therm. Anal. Calorim.*, **2002**, 70, 833-839.
- 20 Simkovic, I., and Csomorova, K. Thermogravimetric analysis of agricultural residues: oxygen effect and environmental impact., *J. Appl. Polym. Sci.*, **2006**, 100, 1318-1322.
- 21 Tomasetti, M., Campanella, L., Aureli, T., and Sammartino, M.P. TG and NMR analysis of commercial plant oil seeds., *Thermochim. Acta*, **1991**, 190, 131-141.
- 22 Tomasetti, M., and Campanella, L., Determination of water in plant samples: a comparative thermogravimetric and NMR study on different species of seeds., *Thermochim. Acta*, **1986**, 105, 179-190.

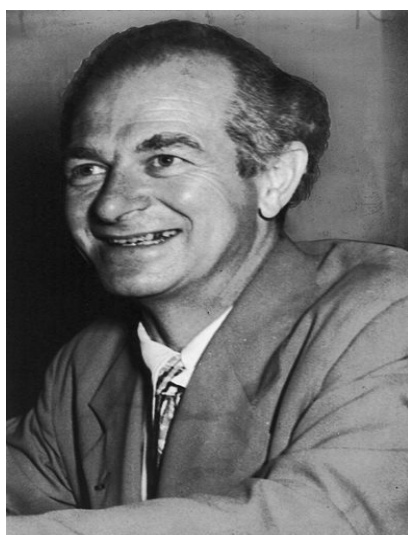
- 23 Tomasetti, M., Campanella, L., Delfini, M., and Aureli, T., Determination of moisture in food flours. A comparative thermogravimetric and NMR study, part 2., *Thermochim. Acta*, **1987**, *120*, 81-95.
- 24 Tomasetti, M., Campanella, L., and Aureli, T., Thermogravimetric analysis of some spices and food products. Comparison with other analytical methods for moisture content determination (part 3). *Thermochim. Acta*, **1989**, *143*, 15-26.
- 25 [www.nal.usda.gov](http://www.nal.usda.gov)
- 26 Meier, P.C., and Zund, R.E., *Statistical methods in analytical chemistry. Volume 123 in Chemical Analysis: a series of monographs on analytical chemistry and its applications*. John Wiley and sons, inc. **1993**, chapter 1.
- 27 Neustadt, M.H. An improved Soxhlet extractor, *Ind. Eng. Chem.*, **1942**, *14*, 431.
- 28 Hanson, J. *Practical manuals for genebanks: No 1. Procedures for handling seeds in genebanks.*, IBPGR publications, Rome. **1985**.
- 29 Van Handel, E. Rapid determination of glycogen and sugars in mosquitoes, *J. Am. Mosq. Control Assoc.*, **1985**, *1* (3), 299-301.
- 30 Ova, M.A.O., Palcios, C.A.M., and Real de Leon, E., *Manual de tecnicas para laboratorio de nutricion de peces y crustaceos. PROGRAMA COOPERATIVE GUBERNAMENTAL FAO. GCP/RLA/102/ITA Proyecto Qauila 2, documento de camp no 7. Italy. Food and Agriculture organization. Available from internet:*  
<http://www.fao.org/docrep/field/003/AB489S/AB489S00.htm>, date of access, 2009.

# CHAPTER 4: EXPLORATIVE ANALYSIS OF SEEDS AND BEANS BY SOLID STATE $^{13}\text{C}$ NMR SPECTROSCOPY

*“Satisfaction of one's curiosity is one of the greatest sources of happiness in life.”*

Linus Carl Pauling

February 28, 1901 – August 19, 1994



Picture obtained from [http://en.wikipedia.org/wiki/Linus\\_Pauling](http://en.wikipedia.org/wiki/Linus_Pauling).

#### 4.1 INTRODUCTION TO SOLID STATE NMR SPECTROSCOPY

In 1936 Gorter attempted to obtain an NMR signal for  $^7\text{Li}$  present in crystalline lithium fluoride as well as  $^1\text{H}$  in crystalline potassium alum<sup>1</sup>. He was however unsuccessful. Six years later Gorter and Broer again attempted to obtain the  $^7\text{Li}$  nuclei signal this time in solid lithium chloride as well as the  $^{19}\text{F}$  nuclei signal in solid potassium fluoride but again without success<sup>1</sup>. The first successful NMR experiments were finally conducted in 1945 by two independent groups working on bulk materials. One was conducted by Purcell *et al.* from Harvard University and the other by Bloch *et al.* from Stanford University<sup>1</sup>. Bloch's group found the signal for  $^1\text{H}$  in water in the liquid state while Purcell *et al.* found the NMR signal for  $^1\text{H}$  in solid paraffin wax. This was arguably the first successful solid state NMR experiment. Purcell *et al.* then went on to a full investigation of NMR relaxation in solids, liquids and gases, these studies laying the basis for further understanding of nuclear relaxation in all forms of matter<sup>1</sup>. A more formal treatment of this concept was given in 1954 by Kubo and Tomita with minor changes in relaxation expressions<sup>1</sup>.

The first British pioneer in NMR spectroscopy was Dr Bernard Rollin from Oxford University. In 1946 he built a very simple, elegant NMR spectrometer of novel design and by November of that year he had published his first paper in *Nature* announcing the detection of  $^1\text{H}$  and  $^9\text{F}$  NMR signals in a range of liquids and solids and the measurement of their relaxation times. In 1947 Hatton reported the first low temperature NMR measurements of  $T^1$  and  $T^2$  values in solid hydrogen and other materials down to 1 Kelvin<sup>1</sup>.

All studies up to this time period had indicated the importance of molecular motion and its modulation of nuclear dipole interactions as sources of nuclear relaxation in a wide range of materials. However, information on the basic understanding of relaxation in crystals such as calcium fluoride, potassium alum and other ionic salts had not yet been obtained, and this was mostly due to the fact that molecules or ions in these crystalline salts displayed no significant nuclear motion, since the lattice is relatively rigid. Bloembergen (who was part of Purcell's group at Harvard) found that the relaxation in these crystals and ionic salts was due to paramagnetic impurities, supplemented by nuclear spin exchanges<sup>1</sup>. This promoted diffusion of energy to and from paramagnetic centres and through them to the lattice. It was concluded that the magnetic dipolar interactions between nuclei was the primary source for the NMR spectrum of a solid, while the width and shape and time dependence of these

interactions was the source of relaxation<sup>1</sup>. At this stage it was understood that a study of the NMR spectra of solids could give information on the nuclei in solid structures of molecules and groups, while a study of the NMR relaxation, particularly as a function of time, could give information on dynamic behaviour of molecules and groups in the solid state<sup>1</sup>.

Further research on several topics in solid state NMR have significantly contributed to the understanding of structure in solids, the dynamics within solids, and of solids in certain environments, conformational motion, magic-angle spinning, NMR imaging, and many other phenomena<sup>1</sup>.

Most of solid state NMR spectroscopy's success lies in the variety of techniques that can be used to detect or investigate several nuclear properties, such as internuclear distances, anisotropy, torsion angles, atomic orientations, spin diffusion, molecular dynamics and exchange processes. Another advantage of NMR spectroscopy lies in the high sensitivity and analytical high resolution of the technique, due to the development of Magic Angle Spinning (MAS)<sup>2</sup>.

Although high resolution solid state NMR spectroscopy has been applied to many fields, this study focuses on the food industry, specifically with application of NMR spectroscopy to seeds and beans. Seeds and beans have a complex composition of mainly oils and fats, proteins and carbohydrates. Solid state <sup>1</sup>H and <sup>13</sup>C NMR spectroscopy can be used to examine these compositions as well as provide information about their specific organization at cellular and macroscopic level as discussed further in this chapter<sup>3-17</sup>.

Solid state NMR spectroscopy can distinguish between solid-like domains and liquid-like domains. Resonances representing <sup>13</sup>C carbons in for instance oils are found in liquid-like domains while resonances representing carbons in for instance carbohydrate and protein carbons are found in solid-like domains. Different solid state NMR spectroscopic techniques are used to detect these: Cross Polarization-Magic Angle Spinning (CP-MAS) NMR spectroscopy is used for solid-like domains while Single Pulse Excitation-Magic Angle Spinning (SPE-MAS) spectroscopy is used for liquid-like domains<sup>18</sup>.

## 4.2 SOLID STATE NMR TECHNIQUES APPLIED TO ANALYSIS OF SEEDS AND BEANS

### 4.2.1 Heteronuclear decoupling interactions

In order to understand the techniques discussed above, a basic understanding of heteronuclear dipolar coupling interactions in a solid is required. Heteronuclear dipolar coupling arises from the interaction between nuclear magnetic moments of two different nuclear spins. The term **I** is usually used for abundant spins such as  $^1\text{H}$  nuclei while **S** is used for rare spins such as  $^{13}\text{C}$  or  $^{15}\text{N}$  nuclei. When these spins are placed in an external magnetic field, the Zeeman interaction describes the energy of spin **I** based on the orientation of the spin, whether it is parallel (spin-up) or anti-parallel (spin-down) with respect to the magnetic field;

$$E_{\text{Zeeman}} = -\hbar\gamma B_0 m_I$$

where  $\gamma$  = gyromagnetic ratio,  $B_0$  = external magnetic field,  $m_I$  = nuclear spin quantum number.

When spin **S** is aligned parallel or anti-parallel to the external magnetic field ( $B_0$ ), the spin (**S**) will be influenced by the magnetic field produced by spin **I** and vice versa, as long as the two spins are in reasonable proximity to each other ( $<10\text{\AA}$ ). The magnetic field produced by spin **I** can either subtract or add to the external field felt by spin **S** depending on the orientation of spin **I**. This can lead to either an increase or decrease in the effective local magnetic field felt at the site of spin **S**, consequently changing its resonance frequency. The degree to which spin **I** affects the magnetic field at spin **S** is characterized by the strength of the heteronuclear dipolar coupling. Consequently the Hamiltonian equation is used:

$$H_{\text{IS}} = -d(3\cos^2\theta - 1)I_z S_z$$
$$d = \left( \frac{\mu_0}{4\pi} \right) \frac{\hbar\gamma_I\gamma_S}{r_{\text{IS}}^3}$$

where  $r_{\text{IS}}$  = internuclear distance,  $\mu_0$  = permeability of free space,  $\gamma$  = gyromagnetic ratios of **I** and **S**,  $I_z$  and  $S_z$  = z components of nuclear spin angular momentum of operators **I** and **S**,  $\theta$  = orientation of the internuclear vector with respect to the orientation of the external magnetic field (see Figure 4.1),  $d$  = dipolar constant<sup>2</sup>

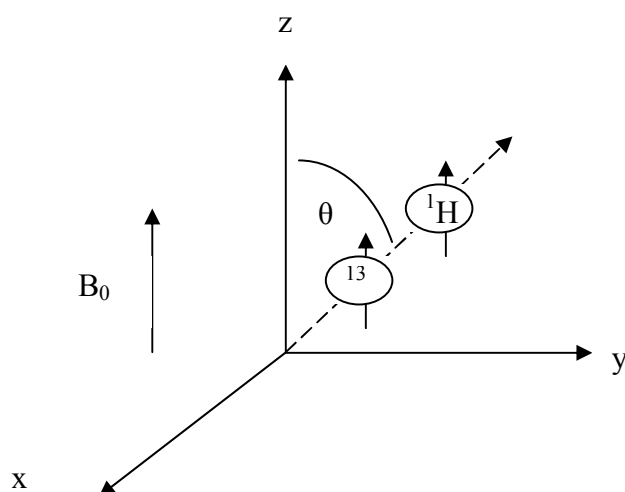


**Figure 4.1:** An illustration of  $\theta$ , which is the angle between the  $^1\text{H}$ - $^{13}\text{C}$  bond vectors and the direction of the external magnetic field  $B_0$ <sup>2</sup>.

Powder samples consist of many crystallites with random orientations. Nuclear spin interactions that affect solid state NMR spectra are chemical shielding, dipole-dipole coupling and quadrupole coupling. All these depend on crystallite orientation and are said to be anisotropic. This leads to NMR spectra with broad lines called powder patterns. The different molecular orientations give rise to different spectral frequencies. There are two techniques that can be used to increase resolution. Magic angle spinning is one of them<sup>19</sup>.

#### 4.2.2 Magic angle spinning (MAS)

This technique is used to remove effects of chemical shift anisotropy due to dipolar interactions and to assist in the removal of heteronuclear dipolar coupling effects. It is also used to narrow resonances from quadrupolar nuclei. In solution NMR spectroscopy the chemical shift anisotropy, dipole coupling, etc, is rarely observed due to the rapid isotropic tumbling of molecules that averages out the molecular orientation dependence of transition frequencies to zero, on the NMR timescale. MAS essentially attempts the same for solids, resulting in the powder pattern being

reduced to a single resonance at the isotropic shift by adjusting the rate of spinning<sup>2,19</sup>.

Spinning of the sample has to be fast compared to the anisotropy of the interaction. This usually means the spinning should be three to four times the size of the anisotropy (in Hz). Slow spinning speeds will cause the formation of spinning sidebands which are sharp lines radiating out from the isotropic shift. In such a situation where spinning sidebands are observed, in order to detect the isotropic chemical shift, the easiest way is by changing the spin speed, and comparing spectra. The chemical shift anisotropy signal does not shift on the ppm scale during different spinning speeds. The MAS technique makes use of what is referred to as a magic angle. When the vector between the two nuclei makes an angle of  $\theta = 54.74^\circ$  (the magic angle) with respect to the static magnetic field, the term in the Hamiltonian equation becomes zero:

$$3\cos^2\theta - 1 = 0$$

The chemical shift anisotropy becomes averaged out by rapidly spinning the powder sample at that magic angle with respect to magnetic field<sup>2,19</sup>. Figure 4.2 illustrates this for cis – and trans-polyacetylene taken from the article by Voelkel *et al*<sup>20</sup>. The <sup>13</sup>C NMR spectrum for the stationary powder sample is observed, with broad signals and spectral overlap. As soon as the sample becomes rotated at the magic angle, the signals become sharper and spectral resolution is increased.

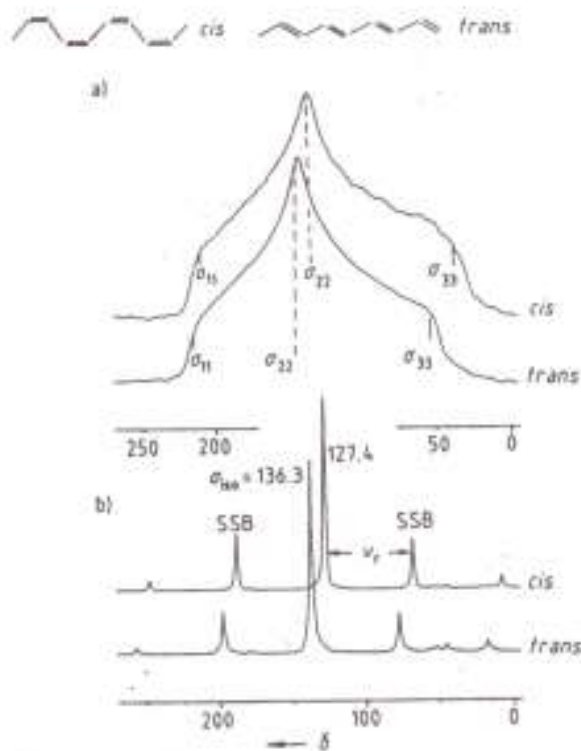


**Figure 4.2:** The  $^{13}\text{C}$  NMR spectra of cis – and trans-polyacetylene taken from Voelkel *et al.*<sup>20</sup> In a) the  $^{13}\text{C}$  NMR spectrum for the stationary powder sample is observed, with b) as the sample is rotating at the magic angle.

#### 4.2.3 Cross-Polarization (CP)

CP assists in observing dilute spins such as  $^{13}\text{C}$  nuclei. The difficulty with observing dilute spins is due to the nuclei having low natural abundance which causes poor signal-to-noise ratios as well as having very long relaxation times. The CP pulse sequence is used to remedy these problems. CP occurs because of the tendency of magnetization to flow from highly polarized nuclei to nuclei with lower polarizations when the two are brought in contact. Therefore the dilute nucleus X (such as  $^{13}\text{C}$ ,  $^{31}\text{P}$  or  $^{15}\text{N}$ ) derives its magnetization by polarization transfer from a nearby network of abundant spins such as  $^1\text{H}$  or any spin  $\frac{1}{2}$  nucleus. Magnetization is transferred from the neighbouring protons to X and back to  $^1\text{H}$ . This leads to a higher sensitivity of detection of the X nucleus<sup>2,19</sup>.

### 4.3 SOLID STATE NMR OF SEEDS AND BEANS: LITERATURE REVIEW

Several studies have been carried out using solid state NMR spectroscopy to investigate the liquid and solid domains of seeds and beans.

Bardet *et al.* used solid state NMR spectroscopy to examine the structural features of plant seeds including *Lactuca Sativa*, *Arabidopsis Thaliana* and *Pisum Sativum*<sup>3</sup>. The researchers examined the different parts of the seeds, including the teguments, cotyledons and embryonic axes as well as the seed as a whole and showed that with a combination of MAS experiments they were able to characterize the liquid and solid domains of the major components<sup>3</sup>.

De Oliveria *et al.* investigated the five layers of the external coat of seeds from *Magonia Pubescens*<sup>6</sup>. <sup>13</sup>C CP-MAS NMR spectroscopy of three of the layers was used to determine the chemical composition of each, while histochemical-light and Scanning Electron Microscopy (SEM) examination of the external coat showed the 3D organization of a gel extruded from the five regions of the external seed coat during swelling processes in water. Carbohydrates containing vicinal hydroxyls and some with acidic polysaccharides were observed to be present in the cytoplasm. Phenols were detected in all layers except the second layer. Lignins and/or tannins were present in the three innermost layers. SEM indicated that the gel had an extruded cylindrical, laminated structure. Two anionic components in the cells of the second layer were observed. In this study solid state NMR spectroscopy proved to be more a sensitive and semi-quantitative technique compared to light microscopy<sup>4</sup>.

Gussoni worked on the seeds of *Azalia cuanzensis*, by using 2D NMR imaging to give information on the surface and structural details of the interior<sup>5</sup>. This was done in order to identify and localize the major constituents and their morphological and structural details, specifically the embryo (an immature plant inside the seed coat), oil and water distribution. Spin-echo NMR imaging and <sup>13</sup>C MAS NMR spectroscopy in turn were used to study the oil, sugar and lignin distribution, and to localize and characterize the major organic constituents<sup>5</sup>.

Solid state NMR studies have also been carried out on compounds extracted from seeds and beans such as starches and proteins.

Cheetham *et al.* used <sup>13</sup>C CP-MAS NMR spectroscopy to monitor the crystalline changes of natural maize starches caused by certain treatments<sup>8</sup>. Such crystalline changes could be determined in terms of the local molecular structure and

conformational order in maize starches. Starches containing different ratios of amylose to amylopectin were examined in different conditions, including dry and hydrated states, native and iodinated states. The  $^{13}\text{C}$  chemical shifts, relative resonance intensities, line-widths and spectral shapes were compared at different moisture contents. The researchers found that by working in a 10 % moisture state, only a small difference in amylose levels could be detected. At 30 % moisture, an increased degree of crystallinity was observed and the signals due to amorphous materials disappeared. Treatment with iodine vapour led to an increase in V-type amylose in high amylose samples, but with a decrease in crystallinity<sup>6</sup>.

Richard *et al.* investigated the interaction of  $\beta$ -purothionin, which is an antimicrobial protein found in the endosperm of wheat seeds, with dimyristoylphosphatidylglycerol (DMPG) by solid state  $^{31}\text{P}$  NMR and infrared spectroscopy<sup>7</sup>. The study was done to determine the organization and dynamics of DMPG in the presence and absence of protein and it was found that protein does not induce formation of non-lamellar phases in DMPG. Solid state 2D exchange NMR spectroscopy showed that the protein decreased the lateral diffusion of DMPG in the fluid phase. Perturbations into the polar and non-polar regions of the phospholipid bilayers were also investigated and it was found the insertion of protein occurred at the hydrophobic core of the lipid bilayer. The protein was found to modify the lipid packing at the surface of the bilayer to increase accessibility to the water at the interfacial region<sup>7</sup>.

Studies on the mobility of the solids present in the seeds and beans have been carried out using NMR spectroscopic techniques. One such technique that is of interest for seeds and beans is the variable contact time (VCT) array experiment used with CP-MAS spectroscopy. VCT experiments allow the estimation of a proton spin-lattice relaxation time in the rotating frame ( $T_{1\rho}^{\text{H}}$ ), which is a parameter that is a measure of intermolecular magnetic interactions, and is related to sample spatial homogeneity.  $T_{1\rho}^{\text{H}}$  depends on the extent of dipolar interaction which is dominated by near neighbour spin diffusion.

Jarvis *et al.* used CP-MAS NMR spectroscopy to investigate the cell walls of lupin seed cotyledons, nasturtium endosperm, celery collenchyma, carob bean and fenugreek<sup>8</sup>. It was found that celery collenchymas cell walls gave spectra typical of dicot primary cell walls; carob and fenugreek were dominated by signals in the NMR spectrum assigned to galactomannans which indicated little sign of crystalline order.

For nasturtium, spectra largely indicated the presence of a xyloglucan. The conformation of the glucan core chain of this xyloglucan appeared to be between that of the solution form and solid form of cellulose. For lupin there were signals in the NMR spectra representing  $\beta(1,4')$ -D galactan<sup>8</sup>.

Tavares *et al.* wanted to gain information on the chemical and physical microstructure of seeds in mango fruits in order to understand the molecular behaviour and classification of seeds into their different mango groups<sup>9</sup>. The starches from *Magnifera Indica* Vc Bourbon and Espada were used. CP-MAS experiments were carried out and <sup>1</sup>H-spin-lattice relaxation times were determined. CP-MAS indicated three signals for Bourbon and two broad signals for Espada. Variable contact time decay experiments confirmed that these starches were amorphous and present in one predominant rigid domain. The mango fruits analyzed by delayed contact time experiments and <sup>13</sup>C decays showed that the polysaccharides were heterogeneous and contained one rigid domain<sup>9</sup>.

Calucci *et al.* used high and low resolution NMR spectroscopy to study the effects of aging of the flour of wheat seeds, by looking at their structural and dynamic properties in dry and hydrated states. Identification and characterization of domains with different mobilities were done using <sup>13</sup>C direct excitation (DE) and CP-MAS, <sup>1</sup>H static and MAS experiments as well as <sup>1</sup>H spin-lattice relaxation time measurements of molecular motions in different frequency ranges<sup>10</sup>. The main components were found to be glassy phase starch and gluten proteins and the mobile fraction which contained lipids and water. After aging and hydration a lower proportion of rigid domains and increased dynamics were found<sup>10</sup>.

Vieira *et al.* used solid state NMR spectroscopy to look at the hydrated powders and gels of the locust bean gum galactomannan (LBG) and Konjac glucomannan (KGM) which are used as thickeners and gelling agents in the food industry<sup>11</sup>. The researchers looked specifically at the changes in relative spectral intensities, cross-polarization dynamics and relaxation times by doing hydration studies of 0-90 % moisture on the powders and gels. It was found that LBG powders increased molecular motions at 108 Hz, probably due to the enhanced motion for the non-aggregating segments of the chain ends. In contrast to that the slower motions (104-105 Hz) were enhanced only slightly at 90 % hydration. The LBG gel had a higher spatial distinction between aggregated and non-aggregated segments than hydrated powder. Relaxation times indicated higher mobility for galactose-ramified segments,

compared to linear mannose segments. KGM hydration dynamics were similar to LGB but the gel was more rigid. Glucose residue mobility was probably hindered due to preferential involvement in chain aggregation<sup>11</sup>.

Bootten *et al.* identified carbons with two different mobilities in the primary cell wall of the xyloglucans of mung beans using solid state <sup>13</sup>C NMR spectroscopy<sup>12</sup>. Glucose in the polysaccharides of the cell wall was labelled at either C1 or C4 with a <sup>13</sup>C-isotope and the proportions of <sup>13</sup>C-isotopes were increased in cell wall polysaccharides to improve the signal to noise ratio and therefore improve sensitivity<sup>12</sup>. Etiolated hypocotyls of mung beans were used and the mobility of the xyloglucans carbons investigated using CP-MAS and Proton Spin Relaxation Editing (PSRE). Spin-echo relaxation and rotating-frame experiments were done to detect partly rigid xyloglucans carbons. Two carbons with different mobilities were found, namely those xyloglucans with a rigid glucan backbone and those with a partly rigid backbone. The latter were determined to be predominant by quantification. It was concluded that no xyloglucans were located within the cellulose microfibrils. Only a small proportion of total surface area of the cellular microbiology was consistent with recent models<sup>12</sup>.

Bardet *et al.* carried out solid state <sup>13</sup>C NMR spectroscopy experiments to investigate the effects of gamma radiation on vegetable seeds, including *Pisum Sativum* and *Latuca Sativa*, since at certain dosages the absorbed radiation can lead to the inhibition of germination<sup>13</sup>. SP and CP-MAS experiments were used to characterize liquid and solid domains and it was found that in the liquid domains, the triacylglycerols were the most sensitive to radiation. The main structural changes were in the embryonic axes of the seeds when water-imbibed before irradiation<sup>13</sup>.

Nascimento *et al.* analysed the seed components of the seed of Sorva (*Couma utilis*), which is a native fruit of the Amazon state in Brazil, by <sup>1</sup>H and <sup>13</sup>C high resolution solid state NMR spectroscopy using techniques such as <sup>1</sup>H MAS and <sup>13</sup>C MAS as well as VCT experiments<sup>14</sup>. The NMR results indicated that the sorva seeds consisted mainly of polysaccharides, glycoproteins and triacylglycerols. The VCT experiments on the seed starch indicated that it was a heterogenous rigid sample of polysaccharides, proteins and lipids. It was concluded that it was possible to characterize the main components without any modification<sup>14</sup>.

Kou *et al.* worked on the mould of conidia germination which was used as microbial probe of food stability in sucrose, starch and sucrose/starch systems<sup>15</sup> which are

present in seeds and beans. Various NMR and DSC methods were used to characterize water and solid mobility and glass transition temperature of the respective systems. DSC and empirical calculation were used to measure glass transition temperatures and  $^1\text{H}$  NMR experiments included effective spin-spin relaxation rate measurements and spin-lattice relaxation rate measurements, while  $^{13}\text{C}$  NMR spin-lattice relaxation rate measurements in the rotating frame were also used ( $T_{1\rho}^{\text{H}}$ ). The water content and  $^2\text{H}$  NMR relaxation rates did not predict the mould germination time. The researchers concluded that the self-diffusion coefficient, translational mobility of water, the DSC Tg (overall system mobility),  $^1\text{H}$  NMR relaxation rates and  $^{13}\text{C}$   $T_{1\rho}^{\text{H}}$  (solids mobility) were alternative measurements to supplement a water content measurement to predict food stability and safety<sup>15</sup>.

Separovic *et al.* looked at the mobility of protein in powders of seeds and beans at different hydration levels in relation to their aggregation and activity<sup>16</sup>. Various techniques were used including  $^{13}\text{C}$ ,  $^{15}\text{N}$ ,  $^1\text{H}$ ,  $^2\text{H}$  and  $^{17}\text{O}$  MAS experiments, High Performance Size Exclusion Chromatography (HPSEC) and bioassays. It was found that water content led to the change in mobility of protein molecules and aggregation and activity strongly related to the change in molecular mobility<sup>16</sup>.

Fransen *et al.* used CP-MAS NMR experiments to identify soybean cellulose and pectin extracts and to investigate the kinetics of cross-polarization<sup>17</sup>. The researchers used *in vitro* incubation of the cellulose (extracted from soy hull) and pectin (extracted from the endosperm) with sheep rumen fluid. VCT CP-MAS NMR experiments of the cellulose fraction during incubation indicated that the cellulose degraded in a layer-by-layer way<sup>17</sup>.

In summary, the general types of information that have been obtained to date by solid state NMR spectroscopy experiments on seeds and beans are:

- Investigation of liquid and solid domains
  - in seeds and beans as a whole
  - of extracted compounds such as starch and protein
- Morphology such as structural features, crystalline changes, molecular structure, conformation order, chemical and physical microstructure
  - of whole seeds
  - cotyledons

- teguments
- embryonic axis
- Characterization of liquid and solid domains
- Quantification of liquid and solid domains and relative amount of domains
- Mobility of solids
  - in whole seed
  - in extracted components
- Packing of domains

Since it is not known how the solid and liquid-like components are packed within the seed and beans and how they are present with respect to each other, domains could occur in which packing and interaction of these components would be different. In this study possible packing for different domains is suggested as illustrated in Figure 4.3. In domain A, the solid-like components and liquid-like components are clearly separated from each other with respect to packing. In domain B, the liquid-like components are closely packed to the solid-like components on the surface only. In domain D the liquid like components are packed in such a way that they are protruding from the solid-like components and in domain C the liquid-like components are trapped within the solid-like components.

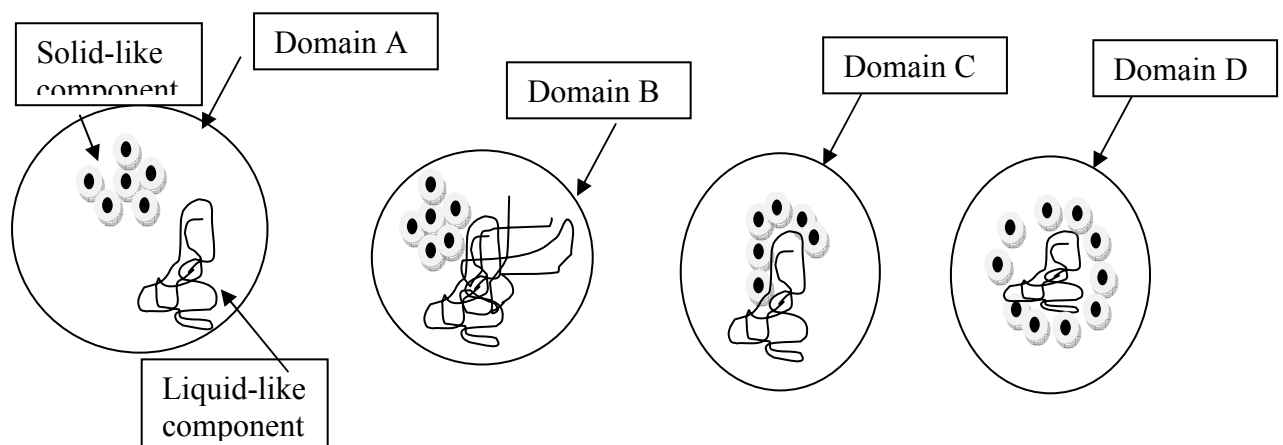


**Figure 4.3:** Illustration of possible packing of components of seeds and beans within domains.

#### 4.4 AIMS OF THIS STUDY

In this chapter solid state  $^{13}\text{C}$  NMR spectroscopy was used to explore the components present in South African produced seeds and beans with the aim of gaining insight into the different degradation profiles observed in the TGA experiments.  $^{13}\text{C}$  Cross-Polarization-Magic Angle Spinning (CP-MAS) and  $^{13}\text{C}$  Single Pulse Excitation-Magic Angle Spinning (SPE-MAS) experiments were carried out to obtain spectra of the solid-like and liquid-like components respectively, present in each seed and bean. Variable Contact Time (VCT) experiments were also carried out to compare the relaxation rates in the rotating frame for the seeds and beans to yield additional information on the liquid-like and solid-like components present in the samples.

#### 4.5 RESULTS AND DISCUSSION

Solid state  $^{13}\text{C}$  SPE-MAS NMR spectra and solid state  $^{13}\text{C}$  CP-MAS NMR spectra were obtained for seeds (sunflower, poppy, sesame and pumpkin seeds) and beans (soy, black, mung and kidney beans). The  $^{13}\text{C}$  SPE-MAS experiments were expected to give information on the mobile liquid-like components present in the samples, which in the case of seeds and beans would be the fatty acid or triacylglycerol (oil) components while the  $^{13}\text{C}$  CP-MAS experiments were expected to give information on the less mobile solid-like components present in the samples, which in the case of seeds and beans would be the carbohydrates, proteins, celluloses, etc<sup>21</sup>.  $^{13}\text{C}$  CP-MAS experiments were collected at spinning speed of 5 kHz and 7 kHz in order to aid in the detection and elimination of spinning side bands. All spectra shown in this chapter were those collected using a spinning speed of 7 kHz.

##### 4.5.1 Seeds

###### 4.5.1.1 $^{13}\text{C}$ Single Pulse Excitation-Magic Angle Spinning experiments

The  $^{13}\text{C}$  SPE-MAS NMR spectra of four seed flour samples (sesame, poppy, sunflower and pumpkin seeds) were obtained. These spectra were found to be similar to the  $^{13}\text{C}$  NMR spectrum of a vegetable oil in solution as illustrated using marula oil in Figure 4.4. The  $^{13}\text{C}$  NMR spectrum of marula oil has been fully assigned<sup>22,23</sup> (as discussed in Chapter 1) and was used for comparison to the  $^{13}\text{C}$  SPE-MAS NMR spectra of the four seed flour samples. Figure 4.4 gives the assignment of the  $^{13}\text{C}$  NMR spectrum of marula oil indicating the signals

representing the carbonyl carbons (C=O) of oleic and linoleic fatty acids, the signals of the glycerol backbone carbons and signals representing aliphatic and allylic carbons (CH double bond carbons).

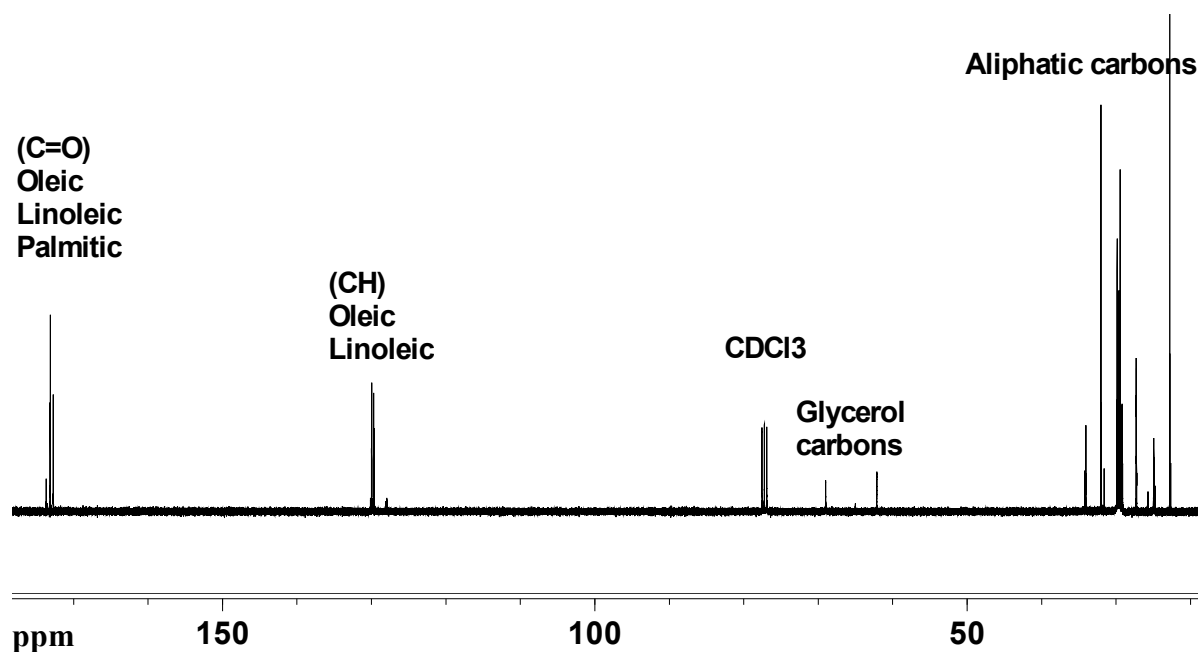


**Figure 4.4:** Solution state  $^{13}\text{C}$  NMR spectrum of marula oil.

From comparison of each of the seed powder  $^{13}\text{C}$  SPE-MAS spectra in Figures 4.5 – 4.8 with Figure 4.4, some of the signals can already be assigned by inspection due to their similarity. In all four of the seed flour spectra a small signal is observed around 170 ppm which corresponds to the carbonyl carbon signal for oleic and linoleic acid at 173 ppm in the marula oil spectrum. Around 130 ppm in the  $^{13}\text{C}$  SPE-MAS spectra of the seeds two signals are observed corresponding to the area in the solution state NMR spectrum of marula oil between 130 and 128 ppm where signals representing the carbons of oleic and linoleic double bonds are observed. Around 60 to 70 ppm two signals are observed in the  $^{13}\text{C}$  SPE NMR spectra which are comparable to the glycerol backbone signals at 68 and 62 ppm in the solution spectrum. Between 40 and 20 ppm there are numerous signals seen in each of the four  $^{13}\text{C}$  SPE-MAS seed flour spectra which correspond to the solution state spectrum of marula oil where these signals were assigned to the aliphatic carbons.

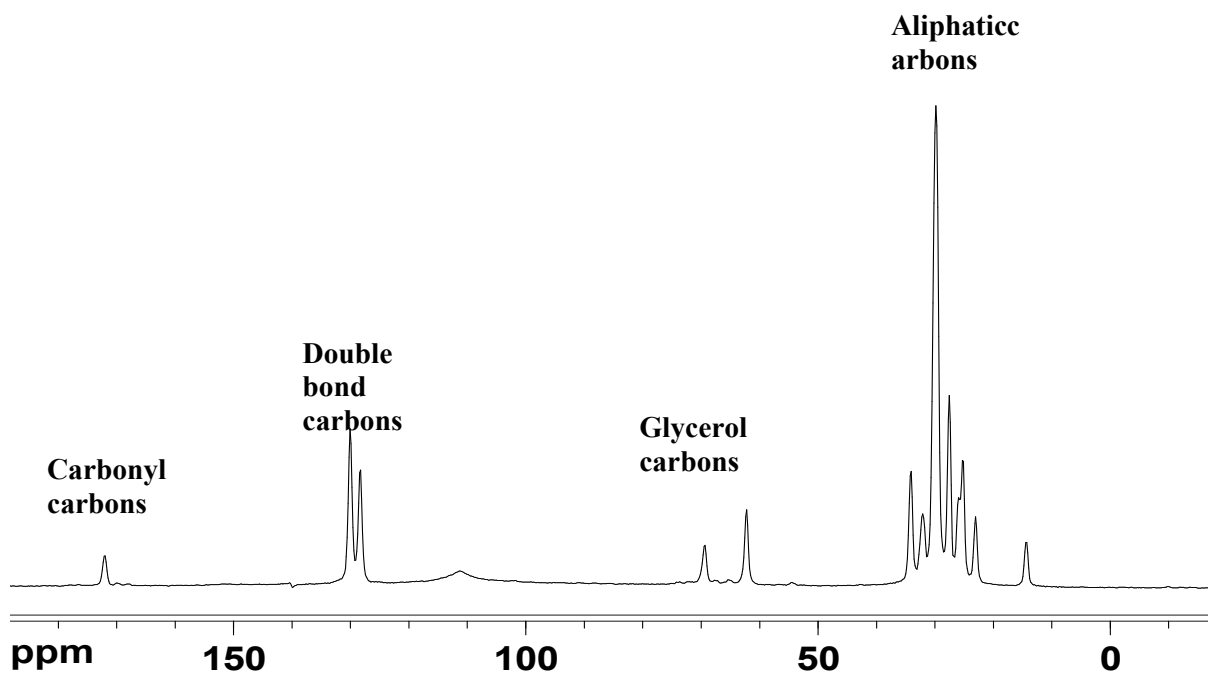


**Figure 4.5:**  $^{13}\text{C}$  SPE-MAS NMR spectrum of poppy seed flour.

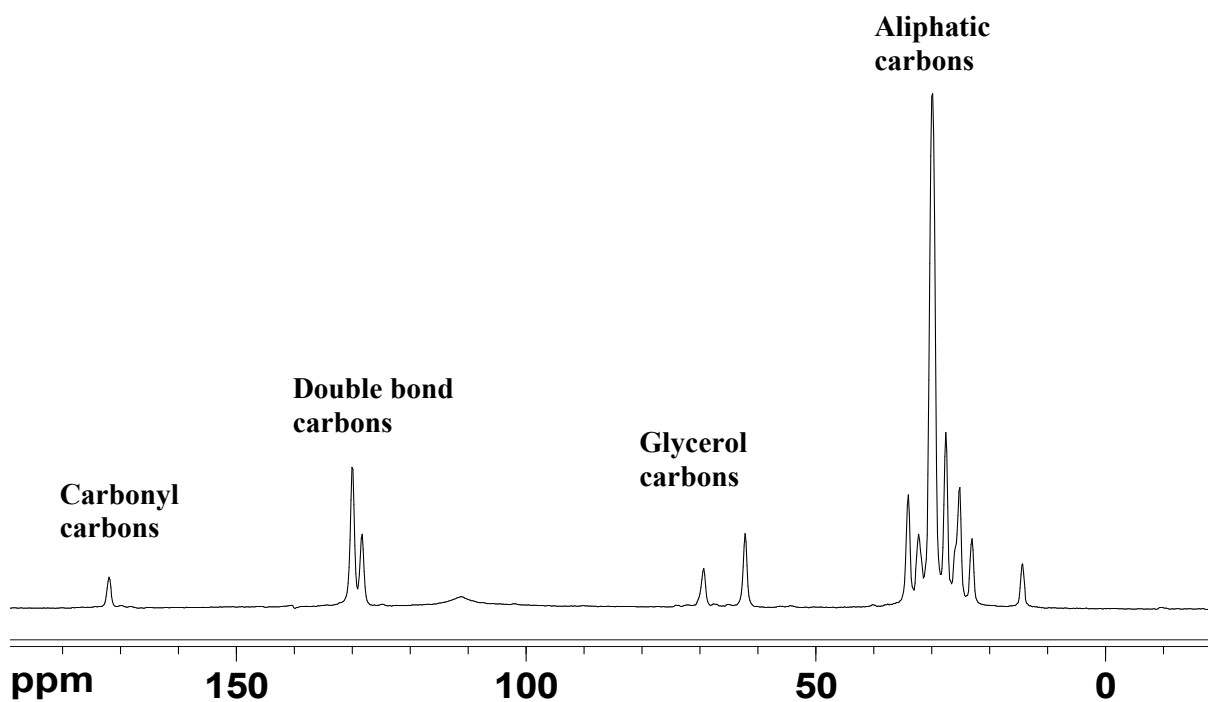


**Figure 4.6:**  $^{13}\text{C}$  SPE-MAS NMR spectrum of pumpkin seed flour.

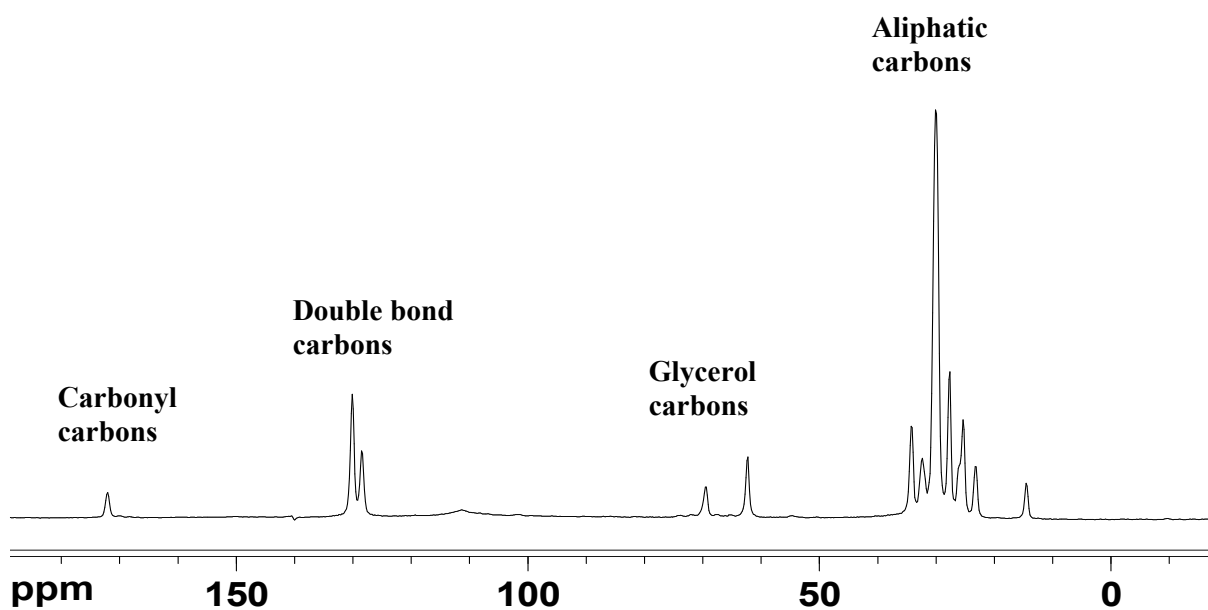


**Figure 4.7:**  $^{13}\text{C}$  SPE-MAS NMR spectrum of sesame seed flour.

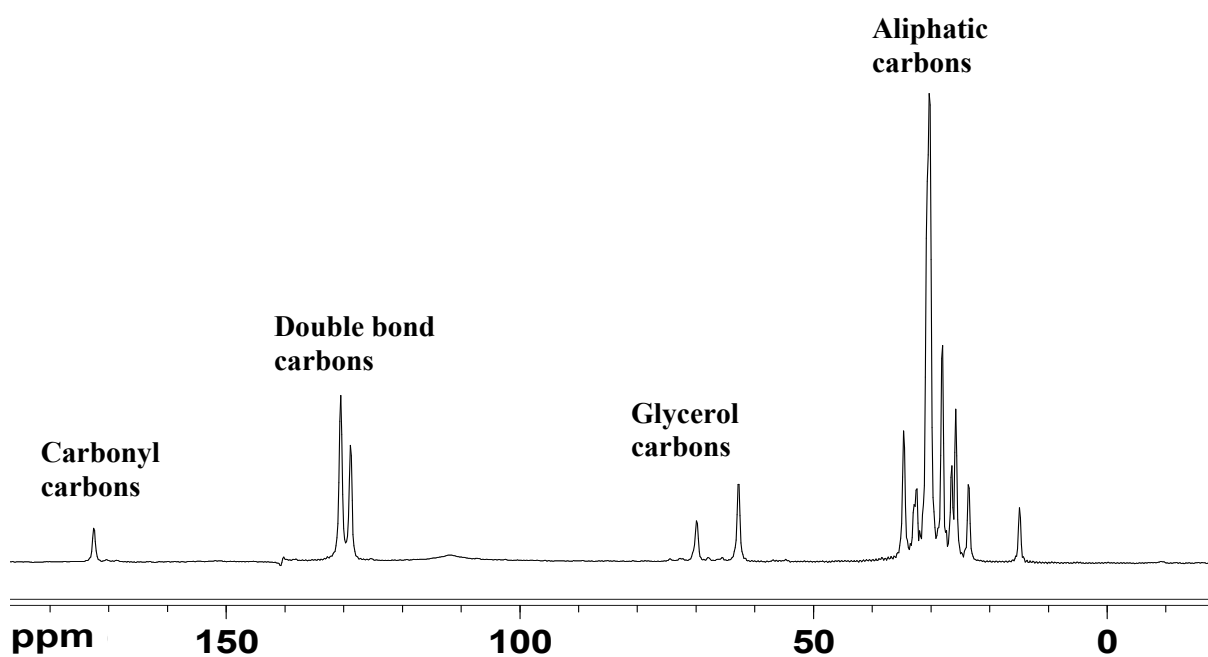


**Figure 4.8:**  $^{13}\text{C}$  SPE-MAS NMR spectrum of sunflower seed flour.

In order to understand the assignments made for the signals of the solution state spectrum of marula vegetable oils and the seeds, the numbering system of the fatty acids of triolein and trilinolein are given in Figures 4.9 and 4.10.

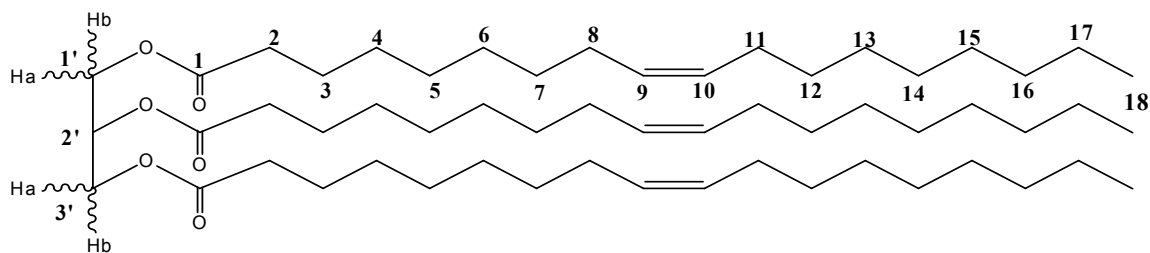


**Figure 4.9:** Numbered structure of triolein.

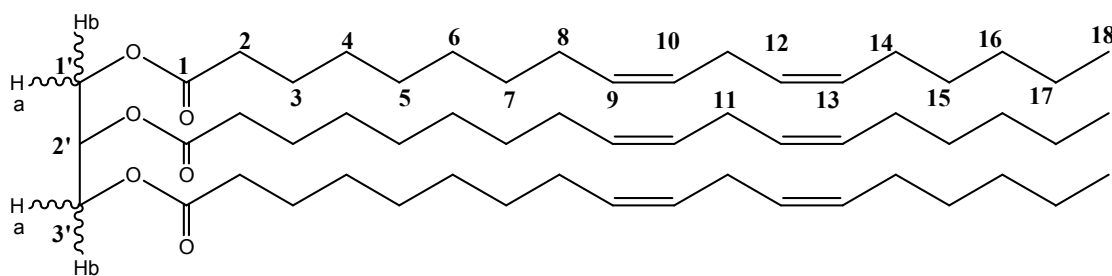


**Figure 4.10:** Numbered structure of trilinolein.

The expansions of the region between 35 and 14 ppm in the solution spectrum of marula oil is shown in Figure 4.11. These were of use for the assignments by inspection of the signals for the corresponding regions in the four seed flours as shown for the  $^{13}\text{C}$  SPE-NMR spectrum of poppy seed flour in Figure 4.12.

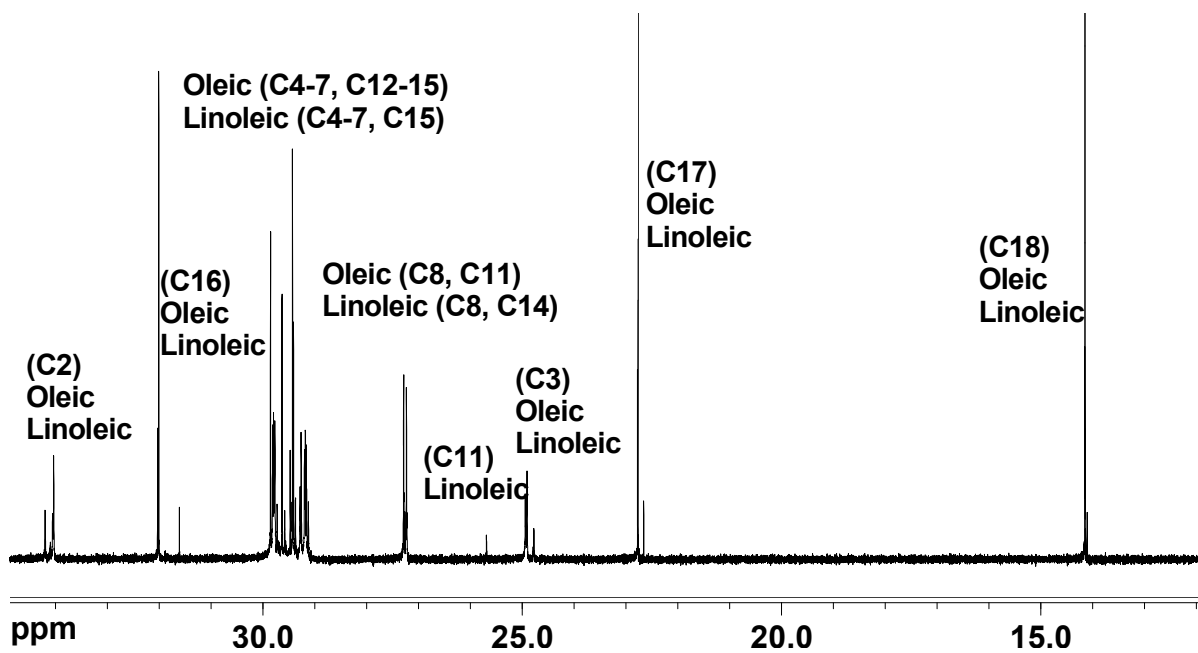


**Figure 4.11:** Expanded solution state  $^{13}\text{C}$  NMR spectrum of marula oil showing the 35 to 14 ppm region.

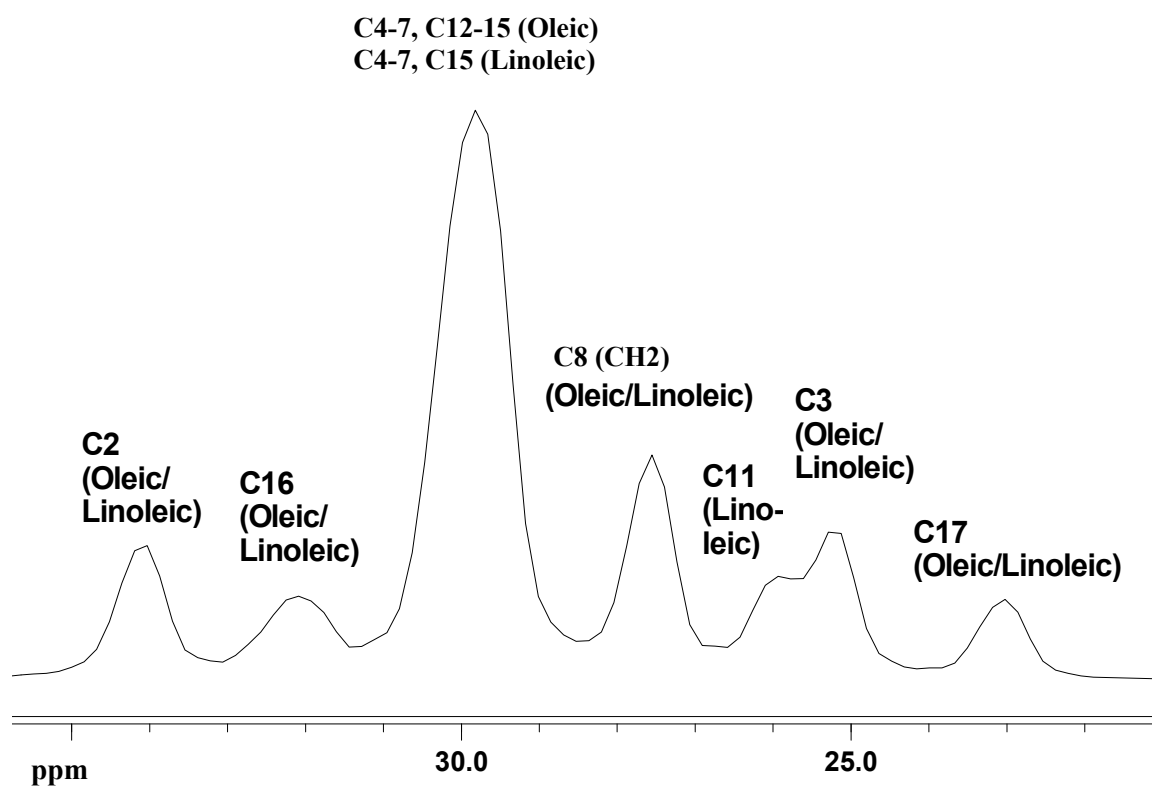


**Figure 4.12:** Expanded  $^{13}\text{C}$  SPE-MAS NMR spectrum of poppy seed flour showing the 35 to 22 ppm area.

In Figure 4.11 the  $^{13}\text{C}$  NMR spectra of marula oil shows signals representing C-2 for oleic and linoleic fatty acids around 34 ppm, C-16 for oleic and linoleic fatty acids around 32 ppm, C-8 and C-11 for oleic fatty acid and C-8 and C-14 for linoleic fatty acid around 28 ppm. C-11 for linoleic acid is observed at 27 ppm and C-3 for oleic and linoleic fatty acids around 25 ppm, C17 for oleic and linoleic fatty acids at 24 ppm and  $\text{CH}_3$  C-18 for oleic and linoleic fatty acids around 14 ppm. All of these solution state signals are observed in the  $^{13}\text{C}$  SPE-MAS NMR spectra of the four seed powders at similar ppm values as indicated in the expanded  $^{13}\text{C}$  SPE-MAS NMR spectrum of poppy seed in Figure 4.12. In the literature Bardet *et al.* assigned the signal around 30 ppm to the  $\text{CH}_2$  of C-18 of oleic and linoleic chains. This is ambiguous since C-18 is the last carbon in the chain for both of these fatty acids and therefore we believe this assignment to be incorrect. Consequently we have

assigned the signal to that of C-4 to 7, C-12 to 15 in oleic and C-4 to 7, C-15 in linoleic as compared to that of the solution state NMR spectrum.

Bardet *et al.* assigned each of the signals in the  $^{13}\text{C}$  SPE-MAS and  $^{13}\text{C}$  CP-MAS spectra of *Pisum sativum*<sup>13,21</sup>. This was done by analyses of model compounds such as proteins, lipids and sugars, of the expected compounds present in the product as well as analysis of the extracted compounds<sup>13,21</sup>. Comparison of the assignments made by Bardet *et al.*, combined with the strong correlation of the signals in the  $^{13}\text{C}$  SPE-MAS NMR spectra to the solution state  $^{13}\text{C}$  NMR spectrum of marula oil, led to the assignment of the signals in the  $^{13}\text{C}$  SPE-MAS NMR spectra of the four seeds of interest, namely poppy, sesame, pumpkin and sunflower seeds. These assignments are given in Table 4.1 as well as indicated on the spectra in Figures 4.5-4.8, 4.12.

**Table 4.1:** Assignment of the  $^{13}\text{C}$  NMR SPE-MAS spectra of poppy, sesame, pumpkin and sunflower seeds by comparison to literature assignments<sup>3</sup>

Assignment	Chemical shift (ppm)
Oleic/Linoleic (C=O)	172
Oleic/Linoleic (CH)	130
Linoleic (CH)	128
Glycerol (C-β)	69
Glycerol (C-α)	62
Oleic (C-2)	34
Oleic/Linoleic (C-16)	32
Oleic (C4-7, C12-15)/ Linoleic (C4-7, C15)	30
Linoleic (C-8, C-14)/ Oleic (C-8, C-11)	28
Linoleic (C-11)	26
Oleic/Linoleic (C-3)	25
Oleic/Linoleic (C-17)	23
Oleic/Linoleic (C-18: CH <sub>3</sub> )	14

#### 4.5.1.2 $^{13}\text{C}$ Cross-Polarization-Magic Angle Spinning experiments

The  $^{13}\text{C}$  CP-MAS NMR spectra of the four seed flour samples (poppy, sesame, sunflower and pumpkin seeds) are shown in Figures 4.13-4.16 with the spinning sidebands indicated as \* and \*. As mentioned in the previous section Bardet *et al.* assigned each of the signals in the  $^{13}\text{C}$  SPE-MAS and  $^{13}\text{C}$  CP-MAS spectra of *Pisum sativum*. Therefore assignments of the  $^{13}\text{C}$  CP-MAS NMR spectra of the four seed

flours were done by comparison to the assignments made by Bardet *et al.* These assignments are given in Table 4.2.

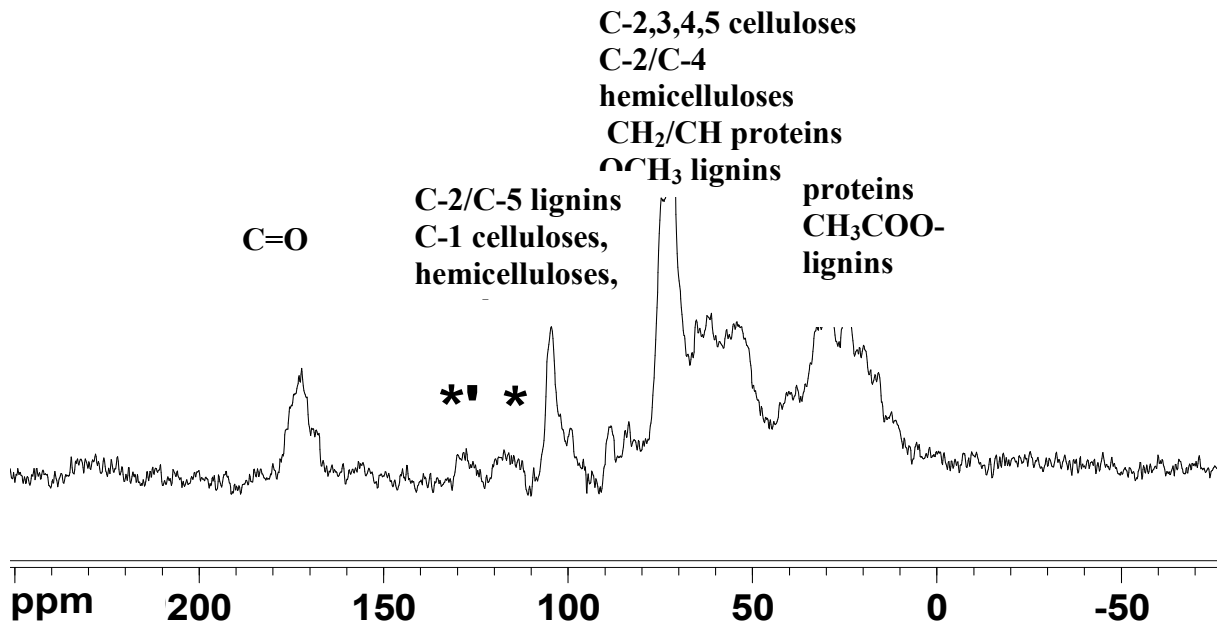


Figure 4.13:  $^{13}\text{C}$  CP-MAS NMR spectrum of poppy seed flour.

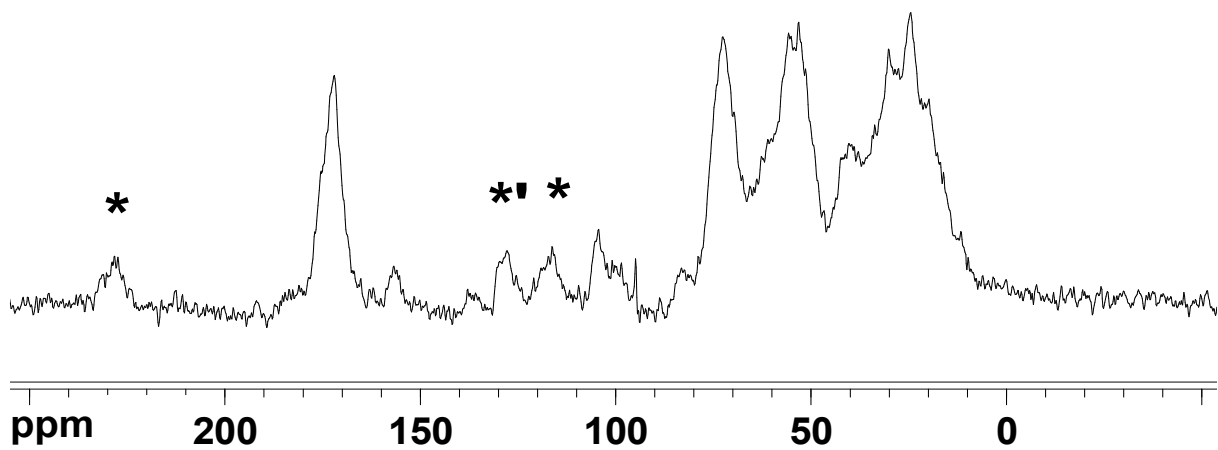
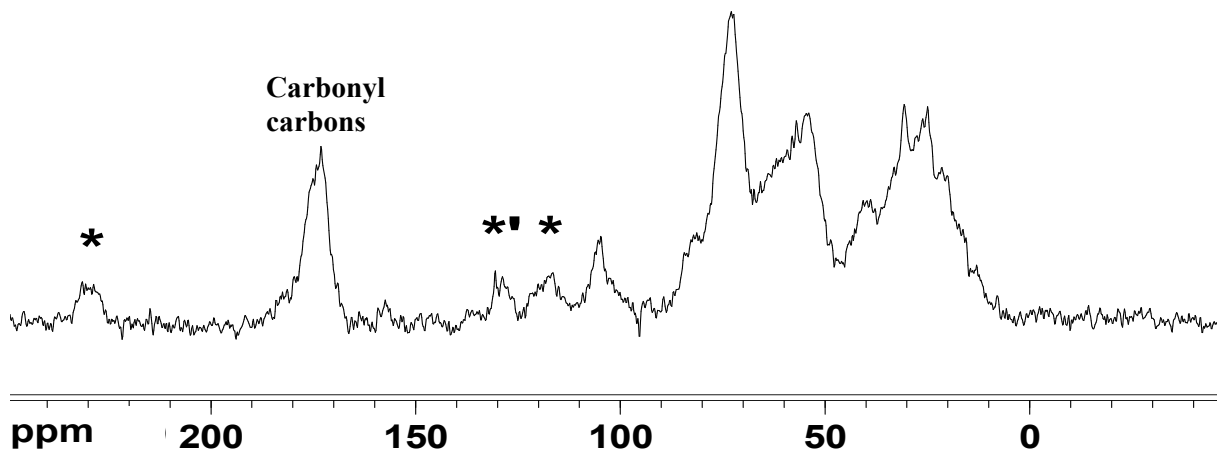
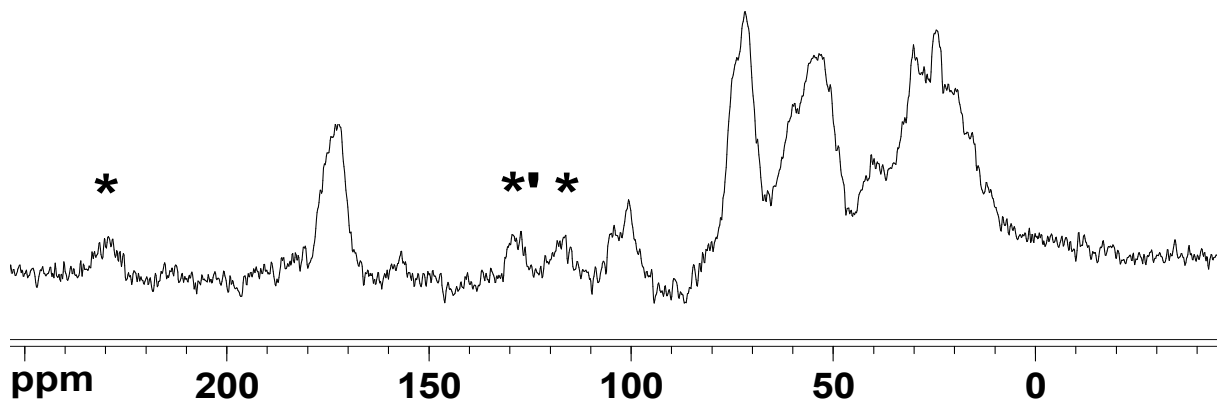


Figure 4.14:  $^{13}\text{C}$  CP-MAS NMR spectrum of pumpkin seed flour.



**Figure 4.15:**  $^{13}\text{C}$  CP-MAS NMR spectrum of sesame seed flour.



**Figure 4.16:**  $^{13}\text{C}$  CP-MAS NMR spectrum of sunflower seed flour.

**Table 4.2:** Assignment of the  $^{13}\text{C}$  NMR CP-MAS spectra of seeds obtained from the literature<sup>3</sup>.

Assignment	Chemical shift (ppm)
C=O (in esters, acids) of lignins, hemicelluloses and proteins	~175
Aromatic carbons in lignins	~130
Aromatic units in lignins	
Anomeric ring carbons (C-1) of cellulose, hemicelluloses and starch	~108-100
C-2/C-4 in celluloses	~90-75
C-3/C-5 in celluloses	
C-2/C-3 in hemicelluloses	~70
C-6 in celluloses	
C-5 in hemicelluloses	~65-60
CH/CH <sub>2</sub> in proteins	
OCH <sub>3</sub> in lignins	~55
Proteins	~40-30
CH <sub>3</sub> COO- in hemicelluloses	~20

The  $^{13}\text{C}$  CP-MAS NMR spectra in Figures 4.13-4.16 all appear similar, with no signals present around 130 ppm representing the aromatic carbons. However the signals due to the spinning sidebands are in the same area of the spectrum and could lead to spectral overlap. Signals around 175 ppm represent carbonyl carbons; signals around 130 ppm represent aromatic carbons in lignins; signals between 108 and 100 ppm represent aromatic units in lignins as well as anomeric ring carbons (C-1) of cellulose, hemicelluloses and starch; signals between 90 and 75 ppm represent C2/C-4 in celluloses while carbons around 70 ppm represent C-3/C-5 in celluloses as well as C-2/C-3 in hemicelluloses; signals between 65 and 60 ppm represent C-6 in celluloses and C-5 in hemicelluloses; around 55 ppm signals representing CH/CH<sub>2</sub> in proteins are observed as well as OCH<sub>3</sub> carbons in lignins; protein signals are observed between 40 and 30 ppm and CH<sub>3</sub>COO- carbon signals are present around 20 ppm.

The lack of good resolution, broad overlapping signals, and very noisy spectra of the four seeds are an indication that the signals of the liquid-like components are also being detected by this technique.

#### 4.5.1.3 Comparison of TGA and Solid-state NMR results

The  $^{13}\text{C}$  NMR SPE-MAS of all four seed flours (namely poppy, sesame, sunflower and pumpkin seeds) were similar with well defined spectra and sharp signals. The same similarity was observed between the  $^{13}\text{C}$  CP-MAS NMR spectra of the four seeds however this time the spectra were similar due to them all containing similar, broad overlapping signals.

The liquid-like components present in seeds are due to the oil. The oil contents of each of the four seeds were determined in the previous chapter (Chapter 3) by TGA and Soxhlet extraction and found to be 43.1 % for poppy seed, 44.6 % for pumpkin seed, 57.6 % for sesame seed and 56.9 % for sunflower seed (TGA results). These values were all high indicating a large amount of oil present in the seeds. This correlates well with what is observed in the  $^{13}\text{C}$  SPE-MAS spectra of the four seed powders due to the high signal to noise ratio obtained with few scans.

The seeds however had very low solid-like component contents (proteins) as was determined by TGA and Dumas-combustion method. The protein contents were 21.1 % for poppy seed, 34.2 % for pumpkin seed and 23.3 % for sesame seed. With comparison to the high values of oil present in these seeds (above 40 % for all four seeds), the solid-like components are in minority and consequently liquid-like components (oil) are also detected by the  $^{13}\text{C}$  CP-MAS NMR technique. The broadness of the carbonyl carbon and aromatic signals are due to the presence of high content of oil, as well as the signal overlap that is observed between 110-60 ppm and 40-10 ppm.

In conclusion, the two techniques gave qualitative results on the presence of the components in seeds, indicating that the seeds contained a high content of mobile oil-like compounds and a low content of lesser mobile solid-like components. This is indeed what was found from results by TGA in Chapter 3. For the first time the  $^{13}\text{C}$  NMR SPE-MAS and  $^{13}\text{C}$  CP-MAS NMR spectra of sesame, sunflower, poppy and pumpkin seeds have been assigned and although the techniques could not be used to differentiate between the four different seeds nor could it be used to yield any quantitative results, the qualitative data obtained from the techniques could be supplemented by the TGA quantitative data observed.

## 4.5.2 Beans

### 4.5.2.1 $^{13}\text{C}$ Single Pulse Excitation-Magic Angle Spinning experiments

Figures 4.17-4.20 show the  $^{13}\text{C}$  SPE-MAS NMR spectra of the four bean flours (soy, kidney, black and mung beans). The  $^{13}\text{C}$  SPE-MAS spectra of the bean flours show similar signals yet very significant differences to those observed for the seeds in Figures 4.5–4.8.

From comparison of each of the bean flour  $^{13}\text{C}$  SPE-MAS spectra with those of the seeds in Figures 4.4-4.7 and the solution spectrum of marula oil in Figure 4.8, some of the signals can already be assigned by inspection due to their similarity. In all four of the bean spectra a small signal is observed around 170 ppm which corresponds to the carbonyl carbon signal for oleic and linoleic acid at 173 ppm in the marula oil spectrum. Around 130 ppm in the  $^{13}\text{C}$  SPE-MAS spectra two signals are observed corresponding to the area in the solution state NMR spectrum of marula oil between 130 and 128 ppm where signals representing the carbons of oleic and linoleic double bonds are observed. Around 70 to 60 ppm two signals are observed in the  $^{13}\text{C}$  SPE-MAS NMR spectra which are comparable to the glycerol backbone signals at 68 and 62 ppm in the solution spectrum. Between 40 and 20 ppm there are numerous signals seen in each of the four  $^{13}\text{C}$  SPE-MAS seed spectra which correspond well to the solution state spectrum of marula oil where these signals were assigned to the aliphatic carbons. Expansion of the region between 40 and 20 ppm also indicated signals corresponding to C-2 for oleic and linoleic fatty acids around 34 ppm, C-16 for oleic and linoleic fatty acids around 32 ppm, the  $\text{CH}_2$  C-18 for oleic and linoleic fatty acids around 30 ppm, C-8 and 11 for oleic fatty acid and C-8 and 14 for linoleic fatty acid around 27 ppm. C-11 for linoleic acid is observed at 27 ppm and C-3 for oleic and linoleic fatty acids around 25 ppm, C-17 for oleic and linoleic fatty acids at 23 ppm and  $\text{CH}_3$  C-18 for oleic and linoleic fatty acids around 14 ppm.

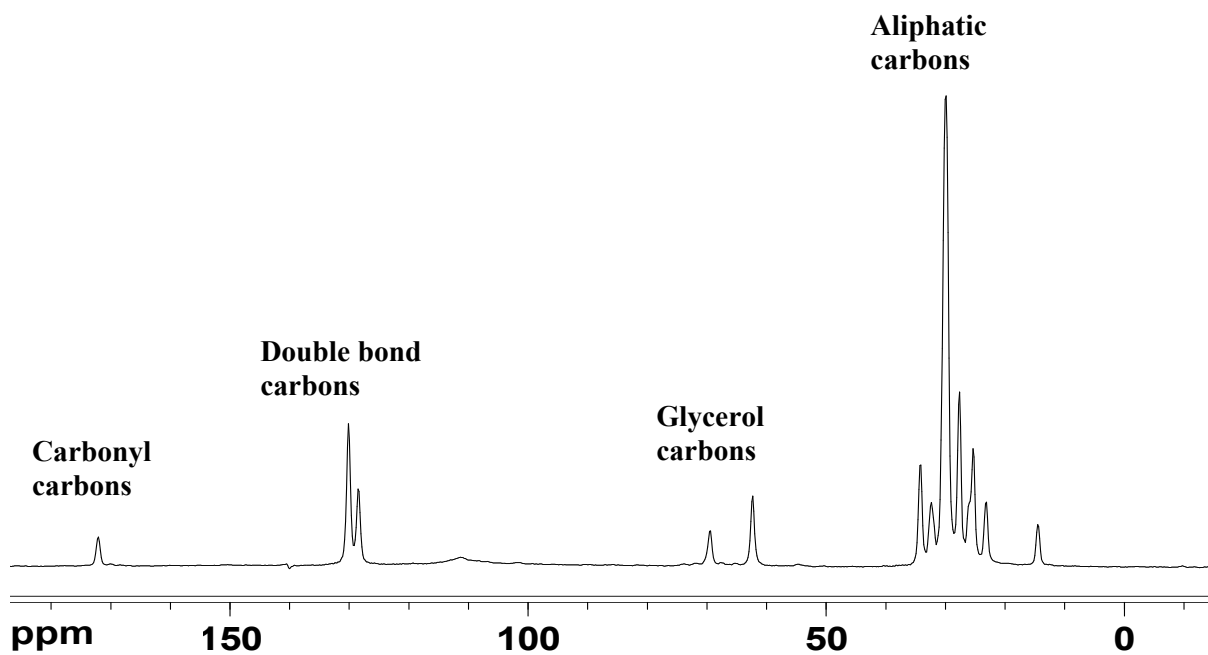


Figure 4.17:  $^{13}\text{C}$  SPE-MAS NMR spectrum of black bean flour.

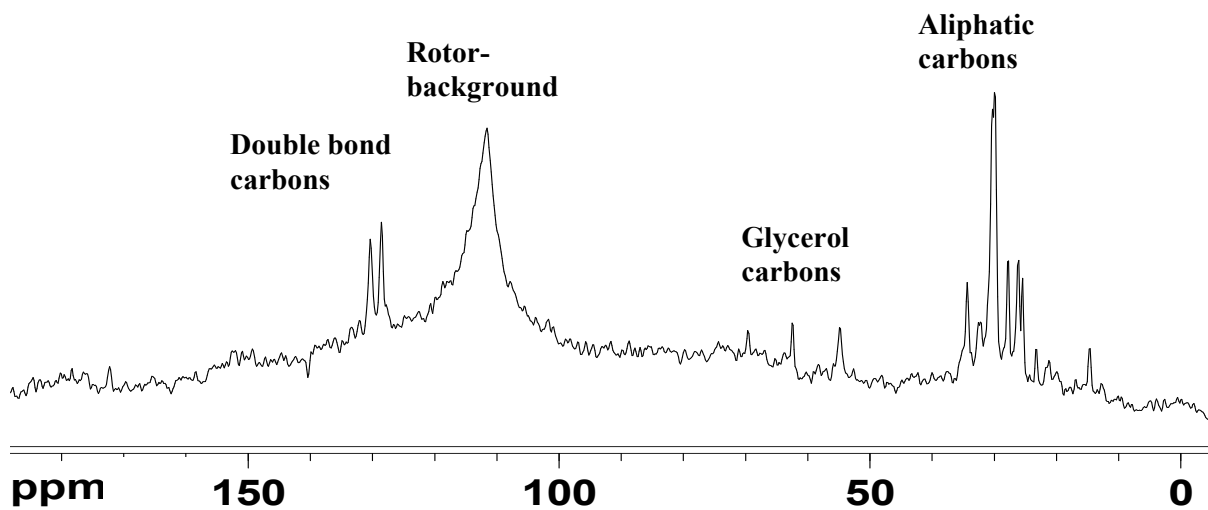


Figure 4.18:  $^{13}\text{C}$  SPE-MAS NMR spectrum of kidney bean flour.

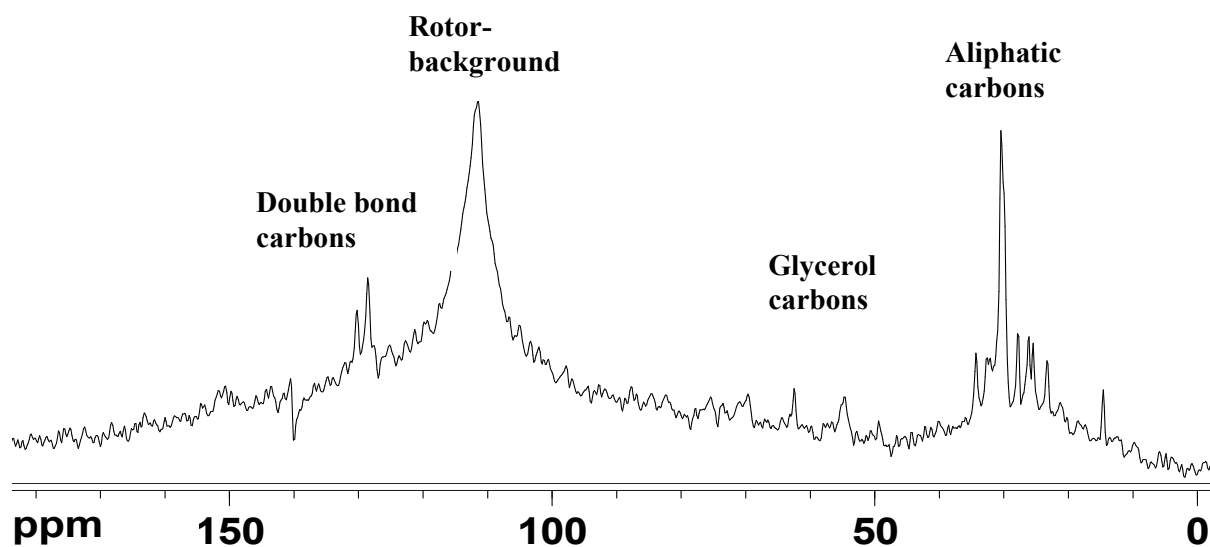


Figure 4.19:  $^{13}\text{C}$  SPE-MAS NMR spectrum of mung bean flour.

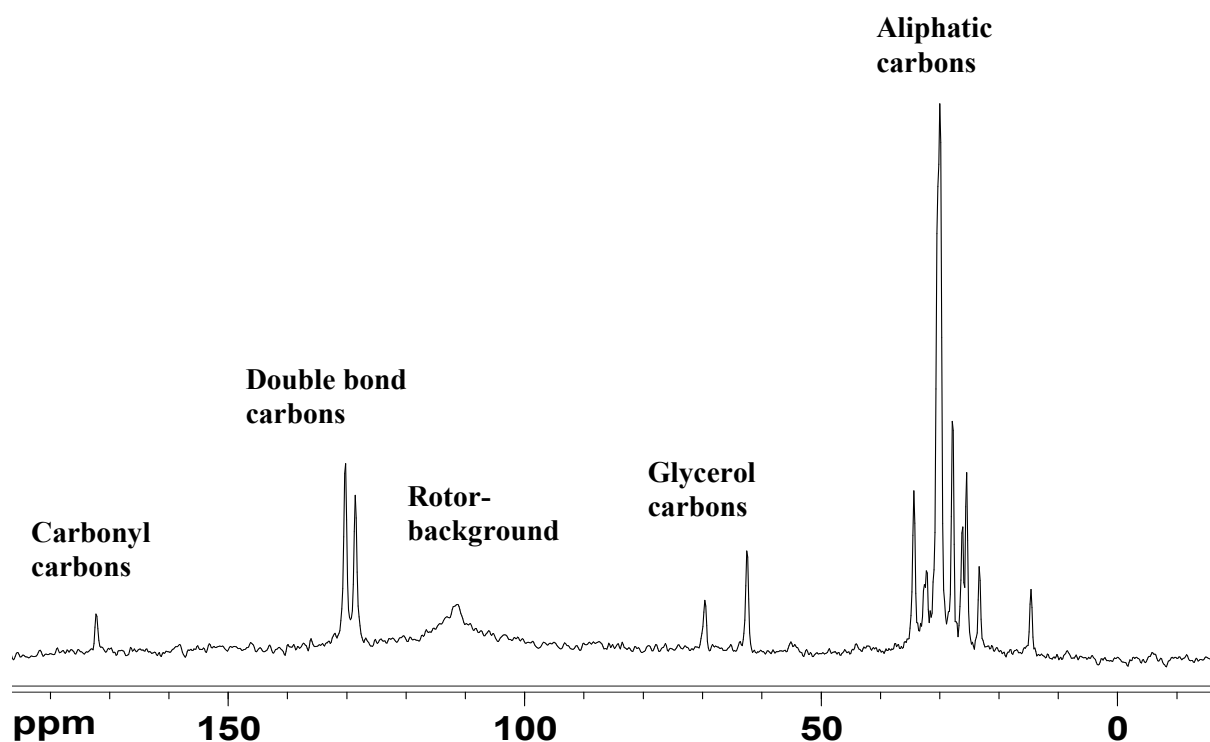


Figure 4.20:  $^{13}\text{C}$  SPE-MAS NMR spectrum of soybean flour.

As was the case for the seed flours, the assignments of the  $^{13}\text{C}$  SPE-MAS spectra of the bean flours were done by comparison to the assignments done by Bardet *et al*<sup>13,21</sup> and the solution state  $^{13}\text{C}$  NMR spectrum of marula oil. The assignments were the same as for seeds (see Table 4.1) and are indicated on the spectra in Figures 4.17-4.20. The peak observed around 111 ppm in all the spectra is due to the

background noise from the rotor. Notice this peak is much larger in kidney bean and mung bean spectra.

Unlike in the case of the seeds, the  $^{13}\text{C}$  SPE-MAS spectra of the bean flours were not all similar to each other. The  $^{13}\text{C}$  SPE-MAS spectrum of black bean flour indicates sharp well-defined signals and good signal to noise ratio representative of a high quantity of mobile oil components. Soybean flour also has a  $^{13}\text{C}$  SPE-MAS spectrum with sharp signals but its signal to noise ratio is worse than that of black bean indicating the presence of solid-like components. The  $^{13}\text{C}$  SPE-MAS spectra of kidney and mung bean flours are very noisy, an indication of a high content of solid like components being detected by this technique.

#### 4.5.2.2 $^{13}\text{C}$ Cross-Polarization-Magic Angle Spinning experiments

The  $^{13}\text{C}$  CP-MAS NMR spectra of the four bean flour samples are shown in Figures 4.21-4.24. As mentioned in the previous section Bardet *et al.* assigned each of the signals in the  $^{13}\text{C}$  SPE-MAS and  $^{13}\text{C}$  CP-MAS spectra of *Pisum sativum*. Therefore assignments of the  $^{13}\text{C}$  CP-MAS NMR spectra of the four bean flours were done by comparison to the assignments made by Bardet *et al.* These assignments are given in Table 4.2.

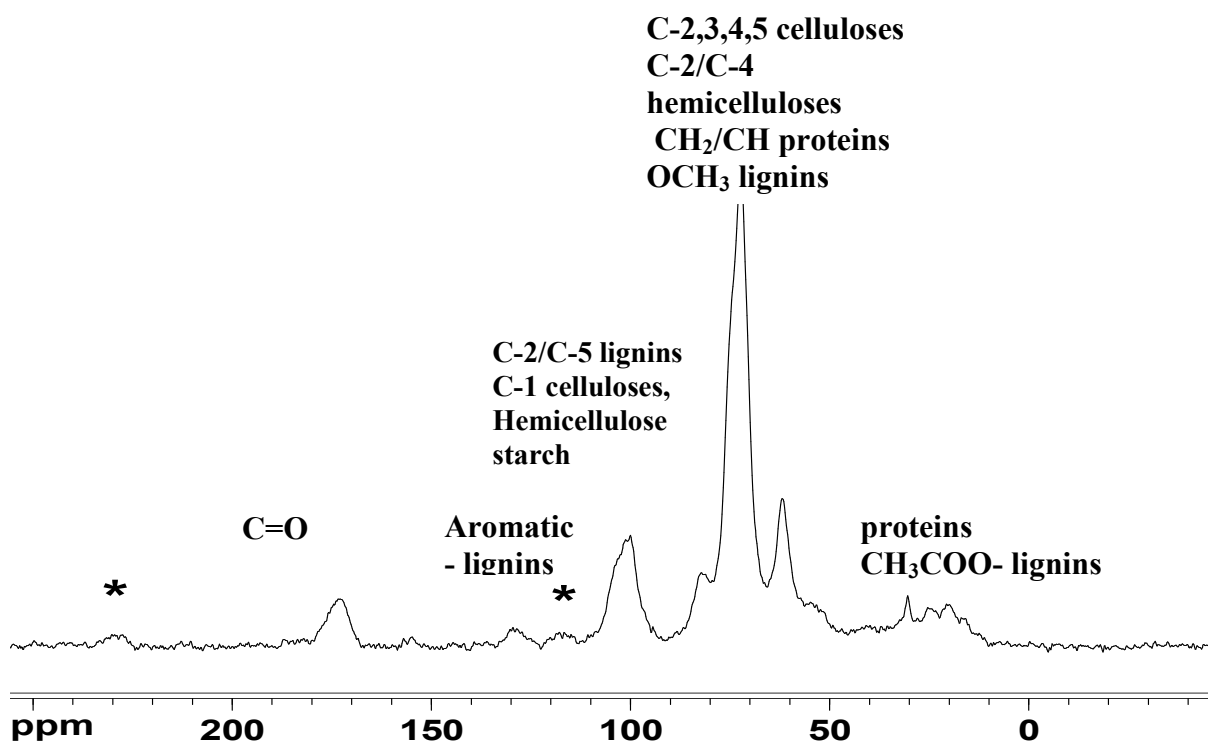


Figure 4.21:  $^{13}\text{C}$  CP-MAS NMR spectrum of black bean flour.

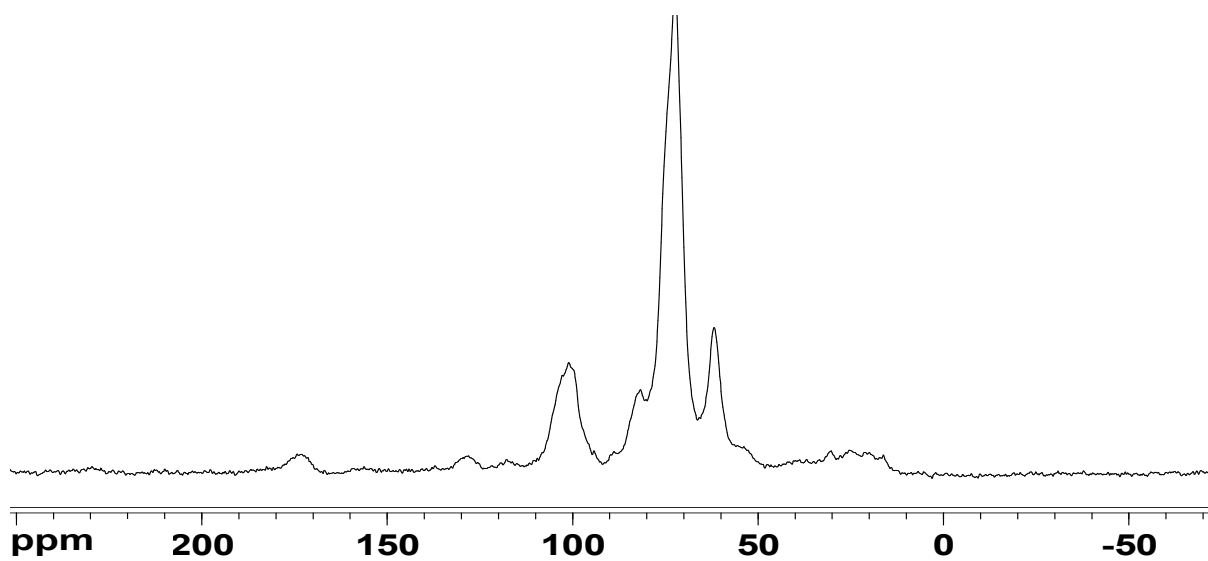


Figure 4.22:  $^{13}\text{C}$  CP-MAS NMR spectrum kidney bean flour.

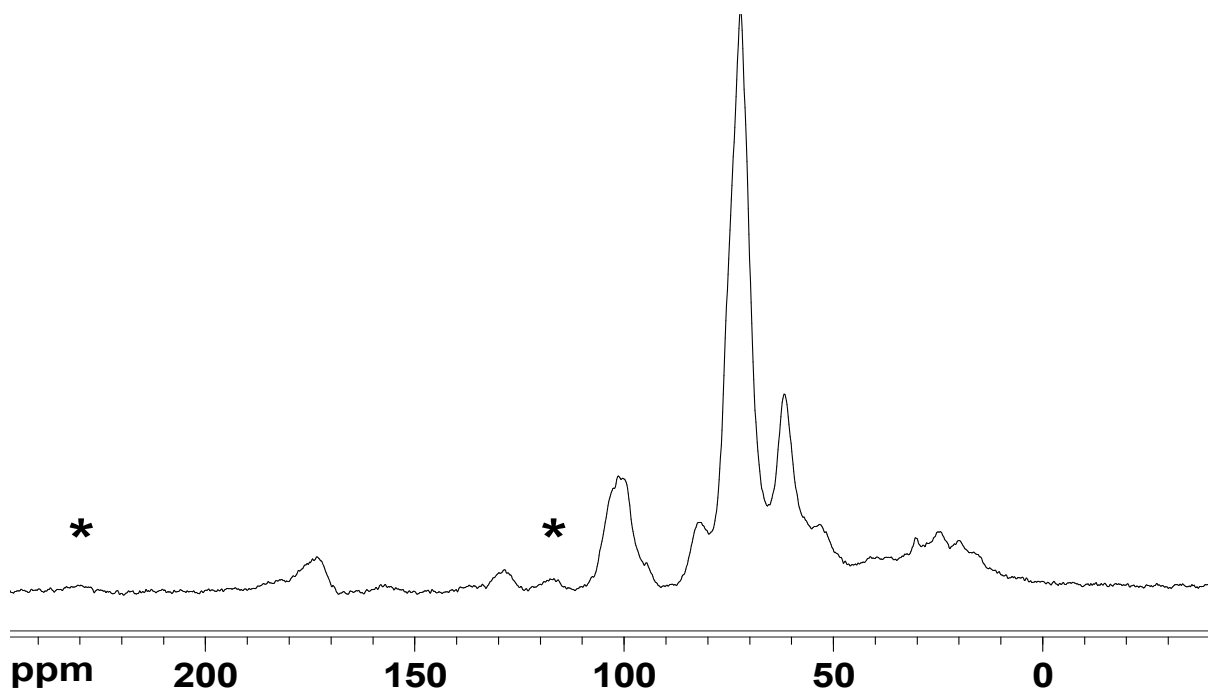
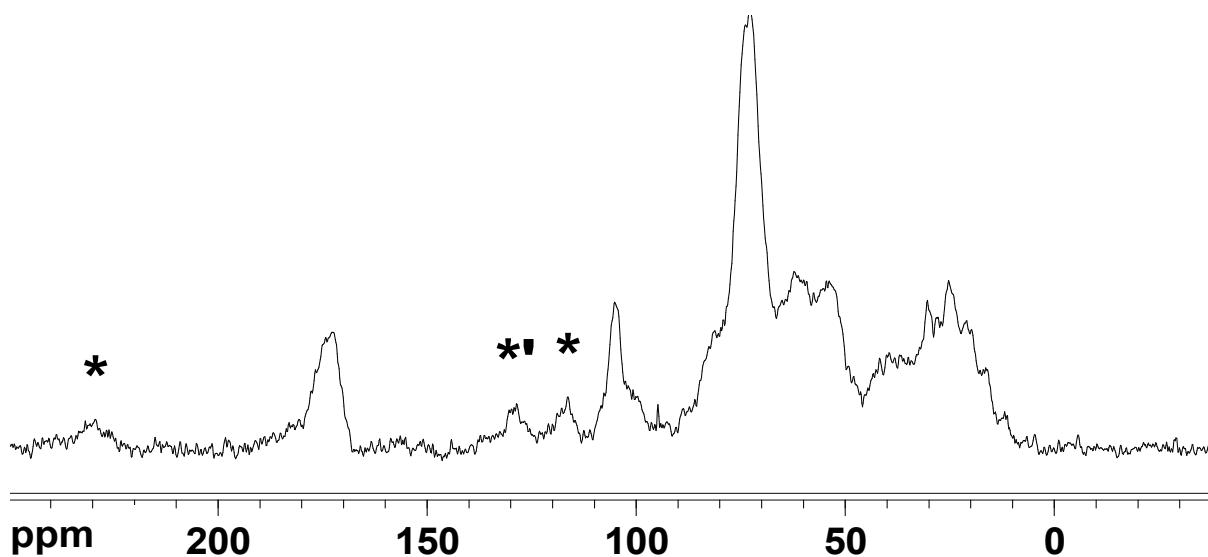


Figure 4.23:  $^{13}\text{C}$  CP-MAS NMR spectrum of mung bean flour.



**Figure 4.24:**  $^{13}\text{C}$  CP-MAS NMR spectrum of soybean flour.

The  $^{13}\text{C}$  CP-MAS NMR spectra in Figures 4.21-4.24 are all fairly similar with the exception of soybean flour. Signals around 175 ppm represent carbonyl carbons; signals around 130 ppm represent aromatic carbons in lignins; signals between 108 and 100 ppm represent aromatic units in lignins as well as anomeric ring carbons (C-1) of cellulose, hemicelluloses and starch; signals between 90 and 75 ppm represent C2/C-4 in celluloses while carbons around 70 ppm represent C-3/C-5 in celluloses as well as C-2/C-3 in hemicelluloses; signals between 65 and 60 ppm represent C-6 in celluloses and C-5 in hemicelluloses; around 55 ppm signals representing CH/CH<sub>2</sub> in proteins are observed as well as OCH<sub>3</sub> carbons in lignins; protein signals are observed between 40 and 30 ppm and CH<sub>3</sub>COO- carbon signals are present around 20 ppm.

The spectra of black, mung and kidney bean flours are all similar with good spectral resolution. The spectrum of soybean however is different with broad signal overlap. This lack of good resolution, broad overlapping signals, and very noisy spectra of soybean is an indication that the signals of the liquid-like components are also being detected by the technique.

#### 4.5.2.3 Comparison of TGA and Solid-state NMR results

The  $^{13}\text{C}$  NMR SPE-MAS of all four bean flours (namely black, kidney, mung and soybeans) were similar with bad signal to noise and significant background noise being observed. The same similarity was observed between the  $^{13}\text{C}$  CP NMR spectra of the four beans however this time sharp signals with high signal-to-noise were observed with the exception of soybean.

TGA determined the sum of two of the solid-like components (namely carbohydrates and proteins) to be 59.6 % for black bean, 59.8 % for kidney bean, 62.4 % for mung bean and 70.7 % for soybean. These values are all fairly high and the presence of this high content of solid-like components is observed in the  $^{13}\text{C}$  CP NMR of the bean flours indicated by the sharp signals and well-defined spectra. The broader signals detected in the  $^{13}\text{C}$  CP NMR spectrum of soybean flour can be attributed to the presence of the mobile components (oil) in the seed that is also being detected.

According to TGA, the oil content of black bean was found to be 2.6 %, for kidney bean 0.8 %, for mung bean 2.3 % and for soybean 17.6 %. Based on these values and comparison to the well defined spectra for the seeds, it could be expected that the highest oil containing bean, namely soybean with 17.6 % oil content, would have the best defined  $^{13}\text{C}$  SPE-MAS spectrum with the clearest signals of the four bean flours. This is however not the case since black bean flour had the best spectrum. Then there is the situation of mung bean, with 2.3 % oil content, having several broad signals in its  $^{13}\text{C}$  SPE-MAS NMR spectrum, while black bean with only 3 % more oil content than mung bean has a much better defined spectrum. Thus the better defined  $^{13}\text{C}$  SPE-MAS NMR spectrum with clear signals is not an indication of the higher oil content in beans.

The noise observed in the kidney bean and mung bean spectra as well as the noise in the soybean spectrum is due to the high content of solid like components that are also detected by the SPE-MAS technique. These high values of solid-like components influence the  $^{13}\text{C}$  SPE-MAS spectra and the spectrum becomes noisier with broader peaks. For mung bean and kidney bean it was observed that a high presence of solid-like components was present which greatly affected the spectrum with its low concentration of oils present.

The two techniques gave qualitative results on the presence of the components in beans, indicating that the beans contained a higher content of solid-like compounds

and a lower content of mobile liquid-like components than the seeds. This is indeed what was found from results by TGA in Chapter 3.

Although the  $^{13}\text{C}$  NMR SPE-MAS and  $^{13}\text{C}$  CP-MAS NMR techniques could not be used to differentiate between four beans, in conjunction with the quantitative TGA results, it was possible to understand and identify the differences in the spectra of the beans. Specifically beans such as soybeans that contain a higher content of oil could be singled out.

#### **4.5.3 Variable Contact Time application**

Variable Contact Time (VCT) is an application of the  $^{13}\text{C}$  CP-MAS technique used to estimate  $T_{1\rho}\text{H}$  values which represent the proton spin-lattice relaxation time in the rotating frame.  $T_{1\rho}\text{H}$  depends on the extent of dipolar interaction which is dominated by near neighbor spin diffusion. The experiment is carried out by varying the contact time in successive steps to map out the build-up of rare spin magnetization<sup>24</sup>. For the seeds and beans of interest to this study, the  $T_{1\rho}\text{H}$  values were determined for three signals present in the  $^{13}\text{C}$  CP-MAS spectrum. These included the signal around 100 ppm representing the aromatic carbons in lignins, and anomeric (C-1) carbons in hemicelluloses, cellulose and starch; the signals around 70 ppm representing the C-2,3,5 carbons in celluloses and C-2,3 in hemicelluloses; and around 60 ppm representing C-6 in cellulose and C-5 in hemicellulose.

Using this experiment several data points of signal intensity were acquired for carbons in a sample with respect to contact time. The signal intensity values were plotted on the y-axis of a graph with the corresponding contact time values on the x-axis. For all three signals similar curves were obtained and for the purpose of this study only the curve around 70 ppm will be discussed. Figure 4.25 illustrates the curves obtained for the seeds and beans for the carbons around 70 ppm.

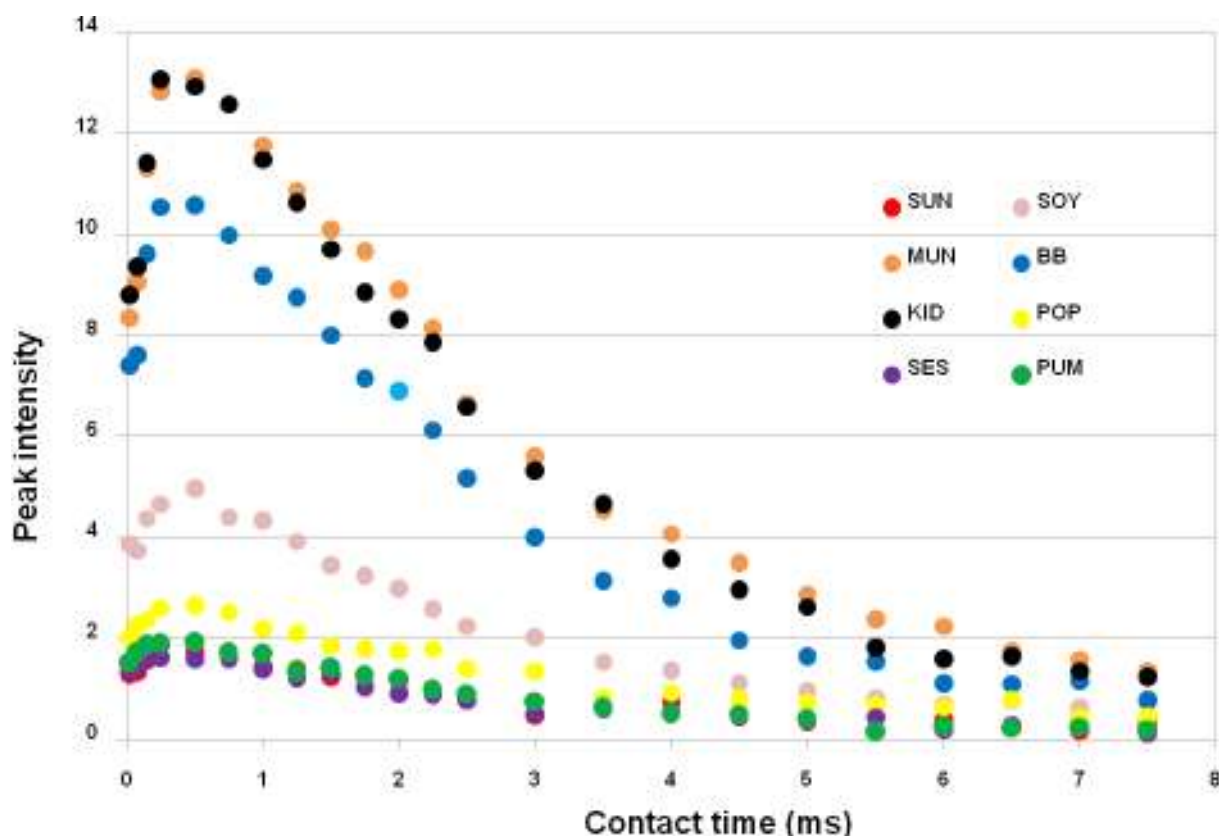


**Figure 4.25:** Curve representing the  $T_{1\rho}H$  relaxation of the carbons around 70 ppm with respect to contact time.

Notice that the curves for all four seeds are grouped together at the bottom of the graph while the curves for the beans are grouped together at the top of the graph with exception of soybean that is found to be in the middle. This grouping together of curves for seeds and beans is an indication that the components in all seeds have similar relaxation rates and components in all beans have similar relaxation rates, but that the overall relaxation rates of seeds differ from those of beans.

Investigating the curve in more detail, not only can information be obtained on  $T_{1\rho}H$  values but also on the cross-polarization (CP) build-up rate from the surrounding protons to the carbon of interest. Looking at Figure 4.26, the initial rise of the curve illustrates this CP build-up rate. This is indicated on the curves with a black line. Notice that by inspection of the relative increase in CP rate (by looking at the slope of the line), the CP build-up rate is much larger for the beans than for the seeds. This could be an indication that the cross-polarization from the protons to the carbons in the beans is much faster than for the seeds.

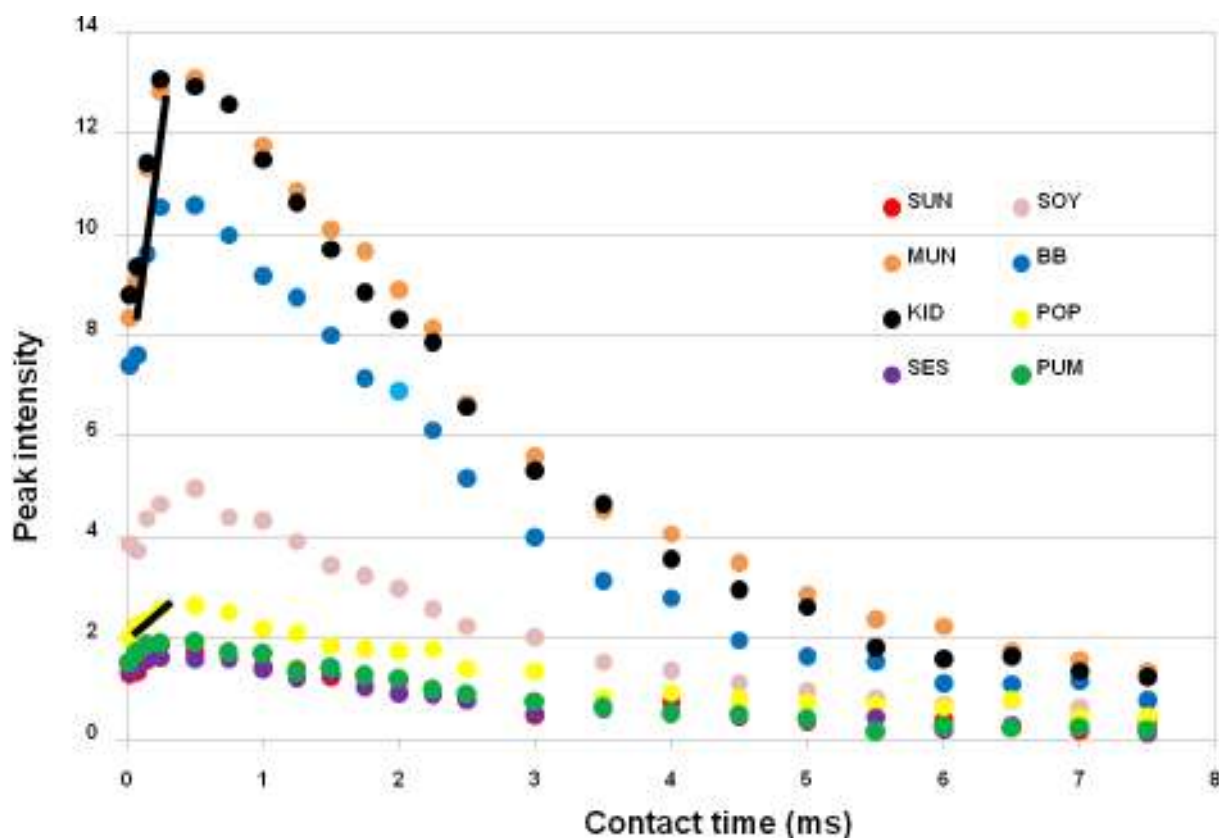


**Figure 4.26:** Curve representing the  $T_{1\rho}H$  relaxation of starch carbons at 70 ppm with respect to contact time with the sharper CP rate for beans than seeds indicated.

The rate of decrease of the curves is an indication of the relaxation rates. Notice again that the rate of decrease for the beans seems to be much larger than for the seeds with respect to the same range of contact time (on the x-axis) as indicated in Figure 4.27. This could be an indication that the carbons relax much faster in the rotating frame in the beans than the seeds.

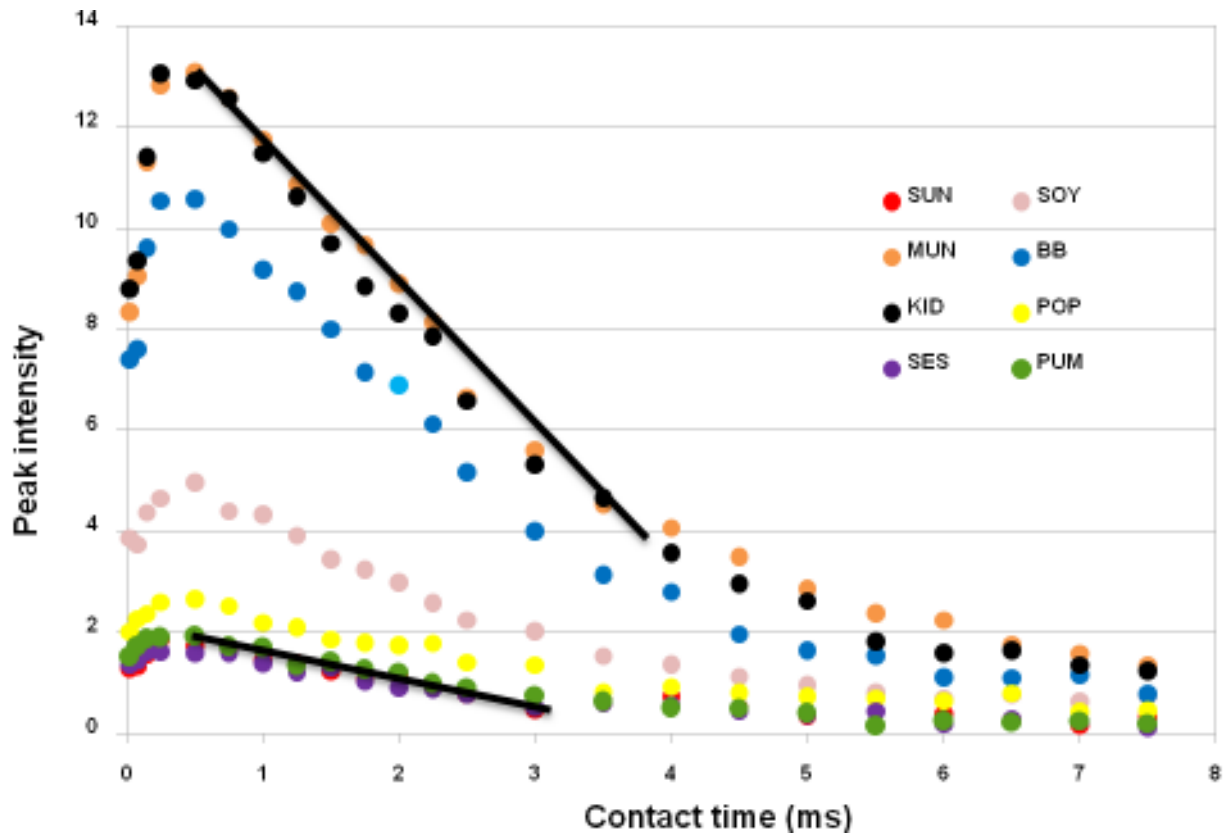


**Figure 4.27:** Curve representing the  $T_{1\rho}H$  relaxation of starch carbons at 70 ppm with respect to contact time with indication of the sharper decrease of relaxation for beans than seeds.

Several equations are available in the literature as fitting models to determine the  $T_{1\rho}H$  values. Below some of these equations are discussed.

$T_{1\rho}H$  values were determined with the following linear equation<sup>15</sup>:

$$\ln I(t) = \ln I_0 - t / T_{1\rho}H$$

where  $I_0$  is the peak height at time  $t = 0$ , and  $I(t)$  is the peak height at time  $t$  ( $t = \tau$ ).

This equation can be rewritten as follows:

$$\ln I(t) = -t / T_{1\rho}H + \ln I_0$$

Consequently this equation looks similar to that of a linear line:

$$y = mx + c$$

Where  $t$  are the  $x$ -values,  $\ln I_0$  the intercept,  $\ln I(t)$  the  $y$ -values and  $(-T_{1\rho}H)$  the gradient.

Therefore by fitting this equation to each of the points of interest,  $T_{1\rho}H$  values could be determined from the slope ( $1/ T_{1\rho}H$ ). In order to fit this equation, it was necessary to re-plot the data, since the log of the signal intensity used on the y-axis is plotted against the contact time on the x-axis (Figure 4.28).

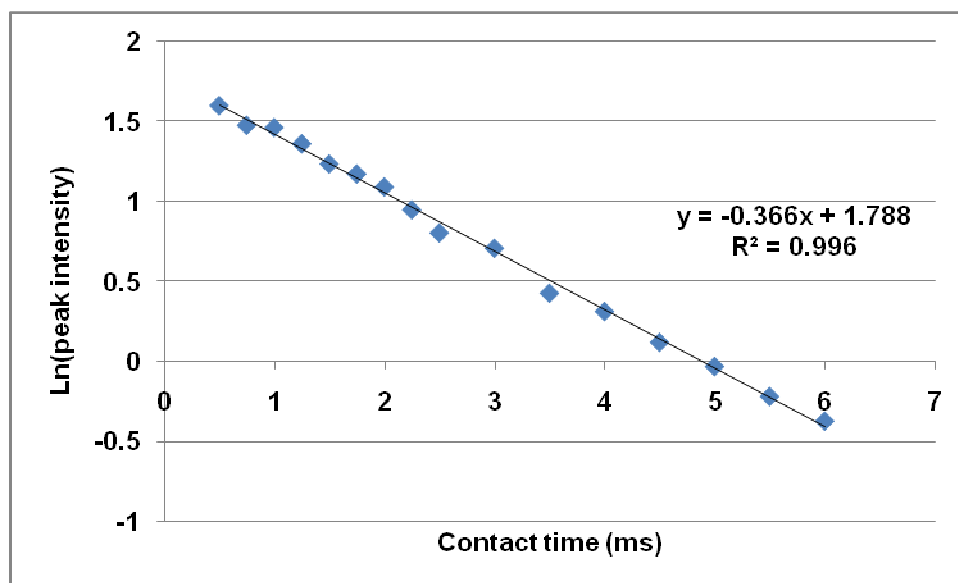


**Figure 4.28:** Log of the peak intensity plotted against contact time for determination of the  $T_{1\rho}H$  relaxation of carbons at 70 ppm for soybeans.

This equation was fitted to the curves of the carbons at 70 ppm and the  $T_{1\rho}H$  relaxation rates obtained using this method for the starch carbons are given in Table 4.3. The problem with this fitting lies in the fact that the VCT experiment itself incorporates both the liquid-like and solid-like components both present at one signal in the spectrum. For instance carbons for starch and glycerol are both represented by one signal at 70 ppm. Therefore it is possible to obtain two separate  $T_{1\rho}H$  values for one signal and hence our observation of the two separate decay periods: upon inspection of the data plotted in Figure 4.27, there seems to be two separate decay periods and not just one as expected. These are clearly indicated in Figure 4.29.

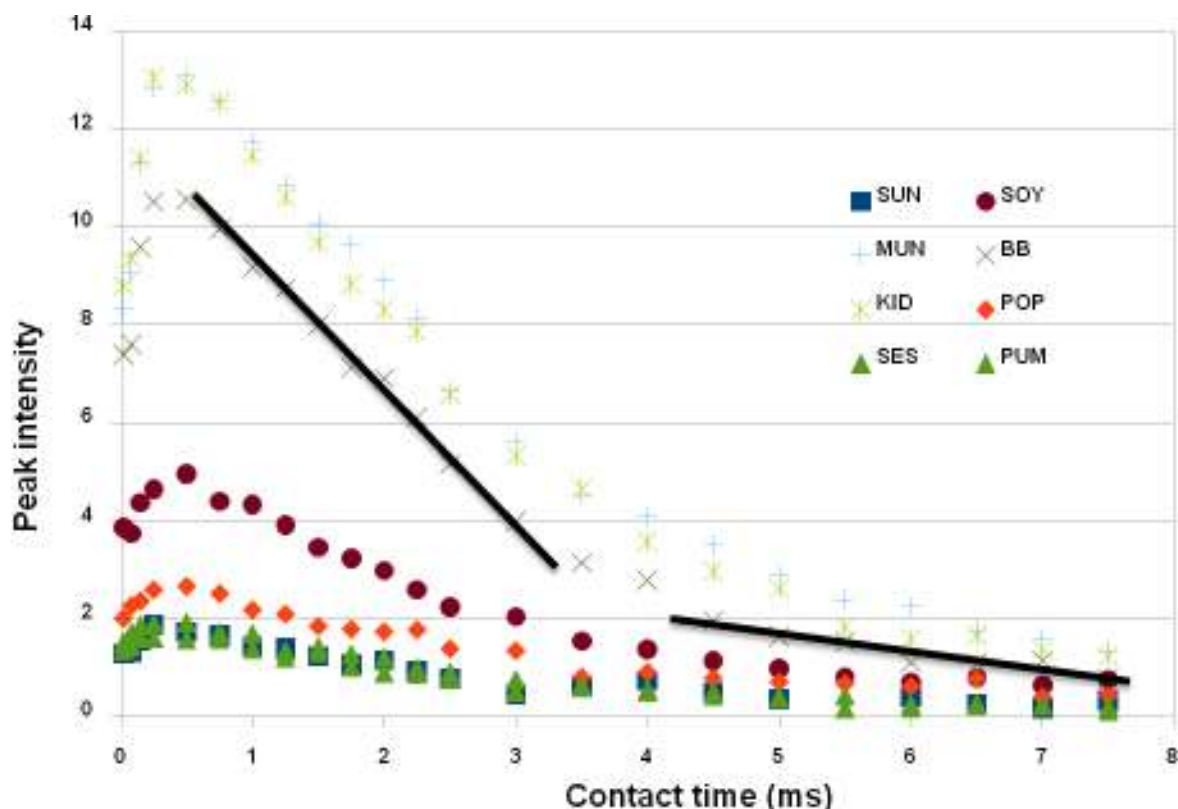


**Figure 4.29:** Curve representing the  $T_{1\rho}H$  relaxation carbons at 70 ppm with respect to contact time with indication of a linear line fitted to two separate relaxation rates.

Notice that due to the observation of the two different phases of relaxation, the above linear equation was not only fitted to the data for the full decay but also taking into account the possibility of two phases most likely due to the presence of carbons of starch and glycerol both being detected by the VCT technique. The decision of which points to use for the fitting of the two phases was done by inspection of linear points on the original curve (Figure 4.30) and not from the plot of the log of the peak intensity against contact time (Figure 4.28). This is illustrated for soybean in Figure 4.32. Values are given in Table 4.3.

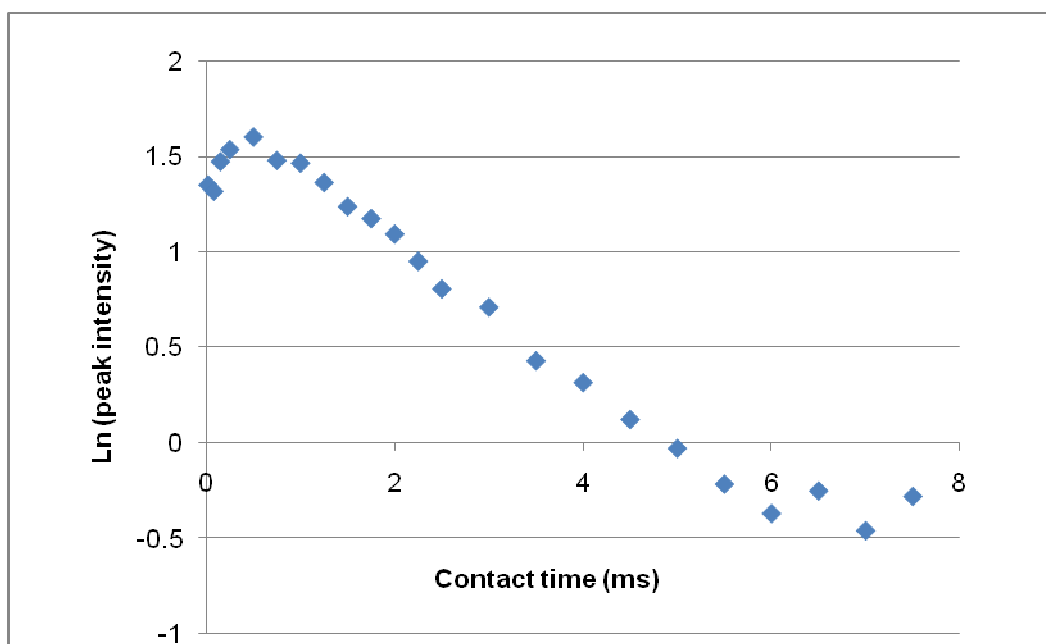


**Figure 4.30:** Plot of the log of the peak intensity against contact time representing the  $T_{1\rho}H$  relaxation of carbons at 70 ppm for soybean.

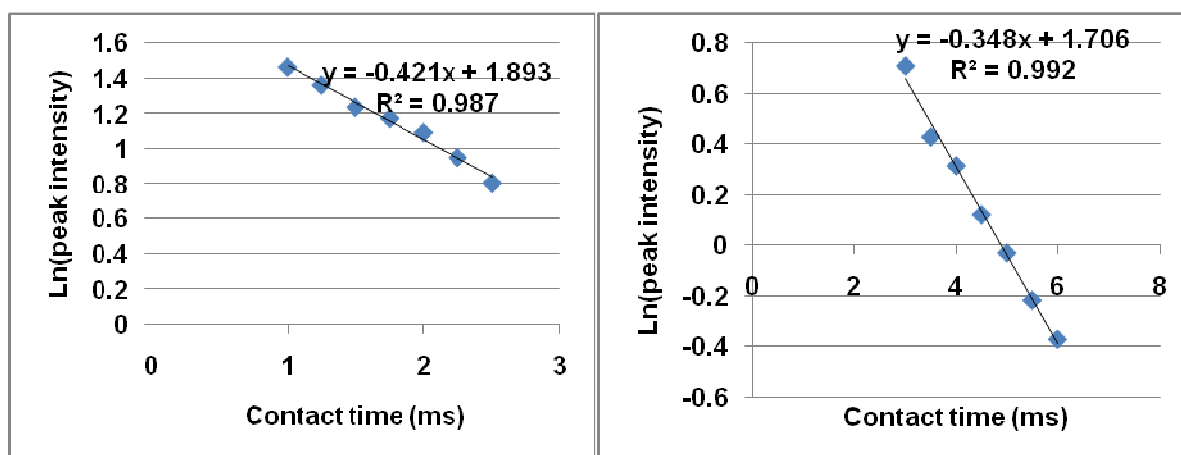


**Figure 4.31:** The plots for determination of  $T_{1\rho}H$  relaxation of carbons at 70 ppm for soybean with a linear line fitted for each of the two phases.

Standard errors for each  $T_{1\rho}H$  value were determined with the following equations.

$$S_{y/x} = \left[ \frac{\sum_i (y_i - \hat{y}_i)^2}{n - 2} \right]^{1/2}$$

where  $y_i$  is the measured signal value and  $\hat{y}_i$  the corresponding value of  $y$  on the fitted straight line at the same value of  $x$ .

$$S_b = \frac{S_{y/x}}{\left[ \sum_i (x_i - \bar{x})^2 \right]^{1/2}}$$

where  $S_b$  is the standard deviation of the slope and therefore equals the standard deviation error of  $T_{1\rho}H$ .

**Table 4.3:**  $T_{1\rho}H$  values determined for seeds and beans for peak at 70 ppm

	Single phase		Two phases			
	$T_{1\rho}H$ (ms)		$T_{1\rho}H_a$ (ms)		$T_{1\rho}H_b$ (ms)	
<b>SEEDS</b>						
POP	3.61 ±	0.02	3.21 ±	0.02	5.65 ±	1.46
PUM	2.62 ±	0.02	3.24 ±	0.02	2.95 ±	0.01
SES	3.00 ±	0.02	2.49 ±	0.06	3.66 ±	0.07
SUN	2.52 ±	0.04	2.52 ±	0.04	5.85 ±	0.16
<b>BEANS</b>						
BB	2.36 ±	0.01	3.37 ±	0.01	2.28 ±	0.02
KID	2.75 ±	0.01	3.29 ±	0.01	2.44 ±	0.02
MUN	2.95 ±	0.01	3.68 ±	0.01	3.15 ±	0.01
SOY	2.73 ±	0.01	2.38 ±	0.02	2.87 ±	0.07

Looking at the data in Table 4.3, there is no definite distinction between the  $T_{1\rho}H$  values for the seeds and those for the beans.

A second equation was used for the fitting of the data which assumes a one-phase situation and incorporates all the data points namely the rising (CP transfer) and falling (relaxation) for the curve<sup>15</sup>:

$$M = M_0 \frac{\exp\left(\frac{-t}{T_{1p}}\right) - \exp\left(\frac{-t}{T_{CH}}\right)}{1 - \frac{T_{CH}}{T_{1p}}}$$

where  $M$  = signal intensity,  $M_0$  = calculated maximum signal intensity,  $t$  = contact time,  $T_{1\rho}$  = proton spin lattice relaxation time in the rotating frame, and  $T_{CH}$  = time constant for cross polarization exponential.

This data was fitted using Sigmaplot 9.0 software and is illustrated in Figure 4.32 for mung bean at 70 ppm. Notice that although the fitting is fairly good it is not accurate enough.

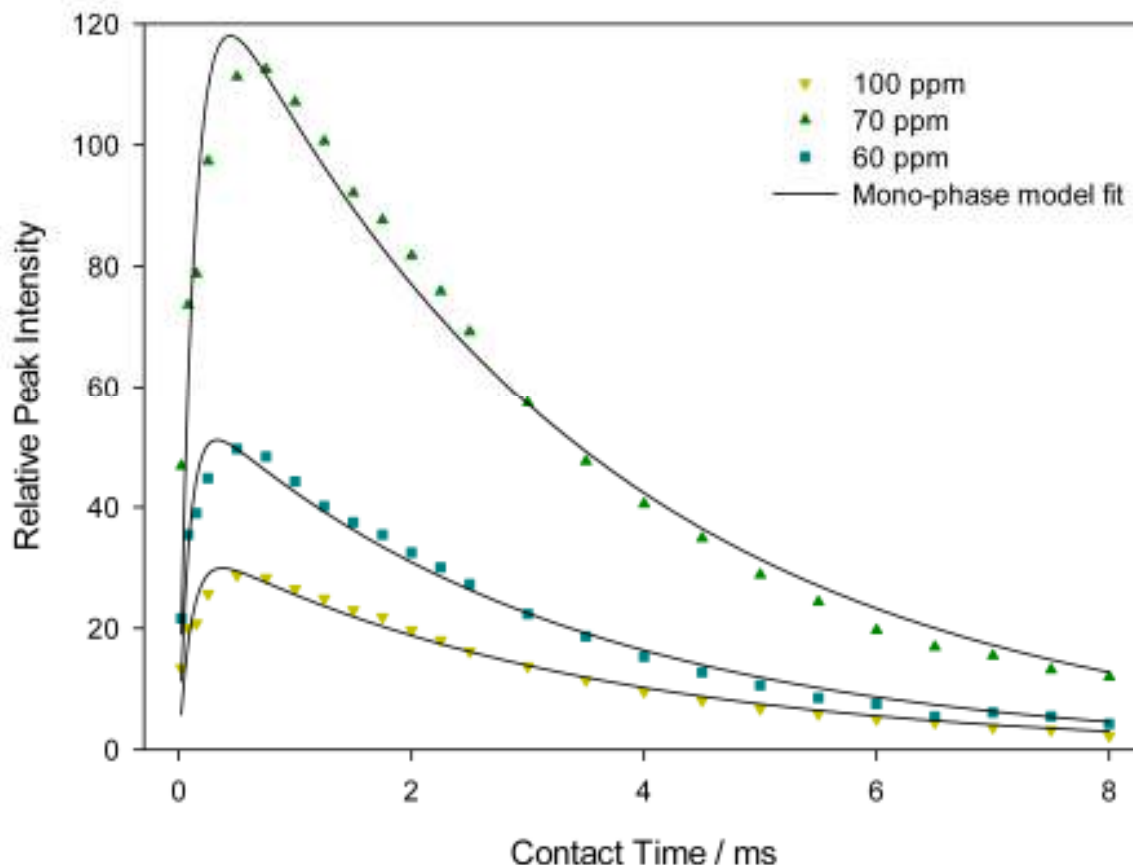


**Figure 4.32:** One-phase fitted equation to starch carbons at 70 ppm relaxation data for mung bean.

$T_{1\rho}H$  values and standard errors for the seeds and beans were calculated from the fitted equation and results are given in Table 4.4. Looking at the data in Table 4.4, once again there is no definite distinction between the  $T_{1\rho}H$  values for the seeds and those for the beans. This however could be due to the fit of the data not being quite as accurate as would be liked and that this data is generated from a fit that only takes into account relaxation values for one phase. On average the errors are higher for this method than the previous method.

**Table 4.4:**  $T_{1\rho}H$  values determined for seeds and beans for peaks at 100, 70 and 60 ppm using a single phase fit.

	100 ppm	70 ppm	60 ppm
	$T_{1\rho}H$ (ms)	$T_{1\rho}H$ (ms)	$T_{1\rho}H$ (ms)
<b>SEEDS</b>			
SUN		3.31 ± 0.33	3.95 ± 0.36
POP	4.07 ± 0.31	3.57 ± 0.23	2.75 ± 0.14
PUM	2.89 ± 0.32	3.14 ± 0.25	3.08 ± 0.35
SES	3.06 ± 0.19	3.10 ± 0.17	
<b>BEANS</b>			
SOY	3.75 ± 0.31	3.31 ± 0.27	
MUN	3.28 ± 0.26	3.34 ± 0.25	3.15 ± 0.21
BB	3.16 ± 0.30	3.29 ± 0.31	1.70 ± 0.14
KID	2.99 ± 0.25	3.04 ± 0.23	2.55 ± 0.17

In order to incorporate two phases, the same equation can be used with an adjustment<sup>17</sup>. This is essentially the same equation observed previously but applied to the presence of two phases:

$$M = M_{0A} \frac{\exp\left(\frac{-t}{T_{1\rho A}}\right) - \exp\left(\frac{-t}{T_{CH A}}\right)}{1 - \frac{T_{CH A}}{T_{1\rho A}}} + M_{0B} \frac{\exp\left(\frac{-t}{T_{1\rho B}}\right) - \exp\left(\frac{-t}{T_{CH B}}\right)}{1 - \frac{T_{CH B}}{T_{1\rho B}}}$$

where the additional suffixes A and B refer to phases A and B, respectively.

This data was once again fitted using Sigmaplot 9.0 software and is illustrated in Figure 4.33 for mung bean at 70 ppm. Notice that this time the fitting is very good, especially when compared to the fitting in Figure 4.32.

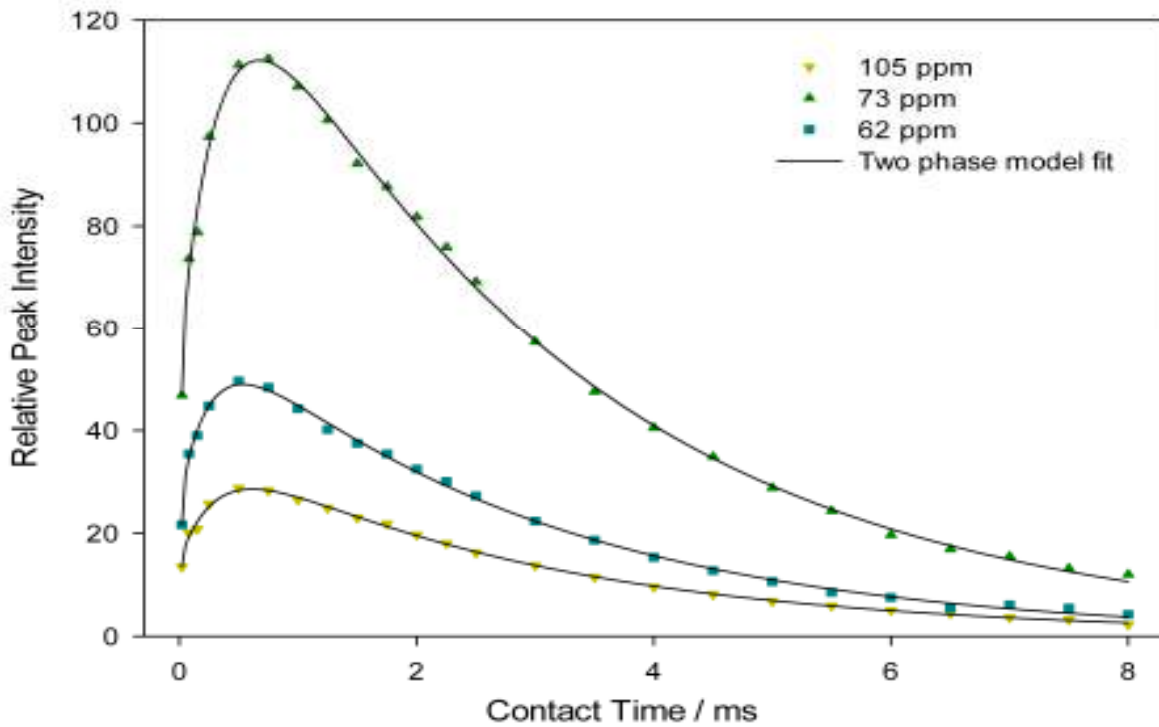


**Figure 4.33:** Two-phase equation fitted to 70 ppm relaxation data for mung bean.

**Table 4.5:**  $T_{1\rho}H$  values determined for seeds and beans for signals at 100, 70 and 60 ppm for two domains.

	100 ppm			70 ppm			60 ppm		
	$T_{1\rho}H$ (ms)			$T_{1\rho}H$ (ms)			$T_{1\rho}H$ (ms)		
<b>SEEDS</b>									
SUN				3.24	±	0.36	4.83	±	0.54
				1.92	±	0.79	1.41	±	0.77
POP	1.38	±	5.05	4.07	±	0.30	5.14	±	1.70
	4.08	±	4.29	1.47	±	0.57	1.54	±	0.42
PUM	3.03	±	1.74	3.20	±	0.18	3.00	±	2.23
	0.61	±	3.37	1.55	±	0.85	1.04	±	4.54
SES				3.24	±	0.71	3.85	±	14.60
				1.00	±	0.62	1.36	±	10.79
<b>BEANS</b>									
SOY	6.69	±	0.72	1.77	±	0.30	3.45	±	1.29
		±	127.3		±			±	
	0.95		4	3.92		0.28	1.10		1.19
MUN	3.83	±	0.54	2.76	±	0.86	2.87	±	2.57
	2.30	±	0.36	3.31	±	1.61	2.72	±	3.83
BB	2.91	±	0.25	2.76	±	0.39	2.12	±	0.83
	2.91	±	0.31	2.76	±	0.43	0.52	±	1.07
KID	2.82	±	0.28	2.65	±	0.19	2.78	±	0.07
	0.78	±	0.56	2.65	±	0.51	1.22	±	0.22

$T_{1\rho}H$  values and standard errors for the seeds and beans were calculated from the fitted equation and results are given in Table 4.5. Looking at the data in Table 4.5, once again there is no definite distinction between the  $T_{1\rho}H$  values for the seeds and those for the beans.

At this stage of preliminary studies on the determination of  $T_{1\rho}H$  values of seeds and beans, looking at the different fitted models and various results obtained in Tables 4.3-4.5, no conclusions can be drawn on the  $T_{1\rho}H$  values themselves. However VCT experiments have indicated that not only the solid-like components are detected by this technique but liquid-like components as well. Therefore when working with fitting models to determine the  $T_{1\rho}H$  values of the components present in seeds and beans, one-phase models have proven to not be sufficient and two-phase models (due to the presence of liquid-like and solid-like components detected by the technique) should rather be used. Further investigation is required to determine the exact  $T_{1\rho}H$  values of the components in each of the seed and bean samples and an explanation as to what they mean.

#### **4.6 CONCLUSIONS**

In conclusion, the Solid State NMR studies carried out gave valuable information on the solid-like and liquid-like components within seeds and beans.  $^{13}\text{C}$  SPE-MAS NMR spectroscopy indicated that overall seeds contained a higher content of liquid-like components (oil) than for beans. In turn the  $^{13}\text{C}$  CP-MAS NMR spectra indicated that beans had a higher content of solid-like components (protein and carbohydrates) than for seeds.

The  $^{13}\text{C}$  SPE-MAS and  $^{13}\text{C}$  CP-MAS techniques complemented each other beautifully.

For the seeds: All four the seeds had well-defined, clear  $^{13}\text{C}$  SPE-MAS spectra indicating that a high content of liquid-like components were present, while the  $^{13}\text{C}$  CP-MAS spectra of all four of the seeds had noisy spectra with spectral overlap and broad signals indicating a low solid-like component content but a high liquid-like component content.

For the beans: Where the  $^{13}\text{C}$  SPE-MAS spectra indicated that soybean had a higher content of liquid-like components (oil) present compared to the other three beans, with noisy spectra for kidney, mung and black bean indicated a high content of solid-

like components present, the  $^{13}\text{C}$  CP-MAS NMR spectra of soybean was noisy due to high liquid-like content and well-defined spectra for mung, kidney and black beans.

These conclusions correlated very well with the content of liquid-like components (oil) and solid-like components (proteins and carbohydrates) that was determined by conventional methods and TGA.

Preliminary studies using  $T_{1\rho}\text{H}$  experiments on the components present in the seeds and beans have led to a few observations. Firstly the CP build-up rate is much larger for the beans than those of the seeds. Secondly the carbons relax much faster in the rotating frame in the beans than the seeds. Thirdly a model using a two-phase fit in order to determine  $T_{1\rho}\text{H}$  values seem to be more accurate. At this stage of the study the implications of these three observations is yet unknown.

Since this was only a preliminary study, further NMR related investigation is however required to explain these observations fully.

## **4.7 EXPERIMENTAL**

### **4.7.1 Sample preparation for Solid State NMR spectroscopy**

All seeds (poppy, sesame, sunflower, pumpkin) and beans (soy, black, mung, kidney) were ground to a flour using a coffee and spice grinder. Flour samples were packed as is except for sunflower and sesame seeds. Due to the high fat content in the seeds, the excess oil in the flour was absorbed onto filter paper before packing to stop oil leaking from the rotor during the experiments and causing the rotor plugs to slip out (this happened initially during optimisation of the sample preparation).

### **4.7.2 Collection of Solid State $^{13}\text{C}$ NMR spectra**

Solid state spectra were obtained on a **Varian VNMRS 500 MHz Solids NMR Spectrometer**, operating at 125.686 MHz for  $^{13}\text{C}$ . A zirconium oxide rotor of 6 mm diameter was used at spinning rates of 5 and 7 kHz for  $^{13}\text{C}$  CP-MAS; 5 kHz for  $^{13}\text{C}$  SPE-MAS experiments, and 7 kHz for VCT experiments.  $^{13}\text{C}$  SPE-MAS experiments were obtained with a delay of 0.3 s using 256 scans and a block size of 4, while  $^{13}\text{C}$  CP-MAS experiments were obtained with a delay of 5 s using 5 000 scans and a block size of 4. Line broadening of 40 Hz was applied when processing all MAS spectra.

### 4.7.3 Variable Contact Time experiment (VCT)

The above instrument was used with a spin-lock time ranging from 200 to 8 000  $\mu$ s. Proton  $T_{1\rho}$  (further referred to as  $T_{1\rho}H$ ) values were determined from the intensity decay of  $^{13}C$  peaks with increasing contact times as discussed in the earlier text.

## 4.8 REFERENCES

- 31 Andrew, E.R., and Szczesniak, E., A historical account of NMR in the solid state. *Prog. Nucl. Mag. Sp.*, **1995**, 28, 11-36.
- 32 Laws, D.D., Bitter, H.M.L., Jerschow, A., Solid state NMR spectroscopic methods in chemistry, *Angew. Chem. Int. Ed.* **2002**, 41, 3096-3129.
- 33 Bardet, M., Foray, M.F., and Guillermo, A., High-Resolution solid state NMR as an analytical tool to study plant seeds, *Modern Magnetic Resonance*, **2006**, 1755-1759
- 34 de Oliveira, C.M.R., Lacomini, M., Alquini, Y., and Gorin, P.A.J., Microscopic and NMR analysis of the external coat from seeds of *Magonia pubescens*, *New Phytol.*, **2001**, 152, 501-509.
- 35 Gussoni, M., Greco, F., Pegna, M., Bianchi, G., and Zetta, L., Solid state and microscopy NMR study of the chemical constituents of *Azelia cuanzensis* seeds, *Magn. Reson. Imaging*, **1994**, 12 (3), 477-486.
- 36 Cheetham, N.W.H., and Tao, L., Solid state NMR studies on the structural and conformational properties of natural maize starches, *Carbohydr. Polym.*, **1998**, 36, 285-292.
- 37 Richard, J., Kelly, I; Marion, D; Pezolet, M; and Auger, M., Interaction between beta-purothionin and dimyristoylphosphatidylglycerol: A  $^{31}P$ -NMR and infrared spectroscopic study, *Biophys. J.*, **2002**, 83 (4), 2074-2083.
- 38 Jarvis, M.C., and Apperley, D.C., Direct observation of cell wall structure in living plant tissues by solid state  $^{13}C$  NMR spectroscopy, *Plant Physiol.*, **1990**, 92, 61-65.
- 39 Tavares, M.I.B., Bathista, A.L.B.S., Silva, E.O., Filho, N.P., and Nogueira, J.S., A molecular dynamic study of the starch obtained from the *Magnifera indica* Cv *Bourbon* and *Espada* seeds by  $^{13}C$  solid state NMR., *Carbohydr. Polym.*, **2003**, 53, 213-216.
- 40 Calucci, L., Galleschi, L., Geppi, M., and Mollica, G., Structure and dynamics of flour by solid state NMR: effects of hydration and wheat aging, *Biomacromolecules*, **2004**, 5, 1536-1544.

- 41 Vieira, M.C and Gil, A.M., A solid state NMR study of locust bean gum galactomannan and Konjac glucomanna gels, *Carbohydr. Polym* **2005**, *60*, 469-448.
- 42 Bootten, T.J., Harris, P.J., Melton, L.D., and Newman, R.H., Solid-state  $^{13}\text{C}$  NMR spectroscopy shows that the xyloglucans in the primary cell walls of mung bean (*Vigna radiate L.*) occur in different domains: a new model for xyloglucan-cellulose interactions in the cell wall, *J. Exp. Bot.*, **2004**, *55*, 571-583.
- 43 Bardet, M., Maron, S., Foray, M.F., Berger, M., and Guillermo, A., Investigation of  $\gamma$ -irradiated vegetable seeds with high resolution solid state  $^{13}\text{C}$  NMR, *Radiat. Res.*, **2004**, *161*, 458-463.
- 44 Nascimento, A.M.R., Tavares, M.I.B., and Nascimento, R., Solid state NMR study of *Couma utilis* seeds, *Int. J. Polym. Mater.*, **2007**, *56*, 365-370.
- 45 Kou, Y., Molitor, P.F., and Schmidt  $^{15}\text{N}$  Mobility and stability characterization of model food systems using NMR,  $^{15}\text{N}$  media germination techniques, *J. Food Sci.*, **1999**, *64*, 950-959.
- 46 Separovic, F.; Lam, Y. H.; Ke, X.; Chan, H.-K. A solid-state NMR study of protein hydration and stability., *Pharmaceut. Res.*, **1998**, *15 (12)*, 1816-1821.
- 47 Fransen, C. T. M.; van Laar, H.; Kamerling, J. P.; Vliegthart, J. F. G. CP-MAS NMR analysis of carbohydrate fractions of soybean hulls and endosperm., *Carbohydr. Res.*, **2000**, *328 (4)*, 549-559.
- 48 Bardet, M., Foray, M.F., Bourguignon, J., and Krajewski, P., Investigation of seeds with high-resolution solid state  $^{13}\text{C}$  NMR, *Magn. Reson. Chem.*, **2001**, *39*, 733-738.
- 49 Duer, M.J., Introduction to solid state NMR spectroscopy, Wiley Blackwell, **2004**.
- 50 Voelkel, R., High-Resolution solid-state  $^{13}\text{C}$ -NMR spectroscopy of polymers, *Angew. Chem. Int. Ed. Engl.*, **1988**, *27*, 1468-1483.
- 51 Bardet, M., Foray, M.F., and Guillermo, A., High-resolution solid-state NMR as an analytical tool to study plant seeds, *Modern Magnetic Resonance*, **2006**, *3*, 1755-1759.
- 52 Retief, L., McKenzie J.M., and Koch K.R., A novel approach to the rapid assignment of  $^{13}\text{C}$  NMR spectra of major components of vegetable oils such as avocado, mango kernel and macadamia nut oils, *Magn. Reson. Chem.*, **2009**, *47*, 771-781.
- 53 Retief, L., McKenzie J.M., and Koch K.R., in "Magnetic Resonance in Food Science: Challenges in a Changing World", Identification and quantification of major triacylglycerols in selected South African vegetable oils by  $^{13}\text{C}$  NMR spectroscopy, RSC publishing, London, UK, **2009**, 151-157.

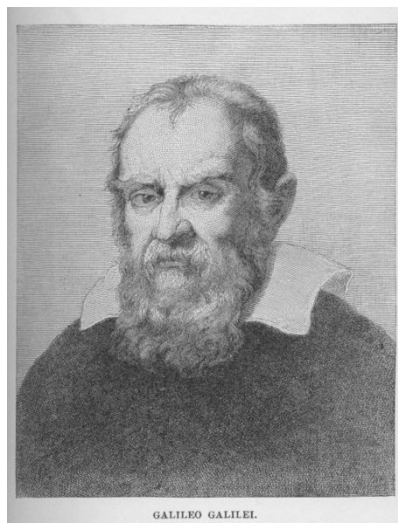
- 54 Ackerman, J. L., A complete introduction to modern NMR spectroscopy, Chapter 15: Solid-state NMR spectroscopy, New York, Wiley, **1998**.

# CHAPTER 5: FINAL CONCLUSIONS

*"Measure what is measurable, and make measurable  
what is not so."*

Galileo Galilei

February, 1564 – January, 1642



Picture obtained from <http://en.wikipedia.org/wiki/Galileo>.

In this dissertation, vegetable oils, seeds and beans were analysed with respect to their oil, protein and carbohydrate content respectively. The vegetable oils included apricot kernel, avocado pear and macadamia nut oils while the seeds included sesame, poppy, pumpkin and sunflower seeds and the beans included soy, mung, kidney and black bean. This chapter summarises the conclusions drawn upon the studies done in this dissertation.

For the analysis of the vegetable oils, high resolution NMR spectroscopy was the technique of interest. Upon phosphorylation of the OH-containing compound present in the vegetable oils (namely the 1,2 DGs; 1,3 DGs; FFAs which were of interest) with 2-chloro-4,4,5,5-tetramethyl dioxaphospholane, the  $^{31}\text{P}$  NMR spectra of the three locally produced vegetable oils, namely apricot kernel; macadamia nut and avocado pear oils, were assigned for the first time. Since these spectra were found to be very similar to those of the  $^{31}\text{P}$  NMR spectra of olive oil as indicated in the literature, the signals were assigned by inspection.

By adding a known amount of cyclohexanol to each of the samples, quantification of the DG and FFA signals were achieved with respect to the cyclohexanol internal standard. Two methods were used for quantitative studies, namely a calibration curve approach (CCA) and a direct correlation approach (DCA). Both methods proved to be useful with CCA found to be more appropriate for determinations of 1,2 DG and 1,3 DG concentrations while DCA gave better information on FFA concentrations.

All oil samples were stored for two different lengths of time and under five different conditions, namely exposed to light, in the dark, in the dark covered in tinfoil, in a freezer at  $-8\text{ }^{\circ}\text{C}$  and in a fridge at  $5\text{ }^{\circ}\text{C}$ . Using the DCA and CCA methods, the best storage conditions for the three vegetable oils were identified. Studies indicated that different storage conditions had an important effect on the minor components and consequently on the freshness of the vegetable oil and stating that vegetable oils should be stored in a dark cupboard or even in a fridge as many consumers and producers claim, is not necessarily accurate as a general rule for all vegetable oils since individual storage conditions seem to affect vegetable oil minor components differently. Overall it seemed that the best storage conditions were storage at  $5\text{ }^{\circ}\text{C}$  and  $-8\text{ }^{\circ}\text{C}$  for apricot kernel, macadamia nut and avocado pear oils. For all oils, the

1,2 DG: 1,3 DG ratio was roughly 1:2. Longer storage periods for all of the oils indicated lower concentrations than for shorter storage periods, possibly due to the precipitation of components out of solution during longer time periods. The effect of storage conditions on these particular vegetable oils, namely apricot kernel, avocado pear and macadamia nut oils have not previously been studied and are reported in this study for the first time.

The moisture, oil, carbohydrate and protein content present in four seeds, namely poppy, sesame, sunflower and pumpkin seeds, and four beans, namely kidney, mung, black and soybeans were determined by TGA analysis and conventional methods such as Soxhlet extraction (oil), Dumas-combustion (protein) and Clegg-Anthrone/UV-VIS (carbohydrates). It was shown that TGA gave valuable information on the contents of seeds and beans. The sample preparations was found to affect the measurements obtained and consequently correct sample preparation conditions were found to be the following: sesame, pumpkin and sunflower seeds were ground into coarse pieces while poppy seed was used whole; soybean and black beans were ground into coarse pieces while the tegument of mung bean and kidney bean were removed and the beans then ground into coarse pieces. The plot of the first derivative of the thermogram with respect to the temperature indicated certain regions of peaks corresponding to the mass loss of the compounds of interest as determined by conventional methods. For seeds, a region consisting of two peaks between 270–480 °C gave quantitative results for the oil and protein content, while for beans, a region between 180-590 °C gave quantitative results for the oil, protein and carbohydrate contents.

It was also suggested that the TGA technique could be used as a subtraction method to determine desired values such as the case discussed for Soxhlet extraction (for determination of oil content) which is a long cumbersome procedure taking about 16 hours. By obtaining results for protein and carbohydrate content by the conventional methods and results from TGA, the oil content of a seed or bean can now be determined by subtracting the protein content (for seeds) or protein and carbohydrate content (for beans). This could significantly shorten analytical times in food laboratories analysing seeds and beans, and while the cost of a TGA instrument may initially be off-putting, the long term financial gain obtained by

significantly shortened analysis times could outweigh the initial financial outlay on the TGA equipment.

Solid State NMR studies were carried out on all above mentioned seeds and beans using two techniques, namely  $^{13}\text{C}$  SPE-MAS NMR to explore the liquid-like components, and  $^{13}\text{C}$  CP-MAS NMR to explore the solid-like components.  $^{13}\text{C}$  SPE-MAS NMR spectroscopy indicated that overall seeds contained a higher content of liquid-like components (oil) than for beans. In turn the  $^{13}\text{C}$  CP-MAS NMR spectra indicated that beans had a higher content of solid-like components (protein and carbohydrates) than for seeds.

For the seeds: All four the seeds had clear, well-defined  $^{13}\text{C}$  SPE-MAS spectra with high signal to noise indicating that a high content of liquid-like components were present, while the  $^{13}\text{C}$  CP-MAS spectra of all four the seeds had noisy spectra with spectral overlap and broad signals indicating a low solid-like component content but a high liquid-like component content.

For the beans: The  $^{13}\text{C}$  SPE-MAS spectra indicated that soybean had a higher content of liquid-like components (oil) present compared to the other three beans, with noisy spectra for kidney, mung and black bean indicating a high content of solid-like components present. In contrast the  $^{13}\text{C}$  CP-MAS NMR spectra of soybean was noisy due to high liquid-like content and well-defined spectra for mung, kidney and black beans were obtained.

These conclusions correlated very well with the content of liquid-like components (oil) and solid-like components (proteins and carbohydrates) that was determined by conventional methods and TGA.

Preliminary studies using  $T_{1\rho}\text{H}$  experiments on the components present in the seeds and beans also led to a few observations. Firstly the CP build-up rate was much larger for the beans than those of the seeds. Secondly the carbons relaxed much faster in the rotating frame in the beans than the seeds. Thirdly a model using a two-phase fit in order to determine  $T_{1\rho}\text{H}$  values seemed to be more accurate.

In overall conclusion, new work that was done in this study included the assignment and quantification of the high resolution  $^{31}\text{P}$  NMR spectra of three locally produced vegetable oils while, namely apricot kernel, avocado pear and macadamia nut oils, using two approaches (one of which was a newly developed direct correlation

approach). New work on the major components of seeds and beans indicated that high resolution solid state  $^{13}\text{C}$  NMR spectroscopy and TGA analysis can be used for the qualitative and quantitative determination of oil, protein and carbohydrate content respectively, in seeds and beans.

**ADDENDUM A:  
PUBLISHED  
ARTICLES**

# A novel approach to the rapid assignment of $^{13}\text{C}$ NMR spectra of major components of vegetable oils such as avocado, mango kernel and macadamia nut oils

Liesel Retief,<sup>a</sup> Jean M. McKenzie<sup>b</sup> and Klaus R. Koch<sup>a\*</sup>



Assignment of  $^{13}\text{C}$  nuclear magnetic resonance (NMR) spectra of major fatty acid components of South African produced vegetable oils was attempted using a method in which the vegetable oil was spiked with a standard triacylglycerol. This proved to be inadequate and therefore a new rapid and potentially generic graphical linear correlation method is proposed for assignment of the  $^{13}\text{C}$  NMR spectra of major fatty acid components of apricot kernel, avocado pear, grapeseed, macadamia nut, mango kernel and marula vegetable oils. In this graphical correlation method, chemical shifts of fatty acids present in a known standard triacylglycerol is plotted against the corresponding chemical shifts of fatty acids present in the vegetable oils. This new approach (under carefully defined conditions and concentrations) was found especially useful for spectrally crowded regions where significant peak overlap occurs and was validated with the well-known  $^{13}\text{C}$  NMR spectrum of olive oil which has been extensively reported in the literature. In this way, a full assignment of the  $^{13}\text{C}$  {1H} NMR spectra of the vegetable oils, as well as tripalmitolein was readily achieved and the resonances belonging to the palmitoleic acid component of the triacylglycerols in the case of macadamia nut and avocado pear oil resonances were also assigned for the first time in the  $^{13}\text{C}$  NMR spectra of these oils. Copyright © 2009 John Wiley & Sons, Ltd.

Supporting information may be found in the online version of this article.

**Keywords:** NMR;  $^{13}\text{C}$ ; olive oil; apricot kernel oil; avocado pear oil; grapeseed oil; macadamia nut oil; mango kernel oil; marula oil; tripalmitolein

## Introduction

Nuclear magnetic resonance (NMR) spectroscopy has found application in the identification and quantitative determination of the major fatty acid components of vegetable oils, in particular olive oil.<sup>[1–5]</sup> One of the significant advantages of NMR spectroscopy is that, unlike other analytical techniques, it does not in general require extraction, separation or chemical modification of the vegetable oil to be analyzed. On the other hand the relatively low sensitivity of NMR spectroscopy limits its use to major and minor components of vegetable oils, rendering it generally unsuitable for analyzing trace components. Of the numerous vegetable oils available, olive oil has been the most widely studied by NMR spectroscopy, presumably in view of its high-value and wide consumption. This has resulted in the need for methods of authentication and the detection of adulteration of olive oil with other vegetable oils such as hazelnut and sunflower oils.<sup>[6–8]</sup>  $^1\text{H}$  NMR spectroscopy has been used in the analysis of olive oil for measuring diglyceride content, determinations of squalene, cyclo-arthenol and Mg-depleted chlorophyll, and analysis of sterols as well as other components responsible for the taste and aroma of olive oil such as acetic acid, *trans*-2-hexenal and formaldehyde.<sup>[1,2]</sup> Although GC (gas chromatography) is the most commonly used technique for the qualitative and quantitative determination of fatty acid residues in vegetable oils,  $^{13}\text{C}$  NMR spectroscopy can also be used for analyzing these major components.<sup>[1–5]</sup> The distinct advantage of using  $^{13}\text{C}$  NMR

spectroscopy in this context is that no chemical derivatization of the sample is required whereas for GC the fatty acid methyl esters must be prepared from the triacylglycerols before analysis is undertaken.  $^{13}\text{C}$  NMR spectroscopy has been successfully used to determine quantitatively the major fatty acid residues in olive oils<sup>[5,7]</sup> and moreover can give direct information about the positional distribution of the fatty acids on the glycerol backbone. Much success has been found in detecting adulteration of olive oil by other oils using  $^{13}\text{C}$  NMR spectroscopy. In conjunction with chemometric methods  $^{13}\text{C}$  NMR spectroscopy can also be used to distinguish between geographic and cultivar-based differences of olive oils.<sup>[1–3,9]</sup>

We have recently become interested in the analysis of other high-value vegetable oils, including apricot kernel, avocado pear, grapeseed, macadamia nut, mango kernel and marula oils. To our knowledge, the  $^{13}\text{C}$  NMR spectra of these oils have not been examined or fully assigned to date. The conventionally used method for the full assignment of  $^{13}\text{C}$  NMR spectra of vegetable

\* Correspondence to: Klaus R. Koch, Department of Chemistry and Polymer Science, Stellenbosch University, Private Bag XI, Matieland 7602, South Africa.  
E-mail: krk@sun.ac.za

<sup>a</sup> Department of Chemistry and Polymer Science, Stellenbosch University, P Bag XI, Matieland, 7602, South Africa

<sup>b</sup> DISA Vascular (Pty) Ltd, PO Box 13397, Mowbray, 7705, South Africa

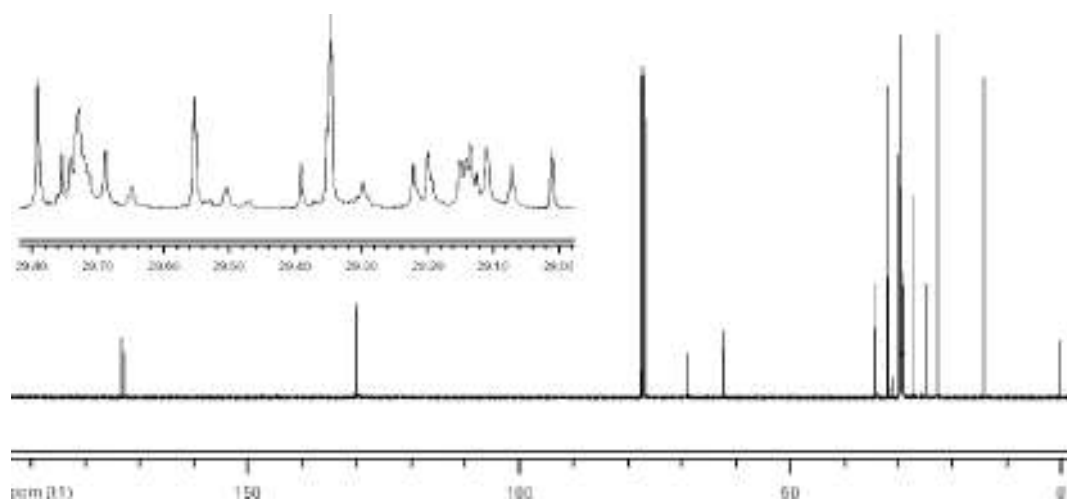


Figure 1.  $^{13}\text{C}$  NMR spectrum of macadamia nut oil in  $\text{CDCl}_3$  with an expansion of the crowded 29 ppm region.

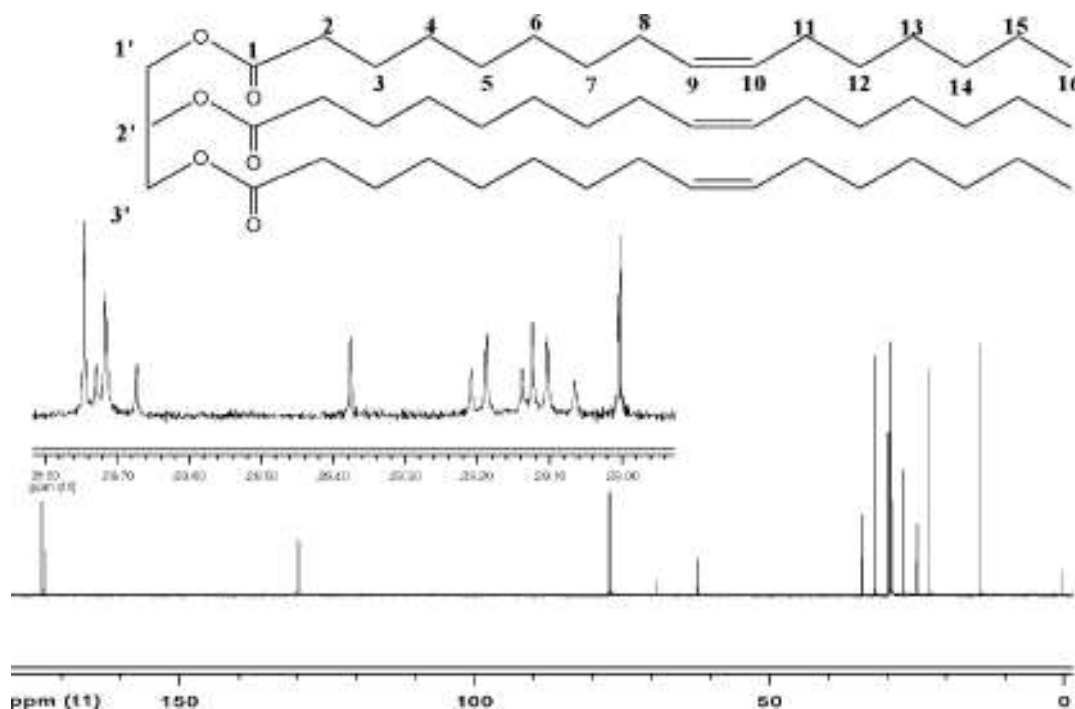


Figure 2.  $^{13}\text{C}$  NMR spectrum of tripalmitolein in  $\text{CDCl}_3$  with an expansion of the crowded 29 ppm region and numbered structure.

oils is by means of standard addition (spiking) of the vegetable oil with a standard triacylglycerol.<sup>[10]</sup> Comparison of the resulting  $^{13}\text{C}$  NMR spectra of the unspiked and spiked vegetable oil leads to the assignment of the  $^{13}\text{C}$  resonances in the NMR spectrum of the different fatty acid components present in the vegetable oil. Besides this method having some practical disadvantages, we found that it was not possible to achieve a full, unambiguous assignment of the  $^{13}\text{C}$  NMR spectra of the desired oils using this technique. Desirous of developing a rapid method for the accurate assignment of the  $^{13}\text{C}$  resonances of the various major components in a vegetable oil, we developed and tested a graphical linear correlation method for the assignment of the  $^{13}\text{C}$  resonances of a vegetable oil. The technique was tested and validated with extra-virgin olive oil, for which the  $^{13}\text{C}$  NMR spectrum has been well characterized in the literature. Using this approach one could

easily achieve the full assignment of the  $^{13}\text{C}$  NMR spectra of six locally produced South African vegetable oils in  $\text{CDCl}_3$  solution.

## Experimental

### Materials and sample preparation

Standard triacylglycerols, tripalmitin, tripalmitolein, tristearin, triolein and trilinolein were purchased from Sigma-Aldrich and used without further purification ( $\geq 99\%$  purity). Samples of olive oil were provided by Brenn-o-Kem (Wolseley, South Africa). Apricot kernel, avocado pear, grapeseed, macadamia nut, mango kernel and marula oils were supplied by Specialized Oils (Paardeneiland, Cape Town, South Africa). All oils were filtered before use. For storage, the oils were flushed with nitrogen gas.

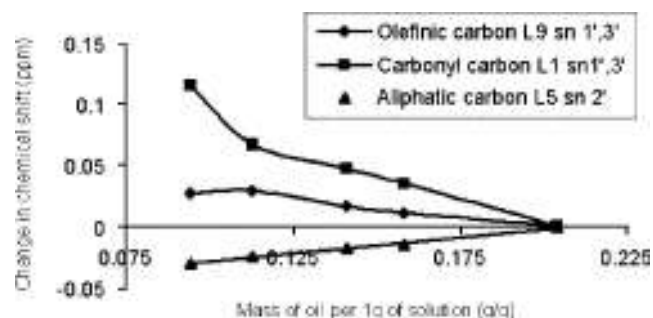


**Figure 3.** Change in chemical shift for different types of carbon atoms plotted against the mass of oil per 1 g of solution.

### $^{13}\text{C}$ NMR data collection and processing

Approximately 100  $\mu\text{l}$  of each oil in 700  $\mu\text{l}$  of  $\text{CDCl}_3$  with TMS as reference was used for NMR analysis at 25  $^\circ\text{C}$ .  $^{13}\text{C}$  NMR spectra were run on a 400 MHz Varian Unity-Inova NMR spectrometer operating at 100 MHz for  $^{13}\text{C}$ . Acquisition parameters similar to those recommended by Mannina *et al.*[10] were used for collecting the  $^{13}\text{C}$  NMR spectra: number of points 256 K; spectral width 195 ppm; relaxation delay: 7 s; acquisition time 4.5 s. When processing, a line-broadening of  $-0.092$  and Gaussian enhancement of 0.7 was used to optimize the resolution of the spectra. The precision of the procedure is estimated by the average half height of the resonances in the crowded region which is at most 0.7 Hz (0.007 ppm). In fact if we do the procedure with the graphical linear correlation method we get even better results, and a precision of  $\pm 0.004$  ppm.

### GC analysis of vegetable oils

Methyl esterification of vegetable oils for GC analysis[11] was carried out as follows: Sodium (0.5 g) was dissolved in 100 ml methanol. The sodium methoxide solution (0.3 g) together with 2 g of the specific vegetable oil was placed in a vial and heat sealed. The heat sealed vial was left for 2 h at 85–90  $^\circ\text{C}$  in an oil bath, with occasionally shaking. GC analysis of the vegetable oil samples was carried out to determine their fatty acid content in order to compare with the  $^{13}\text{C}$  NMR spectroscopy data obtained. 20  $\mu\text{l}$  of each sample was diluted with 1 ml of dichloromethane and 1  $\mu\text{l}$  portions were injected into a HP 5890 Series 2 GC equipped with a fused silica capillary (30 m  $\times$  0.25 mm i.d., 0.2 mm film thickness) coated with a 100% cyanopropylpolysiloxane non-bonded phase. A temperature programmed elution from 40 to 240  $^\circ\text{C}$  at a rate of 4  $^\circ\text{C}/\text{min}$  was used.

## Results and Discussion

The striking superficial resemblance of the  $^{13}\text{C}\{^1\text{H}\}$  NMR spectrum of a typical macadamia nut oil in  $\text{CDCl}_3$ , shown in Fig. 1 to that of  $^{13}\text{C}\{^1\text{H}\}$  NMR spectrum of olive oil, suggests that similar major triacylglycerols are present in all these oils. In order to aid the rapid but unambiguous identification of the individual major triacylglycerols present in all six vegetable oils from their  $^{13}\text{C}\{^1\text{H}\}$  NMR spectra we examined a series of oils and developed a simple method with which to assign all  $^{13}\text{C}\{^1\text{H}\}$  resonances of the major triacylglycerols in such oils. GC analysis was first used to determine the fatty acid components of the triacylglycerols. Although GC analysis is the accepted analytical technique for

**Table 1.** Assignment of  $^{13}\text{C}$  NMR spectrum of tripalmitolein

Carbon	Position on glycerol backbone	Chemical shift (ppm)
C1	sn 1 $^\circ$ , 3 $^\circ$	173.205
	sn 2 $^\circ$	172.795
C2	sn 1 $^\circ$ , 3 $^\circ$	34.021
	sn 2 $^\circ$	34.185
C3	sn 1 $^\circ$ , 3 $^\circ$	24.879
	sn 2 $^\circ$	24.879
C4	sn 1 $^\circ$ , 3 $^\circ$	29.082
	sn 2 $^\circ$	29.044
C5	sn 1 $^\circ$ , 3 $^\circ$	29.167
	sn 2 $^\circ$	29.188
C6	sn 1 $^\circ$ , 3 $^\circ$	29.100
	sn 2 $^\circ$	29.115
C7	sn 1 $^\circ$ , 3 $^\circ$	29.695
	sn 2 $^\circ$	29.709
C8	sn 1 $^\circ$ , 3 $^\circ$	27.162
	sn 2 $^\circ$	27.162
C9	sn 1 $^\circ$ , 3 $^\circ$	129.691
	sn 2 $^\circ$	129.665
C10	sn 1 $^\circ$ , 3 $^\circ$	129.984
	sn 2 $^\circ$	129.995
C11	sn 1 $^\circ$ , 3 $^\circ$	27.220
	sn 2 $^\circ$	27.224
C12	sn 1 $^\circ$ , 3 $^\circ$	29.729
	sn 2 $^\circ$	29.729
C13	sn 1 $^\circ$ , 3 $^\circ$	29.984
	sn 2 $^\circ$	29.986
C14	sn 1 $^\circ$ , 3 $^\circ$ ; sn 2 $^\circ$	31.783
C15	sn 1 $^\circ$ , 3 $^\circ$ ; sn 2 $^\circ$	22.655
C16	sn 1 $^\circ$ , 3 $^\circ$ ; sn 2 $^\circ$	14.094
CHO		68.877
CH <sub>2</sub> O		62.086

fatty acid compound analysis and quantification in vegetable oils, it has the main disadvantage of being a destructive and time-consuming technique since chemical modification (esterification) of the triacylglycerols is required before analysis, unlike  $^{13}\text{C}\{^1\text{H}\}$  NMR spectroscopy. GC analysis of the oils indicated that apricot kernel, avocado pear, grapeseed, macadamia nut, mango kernel and marula oils contained the same major fatty acid components, namely oleic acid, palmitic acid, linoleic acid and stearic acid found in olive oil, although palmitoleic acid not detected in any olive oil samples was observed to be present in macadamia nut and avocado pear oil in significant amounts. With the exception of tripalmitolein, the  $^{13}\text{C}$  NMR spectra of the other triacylglycerols present in the six vegetable oils have previously been assigned by Mannina *et al.*[10]. The full assignment of the  $^{13}\text{C}$  NMR spectrum of a sample of pure tripalmitolein (Fig. 2) was carried out by methodologies given by Mannina *et al.*[10] for other triacylglycerols, and comparison of chemical shift trends observed for mainly triolein (Table 1).

With the aim of developing a rapid method with which to determine the major triacylglycerols present in apricot kernel, avocado pear, grapeseed, macadamia nut, mango kernel and marula oils using  $^{13}\text{C}\{^1\text{H}\}$  NMR spectroscopy we initially investigated the use of the procedure developed for mainly olive oils[10] which involves the addition of standard triacylglycerols

**Table 2.** Assignment of  $^{13}\text{C}$  NMR resonances of the major fatty acid residues in olive oil

Section	Assignment	Position on glycerol backbone	Chemical shift (ppm) measured	Chemical shift (ppm) Literature assignments <sup>[3,4,13]</sup>		
				Vlahov <i>et al.</i> <sup>[3]</sup>	Sacchi <i>et al.</i> <sup>[4]</sup>	Shaw <i>et al.</i> <sup>[13]</sup>
A	P1	sn 1 <sup>o</sup> , 3 <sup>o</sup>	173.236		173.27	173.113
	V/E		173.223			173.101
	O1	sn 1 <sub>o</sub> , 3 <sub>o</sub>	173.204		173.2	173.084
	L1	sn 1 <sup>o</sup> , 3 <sup>o</sup>	173.194		173.17	173.075
	O1	sn 2 <sub>o</sub>	172.837		172.83	172.688
	L1	sn 2 <sup>o</sup>	172.787		172.77	172.679
B	L13	sn 2 <sub>o</sub>	130.198	130.15	130.22	130.105
	L13	sn 1 <sup>o</sup> , 3 <sup>o</sup>	130.191	130.15	130.22	130.097
	O10	sn 2 <sup>o</sup>	130.016	129.96	130.04	129.945
	O10	sn 1 <sub>o</sub> , 3 <sub>o</sub>	130.001	129.94	130.02	129.93
	L9	sn 1 <sup>o</sup> , 3 <sup>o</sup>	129.984	129.91	129.98	129.9
	L9	sn 2 <sub>o</sub>	129.958	129.89	130.01	129.874
	V/E		129.918			
	V/E		129.822			
	O9	sn 1 <sub>o</sub> , 3 <sub>o</sub>	129.702	129.65	129.69	129.64
	O9	sn 2 <sup>o</sup>	129.676	129.63	129.72	129.614
	L10	sn 2 <sup>o</sup>	128.095	128.07	128.12	128.053
	L10	sn 1 <sub>o</sub> , 3 <sub>o</sub>	128.077	128.05	128.11	128.035
	L12	sn 1 <sup>o</sup> , 3 <sup>o</sup>	127.911	127.89	127.94	127.874
	L12	sn 2 <sup>o</sup>	127.899	127.88	127.93	127.862
C	CHO		68.911	68.90		68.8852
	CH2O		62.108	62.06		62.0478
D	O2/L2	sn 2 <sub>o</sub>	34.206	34.16		34.1408
	P2	sn 1 <sub>o</sub> , 3 <sub>o</sub>	34.064	34.01		33.9972
	UK		34.054			
	O2/L2	sn 1 <sub>o</sub> , 3 <sub>o</sub>	34.041	33.990		33.9758
E	P14		31.959	31.940	34.26	31.9283
	O16		31.938	31.920	34.2	31.9074
	UK		31.818	31.80 (UK)		
	L16		31.555	31.53	34.15	31.5167
F	O12		29.796	29.770		29.7586
	O7	sn 2 <sub>o</sub>	29.745			
	P10		29.735	29.720 (UK)		29.6637
	O7/P12	sn 1 <sub>o</sub> , 3 <sub>o</sub>	29.731			
	P11		29.718	29.68 (UK)		
	P8		29.693	29.64 (UK)		
	P7	sn 1 <sub>o</sub> , 3 <sub>o</sub>	29.653			29.6637
	L7	sn 2 <sup>o</sup>	29.650			29.6203
	L7	sn 1 <sup>o</sup> , 3 <sup>o</sup>	29.635			
	O14	sn 2 <sub>o</sub>	29.560	29.54		29.5289
	O14	sn 1 <sup>o</sup> , 3 <sup>o</sup>	29.558	29.54		29.5289
	P5		29.508	29.49		29.4748
	P13		29.397	29.38 (S15)*		29.3688 (S15)*
	L15		29.377	29.36		29.3419
	O13		29.356	29.34		29.3156
	O15		29.353	29.34		29.3156
	P6		29.302	29.28		29.2686
	O5/L5	sn 2 <sub>o</sub>	29.225	29.20		29.1869
	O5/L5	sn 1 <sup>o</sup> , 3 <sup>o</sup>	29.203	29.18		29.1656
	O6/L6	sn 2 <sup>o</sup>	29.153	29.10		
	P4		29.145	29.10		
O6/L6	sn 1 <sup>o</sup> , 3 <sup>o</sup>	29.136	29.10			
O4	sn 1 <sup>o</sup> , 3 <sup>o</sup>	29.114	29.10		29.0717	
L4	sn 1 <sub>o</sub> , 3 <sub>o</sub>	29.108	29.10		29.0717	
O4/L4	sn 2 <sup>o</sup>	29.075	29.05		29.0324	

**Table 2.** (Continued)

Section	Assignment	Position on glycerol backbone	Chemical shift (ppm) measured	Chemical shift (ppm) Literature assignments <sup>[3,4,13]</sup>		
				Vlahov <i>et al.</i> <sup>[3]</sup>	Sacchi <i>et al.</i> <sup>[4]</sup>	Shaw <i>et al.</i> <sup>[13]</sup>
G	O11	sn 2 <sup>o</sup>	27.249	27.22	27.31	27.1477
	O11	sn 1 <sub>o</sub> , 3 <sub>o</sub>	27.245	27.22	27.31	27.1477
	L14		27.226	27.20	27.22	27.1657
	L8		27.214	27.18		27.1815
	O8		27.194	27.16	27.31	27.2009
H	L11		25.653	25.62	25.67	25.6084
	O3	sn 2 <sub>o</sub>	24.908	24.88		24.8605
	L3	sn 2 <sup>o</sup>	24.898	24.88		24.8605
	P3		24.890	24.86	24.84	24.8466
	O3	sn 1 <sup>o</sup> , 3 <sup>o</sup>	24.869	24.84	24.8	24.8239
	L3	sn 1 <sup>o</sup> , 3 <sup>o</sup>	24.861	24.84	24.7	24.8239
I	P15		22.720	22.70 (S17)*	22.82	22.6841 (S17)*
	O17		22.711	22.70	22.8	22.6743
	L17		22.602	22.58	22.61	22.5656
J	P16		14.133	14.09 (S18)*	14.13	14.0824 (S18)*
	O18		14.127	14.09	14.13	14.0769
	UK		14.119			
	L18		14.081	14.05	14.09	14.037

O, olein; P, palmitin; L, linolein; S, saturated; UK, unknown; V/E, vaccenin or eicosenin.

\* The chemical shifts of the omega 1, 2 and 3 carbons (P14, 15 and 16) have been correlated with the corresponding omega carbons in the literature.

(triolein, tristearin, etc.) to the sample of vegetable oil and using deconvolution of the  $^{13}\text{C}\{^1\text{H}\}$  NMR spectrum collected to detect enhancement of particular resonances.<sup>[7,8,10]</sup> Although this approach has been successfully applied to olive and other oils in the literature, its limitations include the time-consuming nature (requiring repeated  $^{13}\text{C}$  NMR spectra to be acquired for each standard triacylglycerol added) and the use of expensive but potentially unavailable pure triacylglycerol standards. In our hands moreover, a major limitation with this standard addition approach was that the complete assignment of the spectra of the six oils of interest was not always possible. Although a large number of  $^{13}\text{C}\{^1\text{H}\}$  resonances in the spectrum could be assigned by inspection and comparison with data in the literature, the method of standard additions could not be applied to all regions in the  $^{13}\text{C}\{^1\text{H}\}$  spectrum, notably in the spectrally crowded  $29 \pm 1$  ppm region in which several  $\text{CH}_2$  carbon resonances are found resulting in significant spectral overlap (Fig. 1). Spiking the oil with a standard in this crowded region leads to the expected intensity increases of specific resonances, but unfortunately can also result in significant loss of resolution due to spectral overlap in this region making clear assignments of individual resonances very difficult if not impossible. This is probably the reason why this region of the  $^{13}\text{C}\{^1\text{H}\}$  spectrum of olive oil has not been fully assigned in the literature to our knowledge. A more invidious problem with the standard additions method is small but detectable concentration dependence of  $^{13}\text{C}\{^1\text{H}\}$  chemical shifts of triacylglycerols and thus the possibility of this leading to peak overlap on addition of the standard; in the case of olive oils a limited concentration dependence of  $^{13}\text{C}\{^1\text{H}\}$  has been reported by Mannina *et al.*<sup>[12]</sup> It is obvious that such concentration dependence of  $^{13}\text{C}\{^1\text{H}\}$  chemical shifts may lead to ambiguity when using the standard addition method for the assignment of the  $^{13}\text{C}$  spectra of vegetable oils. In

this context we propose a new approach to aid in the rapid and reliable assignment of  $^{13}\text{C}$  NMR spectra in vegetable oils.

#### Assignment of $^{13}\text{C}$ NMR spectra using the graphical linear correlation method

The proposed method is based on the reasonable expectation that the  $^{13}\text{C}\{^1\text{H}\}$  chemical shifts of a fatty acid residue of a particular triacylglycerol in a given solvent at a specified concentration should all be affected, to a first approximation, in a similar manner by the factors responsible for the observed concentration dependence. Moreover it may be expected that saturated  $\text{sp}^3$  carbon atoms might be differently affected to unsaturated  $\text{sp}^2$  carbon atoms for a given fatty acid residue (*vide infra*). On this basis it would be reasonable to expect that  $^{13}\text{C}\{^1\text{H}\}$  shifts of all carbon resonances of a fatty acid of a pure, standard triacylglycerol (e.g. triolein, tripalmitin, etc.) would be linearly correlated to the corresponding fatty acid residues of the triacylglycerols in a vegetable oil mixture in a given solvent at a specified concentration range. To test this expectation the dependence of the  $^{13}\text{C}\{^1\text{H}\}$  chemical shifts of concentration changes has been determined for olive oil in  $\text{CDCl}_3$  and we found that for  $\text{sp}^3$  carbon atoms the method is satisfactorily independent on concentration of the vegetable oil within the concentration range of approximately 0.10–0.20 g oil/g of  $\text{CDCl}_3$  solution. Similar trends were found for the other vegetable oils. For each concentration of vegetable oil, the  $^{13}\text{C}\{^1\text{H}\}$  shifts of selected carbon atoms were found to result in linear trends with identical gradients but slightly differing intercepts at 'zero' concentration, which indicates that at a practical concentration range of approximately 0.10–0.20 g oil/g of  $\text{CDCl}_3$  solution, all aliphatic  $^{13}\text{C}\{^1\text{H}\}$  shifts are affected to the same degree, and importantly in a linear fashion as a result of small concentration changes.

This can be clearly seen in Fig. 3 where the chemical shifts of an aliphatic  $sp^3$  carbon L5 of trilinolein is shown to change linearly with a change in concentration from 0.095 to 0.20 g oil/g solution.

Interestingly the concentration dependence of resonances of  $sp^2$ -type carbon atoms (e.g. olefinic and carbonyl carbon atoms) shows a rather more complex non-linear trend (Fig. 3). This suggests that linear concentration dependences for such  $^{13}C\{^1H\}$  shifts and thus correlations cannot generally be expected for such

carbon atoms. As these resonances are in non-crowded spectral regions they are generally easily assigned by inspection in most vegetable oils making this effect not too serious a limitation. Nevertheless we have found that within a limited concentration range (approximately 0.10–0.20 g oil/1 g of  $CDCl_3$  solution) the proposed graphical linear correlation method can, as a first approximation, also be used for assignments of  $sp^2$ -type carbon resonances. Comparing the graphs of the  $sp^2$  and  $sp^3$  (Fig. 3)

**Table 3.** Assignment of  $^{13}C$  NMR resonances of the major fatty acid residues in avocado pear and macadamia nut oil

Carbon	Position	Avocado pear oil (ppm)	Carbon	Position	Macadamia nut oil (ppm)
P1	sn 1 <sup>o</sup> ,3 <sup>o</sup>	173.266	P1	sn 1 <sup>o</sup> , 3 <sup>o</sup>	173.256
Pa1	sn 1 <sup>o</sup> ,3 <sup>o</sup>	173.253	Pa1	sn 1 <sup>o</sup> , 3 <sup>o</sup>	173.243
O1	sn 10,30	173.235	O1/L1	sn 10, 30	173.226
L1	sn 1 <sup>o</sup> ,3 <sup>o</sup>	173.226	O1/Pa1/L1	sn 2 <sup>o</sup>	172.818
O1/Pa1	sn 2 <sup>o</sup>	172.825	L13		130.201
L1	sn 2 <sup>o</sup>	172.815	O10/Pa10	sn 2 <sup>o</sup>	130.017
L13	sn 1 <sup>o</sup> ,3 <sup>o</sup>	130.202	O10/Pa10/L9	sn 1 <sup>o</sup> , 3 <sup>o</sup>	130.003
L13	sn 2 <sup>o</sup>	130.195	L9	sn 2 <sup>o</sup>	129.923
O10/Pa10	sn 2 <sup>o</sup>	130.017	V/E		129.825
O10/Pa10	sn 1 <sup>o</sup> ,3 <sup>o</sup>	130.003	V/E		129.822
L9	sn 2 <sup>o</sup>	129.989	O9/Pa9	sn 10, 30	129.705
L9	sn 1 <sup>o</sup> ,3 <sup>o</sup>	129.962	O9/Pa9	sn 2 <sup>o</sup>	129.679
V/E		129.92	L10	sn 2 <sup>o</sup>	128.093
V/E		129.824	L10	sn 10, 30	128.074
Pa9		129.709	L12	sn 1 <sup>o</sup> , 3 <sup>o</sup>	127.909
O9	sn 1 <sup>o</sup> ,3 <sup>o</sup>	129.704	L12	sn 2 <sup>o</sup>	127.896
O9/Pa9	sn 2 <sup>o</sup>	129.678	CHO		68.907
L10	sn 2 <sup>o</sup>	128.092	CH2O		62.11
L10	sn 10, 30	128.075	O2/Pa2/L2	sn 2 <sup>o</sup>	34.208
L12	sn 1 <sup>o</sup> , 3 <sup>o</sup>	127.91	P2	sn 1 <sup>o</sup> , 3 <sup>o</sup>	34.065
L12	sn 2 <sup>o</sup>	127.898	Pa2	sn 1 <sup>o</sup> , 3 <sup>o</sup>	34.056
CHO		68.913	O2/L2	sn 10, 30	34.043
CH2O		62.114	P14		31.955
O,L,Pa2	sn 2 <sup>o</sup>	34.208	O16		31.933
P2	sn 10,30	34.065	Pa14		31.811
Pa2	sn 1 <sup>o</sup> ,3 <sup>o</sup>	34.056	L16		31.55
O2/L2	sn 1 <sup>o</sup> ,3 <sup>o</sup>	34.042	UK		30.897
P14		31.955	O12		29.792
O16		31.934	Pa12	sn 2 <sup>o</sup>	29.763
Pa14		31.812	Pa12	sn 10, 30	29.755
L16		31.551	O8/Pa7	sn 2 <sup>o</sup>	29.743
O12		29.793	P10	sn1,3	29.731
Pa12	sn 2 <sup>o</sup>	29.763	O8/P12	sn 10, 30	29.729
Pa12	sn 1 <sup>o</sup> ,3 <sup>o</sup>	29.756	Pa7/P11	sn 1 <sup>o</sup> , 3 <sup>o</sup>	29.721
O7	sn 2 <sup>o</sup>	29.743	P9		29.714
P10/Pa7	sn 2 <sup>o</sup>	29.732	P8		29.689
O7/P12/Pa7	sn 1 <sup>o</sup> ,3 <sup>o</sup>	29.728	L7/P7		29.65
P11		29.715	O14		29.554
P8		29.689	P5	sn 1 <sup>o</sup> , 3 <sup>o</sup>	29.505
P7/L7	sn 1 <sup>o</sup> ,3 <sup>o</sup> /sn2(L)	29.65	P13		29.392
L7	sn 10,30	29.633	L15		29.372
O14		29.555	O13		29.353
P5		29.506	O15		29.347
P13		29.393	P6	sn 10, 30	29.298
L15		29.372	O5/L5	sn 2 <sup>o</sup>	29.222
O13/P6		29.353	Pa5	sn 2 <sup>o</sup>	29.216
O15		29.349	O5/L5	sn 10, 30	29.2

**Table 3.** (Continued)

Carbon	Position	Avocado pear oil (ppm)	Carbon	Position	Macadamia nut oil (ppm)
P6	sn 1 <sup>o</sup> ,3 <sup>o</sup>	29.299	Pa5	sn 1 <sup>o</sup> , 3 <sup>o</sup>	29.194
O5/L5	sn 2 <sup>o</sup>	29.222	O6/L6	sn 2 <sup>o</sup>	29.151
Pa5	sn 2 <sup>o</sup>	29.217	Pa6/L6/P4	sn 2 <sup>o</sup> /sn1,3	29.142
O5/L5	sn 1 <sup>o</sup> ,3 <sup>o</sup>	29.201	O6	sn 1 <sup>o</sup> , 3 <sup>o</sup>	29.135
Pa5	sn 1 <sup>o</sup> ,3 <sup>o</sup>	29.194	Pa6	sn 1 <sup>o</sup> , 3 <sup>o</sup>	29.126
O6/L6	sn 2 <sup>o</sup>	29.152	O4/Pa4/L4/P4	sn 1 <sup>o</sup> , 3 <sup>o</sup>	29.111
L6/P4/Pa6	sn 1 <sup>o</sup> ,3 <sup>o</sup>	29.145	O4/Pa4/L4	sn 2 <sup>o</sup>	29.072
O6	sn 1 <sup>o</sup> ,3 <sup>o</sup>	29.135	Pa13		29.011
Pa6	sn 2 <sup>o</sup>	29.126	O11/Pa8	sn 2 <sup>o</sup>	27.246
O4/L4/Pa4	sn 1,3	29.111	O11	sn 1 <sup>o</sup> , 3 <sup>o</sup>	27.243
O4/L4/Pa4	sn 2 <sup>o</sup>	29.073	L14		27.223
Pa13		29.011	L8		27.212
O11/Pa8	sn 2 <sup>o</sup>	27.247	O8		27.193
O11	sn 1 <sup>o</sup> ,3 <sup>o</sup>	27.243	Pa11		27.187
L14		27.224	L11		25.651
L8		27.212	O3/Pa3/L3	sn 2 <sup>o</sup>	24.905
O8		27.193	P3		24.888
Pa11		27.188	O3/Pa3/L3/P3	sn 1 <sup>o</sup> , 3 <sup>o</sup>	24.865
L11		25.651	P17		22.717
O3/Pa3	sn 2 <sup>o</sup>	24.906	O17		22.707
L3	sn 2 <sup>o</sup>	24.896	Pa15		22.681
P3	sn 1 <sup>o</sup> ,3 <sup>o</sup>	24.888	L17		22.598
O3/L3/Pa3	sn 1 <sup>o</sup> ,3 <sup>o</sup>	24.866	P16		14.131
P15		22.717	O18		14.125
O17		22.707	Pa16		14.117
Pa15		22.682	L18		14.085
L17		22.599			
P16		14.131			
O18		14.125			
Pa16		14.116			
L18		14.084			

O, olein; P, palmitin; Pa, palmitolein; L, linolein; UK, unknown; V/E, vaccenin or eicosenoin; FFA, free fatty acid.

carbon atoms, it can be seen that as the concentration increases the chemical shifts of the  $\text{sp}^2$  carbon atoms move upfield, while the  $\text{sp}^3$  carbon atoms chemical shifts move downfield. It is therefore evident that the  $\text{sp}^2$  and  $\text{sp}^3$  carbon atoms are affected very differently with a change in concentration, and thus they should clearly not be plotted on the same graph.

On the basis of these observations therefore, we have tested a new method for the possible assignment of  $^{13}\text{C}\{^1\text{H}\}$  resonances of triacylglycerols in vegetable oils by establishing a correlation of the observed  $\delta^{13}\text{C}\{^1\text{H}\}$  of the various peaks of the major components with those of the pure component obtained under similar conditions at similar concentrations. The graphical correlation method therefore consists of correlating the chemical shift values of defined fatty acid carbon atoms in the standard triacylglycerols (triolein, tripalmitin, etc.) with the corresponding peaks present in the  $^{13}\text{C}\{^1\text{H}\}$  NMR spectrum of the vegetable oil. Essentially we employ the following modus operandi: Firstly, the  $^{13}\text{C}\{^1\text{H}\}$  NMR spectrum of the vegetable oil is divided into sections each representing different carbon atoms of the same type present in the triacylglycerols. Section A covers the  $^{13}\text{C}$  resonances due to the carbonyl  $\text{sp}^2$ -carbon resonances, Section B those of the olefinic  $\text{sp}^2$ -carbons, while Sections D–J shows the crowded spectral region due to aliphatic  $\text{sp}^3$ -carbon  $^{13}\text{C}$  signals (Table 2).

Certain of these regions are easily assigned by inspection using the relative percentages of each fatty acid residue present in the oil as determined by GC analysis and can be approximately related (If necessary quantitative  $^{13}\text{C}\{^1\text{H}\}$  NMR spectra can be recorded to confirm this (see ref 5).) to resonance intensities in the NMR spectrum, which further assists in assigning such additional resonances by inspection. In addition it is known from the work of Vlahov *et al.*<sup>[3]</sup> that carbons from a saturated fatty acid chain is generally observed somewhat further upfield than the equivalent carbon in an unsaturated fatty acid chain. These concepts can be applied in order to assign Sections A, B, E, I and J. Subsequently by plotting the  $^{13}\text{C}\{^1\text{H}\}$  chemical shifts of each of all unambiguously assigned  $^{13}\text{C}\{^1\text{H}\}$  resonances of a particular fatty acid residue in the vegetable oil on the y-axis against the  $^{13}\text{C}\{^1\text{H}\}$  shift of that resonance in the standard triacylglycerol along the x-axis, one obtains a remarkably linear correlation as shown for instance for trilinolein in macadamia nut oil in Fig. 4.

This highly linear correlation thus facilitates the assignment of the remaining  $^{13}\text{C}\{^1\text{H}\}$  resonances, which were not directly assignable by inspection particularly in a spectrally crowded region encompassing the aliphatic carbon resonances. It is thus possible by using a previously assigned  $^{13}\text{C}\{^1\text{H}\}$  shift of the pure triacylglycerol (obtained from the literature or preferably from a

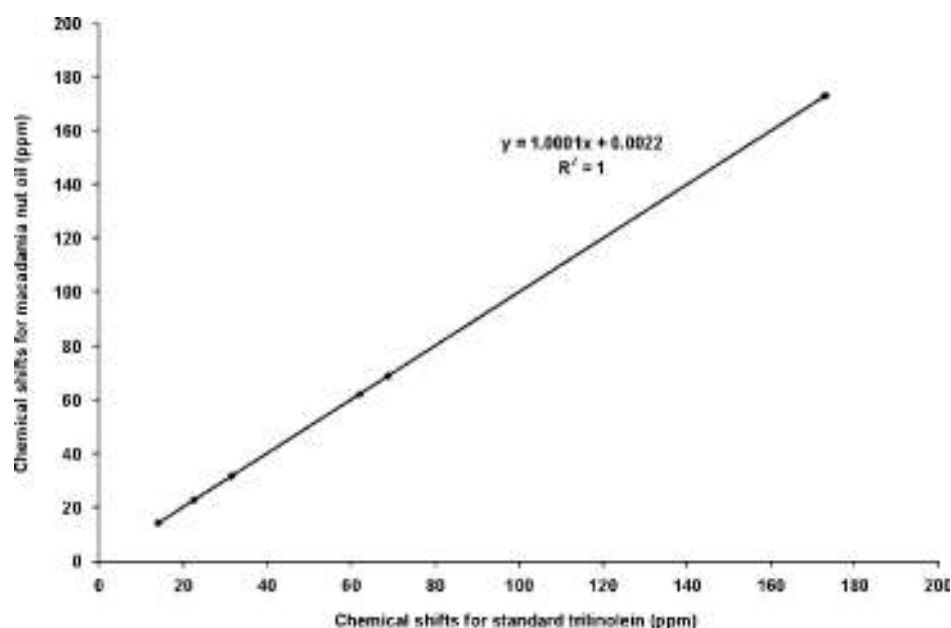


**Figure 4.** Linear correlation obtained from plotting the chemical shifts of the  $sp^3$  carbon resonances belonging to standard trilinolein against those in macadamia nut oil.

$^{13}C\{^1H\}$  spectrum of a sample of pure triacylglycerol recorded in the same sample and approximate concentration plotted as ordinate) to predict the corresponding chemical shift value of the corresponding  $^{13}C\{^1H\}$  shift of that component in the oil as abscissa (Fig. 4).

In this way all the relevant  $^{13}C$  resonances can be assigned to the appropriate carbon of the fatty acid residues, particularly in the crowded spectral region of the  $^{13}C\{^1H\}$  NMR spectrum. This method is most suitable for application in regions D, F, G and H where significant spectral overlap occurs and for the same  $sp^3$  carbon type. Moreover the degree of linearity obtained by regression analysis (as measured by the regression coefficient  $r^2$ ) is sensitive to the correct assignment since miss-assignments result in the rapid deviation of the  $r^2$  from close to 1, typically correct assignments lead to  $r^2$  values of 0.999. This linear method is only used for the  $sp^3$  hybridized carbons as the carbonyl and olefinic  $sp^2$  carbon can easily be assigned by inspection. Indeed the  $sp^2$  and  $sp^3$  carbons should not be used on the same linear graph as a result of their non-linear concentration dependence shown previously (Fig. 3), although for very similar concentrations of standard triacylglycerol and vegetable oil in the same solvent remarkable linear correlations of the  $^{13}C\{^1H\}$  shifts for all carbon types also result. The limitation due to the variable concentration dependencies of the  $^{13}C\{^1H\}$  shifts of  $sp^2$  and carbonyl type carbon atoms is not a serious limitation in this context, since resonances resulting from such carbon atoms are generally easily assigned by inspection of other methods.

#### Validation and assignment of $^{13}C\{^1H\}$ of vegetable oils

Assessment and validation of the linear correlation method described here was first carried out by application to the well-known  $^{13}C\{^1H\}$  spectrum of olive oil, previously assigned and reported extensively in the literature<sup>[3,4,13]</sup> as shown in Table 2. A comparison of the assignment obtained using the graphical linear correlation method with those from the literature confirms that these  $^{13}C\{^1H\}$  assignments agree well with those found by

other researchers for all carbon atoms of each fatty acid residue of the major triacylglycerols in olive oil. The various  $^{13}C\{^1H\}$  chemical shift values for spectral regions A, B, C, E, I and J correspond well with published data<sup>[3,4,13]</sup> with some exceptions in other regions: C-2 of all fatty acid residues present in section D corresponds reasonably well with the literature,<sup>[4]</sup> however the resonances of the C-2 atoms of triolein and trilinolein in the  $\alpha$  positions of the glycerol backbone were clearly separated in our  $^{13}C\{^1H\}$  spectrum and could therefore be separately assigned; Shaw *et al.* found only one resonance representing both these carbon atoms, presumably due to fortuitous overlap. Although most assignments in spectral section G correlate with published data,<sup>[3]</sup> we also observed two resolved resonances for C-8 of the olein residue, indicating separate peaks for C-8 in the  $\alpha$  and  $\beta$  positions, whereas Shaw *et al.* report only a single resonance for this carbon atom. The same pertains for C-3 of the olein and linolein residues in spectral region H, for which separate resonances could be observed and assigned. Upon first glance, region F appears more difficult to assign unambiguously which probably accounts for why several of these resonances have not previously been assigned in the literature to our knowledge. Nevertheless using our proposed correlation method, it becomes relatively straight forward to assign some of these resonances, some of the unassigned resonances in this section could also be due to the vaccenin or eicosenoin residues or possibly some other saturated residues not previously reported or detected by  $^{13}C\{^1H\}$  NMR (due to their low concentrations) which are likely to mostly overlap with the palmitin  $^{13}C\{^1H\}$  resonances. Since palmitin is the major saturated component present in olive oil, the assignment of the saturated resonances was carried out using the tripalmitin chemical shifts as a reference. As expected for olive oil, saturated fatty acid residues, for instance for palmitin, are known not to be present in the  $\beta$  position of a triacylglycerol.<sup>[11]</sup> This is thought to be due to the observation that in natural olive oils saturated fatty acid residues such as palmitin are found at the  $\beta$  position of the triacylglycerols in amounts of less than 2%. Indeed, the presence of substantial amounts of palmitin in the  $\beta$  position of the glycerol

**Table 4.**  $^{13}\text{C}$  NMR assignments for grapeseed and apricot kernel oil

Carbon	Position	Grapeseed oil (ppm)	Carbon	Position	Apricot kernel oil (ppm)
FFA		173.813	P1		173.244
P1		173.252	UK		173.231
O1	sn 1 <sup>o</sup> ,3 <sup>o</sup>	173.221	O1	sn 1 <sup>o</sup> , 3 <sup>o</sup>	173.212
L1	sn 10,30	173.21	L1	sn 10, 30	173.202
UK		172.812	L1	sn 2 <sup>o</sup>	172.805
L1/O1	sn 2 <sup>o</sup>	172.801	O1	sn 2 <sup>o</sup>	172.794
UK		145.14	L13	sn 10, 30	130.203
L13	sn 2 <sup>o</sup>	130.204	L13	sn 2 <sup>o</sup>	130.195
L13	sn 10,30	130.196	O10	sn 20	130.016
O10	sn 20	130.018	O10	sn 10, 30	130.002
O10	sn 1 <sup>o</sup> ,3 <sup>o</sup>	130.002	L9	sn 2 <sup>o</sup>	129.987
L9	sn 10,30	129.988	L9	sn 10, 30	129.962
L9	sn 2 <sup>o</sup>	129.962	O9	sn 1 <sup>o</sup> , 3 <sup>o</sup>	129.703
O9	sn 1 <sup>o</sup> ,3 <sup>o</sup>	129.703	O9	sn 2 <sup>o</sup>	129.677
O9	sn 20	129.676	L10	sn 10, 30	128.092
L10	sn 2 <sup>o</sup>	128.091	L10	sn 2 <sup>o</sup>	128.074
L10	sn 1 <sup>o</sup> ,3 <sup>o</sup>	128.072	L12	sn 2 <sup>o</sup>	127.908
L12	sn 10,30	127.906	L12	sn 10, 30	127.897
L12	sn 2 <sup>o</sup>	127.894	CHO		68.908
CHO		68.908	CH2O		62.106
CH2O		62.109	O2	sn 20	34.204
L2/O2		34.196	L2	sn 2 <sup>o</sup>	34.199
P2		34.06	P2		34.062
L2/O2	sn 1 <sup>o</sup> ,3 <sup>o</sup>	34.032	O2	sn 1 <sup>o</sup> , 3 <sup>o</sup>	34.04
P14		31.948	L2	sn 1 <sup>o</sup> , 3 <sup>o</sup>	34.034
O16		31.927	P14		31.953
L16		31.545	O16		31.932
UK		30.899	UK		31.811
O12		29.787	L16		31.549
O7	sn 2 <sup>o</sup>	29.737	UK		30.895
O7/P10	sn 1 <sup>o</sup> ,3 <sup>o</sup>	29.725	O12		29.791
P12		29.718	UK		29.762
P11		29.708	O7	sn 2 <sup>o</sup>	29.742
P8		29.683	O7/P10,12	sn 10, 30	29.727
L7	sn 2 <sup>o</sup>	29.641	P11		29.713
L7	sn 1 <sup>o</sup> ,3 <sup>o</sup>	29.627	P8	sn 2 <sup>o</sup>	29.687
O14		29.548	L7	sn 10, 30	29.645
P5		29.499	L7	sn 2 <sup>o</sup>	29.631
P13		29.386	O14		29.553
L15		29.367	UK		29.528
O13		29.347	P5	sn 1 <sup>o</sup> , 3 <sup>o</sup>	29.503
O15		29.341	UK		29.47
P6		29.293	P13		29.391
L5/O5	sn 2 <sup>o</sup>	29.215	L15		29.371
L5/O5	sn 10,30	29.194	O15,13	sn 10,30	29.346
L6/O6	sn 20	29.147	P6		29.298
L6/O6/P4	sn 1 <sup>o</sup> ,3 <sup>o</sup>	29.133	O5/L5	sn 2 <sup>o</sup>	29.22
L4/O4	sn 10,30	29.1	O5/L5	sn 10, 30	29.199
L4/O4	sn 2 <sup>o</sup>	29.062	O6/L6/P4	sn 2 <sup>o</sup>	29.15
O11	sn 2 <sup>o</sup>	27.242	O6/L6	sn 1 <sup>o</sup> , 3 <sup>o</sup>	29.133
O11	sn 10,30	27.238	O4	sn 10, 30	29.11
UK		27.231	L4	sn 1 <sup>o</sup> , 3 <sup>o</sup>	29.105
L14		27.219	O4	sn 2 <sup>o</sup>	29.071
L8		27.208	L4	sn 20	29.067
O8		27.188	UK		29.01
L11		25.647	O11		27.242

**Table 4.** (Continued)

Carbon	Position	Grapeseed oil (ppm)	Carbon	Position	Apricot kernel oil (ppm)
O3	sn 2 <sup>o</sup>	24.901	L14		27.222
	sn 2 <sup>o</sup>	24.892	L8		27.211
L3		24.883	O8		27.191
P3					
O3	sn 1 <sup>o</sup> ,3 <sup>o</sup>	24.861	L11		25.65
L3	sn 1 <sup>o</sup> ,3 <sup>o</sup>	24.854	O3	sn 2 <sup>o</sup>	24.905
P15		22.713	L3	sn 10, 30	24.896
O17		22.703	P3		24.887
L17		22.595	O3	sn 1 <sup>o</sup> , 3 <sup>o</sup>	24.865
P16		14.131	L3	sn 20	24.858
O18		14.125	P15		22.716
L18		14.084	O17		22.706
			UK		22.699
			UK		22.682
			L17		22.598
			UK		14.131
			O18		14.125
			P16		14.118
			L18		14.085

O, olein; P, palmitin; Pa, palmitolein; L, linolein; UK, unknown; V/E, vaccenin or eicosenoin; FFA, free fatty acid.

backbone in olive oil in particular indicates adulteration.<sup>[1]</sup>The good agreement between our assignments derived from the graphical correlation method and published data for olive oils, acceptably validates the proposed method.

Using the proposed graphical correlation method developed here, we were able to fully assign the  $^{13}\text{C}$  NMR spectra of all six vegetable oils in  $\text{CDCl}_3$  solution without recourse to the method of standard additions. The maximum relative error determined for the  $^{13}\text{C}\{^1\text{H}\}$  shifts of  $\text{sp}^3$  carbon atoms is  $\pm 0.004$  ppm and for the  $\text{sp}^2$  carbon atoms is  $\pm 0.036$  ppm under our conditions. The assignments for macadamia nut and avocado pear oils are shown in Table 3, grapeseed and apricot kernel oils in Table 4 and mango kernel and marula oils in Table 5, and the ease with which these were carried out is an indication of the simplicity of the method presented earlier. In principle, under carefully controlled conditions we believe that this simple correlation method of assignment may compliment the more time-consuming standard additions methodology, as well as more elaborate spectroscopic methods such as  $^{13}\text{C}$ - $^{13}\text{C}$  correlations spectroscopy (e.g. INADEQUATE), and be suitable for the assignment of  $^{13}\text{C}\{^1\text{H}\}$  spectra of similar vegetable oils not previously studied by NMR spectroscopy, something currently underway in our laboratory.

## Conclusions

In conclusion, the use of simple linear correlations between  $^{13}\text{C}$  NMR shifts of triacylglycerol fatty acid components in vegetable oils against the corresponding chemical shifts of the standard triacylglycerols in the same solvent at concentration ranges of between 0.10 and 0.20 g oil/1 g solution proves to be a simple method to identify and accurately assign the  $^{13}\text{C}$  NMR spectra of the major components in such oils, particularly in crowded spectral regions. These major components included

**Table 5.**  $^{13}\text{C}$  NMR assignments for mango kernel and marula oil

Carbon	Position	Mango kernel oil (ppm)	Carbon	Position	Marula oil (ppm)
UK		178.907	FFA		173.873
UK		178.885	FFA		173.842
FFA		173.898	P1	sn 1 <sup>o</sup> , 3 <sup>o</sup>	173.265
FFA		173.866	O1	sn 1 <sup>o</sup> , 3 <sup>o</sup>	173.234
UK		173.723	L1	sn 1 <sup>o</sup> , 3 <sup>o</sup>	173.223
P1		173.287	O1	sn 2 <sup>o</sup>	172.825
O1	sn 1 <sup>o</sup> , 3 <sup>o</sup>	173.255	L1	sn 2 <sup>o</sup>	172.812
L1	sn 1 <sup>o</sup> , 3 <sup>o</sup>	173.244	L13	sn 2 <sup>o</sup>	130.186
O1	sn 2 <sup>o</sup>	172.844	L13	sn 1 <sup>o</sup> , 3 <sup>o</sup>	130.178
L1	sn 2 <sup>o</sup>	172.834	O10	sn 2 <sup>o</sup>	130.013
UK		145.079	O10	sn 1 <sup>o</sup> , 3 <sup>o</sup>	129.999
L13		130.199	L9	sn 1 <sup>o</sup> , 3 <sup>o</sup>	129.973
O10	sn 1 <sup>o</sup> , 3 <sup>o</sup>	130.017	L9	sn 2 <sup>o</sup>	129.948
O10	sn 2 <sup>o</sup>	130.005	UK		129.717
L9	sn 1 <sup>o</sup> , 3 <sup>o</sup>	129.989	UK		129.707
L9	sn 2 <sup>o</sup>	129.962	O9	sn 1 <sup>o</sup> , 3 <sup>o</sup>	129.701
UK		129.725	O9	sn 2 <sup>o</sup>	129.675
O9	sn 2 <sup>o</sup>	129.705	L10	sn 2 <sup>o</sup>	128.103
UK		129.689	L10	sn 1 <sup>o</sup> , 3 <sup>o</sup>	128.083
O9	sn 1 <sup>o</sup> , 3 <sup>o</sup>	129.679	L12	sn 1 <sup>o</sup> , 3 <sup>o</sup>	127.920
L10		128.094	L12	sn 2 <sup>o</sup>	127.903
L10		128.077	CH <sub>2</sub> O		68.939
L12		127.912	UK		68.332
L12		127.9	UK		65.041
CHO		68.921	CHO		62.127
DAG		68.349	O2/L2	sn 2 <sup>o</sup>	34.212
DAG		65.051	UK		34.105
CH <sub>2</sub> O		62.114	P2		34.069
O2/L2	sn 2 <sup>o</sup>	34.215	O2/L2	sn 1 <sup>o</sup> , 3 <sup>o</sup>	34.047
UK		34.122	UK		34.020
UK		34.106	UK		34.005
P2		34.07	P14		31.976
O2/L2	sn 1 <sup>o</sup> , 3 <sup>o</sup>	34.047	O16		31.955
UK		33.974	L16		31.568
UK		33.958	O12		29.810
P14		31.963	O7	sn 2 <sup>o</sup>	29.757
O16		31.941	UK		29.754
L16		31.557	UK		29.747
O12		29.798	O7	sn 1 <sup>o</sup> , 3 <sup>o</sup>	29.743
P10,12/O7		29.741	P10		29.736
P11		29.726	P12		29.727
P9		29.711	P11		29.719
P8		29.699	UK		29.711
UK		29.679	P9		29.704
P7/L7	sn 1 <sup>o</sup> , 3 <sup>o</sup>	29.661	P8		29.690
L7	sn 2 <sup>o</sup>	29.637	UK		29.670
UK		29.632	L7	sn 2 <sup>o</sup>	29.661
O14	sn 1 <sup>o</sup> , 3 <sup>o</sup>	29.565	P7		29.647
O14	sn 2 <sup>o</sup>	29.562	L7	sn 1 <sup>o</sup> , 3 <sup>o</sup>	29.643
P5		29.515	UK		29.578
UK		29.48	UK		29.576
P13		29.402	UK		29.573
L15		29.378	O14		29.571
O13		29.361	UK		29.525
O15		29.357	P5		29.491
P6		29.307	UK		29.415
UK		29.292	P13		29.391

**Table 5.** (Continued)

Carbon	Position	Mango kernel oil (ppm)	Carbon	Position	Marula oil (ppm)
O5/L5	sn 2 <sup>o</sup>	29.229	O13/L15		29.370
O5/L5	sn 1 <sup>o</sup> , 3 <sup>o</sup>	29.206	O15		29.363
UK		29.187	UK		29.318
O6/L6	sn 1 <sup>o</sup> , 3 <sup>o</sup>	29.158	P6		29.301
P4/L6	sn 1 <sup>o</sup> , 3 <sup>o</sup>	29.149	O5/L5	sn 1 <sup>o</sup> , 3 <sup>o</sup>	29.239
O6	sn 2 <sup>o</sup>	29.141	UK		29.226
O4	sn 1 <sup>o</sup> , 3 <sup>o</sup>	29.119	O5/L5		29.217
L4	sn 2 <sup>o</sup>	29.117	UK		29.201
UK		29.103	UK		29.196
UK		29.088	O6/L6	sn 1 <sup>o</sup> , 3 <sup>o</sup>	29.164
O4/L4	sn 2 <sup>o</sup>	29.08	UK		29.158
O11	sn 1 <sup>o</sup> , 3 <sup>o</sup>	27.252	O6/L6	sn 1 <sup>o</sup> , 3 <sup>o</sup>	29.148
O11	sn 2 <sup>o</sup>	27.248	P4		29.139
UK		27.242	O4		29.126
L14		27.228	L4	sn 2 <sup>o</sup>	29.119
L8		27.217	UK		29.110
UK		27.208	UK		29.093
O8		27.199	O4/L4	sn 1 <sup>o</sup> , 3 <sup>o</sup>	29.088
UK		27.188	O11		27.260
UK		27.183	O11		27.256
L11		25.654	UK		27.249
O3/L3	sn 2 <sup>o</sup>	24.91	L14		27.236
P3		24.892	L8		27.223
UK		24.878	O8		27.204
O3/L3	sn 1 <sup>o</sup> , 3 <sup>o</sup>	24.87	UK		27.197
UK		24.753	UK		27.188
UK		24.737	L11	sn 2 <sup>o</sup>	25.662
P15		22.723	O3		24.917
O17		22.713	L3	sn 1 <sup>o</sup> , 3 <sup>o</sup>	24.906
L17		22.604	P3		24.900
P16		14.133	O3/L3		24.878
O18		14.127	UK		24.742
L18		14.087	UK		24.727
			P15		22.734
			O17		22.724
			L17		22.615
			P16		14.137
			O18		14.132
			L18		14.092

O, olein; P, palmitin; Pa, palmitolein; L, linolein; UK, unknown; V/E, vaccenin or eicosenin; FFA, free fatty acid.

oleic, linoleic and palmitic fatty acids in all six oils and palmitoleic fatty acid in macadamia nut and avocado pear oils. This method has been validated with the well-known  $^{13}\text{C}$  NMR spectrum of olive oil, and has been used to fully assign the  $^{13}\text{C}$  NMR spectra of the triacylglycerol fatty acid residues of six previously unassigned vegetable oils, apricot kernel, avocado pear, grapeseed, macadamia nut, mango kernel and marula oils. This method is reasonably robust and rapidly leads to accurate  $^{13}\text{C}$  NMR assignments in mixtures of triacylglycerols at reasonable concentrations in similar vegetable oils not previously examined, without having to resort to time-consuming additions of pure standards.

### Acknowledgements

We would like to thank Specialized Oils for donating the apricot kernel, avocado pear, grapeseed, macadamia nut, mango kernel and marula oils and Brenn-o-kem for the olive oil. The University of Stellenbosch is acknowledged for financial assistance.

### Supporting information

Supporting information may be found in the online version of this article.

### References

- [1] L. Mannina, A. P. Sobolev, A. Segre, *Spectrosc. Eur.* **2003**, *15*, 6.
- [2] L. Mannina, A. Segre, *Grasas y Aceites* **2002**, *53*, 22.
- [3] G. Vlahov, C. Schiavone, N. Simone, *Magn. Reson. Chem.* **2001**, *39*, 689.
- [4] R. Sacchi, F. Addeo, L. Paolillo, *Magn. Reson. Chem.* **1997**, *35*, S133.
- [5] J. M. McKenzie, K. R. Koch, *S. Afr. J. Sci.* **2004**, *100*, 349.
- [6] L. Diego, G. Gonz'ales, L. Mannina, M. D'Imperio, A. Segre, R. Aparicio, *Eur. Food Res. Technol.* **2004**, *219*, 545.
- [7] G. Vlahov, *Magn. Reson. Chem.* **1997**, *35*, S8.
- [8] J. Mavromoustakos, M. Zervou, G. Bonas, A. Kolocouris, P. Petrakis, *J. Am. Oil Chem. Soc.* **2000**, *77*(4), 405.
- [9] G. Vlahov, A. D. Shaw, D. B. Kell, *J. Am. Oil Chem. Soc.* **1999**, *76*, 1223.
- [10] L. Mannina, C. Luchinat, M. C. Emanuele, A. Segre, *Chem. Phys. Lipids* **1999**, *103*, 47.
- [11] *Off. J. Eur. Commun.* **1991**, *L248*, 1, Commission Regulation (EEC) No 2568/91.
- [12] L. Mannina, C. Luchinat, M. Patumi, M. C. Emanuele, E. Rossi, A. Segre, *Magn. Reson. Chem.* **2000**, *38*, 886.
- [13] A. D. Shaw, A. di Camillo, G. Vlahov, A. Jones, G. Bianchi, J. Rowland, D. B. Kell, *Anal. Chim. Acta* **1997**, *348*, 357.

# IDENTIFICATION AND QUANTIFICATION OF MAJOR TRIACYLGLYCEROLS IN SELECTED SOUTH AFRICAN VEGETABLE OILS BY $^{13}\text{C}$ NMR SPECTROSCOPY

L. Retief<sup>1</sup>, J.M. McKenzie<sup>2</sup> and K.R. Koch<sup>1</sup>

<sup>1</sup>Department of Chemistry and Polymer Science, Stellenbosch University, P Bag X1, Matieland, South Africa, 7602.

<sup>2</sup>Central Analytical Facility, Stellenbosch University, P Bag X1, Matieland, South Africa, 7602

## 1 INTRODUCTION

Vegetable oil production has increased significantly in South Africa in the last decade, due to the use of these oils in the food and cosmetics industry. Apart from olive oils, locally produced oils such marula, apricot kernel, avocado pear, grape seed, macadamia nut, and mango kernel oils are sold for human consumption and widely used in the in the making of handcreams, shampoos and other cosmetic products. Quantitative proton decoupled  $^{13}\text{C}\{^1\text{H}\}$  NMR has been extensively used for the study of olive oils by several groups in order to determine the geographical origin or cultivar variety of the oil, as well as their authentication (1-4). We have become interested in the use of  $^{13}\text{C}\{^1\text{H}\}$  NMR for the determination of major components of South African extra-virgin olive oils particularly the possible detection of adulteration and studying variations in these components as a function of geographic and cultivar origin of olive oils (5).

The aim of our project was to identify and determine the fatty acid content of these oils by means of  $^{13}\text{C}\{^1\text{H}\}$  NMR spectroscopy. The  $^{13}\text{C}\{^1\text{H}\}$  NMR spectra of locally produced marula, apricot kernel, avocado pear, grape seed, macadamia nut, and mango kernel oils are very similar to those of the well-studied olive oil, we attempted to assign their  $^{13}\text{C}\{^1\text{H}\}$  NMR spectra by the method used by Mannina *et al.* for olive oil (1). Mannina *et al.* achieved assignment of the  $^{13}\text{C}\{^1\text{H}\}$  spectra in part by addition of pure Standard triacylglycerols; we shall refer to as the standard-addition method. For our locally produced oils we found however, that full assignment of the  $^{13}\text{C}\{^1\text{H}\}$  spectra was complicated by extensive spectral overlap in crowded regions of the spectrum and some concentration dependence of the  $^{13}\text{C}\{^1\text{H}\}$  resonances of the major components in a given solvent. We here report a  $^{13}\text{C}\{^1\text{H}\}$  method with which to achieve the reliable full assignment of the major triacylglycerol components of the vegetable oils in question, as well as the preliminary quantitative determination of these triacylglycerols.

## 2 EXPERIMENTAL

### 2.1 Materials and sample preparation

Standard triacylglycerols, tripalmitin, tripalmitolein, tristearin, triolein and trilinolein, were purchased from Sigma-Aldrich and used without further purification ( $\geq 99\%$  purity). Samples of olive oil were provided by Brenn-o-Kem (Wolseley, South Africa). Macadamia nut and

avocado pear oil were supplied by Specialized Oils (Paardeneiland, Cape Town, South Africa). All oils were filtered before use. For storage, the oils were flushed with nitrogen gas and refrigerated at -25 °C.

## 2.2 $^{13}\text{C}$ NMR data collection and processing

Approximately 100  $\mu\text{l}$  of each oil in 700  $\mu\text{l}$  of deuterated chloroform with TMS as reference was used for NMR analysis. NMR spectra were run on a 400 MHz Varian <sup>Unity</sup>Inova NMR spectrometer operating at 100 MHz for  $^{13}\text{C}$ . Acquisition parameters described by Mannina *et al.* (10) were used for collecting the  $^{13}\text{C}$  NMR spectra: number of points 256 K; spectral width 195 ppm; relaxation delay: 7 s; acquisition time 4.5 s.

## 2.3 GC analysis of vegetable oils

Methyl esterification of vegetable oils for GC analysis (12) was carried out as follows: Sodium (0.5 g) was dissolved in 100 ml methanol. The sodium methoxide solution (0.3 g) together with 2 g of the specific vegetable oil was placed in a vial and heat sealed. The heat sealed vial was left for 2 hours at 85-90 °C in an oil bath, with occasionally shaking. GC analysis of macadamia nut and avocado pear oil samples was carried out to determine their fatty acid content in order to compare with the  $^{13}\text{C}$  NMR spectroscopy data obtained. 20  $\mu\text{l}$  of each sample was diluted with 1 ml of dichloromethane and 1  $\mu\text{l}$  of the solution was inserted in the gas chromatograph inlet. Analysis was performed on a HP 5890 Series 2 Gas Chromatograph. The column employed was a fused silica capillary (30 m x 0.25 mm i.d., 0.2 mm film-thickness) coated with a 100% cyanopropylpolysiloxane non-bonded phase. The column temperature was programmed from 40 to 240 °C at a rate of 4 °C/min.

# 3 RESULTS

## 3.1 Assignment of standard-additions method

The idea of the  $^{13}\text{C}\{^1\text{H}\}$  NMR spectra by standard-additions method involves the spiking of the vegetable oil with a known standard triacylglycerol, such as for example triolein. The  $^{13}\text{C}\{^1\text{H}\}$  signals representing the fatty acids of triolein that are present in the oil are expected to increase in intensity upon spiking leading to their assignment. We however found some practical disadvantages using this technique. Apart from the standard being expensive and not readily available, the experiments are time-consuming. Our major problem was with the method's lack of reliable use for the 28 – 30 ppm spectral region of the  $^{13}\text{C}\{^1\text{H}\}$  spectrum, which is very crowded (see to figure 1). More importantly, since it is known that  $^{13}\text{C}\{^1\text{H}\}$  chemical shifts of the fatty acids in oils are somewhat concentration dependent in a given solvent (1), this renders assignment of the  $^{13}\text{C}\{^1\text{H}\}$  spectrum particularly in the crowded regions unreliable; for olive oils the 28 – 30 ppm region of the  $^{13}\text{C}\{^1\text{H}\}$  NMR spectra has not been fully assigned in the literature and we believe it may be due to concentration dependence problem (2). Our own observations confirm this as illustrated for the  $^{13}\text{C}\{^1\text{H}\}$  NMR spectrum of olive oil in Figure 1. For this reason for several local vegetable oils we explored an alternative method for the reliable assignment of all peaks in the  $^{13}\text{C}\{^1\text{H}\}$  spectrum.

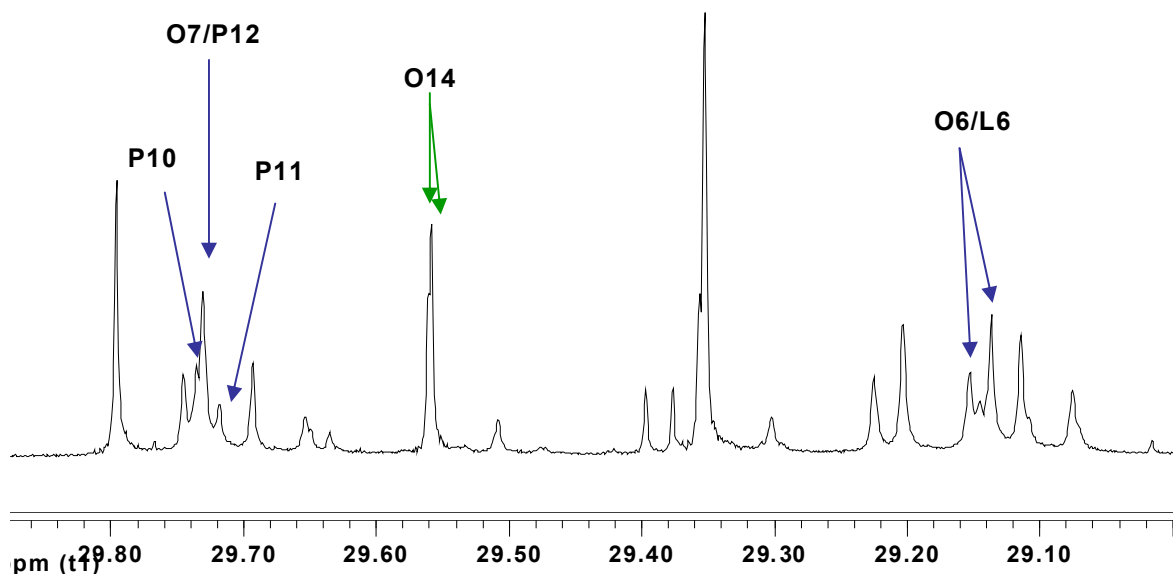


**Figure 1**  $^{13}\text{C}\{^1\text{H}\}$  NMR spectrum of olive oil in  $\text{CDCl}_3$  using TMS as reference at 100 MHz at room temperature.

### 3.2 Linear-graph method

The idea of this method is that the  $^{13}\text{C}$  NMR spectrum of the vegetable oil is divided into separate sections (figure 2), namely Section A for the carbonyl carbons, Section B for the olefinic carbons, section C for the glycerol backbone and sections D-J for the aliphatic carbons.

Division of the  $^{13}\text{C}\{^1\text{H}\}$  spectrum into these sections is convenient because some of these sections are easily assigned by inspection. It is known that  $^{13}\text{C}\{^1\text{H}\}$  signals in the carbonyl region of the spectrum (A) are de-shielded in order of un-saturation, namely the peaks of saturated fragments of the triacylglycerols are most downfield, followed by mono-unsaturated and then polyunsaturated. We also know that the signals due to the carbons in the  $\alpha$  position of the glycerol backbone are usually found more downfield than those in the  $\beta$  position. There is no signal representing the saturated carbons in the  $\beta$  position, which is due to the absence of saturated fatty acids in the  $\beta$  position of the naturally occurring triacylglycerols (3). If there a signal is found in the  $^{13}\text{C}\{^1\text{H}\}$  spectrum which is ascribable to a  $\beta$  position, this indicates possible adulteration. Our proposed 'linear-graph-method' of assignment is based on the premise that if certain  $^{13}\text{C}\{^1\text{H}\}$  peaks in the spectral sections A, B and I can be assigned by inspection for a given component, we expect that these  $^{13}\text{C}\{^1\text{H}\}$  shifts should be approximately linearly correlated to all other  $^{13}\text{C}\{^1\text{H}\}$  peaks of that molecule. We find that this expectation is largely confirmed from our results, particularly if account is taken of the respective type of carbon atom i.e. whether it is a  $\text{sp}^3$  or  $\text{sp}^2$  type (*vide infra*).

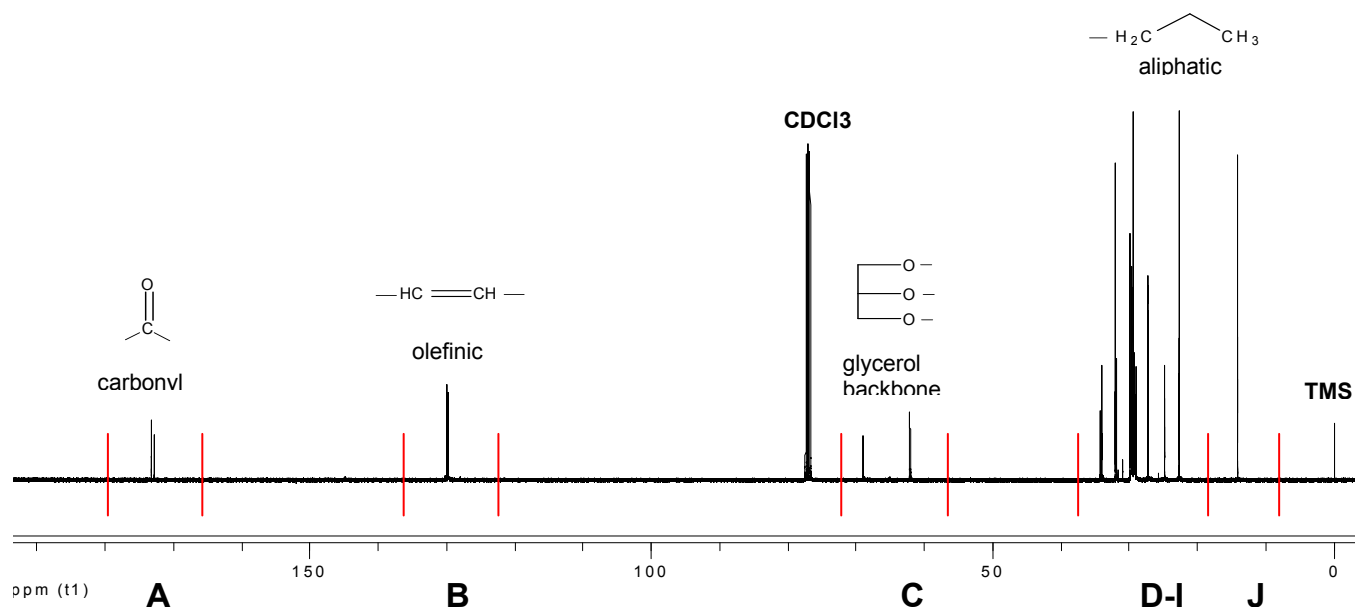


**Figure 2**  $^{13}\text{C}$  NMR spectrum of macadamia nut oil in  $\text{CDCl}_3$  using TMS as reference at 100 MHz at room temperature.

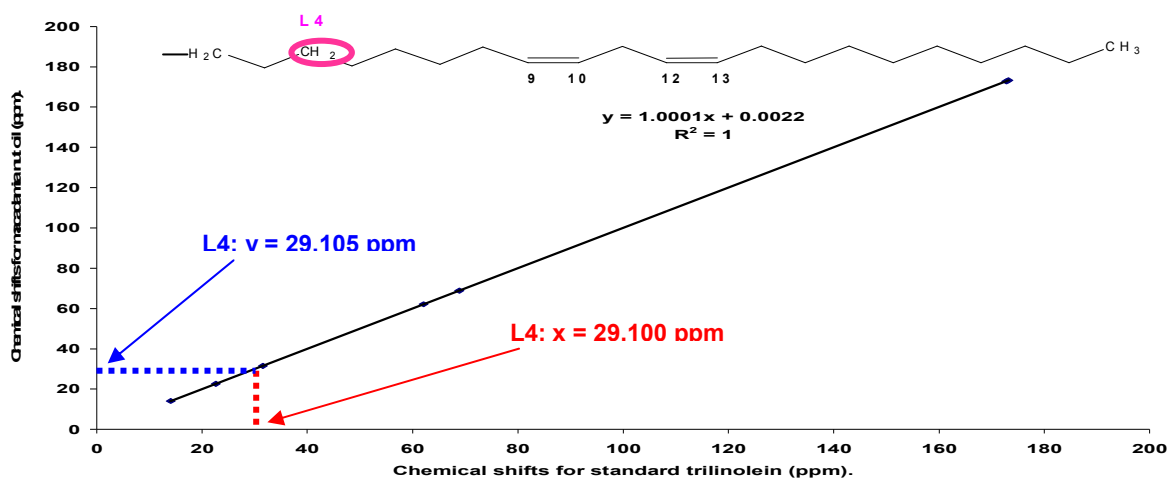


**Figure 3** Linear graph of the chemical shifts in standard trilinolein plotted against the corresponding chemical shifts in macadamia nut oil

Basically our method works as follows: we construct a graph for which on the x-axis the  $^{13}\text{C}\{^1\text{H}\}$  chemical shift of a standard triacylglycerol e.g. trilinolein is plotted against the corresponding carbon atom's  $^{13}\text{C}\{^1\text{H}\}$  shift of that component in the oil, in the same solvent and at the same temperature and approximately similar concentration. The resulting linear excellent correlation may be used as an aid to assign all other  $^{13}\text{C}\{^1\text{H}\}$  for that component in the oil (Figure 3). By way of example, the assignment of C(4) in the linoleic fatty acid chain, which is difficult by inspection since this peak lies in the crowded 28-30 ppm region, is readily obtained from the linear correlation, which so leads to the assignment of that  $^{13}\text{C}\{^1\text{H}\}$  resonance in the vegetable oil spectrum with considerable certainty. We find that this method is remarkably accurate for  $^{13}\text{C}\{^1\text{H}\}$  assignment up to at least one hundredth of a ppm

provided that the  $sp^3$  hybridized carbons and  $sp^2$  hybridized carbons should be plotted on separate graphs.

In order to check the robustness of the the linear-graph-method, and in particular to examine a possible concentration dependance of the  $^{13}C\{^1H\}$  chemical shifts of the various types of carbon atoms of the triacylglycerols, we measured a series of  $^{13}C\{^1H\}$  NMR spectra of different concentration of oil and this is plotted on your x-axis (Figure 4). On the y-axis is the change in chemical shift between each concentration for each type of carbon atom (the aliphatic  $sp^3$  hybridized, carbonyl and olefinic  $sp^2$  hybridized carbon atoms) It can be seen that  $^{13}C\{^1H\}$  shifts of  $sp^3$  hybridized carbon atoms show virtually a linear concentration dependence, being shifted downfield with increasing concentration, while the  $sp^2$  carbon atoms undergo a non-linear upfield shift with increasing concentration. This suggests that our method is concentration independant for  $sp^3$  carbon atoms, while for practical oil concentrations ammenable to  $^{13}C\{^1H\}$ NMR analysis, even  $^{13}C\{^1H\}$  shifts of  $sp^2$  carbon atoms show an approximately linear concentraion dependence.

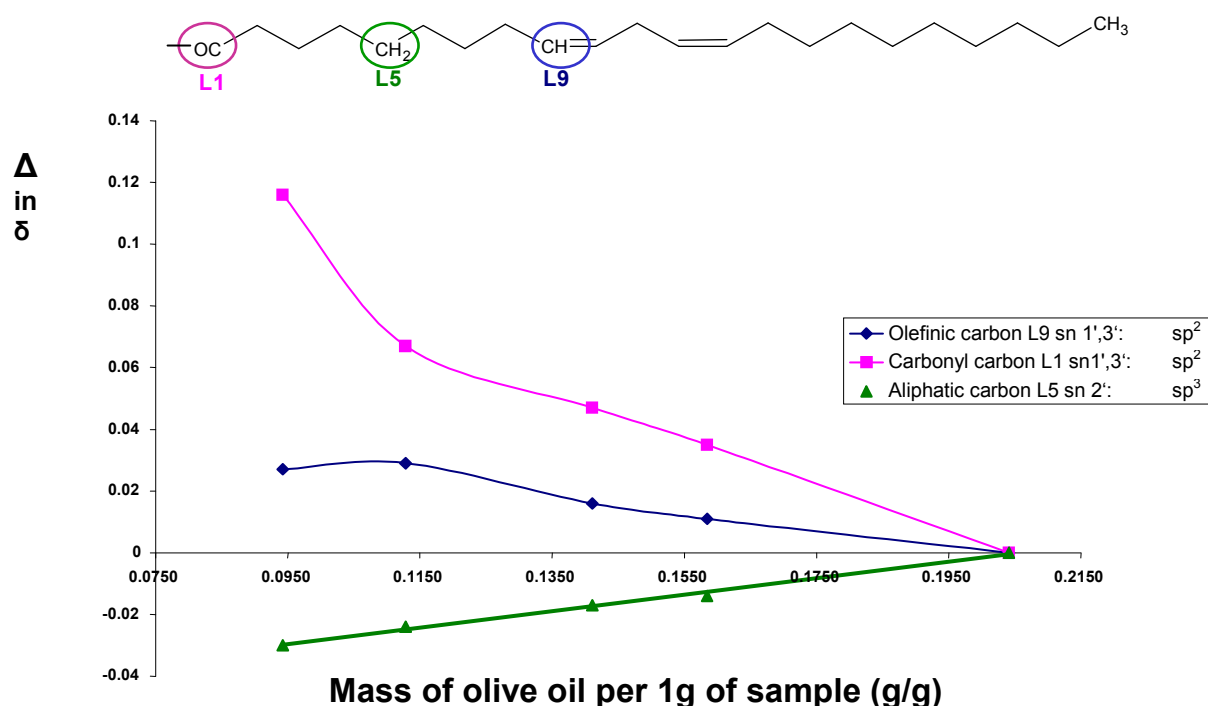


**Figure 4** Graph representing the change in chemical shift between different concentrations of each type of carbon atom in olive oil.

We validated our linear graph method by the assignment of an  $^{13}C\{^1H\}$ NMR spectrum of well studied olive oil in  $CDCl_3$ , finding that our assignments of  $^{13}C\{^1H\}$  chemical shifts compared well to those in the literature (3,4,6) for all the spectral sections (A- J). Moreover it was possible to fully assign the 28 – 30 ppm region of the  $^{13}C\{^1H\}$ NMR spectrum of olive oil shown in Figure 1. Thus for the C(14) of the oleic fatty acid we were able to distinguish between the  $\alpha$  and  $\beta$  positions, as well as suggest assignments of C(7), C(12) and C(11) of the palmitic residue, C(9) and C(6) of oleic residue and C(6) of the linoleic residue, which to the best of our knowledge had not previously been assigned.

With the validation of our method, we were able to apply this the linear-graph-method to the full assignment of the  $^{13}C\{^1H\}$  NMR spectra of the major components in marula, apricot kernel, avocado pear, grape seed, macadamia nut, and mango kernel oils which will be published elsewhere (7).

### 3.3 Quantification of fatty acids

Based on the clear assignment of the major triacylglycerols present in marula, apricot kernel, avocado pear, grape seed, macadamia nut, and mango kernel oils we carried out a preliminary quantitative determination of individual fatty acid using quantitative  $^{13}\text{C}\{^1\text{H}\}$  NMR as applied previously to olive oil (5). For the saturated fatty acids, the carbonyl regions (A) were used, and the  $^{13}\text{C}\{^1\text{H}\}$  were integrated using deconvolution software, which was found to give more reliable integral values for certain signals in the  $^{13}\text{C}\{^1\text{H}\}$  NMR spectrum. For unsaturated fatty acids, the olefinic regions is used (B), and the oleic and linoleic peaks were integrated. These results were compared to those obtained by GC-MS analysis (table 1).

Comparison of fatty acid content as determined by GC with NMR analysis.

		Oleic %	Palmitoleic %	Linoleic %	Vaccenic/ Eicosenoic %	Saturated %
Apricot kernel	GC	63 ± 3.15	1 ± 0.05	31 ± 1.55	< 1	5 ± 0.25
	NMR	61 ± 0.39	nd	31 ± 0.56	nd	8 ± 0.27
Avocado pear	GC	50 ± 2.50	7 ± 0.35	6 ± 0.30	< 1	30 ± 1.50
	NMR	62 ± 0.40		12 ± 0.22	5	21 ± 0.70
Grape seed	GC	12 ± 0.60	< 1	72 ± 3.60	1	14 ± 0.70
	NMR	14 ± 0.09	nd	75 ± 1.36	nd	12 ± 0.40
Macadamia nut	GC	60 ± 3.00	22 ± 1.10	1 ± 0.05	< 1	15 ± 0.75
	NMR	56 ± 0.36	16	nd	7	21 ± 0.70
Mango kernel	GC	50 ± 2.50	< 1	7 ± 0.35	nd	42 ± 2.10
	NMR	56 ± 0.36	nd	10 ± 0.18	nd	34 ± 1.13
Marula	GC	67 ± 3.35	< 1	3 ± 0.15	1 ± 0.05	28 ± 1.70
	NMR	72 ± 0.46	nd	7 ± 0.13	nd	21 ± 0.70

The relative uncertainties for GC analysis were determined based on the maximum 5% relative error expected for this technique for oils (8) and those for NMR analysis were determined similarly as we reported previously for olive oil by quantitative  $^{13}\text{C}\{^1\text{H}\}$  NMR spectroscopy (5). As can be seen within experimental error the amounts of major fatty acid components in the six vegetable oils obtained by both GC and  $^{13}\text{C}\{^1\text{H}\}$  NMR compare fairly well.

## 4 CONCLUSIONS

In conclusion, we believe that the “linear graph method” for the assignment of the  $^{13}\text{C}\{^1\text{H}\}$  chemical shifts of vegetable oil components, particularly in crowded spectral regions is a valuable aid in this regard. We found the method essentially concentration independent for  $\text{sp}^3$  carbon atoms at most practical concentrations, while for  $\text{sp}^2$  carbon atoms there is only a limited range of concentrations applicable to this method. Nevertheless it is possible to fully assign the  $^{13}\text{C}\{^1\text{H}\}$  NMR spectra of these six oils. Quantitative  $^{13}\text{C}\{^1\text{H}\}$  NMR spectroscopy is a suitable method for the rapid determination of the major fatty acids components in six South African vegetable oils with acceptable accuracy and precision.

## Acknowledgements

Financial assistance from the NRF and Stellenbosch University is gratefully acknowledged.

## References

1. L. Mannina, Sobolev, A.P. and Segre, A. *Spectrosc. Eur.* 2003, **15**, 6-14.
2. L. Mannina, L, and Segre, A. *Grasas y Aceites.* 2002, **53**, 22-33.
3. G. Vlahov, *Magn. Reson. Chem.* 2001, **39**, 689-695.
4. R. Sacchi, R, Addeo, F. and Paolillo, L., *Magn. Res. Chem.* 1997, **35**, S133-S145.
5. J.M. McKenzie, and Koch, K.R., *S. Afr. J. Sci.* 2004, **100**, 349-354
6. A.D. Shaw, di Camillo, A, Vlahov, G. Jones, A. Bianchi, G. Rowland, J. And Kell, D.B, *Anal. Chim. Acta.* 1997, **348**, 357-374.
7. L. Retief, McKenzie, J. and Koch, K.R., *Magn. Res. Chem.* 2008
8. M. Schreiner, *Journal of Chromatography A*, 2005, **1095**, 126-130

## LIST OF FIGURES

Figure 1.1: Percentage oil crop production per continent, adapted from data provided by FAO .....	15
Figure 1.2: Percentage oil crop production within Africa, adapted from data provided by FAO .....	16
Figure 1.3: Structure and numbering of a basic saturated fatty acid .....	20
Figure 1.4: The structure and constituents of a triacylglycerol, where $R^n$ represents a hydrocarbon chain and $R^{1,2,3}$ represents three possibly different hydrocarbon chains	21
Figure 1.5: Structure indicating a hypothetical positional distribution of different fatty acids on the glycerol backbone of a natural occurring TG.....	21
Figure 1.6: Numbering scheme for tripalmitin.....	22
Figure 1.7: General structures of diacyl-, monoacylglycerols and fatty acid compounds	23
Figure 2.1: $^{31}\text{P}\{^1\text{H}\}$ NMR spectrum of derivatized apricot kernel oil.....	52
Figure 2.2: $^{31}\text{P}\{^1\text{H}\}$ NMR spectrum of derivatized avocado pear oil .....	53
Figure 2.3: $^{31}\text{P}\{^1\text{H}\}$ NMR spectrum of derivatized macadamia nut oil.....	53
Figure 2.4: $^{31}\text{P}\{^1\text{H}\}$ NMR spectrum of derivatized virgin olive oil taken from Vigli <i>et al</i>	54
Figure 2.5: Illustration of the derivatization of the labile hydrogens present in 1,2 DG; 1,3 DG; FFA and cyclohexanol with 2-chloro-4,4,5,5-tetramethyldioxaphospholane .....	57
Figure 2.6: Calibration curve for 1,2 dipalmitin (1,2 DG standard) .....	59
Figure 2.7: Calibration curve for 1,3 dilinolein (1,3 DG standard).....	60
Figure 2.8: Calibration curve for oleic acid (FFA standard) .....	60
Figure 2.9: Variation in 1,2 DG concentration with different storage methods for apricot kernel oil using the direct correlation approach (DCA) and the calibration curve approach (CCA), with error bars ranging from 3.7 % (CCA) to 10.4 % (DCA) .....	65

Figure 2.10: Variation in 1,3 DG concentration with different storage methods for apricot kernel oil using the direct correlation approach (DCA) and the calibration curve approach (CCA), with error bars ranging from 1.3 % (CCA) to 10.4 % (DCA) .....	66
Figure 2.11: Variation in FFA concentration with different storage methods for apricot kernel oil using the direct correlation approach (DCA) and the calibration curve approach (CCA), with error bars ranging starting from 10.4 % (DCA).....	67
Figure 2.12: Variation in 1,2 DG concentration with different storage methods for macadamia nut oil using the direct correlation approach (DCA) and the calibration curve approach (CCA), with error bars ranging from 1.5 % (CCA) to 10.4 % (DCA) .....	68
Figure 2.13: Variation in 1,3 DG concentration with different storage methods for macadamia nut oil using the direct correlation approach (DCA) and the calibration curve approach (CCA), with error bars ranging from 0.2 % (CCA) to 10.4 % (DCA)	69
Figure 2.14: Variation in FFA concentration with different storage methods for macadamia nut oil using the direct correlation approach (DCA) and the calibration curve approach (CCA), with error bars starting from 8.1 % (CCA) .....	71
Figure 2.15: Variation in 1,2 DG concentration with different storage methods for avocado pear oil using the direct correlation approach (DCA) and the calibration curve approach (CCA), with error bars ranging from 2.1 % (CCA) to 10.4 % (DCA) .....	72
Figure 2.16: Variation in 1,3 DG concentration with different storage methods for avocado pear oil using the direct correlation approach (DCA) and the calibration curve approach (CCA), with error bars ranging from 0.09 % (CCA) to 10.4 % (DCA) ....	74
Figure 2.17: Variation in FFA concentration with different storage methods for avocado pear oil using the direct correlation approach (DCA) and the calibration curve approach (CCA), with error bars starting from 3.6 % (CCA) .....	75
Figure 3.1: Total production quantities (in tonnes) of certain beans and seeds worldwide, adapted from data provided by FAO .....	82
Figure 3.2: Production quantities as a percentage of the world total (in tonnes) as produced in separate continents, adapted from data provided by FAO.....	82

Figure 3.3: Production quantities of pumpkins, squash and gourds in various African countries as a percentage of the total tonnes produced in Africa, adapted from data provided by FAO .....	84
Figure 3.4: Production quantities of sesame seeds in various African countries as a percentage of the total tones produced in Africa, adapted from data provided by FAO .....	85
Figure 3.5: Production quantities of sunflower seeds in various African countries as a percentage of the total tonnes produced in Africa, adapted from data provided by FAO .....	86
Figure 3.6: Production quantities of soybeans in various African countries as a percentage of the total tonnes produced in Africa, adapted from data provided by FAO .....	87
Figure 3.7: Production quantities of dry beans in various African countries as a percentage of the total tonnes produced in Africa, adapted from data provided by FAO .....	89
Figure 3.8: The TGA Q500 instrument from TG Instruments .....	91
Figure 3.9: Examples of a TGA and DTG thermogram for soybean.....	91
Figure 3.10: DTG curves of the seeds.....	99
Figure 3.11: DTG curves of the beans .....	100
Figure 3.12: Screen shot of the main view of the FindGraph software, indicating the maximum and minimum values obtained from the DTG of a soybean sample.....	101
Figure 3.13: Screen shot indicating the standard error for the equation describing the DTG of a soybean sample as found by the FindGraph software.....	102
Figure 3.14: DTG thermogram of soybean with indication of the peak due to moisture loss .....	105
Figure 3.15: Graph illustrating the DTG thermogram for pumpkin seed with indication of the peaks of interest for oil and protein content.....	111
Figure 3.16: Graph illustrating the DTG of soybean with indication of the region of interest for oil, protein and carbohydrate content .....	117
Figure 4.1: An illustration of $\theta$ , which is the angle between the $^1\text{H}$ - $^{13}\text{C}$ bond vectors and the direction of the external magnetic field $B_0$ .....	130

Figure 4.2: The $^{13}\text{C}$ NMR spectra of cis – and trans-polyacetylene taken from Voelkel <i>et al.</i> <sup>20</sup> In a) the $^{13}\text{C}$ NMR spectrum for the stationary powder sample is observed, with b) as the sample is rotating at the magic angle .....	132
Figure 4.3: Illustration of possible packing of components of seeds and beans within domains.....	138
Figure 4.4: Solution state $^{13}\text{C}$ NMR spectrum of marula oil.....	140
Figure 4.5: $^{13}\text{C}$ SPE-MAS NMR spectrum of poppy seed flour.....	141
Figure 4.6: $^{13}\text{C}$ SPE-MAS NMR spectrum of pumpkin seed flour.....	141
Figure 4.7: $^{13}\text{C}$ SPE-MAS NMR spectrum of sesame seed flour.....	142
Figure 4.8: $^{13}\text{C}$ SPE-MAS NMR spectrum of sunflower seed flour.....	142
Figure 4.9: Numbered structure of triolein.....	143
Figure 4.10: Numbered structure of trilinolein .....	143
Figure 4.11: Expanded solution state $^{13}\text{C}$ NMR spectrum of marula oil showing the 35 to 14 ppm region .....	143
Figure 4.12: Expanded $^{13}\text{C}$ SPE-MAS NMR spectrum of poppy seed flour showing the 35 to 22 ppm area.....	144
Figure 4.13: $^{13}\text{C}$ CP-MAS NMR spectrum of poppy seed flour.....	146
Figure 4.14: $^{13}\text{C}$ CP-MAS NMR spectrum of pumpkin seed flour.....	146
Figure 4.15: $^{13}\text{C}$ CP-MAS NMR spectrum of sesame seed flour .....	147
Figure 4.16: $^{13}\text{C}$ CP-MAS NMR spectrum of sunflower seed flour .....	147
Figure 4.17: $^{13}\text{C}$ SPE-MAS NMR spectrum of black bean flour.....	151
Figure 4.18: $^{13}\text{C}$ SPE-MAS NMR spectrum of kidney bean flour.....	151
Figure 4.19: $^{13}\text{C}$ SPE-MAS NMR spectrum of mung bean flour .....	152
Figure 4.20: $^{13}\text{C}$ SPE-MAS NMR spectrum of soybean flour.....	152
Figure 4.21: $^{13}\text{C}$ CP-MAS NMR spectrum of black bean flour.....	153
Figure 4.22: $^{13}\text{C}$ CP-MAS NMR spectrum kidney bean flour.....	154
Figure 4.23: $^{13}\text{C}$ CP-MAS NMR spectrum of mung bean flour .....	154
Figure 4.24: $^{13}\text{C}$ CP-MAS NMR spectrum of soybean flour.....	155

Figure 4.25: Curve representing the $T_{1\rho}H$ relaxation of the carbons around 70 ppm with respect to contact time .....	158
Figure 4.26: Curve representing the $T_{1\rho}H$ relaxation of starch carbons at 70 ppm with respect to contact time with the sharper CP rate for beans than seeds indicated . .....	159
Figure 4.27: Curve representing the $T_{1\rho}H$ relaxation of starch carbons at 70 ppm with respect to contact time with indication of the sharper decrease of relaxation for beans than seeds.....	160
Figure 4.28: Log of the peak intensity plotted against contact time for determination of the $T_{1\rho}H$ relaxation of carbons at 70 ppm for soybeans .....	161
Figure 4.29: Curve representing the $T_{1\rho}H$ relaxation carbons at 70 ppm with respect to contact time with indication of a linear line fitted to two separate relaxation rates. .....	162
Figure 4.30: Plot of the log of the peak intensity against contact time representing the $T_{1\rho}H$ relaxation of carbons at 70 ppm for soybean .....	163
Figure 4.31: The plots for determination of $T_{1\rho}H$ relaxation of carbons at 70 ppm for soybean with a linear line fitted for each of the two phases .....	163
Figure 4.32: One-phase fitted equation to starch carbons at 70 ppm relaxation data for mung bean .....	165
Figure 4.33: Two-phase equation fitted to 70 ppm relaxation data for mung bean .....	167
Scheme 1.1: Acid-catalysed hydrolysis of the TGs present in vegetable oils.....	28
Scheme 1.2: Figure illustrating the breakdown of TGs into DGs and FFAs and the FFA catalysed isomerisation between 1,2 DGs and 1,3 DGs .....	29
Scheme 1.3: Free fatty acid-catalysed of the isomerisation of 1,2 DG to 1,3 DG present in vegetable oils .....	30
Scheme 2.1: Schematic representation of the reaction of 2-chloro-4,4,5,5-tetramethyldioxaphospholane with the OH-groups present in the minor components yielding the minor component (R) containing a tetramethyldioxaphospholinate group.....	50

## LIST OF TABLES

Table 1.1: Some common fatty acids with their IUPAC and trivial names .....	20
Table 1.2: Chromatographic and other analytical techniques for the measurement of chemical properties of vegetable oils .....	24
Table 2.1: Assignment of the $^{31}\text{P}\{^1\text{H}\}$ NMR spectra of derivatized apricot kernel, avocado pear and macadamia nut oils with comparison to those of derivatized olive oil .....	55
Table 2.2: Table presenting the integration of the $^{31}\text{P}\{^1\text{H}\}$ signals and conversion of values to concentration of apricot kernel oil .....	58
Table 2.3: Concentration in $\mu\text{mol/ml}$ of 1,2 DGs; 1,3 DGs and FFAs present in fresh apricot kernel, avocado pear and macadamia nut oils .....	58
Table 2.4: True slope and intercept at 95 % CL of the standard calibration curves	59
Table 2.5: Concentration in $\mu\text{mol/ml}$ of 1,2 DGs; 1,3 DGs and FFAs present in fresh apricot kernel, avocado pear and macadamia nut oils .....	61
Table 2.6: LOD and LOQ values determined for apricot kernel, avocado pear and macadamia nut oil analysis by NMR spectroscopy .....	62
Table 3.1: Thermal analysis techniques .....	90
Table 3.2: Standard errors of the equations fit to the DTGs of seeds and beans based on their full data and from increasing temperature only.....	103
Table 3.3: Calculations of moisture content by gravimetry .....	104
Table 3.4: Moisture content determined by TGA and the oven gravimetry method	106
Table 3.5: Moisture content determination by TGA and the gravimetric method using different sample preparation.....	108
Table 3.6: Values used for the calculation of fat content .....	109
Table 3.7: Protein determination using EDTA and Alfalfa as standards .....	110
Table 3.8: Comparison of the fat and protein content values of seeds determined by Soxhelt and Dumas combustion respectively with DTG results .....	112
Table 3.9: Sum of the oil and protein percentage content obtained for each seed	

with 95 % CL* by various methods .....	113
Table 3.10: Values used for the calculation of fat content .....	115
Table 3.11: Protein determination using EDTA and Alfalfa as standards .....	116
Table 3.12: Determination of the carbohydrate content in beans .....	116
Table 3.13: Comparison of fat, carbohydrate and protein content values for beans determined by conventional methods and DTG .....	118
Table 3.14: Sum of oil, protein and carbohydrate (% w/w) content obtained for each type of bean at 95 % CL by various methods.....	119
Table 4.1: Assignment of the <sup>13</sup> C NMR SPE-MAS spectra of poppy, sesame, pumpkin and sunflower seeds by comparison to literature assignments .....	145
Table 4.2: Assignment of the <sup>13</sup> C NMR CP-MAS spectra of seeds obtained from the literature .....	148
Table 4.3: T <sub>1ρ</sub> H values determined for seeds and beans for peak at 70 ppm .....	164
Table 4.4: T <sub>1ρ</sub> H values determined for seeds and beans for peaks at 100, 70 and 60 ppm using a single phase fit.....	166
Table 4.5: T <sub>1ρ</sub> H values determined for seeds and beans for signals at 100, 70 and 60 ppm for two domains .....	167